# The molecular bases underlying chromosome fragility at Replication Slow Zones in *Saccharomyces cerevisiae*

## Nadia Hashash

**A thesis submitted to University College London in fulfilment of the requirements for the degree of Doctor of Philosophy**

**December 2008**

Division of Stem Cell Biology and Developmental Genetics
National Institute for Medical Research
The Ridgeway
Mill Hill
London
NW7 1AA

1

# Declaration

"I, **Nadia Hashash**, confirm that the work presented in this thesis is my own. Where information has been derived from other sources, I confirm that this has been indicated in the thesis"

**Signed**  ............................................................  **Date**  ............................................................

# Abstract

Chromosome rearrangements such as translocations and deletions are frequently associated with human cancers. Such rearrangement of the chromosome can be initiated by a DNA break (DSB) that, when inappropriately repaired, may alter chromosome structure. Mammalian common fragile sites are the best-characterised, naturally occurring breakage-prone regions and are deleted or rearranged in many tumour cells. Analogous chromosomal regions also exist in the budding yeast, *S. cerevisiae*. One example of a yeast fragile site is the replication slow zone (*RSZ*), so called because the rate of replication fork progression through these regions is slow compared to other regions within the same chromosome. Inactivation of the essential checkpoint kinase, Mec1, in *mec1-ts* mutants results in replication fork stalling followed by chromosome breakage at *RSZs*. Interestingly, inhibition of ATR, the mammalian homologue of Mec1, also leads to chromosome instability at common fragile sites, suggesting that the mechanism by which endogenous DSBs are generated is conserved between yeast and mammals. This study aims to enhance our current understanding of common fragile sites using yeast *RSZs* as a model.

First, *RSZs* were characterised in terms of chromosomal features and determinants in order to identify similarities between *RSZs* and mammalian common fragile sites and to assess whether yeast *RSZs* as a suitable system for studying common fragile sites in more complex organisms.

Next, the mechanism underlying chromosome fragility at *RSZs* was investigated by examining the contribution of various chromosomal processes to break formation at these sites. These include: (*i*) replication fork restart processes (*ii*) spindle force, (*iii*) chromosome condensation and decatenation, (*iv*) chromosome segregation, and (*v*) cytokinesis. The analyses suggest that chromosome breakage within *RSZs* requires the actions of the evolutionarily conserved type II topoisomerase and condensin complex.

Finally, factors involved in maintaining the stability of *RSZs* were also explored. The Rrm3 helicase and Psy2 phosphatase complex were found to suppress chromosome breakage at *RSZs* in a manner dependent on Tel1, another checkpoint kinase. These findings suggest that Tel1 is somehow implicated in chromosome stability at *RSZs*.

The findings presented in this study further our understanding of RSZs and the molecular bases governing their fragility, providing some insight into the mechanism of fragile site instability in mammals.

# Table of Contents

# List of Figures

# List of Tables

# List of Abbreviations

| | |
|---|---|
| 1C | One cell (haploid) DNA content |
| 2C | Two cell (diploid) DNA content |
| 2D | Two dimensional |
| $^{32}$P | 32-phosporous |
| 5'FOA | 5'-fluoro-orotic acid |
| 5'UTR | 5'-untranslated region |
| αF | alpha factor |
| ACS | ARS consensus sequence |
| Amp | ampicillin |
| APC/C | anaphase promoting complex or cyclosome |
| APC/C$^{Cdc20}$ | Cdc20-bound APC/C |
| APC/C$^{Cdh1}$ | Cdh1-bound APC/C |
| APS | ammonium persulphate |
| ARS | autonomously replicating sequence |
| ATM | ataxia telangiectasia mutated |
| ATR | ataxia telangiectasia and Rad3 related |
| ATRIP | ATR interacting protein |
| bp | base pair(s) |
| BrdU | bromodeoxyuridine |
| BSA | bovine serum albumin |
| CDK | cyclin-dependent kinase |
| CDKI | cyclin-dependent kinase inhibitor |
| CEN | centromere |
| CEO | compromised early origin |
| CFU | colony forming units |
| ChIP | chromatin immunoprecipitation |
| DAPI | 4,6-diamino-2-phenylindole |
| DCTP | deoxycytidine triphosphate |
| DDK | Dbf4-dependent kinase |
| dHJ | double Holliday junction |
| DIC | differential interference contrast |

| | |
|---|---|
| D-loop | displacement loop |
| DMSO | dimethyl sulphoxide |
| DNA | deoxyribonucleic acid |
| dNTP | deoxynucleotide triphosphate |
| DSB | double-strand break |
| dsDNA | double-stranded DNA |
| *E. coli* | *Eschericia coli* |
| ECL | enhanced chemiluminescence |
| EDTA | ethlenediaminetetra-acetic acid |
| FA | Fanconi Anemia |
| FACS | fluorescence activated cell sorting |
| FEAR | CDC fourteen early anaphase release |
| FRAP | Fluorescence recovery after photobleaching |
| G1 | gap 1 |
| G2 | gap 2 |
| G2/M | transition from G2 to mitosis (M) |
| G-banding | Giemsa-banding |
| GFP | Green fluorescent protein |
| γH2AX | phosphorylated *S. cerevisiae* H2A or vertebrate H2AX |
| HR | homologous recombination |
| HU | hydroxyurea |
| HPV | human papillomavirus |
| ICL | intra-strand crosslink |
| IR | ionising radiation |
| kb | kilo base (s)/ kilo base pair (s) |
| LB | Luria Bertani |
| LINE(s) | long interspersed nuclear element(s) |
| LMP | low melting point |
| LTR | long terminal repeat |
| M | mitosis |
| *MARs* | matrix association regions |
| *MAT* | mating type locus |
| Mb | mega base pair(s) |
| MBC | carbendazim |

| | |
|---|---|
| MCC | mitotic checkpoint complex |
| MCM | minichromosome maintenance |
| MEN | mitotic exit network |
| MMS | methyl methanesulphonate |
| MOPS | 3-(N-morpholino)propanesulphonic acid |
| NHEJ | non-homologous end-joining |
| $OD_{600}$ | optical density at 600 nm |
| ORC | origin recognition complex |
| PAGE | polyacrylamide gel electrophoresis |
| PBS | phospho-buffered saline |
| PCC | premature chromosome condensation |
| PCNA | proliferating cell nuclear antigen |
| PCR | polymerase chain reaction |
| PEG | polyethylene glycol |
| PFG(E) | pulsed-field gel (electrophoresis) |
| PIKK | phosphatidylinositol-3-OH kinase-like kinase |
| PP1 | type 1 protein phosphatase |
| pre-RC | pre-replicative complex |
| PRR | post-replicative repair |
| R-banding | reverse-Giemsa-banding |
| rDNA | ribosomal DNA |
| RFB | replication fork barrier |
| RFC | replication factor C |
| RNA | ribonucleic acid |
| RNase | ribonuclease |
| RNR | ribonucleotide reductase |
| RPA | replication protein A |
| rpm | revolutions per minute |
| RSC | remodel the structure of chromatin |
| *RSZ* | replication slow zone |
| S | DNA synthesis |
| SAC | spindle assembly checkpoint |
| *S. cerevisiae* | *Saccharomyces cerevisiae* |
| *S. pombe* | *Schizosaccharomyces pombe* |

| | |
|---|---|
| SC | synthetic complete |
| SCE | sister chromatid exchange |
| SD | synthetic dextrose |
| SDS | sodium dodecyl sulphate |
| SDSA | synthesis-dependent strand annealing |
| SGD | *Saccharomyces Genome* database |
| SMC | structural maintenance of chromosome |
| SPB | spindle pole body |
| SPM | sporulation media |
| ssDNA | single-stranded DNA |
| TAE | Tris-acetate EDTA |
| TBE | Tris-borate EDTA |
| TCA | trichloroacetic acid |
| TE | Tris-EDTA |
| TEMED | N,N,N',N'-tetramethyl-ethylenediamine |
| TLS | translesion |
| tRNA | transfer RNA |
| TS | template switching |
| ts | temperature sensitive |
| UV | ultra violet |
| WT | wild type |
| YAC | yeast artificial chromosome |
| YEP | yeast extract peptone |
| YPD | yeast extract peptone dextrose |
| YPG | yeast extract peptone glycerol |

# Acknowledgements

First, I would like to thank my supervisor, Rita Cha, for giving me the opportunity to work on this project and for all her guidance, ideas, and advice over the past three years. Her continued enthusiasm was greatly needed and deeply appreciated.

I express my gratitude to Catherine Freudenreich, Doug Koshland, John Nitiss, Marco Foiani, Oscar Aparicio, Shawn Szyjka, and Virginia Zakian for supplying some of the reagents, strains, and software used in this thesis. I am especially grateful to Katsuhiko Shirahige and Yuki Katou for carrying out the ChIP on chip experiments, and to Peter Rosenthall for his help with the TwistFlex analysis. I would also like to express my appreciation to the members of my thesis committee: Robin Lovell-Badge, Jonathan Millar, and Tony Carr, for their numerous suggestions and ideas, and for taking time out of their busy schedules to discuss my project.

A huge thank-you to all the members of the "ChaChaCha lab" and Yeast Genetics Division, both past and present, for creating a stimulating and fun working environment. I would especially like to thank Marco for his insightful suggestions and constructive advice, Tony for providing technical support and being an invaluable source of information (yeast related and otherwise), and Caroline for kindly sharing all her formatting tips – and for teaching us all something about organisation skills! A special thank-you to Jesús Carballo for his support, criticisms, encouragement, ideas, advice, and friendship. I would have been lost without it.

Thanks also to Sara and Robyn for enduring my gradual decline to the ranks of "monster flatmate". Hopefully, I'll be able to turn back into a normal, pleasant human being! Finally, I would like to thank Jeremiah for his endless patience and support, and for always making me smile, even when nothing else could.

# Chapter 1

# Introduction

## 1.1    General introduction

Genome instability, manifested as abnormal chromosomes exhibiting deletions or rearrangements, is a hallmark of cancer. Such potentially hazardous chromosome aberrations can arise from inappropriate repair of lesions or breaks in the DNA, which are either caused by exogenous DNA-damaging agents or occur endogenously during the normal life of a cell. Endogenous chromosome breaks can be induced intentionally by the cell in order to perform certain necessary functions. However, endogenous chromosome breakage can also arise accidentally as cells undergo different stages of the cell cycle. Although a multitude of studies have addressed the mechanisms by which broken chromosomes can be repaired, the molecular basis underlying endogenous chromosome breakage remains unknown.

Although endogenous chromosome breakage occurs unintentionally, it has long been known that certain regions of the chromosome are more prone to breakage than other regions in the same chromosome. Chromosome instability at these so-called fragile sites correlates strongly with chromosome abnormalities found in cancer cells. However, despite numerous studies to determine the sequence properties of fragile sites, these sites still remain enigmatic intrinsic parts of human chromosomes in that the molecular basis underlying their fragility remains obscure. What makes these regions inherently more susceptible to breakage than other areas of the chromosome? Fragile sites typically encounter problems during chromosome duplication, which are manifested at later stages of the cell cycle. As fragile sites are natural components of the chromosome structure, it is likely that their fragility is based on at least two factors: the sequence characteristics that render these regions susceptible to breakage,

and the cell cycle event or chromosomal process directly responsible for inducing this instability.

## 1.2   Fragile sites

Mammalian fragile sites are defined as specific regions/loci on chromosomes that preferentially exhibit gaps, constrictions, or breaks on metaphase chromosomes when exposed to certain culture conditions. To date, over 120 different fragile sites have been identified in the human genome (Schwartz et al., 2006). Fragile sites are classified as rare or common depending on their frequency within the population.

### 1.2.1   Rare Fragile sites

Rare fragile sites are seen in only a small proportion of the population (<5%) and segregate in a Mendelian fashion (Lukusa and Fryns, 2008; Sutherland and Richards, 1995). Inducers of rare fragile sites include folate/thymidylate stress, distamycin A, and bromodeoxyuridine (BrdU), all of which can impede DNA synthesis (Lukusa and Fryns, 2008). Replication analysis of folate-sensitive rare fragile sites indicates that these regions replicate very late in S-phase under normal conditions and that this is further delayed until G2 under conditions of thymidylate stress (Hansen et al., 1997; Subramanian et al., 1996). Folate-sensitive rare fragile sites represent loci with expansive mutations in CCG/CGG repeat sequences (Richards and Sutherland, 1994; Sutherland and Richards, 1995). The folate-sensitive rare fragile site FRAXA is responsible for the fragile X syndrome characterised by severe mental retardation (Verkerk et al., 1991). Another folate-sensitive rare fragile site, FRAXE, is also associated with non-specific mental retardation (Gu et al., 1996).

Rare fragile sites that are sensitive to BrdU or distamycin A are characterised by expanded AT-rich minisatellite repeats (Hewett et al., 1998; Yu et al., 1997). The mechanism for cytogenetic expression of both types of rare fragile sites is likely to involve the formation of secondary structures such as hairpins that perturb DNA replication (Hewett et al., 1998; Samadashwily et al., 1997). This, in turn, can lead to chromosome condensation defects in these regions, which are then manifested as

gaps or constrictions on the chromosomes (Hewett et al., 1998; Lukusa and Fryns, 2008).

## 1.2.2   Common fragile sites

In contrast to rare fragile sites, common fragile sites are present in all individuals and can be found on every chromosome, indicating that they are a normal component of the chromosome (Durkin and Glover, 2007; Sutherland and Richards, 1995). However, not all common fragile sites form breaks at the same frequency in that some common fragile sites are more prone to breakage than others. For example, FRA3B at 3p14.2 is the most 'fragile' site in the human genome, exhibiting breaks in 50% of metaphases after treatment with aphidicolin (Durkin and Glover, 2007; Glover and Stein, 1988). Common fragile sites are conserved throughout mammalian evolution (Elder and Robinson, 1989; Smeets and van de Klundert, 1990; Stone et al., 1991; Stone et al., 1993) and have counterparts in yeast (Cha and Kleckner, 2002; Lemoine et al., 2005; Raveendranathan et al., 2006).

Numerous studies have established a link between genomic instability at common fragile sites and the evolution of cancer (Durkin and Glover, 2007; Glover et al., 2005). In addition to gaps and breaks on chromosomes, common fragile sites also exhibit both large and sub-microscopic deletions (Durkin et al., 2008; Wang et al., 1993), translocations (Glover and Stein, 1987; Glover and Stein, 1988), and sister chromatid exchanges (Glover and Stein, 1987), all of which are hallmarks of human cancers. Furthermore, human papillomavirus 16 (HPV-16) that causes cervical cancer is known to integrate its DNA at common fragile site FRA3B (Wilke et al., 1996). It has also been proposed that chromosome breakage at these sites may initiate the breakage-fusion-bridge cycles that lead to gene amplification and tumourigenesis (Coquelle et al., 1997). Moreover, common fragile sites are often located within or spanning tumour suppressor genes. Chromosome deletions and rearrangements within these genes, and specifically at common fragile sites, have been associated with several forms of cancer (reviewed in Durkin and Glover, 2007; Glover et al., 2005).

**1.2.2.1 Features of common fragile sites**

Common fragile sites extend over large regions of the genome, from several hundred kilobases (kb) to over 1 megabase (Mb) (Boldog et al., 1997; Paradee et al., 1996), with breaks or gaps occurring throughout these regions. There is no sequence determinant that defines common fragile sites except that they are relatively AT-rich (Arlt et al., 2002; Boldog et al., 1997; Mishmar et al., 1998; Ried et al., 2000). Unlike rare fragile sites, common fragile sites are not associated with expanded trinucleotide and minisatellite repeat motifs and are, therefore, not induced by nucleotide repeat expansion mutations (Arlt et al., 2002; Mishmar et al., 1998; Schwartz et al., 2006). Additionally, common fragile sites tend to contain more regions of high DNA flexibility compared to non-fragile regions, and it has been suggested that this could aid the formation of abnormal secondary structures that could hinder replication progression (Limongi et al., 2003; Mishmar et al., 1998; Ried et al., 2000; Zlotorynski et al., 2003). Indeed, a yeast artificial chromosome (YAC) carrying a highly flexible region of human common fragile site, FRA16D, can cause fork stalling and increase mutation rates when introduced into yeast cells (Zhang and Freudenreich, 2007). Highly repetitive sequence elements such as 'long interspersed elements' (LINEs) have also emerged as a feature of common fragile sites (Rozier et al., 2004).

Late replication seems to be a defining feature of common fragile sites as these are some of the latest regions of the genome to complete replication, with some sites remaining unreplicated in G2 (Hellman et al., 2000; Le Beau et al., 1998). This observation has lead to the suggestion that common fragile sites are inherently difficult to replicate, possibly because they readily form secondary structures that impede replication. As mentioned above, insertion of a YAC expressing a human common fragile site sequence into yeast causes replication forks to stall at this site (Zhang and Freudenreich, 2007). However, a recent study shows that common fragile site sequences inserted into ectopic sites render these regions fragile despite replicating earlier than endogenous common fragile sites (Ragland et al., 2008). This raises the possibility that late replication alone may not account for the formation of gaps and breaks at common fragile sites, but rather, instability at these sites may also be dependent on inherent sequence determinants. Indeed, not all late-replicating

regions of the genome exhibit chromosome instability. It is, therefore, likely that other factors in addition to late replication contribute to chromosome instability at common fragile sites.

**1.2.2.2 Inducers of chromosome breakage at common fragile sites**

Common fragile sites are normally stable in cultured cells. However, certain conditions are known to induce the accumulation of breaks or gaps at these sites. Common fragile sites are said to be 'expressed' when they display signs of chromosome instability. The most commonly used condition to induce fragile site expression is partial inhibition of DNA replication i.e. under conditions of thymidylate or folate stress or, more commonly, by treatment with low doses of the replication inhibitor, aphidicolin (Durkin and Glover, 2007; Lukusa and Fryns, 2008). The widely held view is that common fragile sites are regions that are inherently difficult to replicate, which renders them particularly sensitive to further inhibition of replication, which generates instability at these sites (Durkin and Glover, 2007).

Proteins involved in cell cycle checkpoints (Arlt et al., 2004; Casper et al., 2002; Durkin et al., 2006; Zhu and Weiss, 2007), in addition to proteins involved in DNA repair (Schwartz et al., 2005), have been implicated in maintaining the stability of common fragile sites. Disruption of genes involved in these processes in cells treated with aphidicolin show an increased incidence of chromosome instability at common fragile sites. However, cells deficient for the checkpoint kinase, ATR (Ataxia telangiectasia and Rad3 related), show a significant increase in common fragile site expression without the addition of aphidicolin suggesting that ATR is critical for stability of common fragile sites during normal cell divisions, as well as under conditions of replication stress (Casper et al., 2002). Consistent with this finding, cells from individuals with Seckel syndrome, a condition characterised by hypomorphic mutations in *ATR*, show increased instability at common fragile sites (Casper et al., 2004). Since the ATR pathway is required for the response to replication stress (see Section 1.9), it is presumed that common fragile sites are regions that frequently accumulate stalled replication forks and that fork collapse at

these sites in the absence of ATR leads to genome instability (Casper et al., 2002; Cimprich, 2003).

The last condition capable of inducing expression of common fragile sites is premature chromosome condensation on replicating chromosomes. Treatment of cells with Calyculin A, a phosphatase inhibitor that induces chromosome condensation at any stage in the cell cycle, induces breaks and gaps within common fragile sites, particularly on chromosomes from late S-phase and G2 cells (El Achkar et al., 2005).

### 1.2.3   Fragile sites in budding yeast

Several studies have reported the existence of similar fragile regions in yeast. Two specific regions of budding yeast chromosome III, FS1 and FS2, were shown to be hotspots for chromosome rearrangements under conditions that slow DNA replication (Lemoine et al., 2005). The preferred site of breakage within these regions seems to involve Ty retrotransposons. FS2, the more common breakpoint of the two, involves a pair of Ty elements placed in a head-to-head configuration. It has been proposed that inverted Ty elements may induce the formation of secondary structures in the DNA, which cause replication forks to stall. Resolution of these secondary structures could result in a recombinogenic DNA break. The finding that recombination between these elements and similar elements on other chromosomes can induce chromosome translocations when DNA replication is compromised suggests a similarity between these sites and common fragile sites in mammals (Lemoine et al., 2005).

Interestingly, chromosome breakage at the same FS2 site was identified independently in a genome-wide study of replication profiles of yeast strains deficient in the essential checkpoint kinases, *MEC1* or *RAD53*, that were treated with the replication inhibitor, hydroxyurea (HU) (Raveendranathan et al., 2006). This region is in close proximity to an active replication origin referred to as a compromised early origin (CEO) due to the observation that this region, which normally fires early, was not replicated efficiently in *mec1* and *rad53* mutants exposed to HU. Seventeen CEOs were identified in this study. The occurrence of

CEOs was not due to a lack of replication initiation at these sites, but rather to problems in replication elongation since replication forks arrested in close proximity to these origins, giving rise to breaks at these sites (Raveendranathan et al., 2006).

Another report shows that chromosome breakage and translocations are enriched on a region of yeast chromosome VII, referred to as the 403 E2 site (Admire et al., 2006). This region contains Ty LTR (long terminal repeats or Δ) elements as well as clusters of tRNA genes, which are known to stall replication forks. Interestingly, chromosome aberrations in this region, were observed particularly after replication stress or in the absence of an intact replication checkpoint (Admire et al., 2006).

The fact that CEO-proximal regions (including FS2) and the 403 site are particularly sensitive to replication stresses and require Mec1, the orthologue of ATR, for stability suggests that these yeast fragile sites may be mechanistically similar to common fragile sites in mammals.

**1.2.3.1 Replication Slow Zones**

Another example of budding yeast fragile site is the replication slow zone (*RSZ*), which shares many similarities with mammalian common fragile sites (Cha and Kleckner, 2002). In wild type cells, replication proceeds more slowly through *RSZs* compared to other regions on the same chromosome, suggesting that these regions are intrinsically difficult to replicate. When a temperature-sensitive allele of *MEC1* is inactivated, replication forks at the *RSZs* stall permanently and the cells eventually accumulate DNA breaks at these sites during their transition into mitosis. Breaks at *RSZs* do not arise at a specific site, but rather occur throughout these broad regions (Cha and Kleckner, 2002).

Mapping *RSZs* on chromosome III revealed that these are large regions of the yeast genome, about 10 kb in size, that occur in alternation with highly active origins of replication and coincide with sites of replication termination. However, *RSZs* are not determined by the location of these origins as altering the pattern of replication origins does not change the pattern of break formation along the chromosome (Cha and Kleckner, 2002). The latter observation suggests that *RSZs* are physically determined regions of the chromosome. Although *RSZs* often contain Ty insertion

hotspots and/or tRNA genes, there is no known sequence or chromosomal determinant that clearly defines a *RSZs* (Cha and Kleckner, 2002).

Like mammalian common fragile sites, chromosome breakage at *RSZs* follows an aberrant replication program and is influenced by Mec1 activity, although the specific role that Mec1 plays at these sites remains unclear. Forks stalled at *RSZs* do not immediately collapse as is expected from checkpoint-deficient cells treated with replication inhibitors (Section 1.9.3). Instead, replication forks at *RSZs* undergo a period of prolonged pausing in which forks are maintained in a replication-competent manner, as cells can retain viability if returned to permissive temperatures within this period. After the period of replication pausing, and some time during the transition to mitosis, the forks stalled at *RSZs* are converted into chromosome breaks (Cha and Kleckner, 2002). The nature of the event that triggers this transformation remains unknown.

Despite numerous studies into common fragile sites in both mammalian and yeast systems, relatively little is known about these chromosomal regions and the mechanism of their expression. The molecular basis, at the primary sequence level, that renders these regions prone to breakage, as well as the precise mechanism that triggers chromosome breakage at these sites, remain unknown. However, it is clear that the underlying phenomenon of chromosome instability at these sites in both yeast and mammals is a problem in DNA replication. It appears that, at common fragile sites in mammals and *RSZs* in yeast, this defect is manifested at later stages in the cell cycle and that checkpoint activity plays a role in their stability. The next part of this chapter will, therefore, survey the events of the eukaryotic cell cycle that are relevant to understanding the processes that culminate in the expression of fragile sites.

## 1.3   Overview of the eukaryotic cell cycle

A basic and fundamental function of a cell is to proliferate.  Proliferation of a cell depends on accurate replication of its genetic material followed by segregation of these duplicated chromosomes to generate two genetically identical daughter cells. These events must be executed in a coordinated and sequential manner to ensure that the genetic information is transmitted to its progeny with high fidelity. Inability to coordinate this highly ordered sequence of events compromises cell viability and genome stability; in multicellular organisms this can lead to tumourigenesis (Lengauer et al., 1998). Although some features of the cell cycle can vary greatly between organisms and/or cell types, the basic organization of the cycle and its control system are essentially the same in all eukaryotic cells. As a result, detailed genetic studies of the budding yeast, *Saccharomyces cerevisiae* (*S. cerevisiae*), and the fission yeast, *Schizosaccharomyces pombe* (*S. pombe*), have proved instrumental in understanding how the eukaryotic cell cycle progresses in yeast as well as in higher eukaryotes (Hartwell et al., 1970; Nurse and Thuriaux, 1980).

The entire cell cycle can be divided into four sequential, temporally and biochemically separate phases: G1 (gap 1), S (DNA synthesis), G2 (gap 2), and M (mitosis) (Hartwell, 1974). Although key cell cycle regulatory events do not always correspond to the boundaries between these phases (Nasmyth, 1996), DNA replication is generally confined to S-phase, whereas nuclear division (i.e. chromosome segregation) is restricted to M-phase. The gap phases, G1 and G2, serve to provide time for the cell to grow and prepare for chromosome duplication or segregation. Once the chromosomes have segregated, the cell/cytoplasm is divided in a process called cytokinesis to give rise to two daughter cells with identical genetic content as the mother cell (Nasmyth, 1996).

Progression through the different stages of the cell cycle is driven by cyclin-dependent kinases (CDKs), whose activity is controlled by periodic transcription of the regulatory cyclin subunits (Mendenhall and Hodge, 1998). These protein complexes exert control through their kinase activities, which are switched on or off at particular points in the cycle. In budding yeast, the major CDK is Cdc28, which is

homologous to *S. pombe* Cdc2 and human CDK1. CDK activity is also negatively controlled by CDK inhibitors (CDKI) (Mendenhall and Hodge, 1998). In yeast, *SIC1* encodes the most important CDKI, which is involved in down-regulating the mitotic CDK-cyclin complex, Cdc28-Clb2, at the end of mitosis (Schwob et al., 1994).

As chromosome breakage at *RSZs* involves defects in DNA replication (S-phase) and a second undetermined event that occurs during the G2/M transition, the following sections will focus on events that take place during these two stages of the cell cycle.

## 1.4   Chromosome duplication

### 1.4.1   Origins of DNA replication

Contrary to replication in prokaryotes, which replicate their small, circular chromosomes from a single origin of replication, eukaryotes from yeast to mammals initiate replication from a large number replication origins along their chromosomes (Toone et al., 1997). This ensures that accurate duplication of the DNA is completed in the right amount of time. However, coordinating replication initiation from multiple origins requires a complex and highly ordered system. The first step in defining replication origins is the assembly of a pre-replicative complex (pre-RC) at the origins in G1. During S-phase, pre-RCs initiate replication by promoting origin unwinding and facilitating the recruitment of the replicative polymerases.

The *S. cerevisiae* genome contains about 300 to 400 origins of replication, all of which comprise DNA sequences, a few hundred of base pairs in length, called autonomously replicating sequence (ARS) elements (Toone et al., 1997). These elements were initially shown to allow replication and stable maintenance of a plasmid (Newlon and Theis, 1993). However, not all ARS sequences in the genome function as replication origins, even if they support the replication of a plasmid. All ARS elements contain an 11 bp ARS consensus sequence (ACS) to which the six subunit origin recognition complex (ORC), a component of the pre-RC, can bind (Bell and Stillman, 1992). In *S. cerevisiae*, ORC is bound to replication origins throughout the cell cycle (Liang and Stillman, 1997).

The ORC is highly conserved among all eukaryotes from yeast to humans; however, identification of ARS sequences in other eukaryotes has proved elusive, suggesting that recruitment of pre-RC components to replication origins may involve other mechanisms in these organisms. For example, in *S. pombe*, AT-rich regions specify replication origins, which are bound by AT hook motifs in the *S. pombe* ORC (Chuang and Kelly, 1999). In humans, any sequence is competent for replication initiation (Schaarschmidt et al., 2004), and in *Xenopus* embryonic systems, initiation is spaced roughly 10 kb apart, irrespective of DNA sequence (Blow et al., 2001; Gilbert, 2001). It has been proposed that the absence of sequence-specification for defining replication origins in these organisms may allow faster initiation of replication and may allow the genome to sustain genetic alterations without compromising replication origins (Gilbert, 2001).

Although the mechanism of ORC recruitment to replication origins differs between eukaryotes, the subsequent steps in pre-RC assembly after ORC binding are conserved among all eukaryotes (Takeda and Dutta, 2005).

## 1.4.2   Initiation of DNA replication

### 1.4.2.1 Assembling the pre-replicative complex (pre-RC)

The first step in the initiation of DNA replication is the highly ordered assembly of the pre-RC on the origins of replication. This occurs in G1 and is regulated by CDK activity (Piatti et al., 1996). After ORC has bound to replication origins within the eukaryotic genome, it directs the recruitment of two other initiation factors, Cdc6 and Cdt1. These, in turn, load the putative replicative helicase, the MCM2-7 complex, onto the origins (Toone et al., 1997). The primary requirement for ORC, Cdc6, and Cdt1 is to recruit MCM2-7 as these proteins become dispensable for initiation after MCM2-7 is loaded (Donovan et al., 1997; Harvey and Newport, 2003).

Formation of the pre-RC, and crucially loading of the Mcm2-7 complex, in G1 'licenses' the origin for initiation. The cell must ensure that replication is licensed for initiation once during each cell cycle as repeated rounds of replication initiation within one cell cycle result in chromosome breakage and genome instability (Blow

and Hodgson, 2002; Lengauer et al., 1998; Nishitani and Lygerou, 2002). Licensing is regulated by CDK activity (Piatti et al., 1996). The increase in CDK activity at the onset of S-phase activates factors required for origin firing and also inhibits the formation of new pre-RCs at replication origins. CDK activity remains high until cyclins are degraded at the end of mitosis. Therefore, CDK activity is at its lowest in early G1 enabling origins to be licensed for replication once again (Takeda and Dutta, 2005). In higher eukaryotes, Geminin, a protein that blocks Mcm 2-7 loading by binding Cdt1, is involved in a second mechanism of preventing re-licensing and re-replication (Maiorano et al., 2004; Saxena et al., 2004; Takeda and Dutta, 2005). Geminin is cell cycle regulated and only binds Cdt1 during S-phase, G2, and early mitosis; so the inhibition of licensing by Geminin is specific to these phases. During mitosis, Geminin is ubiquitinated and either degraded or inactivated allowing origins to be licensed again in G1 (Li and Blow, 2004; Nishitani and Lygerou, 2002).

## 1.4.2.2 Spatial and temporal regulation of origin firing

Although each origin with an assembled pre-RC is competent for replication initiation, only a subset of origins actually fire during S-phase (Anglana et al., 2003; Santocanale and Diffley, 1996). It has been proposed that these extra pre-RCs serve as 'backup' origins, which become activated and facilitate replication if some pre-RCs fail to fire (Anglana et al., 2003; Santocanale and Diffley, 1996; Vujcic et al., 1999). Replication initiation at origins also inhibits the activation of nearby origins, which become passively replicated (Anglana et al., 2003; Brewer and Fangman, 1994; Marahrens and Stillman, 1992). Therefore, initiation of replication from an origin is influenced by the activity of surrounding replication origins.

Replication initiation is also regulated temporally, resulting in a subset of origins that fire early in S-phase and others that fire later in S-phase. The decision as to which origins will replicate early or late is established in G1 (Raghuraman et al., 1997) and may involve factors such as nucleotide availability (Anglana et al., 2003). In addition, the surrounding chromatin structure also plays a role in temporal regulation of origin firing. Early replication origins are associated with the actively transcribed euchromatic regions, while late-replicating origins occur within transcriptionally silent heterochromatic regions such as telomeres (Friedman et al., 1997; Reynolds et

al., 1989). In addition, insertion of an early origin into a heterochromatic region is enough to convert it to a late-firing origin (Friedman et al., 1996), and disruption of heterochromatin allows late origins to fire earlier (Stevenson and Gottschling, 1999). This correlation may be attributed to hyperacetylation of histones in euchromatic regions, making these regions more accessible to replication factors (Vogelauer et al., 2002).

There are also differences in the efficiency of origin firing; some origins fire during every cell cycle, whereas others fire less frequently (Raghuraman et al., 2001). However, how the selection of origins that fire in any one cell cycle is determined remains unclear.

### 1.4.2.3 Initiation of replication

The next step in replication initiation is the conversion of pre-RCs into active replication forks (Figure 1.1). This involves unwinding of the DNA at the replication origins, stabilisation of the single-stranded DNA generated by the unwinding, and loading of the replicative polymerases (Takeda and Dutta, 2005). These events are regulated by the action of two kinases, CDK (Tanaka et al., 2007) and the Dbf4-dependent kinase (DDK) (Yabuuchi et al., 2006). At this stage, replication factors are temporally regulated and associate with each replication origin as it becomes activated during S-phase, suggesting that the mechanisms influencing origin selection and timing may also regulate targeting of these kinases to the origin (Takeda and Dutta, 2005).

The replication initiation factors recruited to a pre-RC include Mcm10, Cdc45, Sld2, Sdl3, Dpb11, and the GINS complex (Forsburg, 2004). Together these proteins constitute the initiation complex, the assembly of which is controlled by CDK activity (Tanaka et al., 2007; Yabuuchi et al., 2006).

After assembling the initiation complex, the replication machinery must be loaded at the origin. This requires the initial unwinding of the DNA duplex at the origin, a process governed by Cdc7-Dbf4 (DDK) activity. DDK phosphorylates Mcm2-7 helicase and may play a role in activating this putative helicase (Takeda and Dutta,

2005). The single-stranded DNA (ssDNA) formed as the origin is unwound is stabilised by association of the ssDNA binding protein, RPA, which further stimulates origin unwinding and promotes the association of DNA polymerase $\alpha$ (pol $\alpha$) (Bell and Dutta, 2002).

Pol $\alpha$ is the first polymerase to be recruited at the unwound replication origin. It is also the only polymerase capable of initiating DNA synthesis *de novo* on single-stranded DNA and is therefore required to generate short RNA primers for both leading and lagging strand synthesis (Bell and Dutta, 2002). After primer synthesis, DNA pol $\alpha$ is replaced with DNA pol $\delta$ and/or DNA pol $\varepsilon$, which display greater processivity and have proofreading exonuclease activity. Both DNA pol $\delta$ and DNA pol $\varepsilon$ associate with the ring-shaped processivity factor called proliferating cell nuclear antigen (PCNA), which encircles the DNA and topologically links the polymerases to the DNA in order to ensure processive DNA synthesis (Jonsson and Hubscher, 1997; Mossi and Hubscher, 1998). PCNA is loaded onto at the replication origin by the clamp loader, RFC1-5 (Mossi and Hubscher, 1998). Experiments with mutants of DNA pol $\delta$ and DNA pol $\varepsilon$ that are defective in proofreading accumulate mismatches on different DNA strands suggesting that these polymerases are responsible for synthesising opposite DNA strands. However, studies in *Xenopus* extracts suggest that DNA pol $\delta$ is the major replicative polymerase and can substitute for DNA pol $\varepsilon$ function (Fukui et al., 2004).

Figure 1.1    Building the replication fork

**1.4.2.4 The replication fork**

The multi-protein replication complex consisting of the DNA polymerases, pol ε and pol δ, and their accessory proteins, PCNA and RFC, is referred to as the replisome (Baker and Bell, 1998). The replicative polymerases can only catalyse DNA synthesis in the 5'-3' direction. However, owing to the opposite polarity of the two template DNA strands, only the 5'-3' leading strand can be synthesised in a continuous manner, whereas the other 3'-5' lagging strand must be synthesised in short 5'-3' fragments known as Okazaki fragments. These fragments are subsequently ligated together to form a continuous DNA strand (Waga and Stillman, 1998).

Firing of the replication origin results in two replication forks that synthesise new DNA strands bi-directionally away from the replication origin. The current thinking, now confirmed in yeast, is that several replisomes are attached to each other and remain stationary throughout the course of DNA replication, generating the so-called 'replication factories' through which the DNA template is fed. In yeast, replication factories can be observed as nuclear foci containing replisome proteins (Kitamura et al., 2006).

**1.4.3   Progression of the replication fork**

During DNA replication, the advancing replication fork faces various obstacles to its progression along the chromosomes. In the presence of DNA damage on the DNA template, or if the production of nucleotides is inhibited, the replicative helicase progresses much more slowly, so that the fork is said to have 'stalled' (Katou et al., 2003; Tercero and Diffley, 2001). Forks can also stall in response to agents that inhibit polymerases but that allow the helicase to continue unwinding the parental duplex (Pacek et al., 2006; Walter and Newport, 2000). Under such conditions, eukaryotic cells activate checkpoint kinases that play essential roles in preventing irreversible collapse of the stalled forks, which would otherwise be fatal for the cell (Lopes et al., 2001; Tercero and Diffley, 2001).

Forks also pause during the normal process of chromosome replication at genetically specified pause sites, which are scattered throughout the genome. The best-characterized programmed pause site in budding yeast is the replication fork barrier (RFB) of ribosomal DNA (rDNA). This element is found in many other species including fission yeast, pea, mouse, and human where it also causes replication forks to pause (Lambert and Carr, 2005). In budding yeast, replication forks at the rDNA locus stall when they encounter a non-histone protein called Fob1, which is tightly bound to the RFB (Kobayashi and Horiuchi, 1996).

Other examples of natural programmed pause sites in yeast include centromeres, telomeres, inactive origins, and the mating type loci (MAT) (Greenfeder and Newlon, 1992; Ivessa et al., 2003; Ivessa et al., 2002; Wang et al., 2001). Replication pausing also occurs at tRNA genes that are transcribed in an opposing direction to the replicative polymerase (Deshpande and Newlon, 1996; Prado and Aguilera, 2005). In all these cases, including the RFB at rDNA, stable fork stalling is an active process that requires the action of the replisome components and checkpoint factors Tof1 and Csm3 (Wang et al., 2001). Release from fork arrest at these sites involves the Rrm3 helicase, which interacts with PCNA and whose helicase activity progresses in the 3'-5' direction (Schmidt et al., 2002). Thus, Rrm3 associates with the replication fork and displaces bound proteins such as Fob1, thereby enabling the fork to progress beyond these sites (Azvolinsky et al., 2006; Calzada et al., 2005). Rrm3 has been described as a "sweepase" that is counteracted by the fork pausing actions of Tof1 and Csm3 (Mohanty et al., 2006).

Replication forks can also stall at different types of DNA structure (Hyrien, 2000). Palindromes and inverted repeats in the primary DNA sequence can stall replication forks in all organisms ranging from *E. coli* to yeast and humans (Akgun et al., 1997; Voineagu et al., 2008). During replication, ssDNA containing an inverted repeat is generated as the helicase unwinds the region. The bases of the inverted repeats on the ssDNA can then pair together to form secondary structures such as DNA hairpins and cruciform structures. Since ssDNA is more prevalent on the lagging strand template to allow priming of the Okazaki fragments, the formation of hairpins is likely to be favoured on this strand (Mirkin, 2006). These structures have been

shown to hinder the progression of the replicative polymerase and, in yeast, require Tof1 and another replisome component, Mrc1, and to counteract this DNA structure-mediated stalling (Voineagu et al., 2008).

In addition to the above, common fragile sites are thought to constitute areas of the chromosome that are intrinsically difficult to replicate (Durkin and Glover, 2007). Similarly, *RSZs* are naturally occurring regions of the chromosome that slow fork progression even in normal, unchallenged conditions (Cha and Kleckner, 2002). As is the case for mammalian common fragile sites, the cause of replication slowing at *RSZs* is also unclear; however, there is some indication that dNTP availability may play a role (Cha and Kleckner, 2002).

### 1.4.4   Cohesion

The two replicated sister chromatids must be held together in order to ensure proper segregation of each sister chromatid to each daughter cell during mitosis. The physical attachment of the two sister chromatids is also important for the formation of the bipolar mitotic spindle as it provides a force to oppose the outward pulling force of the mitotic spindle (Michaelis et al., 1997; Tanaka et al., 2000).

Cohesion of the two sister chromatids is mediated by a multiprotein complex called cohesin. The evolutionarily conserved four-member cohesin complex is composed of the SMC (structural maintenance of chromosomes) proteins, Smc1 and Smc3, and the non-SMC proteins, Scc1/Mcd1/Rad21 and Scc3/Irr1 (Guacci et al., 1997; Michaelis et al., 1997). Cohesin is loaded onto the unreplicated DNA in G1, with the help of Scc2 and Scc4 (Ciosk et al., 2000). However, establishment of a physical connection between the duplicated sister chromatids occurs during DNA replication (Uhlmann and Nasmyth, 1998). The mechanism by which cohesion is established is still unclear; one model suggests that the ring-like cohesin structure encompasses the DNA that is replicated through this ring, whereas another model proposes that each sister chromatid is encircled by a cohesin ring and that sisters chromatids are together by interaction between the two cohesin rings (Huang et al., 2005).

The connection between the two sister chromatids is maintained until mitosis when cohesin is dissolved from the DNA, enabling the two sister chromatids to segregate to opposite poles of the cell (Nasmyth et al., 2000).

### 1.4.5   Replication termination

As replication progresses, the unwinding of the two DNA strands can generate positive supercoiling in front of the replication fork (Schvartzman and Stasiak, 2004). Therefore, topoisomerases such as the type IB topoisomerase (Top1 in budding yeast, sometimes called topo I in other eukaryotes) and the type II topoisomerase, (Top2 in yeast, also referred to as topo II in other eukaryotes) can act as 'swivelases' to relax the supercoils produced during the replication process in order to aid progression of the replication fork (Bermejo et al., 2007; Wang, 2002). Although Top1 and Top2 are used interchangeably during DNA replication, Top1 is considered the main player in the removal of supercoils during DNA replication (Bermejo et al., 2007). However, when two replication forks converge at the completion of DNA replication, the unreplicated region in front of the forks is likely to become too short for topoisomerase I to act on. By allowing the replisomes to rotate, topological stress produced ahead of the converging forks can be transferred behind the forks, generating precatenanes that, upon the completion of replication, become multipley catenated regions that physically link the two sister chromatids (Lucas et al., 2001; Wang, 2002).

Accurate chromosome segregation during mitosis requires the complete removal of catenations linking of the two intertwined strands of DNA. Separation of the intertwined sister chromatids depends on the unique function of the type II topoisomerase in generating a break on both strands of the DNA (Champoux, 2001). Only one type II topoisomerase, Top2, is expressed in yeast, whereas two isoforms of the enzyme act in mammalian cells: topo II α and topo II β, with the former playing the dominant role in decatenation (Champoux, 2001). At the onset of mitosis, Top2 generates a DNA double strand break (DSB) on one sister molecule and passes the other sister through the break, thereby untangling the catenated sister chromatids and enabling their segregation to the daughter cells (Holm et al., 1989;

Lucas et al., 2001). In the absence of Top2, yeast chromosomes are fully duplicated, but the inability to decatenate chromosomes results in incomplete segregation of sister chromatids and chromosome breakage (DiNardo et al., 1984; Holm et al., 1989; Spell and Holm, 1994; Uemura et al., 1987).

On chromosome III, *RSZs* tend to coincide with sites of replication termination raising the possibility that replication termination and decatenation may contribute to chromosome breakage at these sites.

## 1.5  Mitosis

Mitosis is the process by which the cell segregates its duplicated chromosomes to opposite poles of the cell. Mitosis is divided into four main stages: prophase, metaphase, anaphase, and telophase (reviewed by Craig and Choo, 2005). In most eukaryotes, prophase is normally identified by the breakdown of the nuclear envelope (this stage is sometimes called prometaphase); however, yeast cells undergo closed mitoses in which the nuclear membrane stays intact and divides with the cytoplasm at cytokinesis. At the onset of prophase, the chromatin begins to condense, culminating in the condensed mitotic chromosome by the time cells enter metaphase. Although chromosomes in metaphase were originally thought to be in their most compact state, time-lapse studies of rodent chromosomes shows that compaction process continues after metaphase until late anaphase (Mora-Bermudez et al., 2007). The condensation process reduces the volume of the chromosomes to facilitate the segregation of sister chromatids. Spindle microtubules emanating form the duplicated centrosomes (spindle pole bodies or SPBs in yeast) find and capture the chromosomes. At metaphase, chromosomes convene along the metaphase plate. During anaphase, the sister chromatids of each chromosome are segregated towards opposite poles of the cell by the shortening of spindle microtubules. Telophase is the reversal of prophase and prometaphase events, for example chromosomes decondense into chromatin and, in higher eukaryotes, the nuclear envelope is regenerated.

### 1.5.1   Chromosome condensation

In vertebrate cells, chromosomes become individualised during G2 resulting in unseparated sister chromatid cores (Gimenez-Abian et al., 2000). Resolution of the sister chromatid chores into two cytologically distinct sister chromatid cores attached by the centromere occurs in prometaphase, with the final stages of chromosome condensation taking place in metaphase (Gimenez-Abian et al., 1995; Losada et al., 2002). The early stages of chromosome condensation including chromosome individualisation and sister chromatid resolution require the catalytic activity of topoisomerase II (Gimenez-Abian et al., 2000; Gimenez-Abian et al., 1995). Topo II decatenates strands of DNA among different chromosomes giving rise to the individualised chromosomes, whereas topo II-dependent decatenation of DNA strands between the sister chromatids allows their resolution in prometaphase. The catalytic activity of topo II is also involved in linear chromosome compaction at metaphase (Swedlow and Hirano, 2003). Studies in *Xenopus* suggest that topo II is required to establish condensation, whereby it couples condensation to DNA replication, however this activity is dispensable for maintaining chromosomes in the condensed state (Cuvier and Hirano, 2003).

In addition to topo II-dependent sister chromatid resolution during prometaphase, cohesin is removed from the chromosome arms but not from the centromeric regions of chromosomes (Darwiche et al., 1999; Schmiesing et al., 1998; Sumara et al., 2000), and an evolutionarily conserved multi-subunit complex called condensin is loaded onto the chromosome to facilitate its compaction (Losada et al., 2002). The condensin complex is essential for proper chromosome condensation and is composed of two SMC proteins (SMC2/Smc2 and SMC4/Smc4) as well as three non-SMC subunits (CAP-D2/Ycs4, CAP-G/Ycg1, and CAP-H/Brn1) (Hagstrom et al., 2002; Hirano et al., 1997; Kimura and Hirano, 2000; Lavoie et al., 2002; Saka et al., 1994). In yeast, proper loading of condensin and condensation depends on sister chromatid cohesion; however, this is not the case in other eukaryotes (Guacci et al., 1997; Losada and Hirano, 2001). Condensin activity may be regulated by the mitotic CDK. Phosphorylation of the condensin complex by the Cdc2-cyclin B CDK is thought to activate condensin in frogs (Kimura et al., 1998) or mobilise it to

chromatin in fission yeast (Sutani et al., 1999). In contrast, the *S. cerevisiae* CDK, Cdc28, does not seem to regulate condensation in this organism. Instead, the aurora B kinase, Ipl1, plays important roles in maintaining chromosomes in a condensed state in budding yeast (Lavoie et al., 2004; Vas et al., 2007). Aurora B is also involved in regulating condensation in other eukaryotes (Gadea and Ruderman, 2005; Lipp et al., 2007; Mora-Bermudez et al., 2007). Although the exact process by which condensin mediates condensation remains speculative, its *in vitro* biochemical properties suggest condensin may function as an intra-molecular DNA cross-linker by binding two segments within a single chromosome to facilitate its folding (Kimura and Hirano, 1997; Kimura et al., 1999).

Another protein implicated in chromosome condensation is histone H3. Phosphorylation of histone H3 on conserved residues (serine 10, serine 28, and threonine 11) correlates with chromosome condensation in a wide variety of organisms from yeast to human (Goto et al., 1999; Hendzel et al., 1997; Hsu et al., 2000; Preuss et al., 2003; Wei et al., 1998). Phosphorylation at serine 10 is dependent on the aurora B kinase (Ipl1 in yeast) that plays important roles in mitotic chromosome dynamics (de la Barre et al., 2000; Giet and Glover, 2001; Hsu et al., 2000) and is counterbalanced by the activity of type1 phosphatases (PP1) (Hsu et al., 2000; Murnion et al., 2001). While phosphorylation of this residue is essential for condensation in some organisms (Van Hooser et al., 1998; Wei et al., 1998), *S. cerevisiae* strains in which the serine 10 residue of histone H3 has been replaced with a non-phosphorylatable alanine residue show wild type cell cycle progression, suggesting that this modification is dispensable for chromosome condensation in budding yeast (Hsu et al., 2000). However, it has been proposed that phosphorylation of histone H2B may substitute for histone H3 in this mutant (Hsu et al., 2000). Models for the function of histone H3 phosphorylation in mitosis include labelling the chromosome to indicate that they are ready to undergo anaphase, recruiting condensin and/or topo II, or indirectly decreasing the repulsion between nucleosomes thereby facilitating their compaction (Prigent and Dimitrov, 2003). However, the precise role that histone H3 phosphorylation plays in condensation is still unclear.

In *S. cerevisiae*, chromosome condensation is not as extensive as in other eukaryotes; chromosomes in this organism have a compaction ratio, defined as the ratio of DNA length to metaphase chromosome length, of 160 compared to the compaction ratio of 10,000- 20,000 detected in metazoan cells (Guacci et al., 1994; Li et al., 1998; Losada and Hirano, 2001). In addition, chromosome individualisation, sister chromatid resolution, and removal of cohesin from chromosome arms are not detectable in this organism (Losada and Hirano, 2001; Vas et al., 2007). However, inactivation of either Top2 or condensin subunits in *S. cerevisiae* results in defects in chromosome condensation as well as chromosome segregation suggesting that the mechanism by which chromosomes are compacted during mitosis is conserved among all eukaryotes (Freeman et al., 2000; Lavoie et al., 2002; Lavoie et al., 2000; Vas et al., 2007).

Inducing condensation on S-phase chromosomes leads to fragmentation of the chromosomes (Gimenez-Abian et al., 1995) and, as mentioned above, causes common fragile site expression in human lymphocytes (El Achkar et al., 2005; Section 1.2.2.2). However, whether condensation is the actual mechanism by which chromosomes break at fragile sites under normal conditions and whether it is involved in chromosome breakage at *RSZs* remains unknown.

### 1.5.2   Anaphase onset

As mentioned above, the large majority of cohesin is removed from chromosome arms during pro-metaphase in vertebrate cells. This 'prophase pathway' of cohesin removal depends on the Polo-like and the aurora B kinases, which presumably phosphorylate cohesin, and does not involve cleavage of cohesin (Gimenez-Abian et al., 2004; Hauf et al., 2005; Losada et al., 2002; Sumara et al., 2002). However, a subset of cohesin at the centromere is protected from removal by a conserved protein kinase binding protein, Sgo1 (shugoshin), and mediates the cohesion of the two sister chromatids until the onset of anaphase (Kitajima et al., 2004; McGuinness et al., 2005). Sgo1 also protects a small fraction of arm cohesin from dissociation by the prophase pathway (Nakajima et al., 2007). Residual arm cohesins and the centromeric cohesins are removed by another mechanism referred to as the 'separase

pathway' described below (Hauf et al., 2001; Nakajima et al., 2007; Waizenegger et al., 2000). The separase pathway is responsible for the removal of all cohesins in *S. cerevisiae*.

 In all eukaryotes, anaphase onset is defined by the dissolution of centromeric cohesion (Figure 1.2). This is accomplished by the cleavage of the Scc1 subunit of the cohesin complex by the protease, Esp1 (separase) (Hauf et al., 2001; Uhlmann et al., 2000). Phosphorylation of Scc1 by Cdc5 Polo-like kinase is necessary for efficient cleavage of Scc1 by Esp1 (Alexandru et al., 2001). Prior to the onset of anaphase, Esp1 (separase) is maintained in an inactive form by the anaphase inhibitor, Pds1 (securin). Activation of Esp1 requires ubiquitination of Pds1 by the anaphase promoting complex/cyclosome (APC) followed by proteosome-mediated degradation of Pds1 (Ciosk et al., 1998).  Interaction between APC and its specificity factor, Cdc20, targets APC to Pds1. Degradation of Pds1 allows the release and activation of Esp1, which in turn cleaves Scc1 resulting in complete separation of the sister chromatids. Each sister chromatid is now free to segregate to opposite poles of the cell during anaphase (Ciosk et al., 1998; Uhlmann et al., 1999; Uhlmann et al., 2000).

Anaphase, or rather, the pulling force of the mitotic spindle exerted on the chromosome has been implicated in chromosome breakage.  For instance, yeast cells containing dicentric chromosomes, where each centromere is attached to spindles from opposite poles, exhibit elevated levels of chromosome rearrangements, suggesting that chromosomes stretched between the two poles of the cell during anaphase may eventually break (Janson and Tran, 2008). In addition, Mec1-deficient cells that have undergone nuclear division with incompletely segregated chromosomes have been shown to accumulate DNA breaks (Krishnan et al., 2004). Furthermore, chromosome breakage at *RSZs* is prevented by spindle inhibitors (R. Cha, unpublished results). These considerations raise the possibility that chromosome breakage at *RSZs* may be instigated by the spindle force on incompletely replicated chromosomes.

Figure 1.2      Regulation of the metaphase-anaphase transition

### 1.5.3   Exit from Mitosis

In order to exit mitosis and enter the subsequent G1, all the processes that were executed to allow the cell to progress to mitosis must essentially be reversed. Since cell cycle progression is mainly governed by CDK activity, the major step in exiting mitosis involves inactivating the CDK. This is accomplished by up-regulation of the CDK inhibitor (Sic1 in yeast) (Knapp et al., 1996), and by destruction of the mitotic cyclin (Clb2 in yeast) (Schwab et al., 1997). In budding yeast, the central event in both pathways is the activation of the phosphatase, Cdc14, which can then trigger the dephosphorylation of CDK substrates (Visintin et al., 1998).

Throughout the earlier stages of the cell cycle Cdc14 is sequestered in the nucleolus by its interaction with Cfi1/Net1 (Visintin et al., 1999). During early anaphase, both Cdc14 and Net1 are phosphorylated, allowing release of Cdc14 from the nucleolus so that it can diffuse into the nucleus and cytoplasm where it can dephosphorylate its targets (Visintin et al., 2003). Release of Cdc14 from the nucleolus requires the concerted actions of Esp1, Slk19, Spo12, and Cdc5, which collectively constitute the Cdc fourteen early anaphase release (FEAR) network (Stegmeier et al., 2004). The role of Esp1 in the FEAR network is distinct from its function in cohesin cleavage at metaphase (Sullivan and Uhlmann, 2003).  The FEAR network governs processes that are important for successful anaphase including stabilisation of the anaphase spindle, positioning of the anaphase nucleus, and segregation of rDNA (D'Amours and Amon, 2004).

Release of Cdc14 from the nucleolus by the FEAR network is not sufficient for its full activation, in part, because Cdc14 can dephosphorylate itself and Net1 allowing it to re-enter the nucleolus. Maintenance of Cdc14 activity, therefore, requires another set of proteins that form the mitotic exit network (MEN) (Stegmeier and Amon, 2004). Components of the MEN include Tem1, Lte1, the Cdc15 kinase, and the Dbf2-Mob1 kinase. Mutations in these proteins allow cells to undergo normal anaphase; however, Cdc14 activity decreases prematurely resulting in arrest of the cell cycle at the end of anaphase (Stegmeier et al., 2002).  Activation of Tem1 by

Lte1 results in the activation of Cdc15, which in turn activates the Dbf2-Mob1 kinase, the downstream target of the MEN. The Dbf2/Mob1 kinase probably sustains Cdc14 activity by phosphorylating Net1, repelling it from Cdc14 (Stegmeier and Amon, 2004).

The MEN-dependent activation of Cdc14 enables the dephosphorylation of other CDK targets such as Sic1, the transcription factor Swi5, and Cdh1, the second substrate specificity factor for APC. Phosphorylated Sic1 is targeted for ubiquitin-mediated proteolysis, so removal of this phosphorylation by Cdc14 increases Sic1 levels in the cell (Verma et al., 1997; Visintin et al., 1998). Dephosphorylation of both Swi5 and Cdh1 allows these proteins to be imported into the nucleus where they can perform their respective functions (Jaquenoud et al., 2002; Moll et al., 1991). Swi5 is the transcription factor for *SIC1* and, by increasing Sic1 levels, contributes to the overall inhibition of CDK by Sic1 (Knapp et al., 1996; Toyn et al., 1997). Destruction of the mitotic cyclin Clb2 begins at the onset of anaphase by APC$^{Cdc20}$ (Baumer et al., 2000; Yeong et al., 2000). However, a certain subpopulation of Clb2 remains stable, presumably to allow certain telophase events. Complete destruction of Clb2 at the end of telophase requires the interaction of APC with dephosphorylated Cdh1 (Yeong et al., 2000). APC$^{Cdh1}$ activity also contributes to spindle disassembly (Zachariae and Nasmyth, 1999).

The up-regulation of Sic1 and the destruction of Clb2 culminate in the switching off of CDK activity. Low CDK activity enables the formation of pre-RCs at replication origins, permits the licensing of new bud formation, and allows chromosomes to decondense (Haase et al., 2001; Lew and Reed, 1993; Noton and Diffley, 2000; Zachariae and Nasmyth, 1999). CDK inactivation also triggers cytokinesis, the final stage in the cell cycle (Balasubramanian et al., 2000; Field et al., 1999; Figure 1.3).

Figure 1.3    Regulation of mitotic exit and cytokinesis by FEAR and MEN pathways

## 1.6  Cytokinesis

Cytokinesis is the process by which the cytoplasm of a eukaryotic cell is divided to form two daughter cells. In budding yeast, cytokinesis occurs at the bud neck, and involves two ring structures, the septin ring, and the actomyosin ring. Septins are characterised by a GTP-binding domain that is conserved from yeast to man, and their ability to form filaments (Douglas et al., 2005; Lippincott et al., 2001). Septins localise to a broad region around the bud neck in late G1 and remain throughout the rest of the cell cycle (Lippincott et al., 2001). The septin ring is thought to create a scaffold to anchor the actomyosin ring at the bud neck (Douglas et al., 2005; Lippincott and Li, 1998).

In contrast to septin ring formation, the actomyosin ring covers a narrower region of the bud neck and assembles in stages. First, the myosin II heavy chain, Myo1, and its regulatory light chain, Mlc2, are recruited to the ring early in the cell cycle, concomitantly with bud emergence and immediately after the appearance of the septin ring (Balasubramanian et al., 2004). Other components of the actomyosin ring include Mlc1, the essential myosin II light chain, and Hof1/Cyk2, and are recruited during S-phase or the S/G2 transition (Balasubramanian et al., 2004). This is followed by recruitment of the actin ring in late anaphase. This step requires the IQGAP-like protein, Iqg1/Cyk1, and is dependent on the function of some MEN components (Balasubramanian et al., 2004; Frenz et al., 2000). Thus, although many components of the actomyosin ring are recruited earlier in the cell cycle, a functional actomyosin ring only forms during late anaphase, after sister chromatids have properly segregated (Balasubramanian et al., 2004).

Cytokinesis occurs in two stages. First, the septin ring divides into two separate rings. Secondly, the actomyosin ring, which localises between these two septin rings, undergoes constriction (Lippincott et al., 2001). A growing body of evidence suggests that the MEN network may regulate cytokinesis. All MEN proteins localise to the SPB from S/G2 until anaphase, when some MEN components translocate to the bud neck, signifying a role in cytokinesis (Simanis, 2003). In addition, overexpression of *SIC1* is able to rescue the mitotic exit defects of MEN mutants but

not their cytokinesis defects, indicating a separate role for MEN in regulating cytokinesis (Hwa Lim et al., 2003). Although *MEN* mutants are capable of forming an actomyosin ring, septum formation is defective in these mutants (Lippincott et al., 2001). As septum formation affects actomyosin ring contraction, the actomyosin ring is unable to constrict efficiently in these mutants, resulting in a cell separation defect (Lippincott et al., 2001). It has therefore been proposed that the MEN may regulate the splitting of the septin ring, which promotes actomyosin ring contraction (Lippincott et al., 2001).

Cytokinesis has also been implicated in the formation of DNA breaks, particularly on chromosomes that have not completely segregated to the opposite poles of the cells. Yeast cells harbouring mutations in Top2 cannot decatenate the sister chromatids and the entangled chromosomes are unable to segregate properly. It is thought that cytokinesis through chromosomes remaining in the plane of division may generate lethal breaks in these chromosomes (Baxter and Diffley, 2008; DiNardo et al., 1984; Holm et al., 1985). It is therefore conceivable that chromosome breaks at *RSZs* are caused by inappropriate cytokinesis.

## 1.7 Checkpoints that regulate fragile site stability

To ensure successful progression through the cell cycle in an ordered fashion, the different stages of the cell cycle must only be initiated after accurate completion of the previous stage. The cell has evolved multiple checkpoint mechanisms that monitor each stage of the cell cycle and delay entry into the next stage in order for problems to be corrected ensuring the fidelity of cell division (Hartwell and Weinert, 1989). Loss of checkpoint activity leads to genome instability and, in higher eukaryotes, is implicated in the development of cancer (Nojima, 1997).

Checkpoint pathways are essentially signal transduction cascades that involve sensing a problem and transducing a signal in order to obtain an appropriate response. There are three main classes of checkpoint proteins: sensors that detect abnormalities; transducers that relay and amplify the signal; and effectors that act on targets to carry out the checkpoint response.

Common fragile sites in both mammals and yeast appear to depend on checkpoint activity for their stability (Section 1.2). It is now becoming clear that common fragile sites are among the last regions of the chromosome to be replicated and often remain unreplicated in G2 (Debatisse et al., 2006). Additionally, chromosome breaks at *RSZs* occur during G2/M (Cha and Kleckner, 2002). It is therefore likely that checkpoints that prevent the progression into mitosis are implicated in fragile site stability (Arlt et al., 2004). In fact, Debatisse et al (2006) have proposed that these sites could function as "*cis*" acting components of the G2/M checkpoint, signalling to the checkpoint to delay mitosis until the duplication of common fragile sites has been completed. Checkpoints that can induce G2/M arrest include the DNA damage and S-phase checkpoints. Indeed, cells deficient for several DNA damage response proteins have been shown to increase fragile site expression (Arlt et al., 2004; Durkin et al., 2006; Zhu and Weiss, 2007). Furthermore, it has been suggested that breaks at fragile sites are the 'signatures' of replication stress and may therefore require the replication or S-phase checkpoint for stability (Casper et al., 2002). Finally, drugs that prevent mitosis by destabilising the mitotic spindle prevent chromosome breakage at *RSZs* (R. Cha, unpublished results), suggesting that the spindle assembly checkpoint, which monitors chromosome attachment to the mitotic spindle, may also play a critical role in maintaining the stability of these sites.

The following sections describe the basic components of the DNA damage, the S-phase, and the spindle assembly checkpoints.


## 1.8   The DNA damage checkpoint

Cells are constantly exposed to both exogenous and endogenous forms of DNA damage, so maintaining the integrity of the genome is a continuous challenge for the cell. The DNA damage checkpoint monitors the state of DNA throughout the entire cell cycle and responds differently to the various forms of DNA damage.

## 1.8.1   Activating the DNA checkpoint

The key players in the checkpoint response to DNA damage in budding yeast are Mec1 and the closely related kinase Tel1. These checkpoint kinases are widely conserved and are orthologous to ATR and ATM (Ataxia telangiectasia mutated) checkpoint kinases in higher eukaryotes, respectively.  Both Mec1$^{ATR}$ and Tel1$^{ATM}$ belong to the phosphatidylinositol-3-OH kinase-like kinases (PIKK) superfamily (Abraham, 2004). These PIKK kinases are responsible for initiating the checkpoint cascade that reversibly arrests the cell cycle in response to genotoxic stress and coordinates the repair of the damaged DNA (Bartek and Lukas, 2007).

The general consensus is that Mec1$^{ATR}$ is activated in response to RPA-coated single-stranded DNA (ssDNA), whereas Tel1$^{ATM}$ responds to DSBs. However, the rapid resection of DSBs in budding yeast to produce ssDNA consigns Mec1 to the role of the major player in the response to DSBs in this organism (Nyberg et al., 2002). However, partial overlap between Mec1 and Tel1 functions exists in yeast. Strains deleted for *TEL1* are not sensitive to genotoxic stress but increase the sensitivity of cells lacking Mec1 function to the same stresses (Craven et al., 2002; Morrow et al., 1995). Furthermore, overexpression of *TEL1* partially rescues the DNA damage sensitivity of *mec1* mutants (Morrow et al., 1995). Therefore, in yeast, Mec1 is considered the major player in maintaining genomic integrity, with Tel1 playing a secondary role to Mec1.

Checkpoint proteins are often recruited to the site of DNA damage by repair complexes that generate intermediate structures that function as signals to activate the checkpoint response (Figure 1.4A). In higher eukaryotes, the Mre11-Rad50-Nbs1 (MRN) complex acts as a mediator that recognises DSBs and recruits ATM to broken DNA (Harper and Elledge, 2007). In yeast, the similar Mre11-Rad50-Xrs2 (MRX) complex also senses DSBs. Degradation of the 5' strand by the nuclease activity of MRX exposes ssDNA, to which Mec1 is recruited (Figure 1.4B). Mutations that block DSB resection render cells dependent on Tel1 activity for checkpoint activation (Usui et al., 2001). Note that, in higher eukaryotes, ATM appears to stimulate DSB resection and that the ssDNA exposed by this resection leads directly to ATR activation (Cuadrado et al., 2006; Jazayeri et al., 2006).

In addition, checkpoint activation also requires the hetero-trimeric Rad17-Mec3-Ddc1 (or the Rad9-Hus1-Rad1 [9-1-1] complex in mammals) checkpoint clamp, which is thought to be similar to the replication clamp, PCNA. Loading of the checkpoint clamp at sites of DNA damage requires the Rad24/RFC2-5 clamp loader, which is also similar to the RFC1-5 clamp loader utilised for loading PCNA during DNA replication (Harrison and Haber, 2006). Recruitment of the checkpoint clamp and clamp loader to DNA damage occurs independently of Mec1/Tel1 (Melo et al., 2001) but seems to require RPA-coated ssDNA (Lucca et al., 2004; Zou et al., 2003). Interestingly, RPA-dependent recruitment of the checkpoint clamp and clamp loader does not require extensive resection of DSB ends, although minimal resection must occur before the clamp is loaded (Nakada et al., 2004).

It is now evident that chromatin structure is also implicated in early activation of the DNA damage checkpoint. In *S. cerevisiae*, the ATP-dependent chromatin remodeller, the RSC complex (remodel the structure of chromatin), has been shown to function as an early sensor of DSBs and facilitates recruitment of Mec1/Tel1 to the site of damage (Liang et al., 2007). In higher eukaryotes, the chromatin structure of regions flanking a DSB has been implicated in activation of ATM. One possibility is that changes in nucleosome structure or modification of histones surrounding a DSB may constitute the signal for ATM activation (You et al., 2007).

Figure 1.4       The checkpoint response to DNA double strand breaks

## 1.8.2   Amplifying the signal

Following damage detection, the checkpoint transducers and mediators transmit and amplify the checkpoint signal to downstream targets, i.e. the cell cycle machinery and DNA repair machinery (Figure 1.4C). The budding yeast transducers are the Chk2-family kinase Rad53 and the Chk1 kinase (Chk1 in other eukaryotes). Both Rad53 and Chk1 activation require the adaptor protein, Rad9, to bring these kinases into contact with Mec1, although the two kinases bind different domains within Rad9 (Figure 1.4D). Additionally, recruitment of Rad53, but not Chk1, requires phosphorylation of Rad9 by Mec1 (Schwartz et al., 2002). The interaction between Rad53 and the Rad9 adaptor allows the initial, low-level activation of Rad53 by Mec1, which then stimulates its *in trans* autophosphorylation activity (Gilbert et al., 2001; Ma et al., 2006).

## 1.8.3   Effectors of DNA checkpoints

Depending on the stage of the cell cycle at which the DNA lesion was incurred, the cell activates different effectors to stop passage into the subsequent stage of the cell cycle. For example, DNA damage acquired in G1 in higher eukaryotes induces a p53 and Chk2-dependent inhibition of the S-phase-promoting CDKs (Ekholm and Reed, 2000). By contrast, the damage-induced G1 arrest in budding yeast is very weak (Nyberg et al., 2002); although there is some indication that the transcription of G1 cyclins is inhibited, to a limited extent, resulting in delayed entry into S-phase (Sidorova and Breeden, 1997).

As mentioned above, the G2/M checkpoint arrest appears to play a role in fragile site stability. Although BRCA1 is a downstream effector of ATR that plays roles in both the G2/M and S-phase checkpoints, cell lines deficient in the G2/M-specific checkpoint function of BRCA1, exhibit increased levels of chromosome breakage at fragile sites compared to cells lacking the S-phase-specific function (Arlt et al., 2004).

In budding yeast, the DNA damage response effectors that bring about a G2/M arrest target the APC to prevent cells progressing into anaphase (Tinker-Kulberg and Morgan, 1999). In response to DNA damage, Mec1 activates both Rad53 and Chk1 to inhibit the APC-dependent degradation of cohesins (Gardner et al., 1999; Liang and Wang, 2007).

Activated Rad53 specifically blocks the interaction between Pds1 and the APC specificity factor Cdc20, possibly by phosphorylating Cdc20, resulting in the stabilisation of Pds1 and inhibition of entry to anaphase (Agarwal et al., 2003). Rad53 activation also blocks the cell cycle at G2 by inhibiting mitotic exit (Section 1.5.2). Although the mechanism is unclear, it is possible that Rad53 inhibits the polo kinase, Cdc5, thereby preventing activation of the MEN (Sanchez et al., 1999). Inhibition of Cdc5 may also impact on sister chromatid separation, as efficient dissolution of cohesion at anaphase requires phosphorylation of Scc1 by Cdc5 (Alexandru et al., 2001).

In a parallel pathway, activated Chk1 contributes to the metaphase-anaphase arrest by phosphorylating Pds1 (Cohen-Fix and Koshland, 1997; Sanchez et al., 1999). Hyper-phosphorylation of Pds1 is specific to the DNA damage response and requires Chk1 and Rad9, but not Rad53 (Cohen-Fix and Koshland, 1997). Phosphorylation of Pds1 renders it resistant to APC$^{Cdc20}$-dependent ubiquitination and, consequently, reduces its proteolysis (Agarwal et al., 2003). In these ways, activation of Mec1 enables a G2/M arrest in response to DNA damage in budding yeast.

In both mammals and fission yeast the central event leading to a DNA damage-dependent G2/M arrest is inhibition of the mitotic CDK, the Cdc2-cyclin B complex (Rhind and Russell, 1998a; Rhind and Russell, 1998b; Sancar et al., 2004). This is achieved by maintaining the inhibitory phosphorylation of Cdc2. Activation of Chk1 and Chk2 (Cds1 in *S. pombe*) in response to DNA damage increases the activity of the Wee1 kinase, which in turn phosphorylates Cdc2. This inhibitory phosphorylation on Cdc2 is reinforced by the Chk1- and Chk2-dependent inhibition of the Cdc25 phosphatase.

**1.8.3.1 Escape from G2/M arrest as a model for common fragile site expression**

One model for the mechanism of common fragile site expression in mammals proposes that loss of ATR function leads to entry into mitosis with incompletely replicated DNA (Cimprich, 2003). Stalling of a replication fork at a region that is difficult to replicate within the fragile site leads to ATR activation and cell cycle arrest. In the absence of ATR, cells do not arrest and proceed into mitosis with regions of unreplicated DNA. As a result, fragile sites become expressed as gaps consisting of persistent single-stranded DNA and/or DSBs resulting from breakage of these already weakened single-stranded regions upon entry into mitosis (Cimprich, 2003). This model is supported by the finding that overexpression of the Cdc25A phosphatase overrides the G2/M response after treatment with aphidicolin resulting in chromosome breakage at common fragile sites (Cangi et al., 2008).

**1.8.4   DNA repair mechanisms**

Eukaryotic cells have evolved a multitude of repair pathways that contend with the various types of DNA damage that can be acquired during the cell cycle. Of all the types of DNA damage that can occur, the DNA double-strand break is arguably the most dangerous as it can result in chromosome rearrangements and/or cell death (Pierce et al., 2001; van Gent et al., 2001). As DSBs are most relevant type of damage to this thesis, this section will only discuss mechanisms of repairing this type of lesion.

 The two main mechanisms for repair of DSBs are non-homologous end-joining (NHEJ) and homologous recombination (HR) (Figure 1.5). Both NHEJ and HR play major roles in DSB repair in mammalian cells, whereas HR is the predominant mechanism of repair in yeast (Liang et al., 1998; Paques and Haber, 1999). During NHEJ, the two ends of a DSB are ligated together, with minimal processing (reviewed by van Gent et al., 2001). This process involves binding of the Ku70/Ku80 heterodimer to the two ends of a DSB followed by recruitment of the catalytic subunit of DNA-PK, another PIKK that plays important roles in checkpoint response to DNA damage. The Ligase IV-XRCC4 complex is also recruited in order to ligate the two ends back together again. Since NHEJ can promote ligation of two DSB ends

regardless of whether they are in the same chromosome or not, repair of DSBs using this process is not always accurate and may result in loss of genetic information and chromosome translocations (Sancar et al., 2004).

DSB repair by HR uses an intact, homologous sequence to template the repair of a DSB in a process involving members of the conserved *RAD52* epistasis group (Symington, 2002; West, 2003). The first step in the proposed model for DSB repair using HR is the resection of the DSB ends to generate 3' ssDNA overhangs (reviewed in Symington, 2002; Szostak et al., 1983). Resection is inititated by the Mre11-Rad50-Xrs2 (MRX) complex and Sae2, which catalyse a limited amount of DSB end resection (Nakada et al., 2004; Symington, 2002; Szostak et al., 1983). Rapid processing of 3'-tailed DNA ends is achieved by the action of the Sgs1-Dna2 complex or by Exo1-dependent processing in order to yield long 3' ssDNA tails (Zhu et al., 2008; Raynard et al., 2008). RPA on the 3' ssDNA overhangs is removed and replaced by the recombination protein, Rad51, in a process facilitated by Rad52. The Rad51-ssDNA filament can then align with a homologous DNA sequence, usually from the sister chromatid, and initiate strand invasion of the homologous duplex. The 3' end is then extended by DNA synthesis using the homologous duplex as a template, generating the displacement loop (D-loop). At this point, the elongating strand can be displaced by a helicase in a process known as synthesis-dependent strand annealing (SDSA). Alternatively, the D-loop can then pair with the other end of the DSB, and the 3' end of the non-invading strand is also extended, giving rise to two junctions known as the double Holliday junction (dHJ). The dHJ must then be resolved in order to separate the repaired duplexes. As DNA is copied from a homologous sequence during HR, this method of repairing DSBs is more accurate than the error-prone NHEJ pathway.

The mechanism by which DSBs (and other types of DNA damage) are repaired depends on the stage of the cell cycle when the damage is incurred. The primary template for DSB repair by HR is the sister chromatid (Johnson and Jasin, 2000), so this mode of repair is favoured in S- and G2-phases of the cell cycle when a sister chromatid is present (Rothkamm et al., 2003; Takata et al., 1998). Furthermore, a DSB in G2 triggers sister chromatid cohesion, even after cohesion has been

established in S-phase (Strom et al., 2007; Unal et al., 2007). Cohesion probably ensures that the sister chromatids are in close proximity so that repair can occur via HR (Branzei and Foiani, 2008). In G1, the absence of a sister chromatid means that NHEJ is the preferred mechanism of repair (Takata et al., 1998). In addition, high CDK activity in the S- and G2-phases of the cell cycle facilitates the resection stage of HR (Aylon et al., 2004; Ira et al., 2004). Although favoured in G1, NHEJ can be used to repair DSBs at any point in the cell cycle; for example, breaks induced during chromosome segregation are repaired by NHEJ as the highly condensed structure of chromosomes at this stage may hinder the homology search step of HR (Branzei and Foiani, 2008).

Phosphorylation of histone H2A (or the H2AX variant in mammals) by Mec1$^{ATR}$ or Tel1$^{ATM}$ plays an important role in recruiting DNA repair proteins (Paull et al., 2000). Phosphorylated H2A/X, referred to as γH2AX, spans a large region around a DSB site and recruits repair proteins such as Nbs1 or chromatin modifying enzymes in *S. cerevisiae* to the DSB site (Downs et al., 2004; Kobayashi et al., 2002; Rogakou et al., 1998; Shroff et al., 2004).  Recruitment of chromatin remodelling proteins is thought to regulate access of the repair machinery to the DSB, and to restore normal chromosome architecture after repair is complete (Peterson and Cote, 2004). γH2AX is also required for *de novo* association of cohesin around the DSB site in order to facilitate its repair by HR (Strom et al., 2004; Xie et al., 2004).

Figure 1.5        Mechanisms of double strand break repair

## 1.8.4.1 DNA repair at common fragile sites

The DNA repair pathways also play a role at expressed common fragile sites. For instance, RAD51 forms foci at fragile sites and DNA-PKcs is phosphorylated in the presence of aphidicolin (Schwartz et al., 2005). Down-regulation of RAD51, DNA-PKcs, or LIG IV, significantly increases fragile site expression in HeLa cells treated with aphidicolin, suggesting that both HR and NHEJ act at these sites (Schwartz et al., 2005). γH2AX, a marker for DSBs, was found to colocalise with RAD51 and phospho-DNA-PKcs foci and to broken common fragile sites on metaphase chromosomes (Schwartz et al., 2005). These findings lead to the proposal that repair of DSBs formed at common fragile sites by HR and NHEJ pathways may contribute to the elevated level of sister chromatid exchanges found at common fragile sites (Schwartz et al., 2005).

## 1.8.5   Turning off the checkpoint

After successful repair of the DNA damage, the cell must turn off the checkpoint in order to re-renter the cell cycle. Although this process is not very well understood, recent studies indicate that reversal of the activation processes plays an important role. The type 2A-like protein phosphatase Pph3, in a complex with Psy2, binds to activated Rad53 and dephosphorylates it, resulting in its inactivation (O'Neill et al., 2007). The PP2C phosphatases, Ptc2 and Ptc3, can also bind and dephosphorylate Rad53 (Leroy et al., 2003). Similarly, PPM1D/Wip1, the human homologue of Ptc2 and Ptc3, is implicated in recovery from ATM- and ATR-dependent checkpoint arrest (Lu et al., 2005). Dephosphorylation of γH2AX is also important for checkpoint recovery. In yeast, the complete PPP4C complex composed of Pph3, Psy2, and the specificity factor, Ybl046w is required to dephosphorylate γH2AX independently of the role of Pph3-Psy2 complex in deactivating Rad53 (Keogh et al., 2006; O'Neill et al., 2007). Although dephosphorylation of γH2AX in mammals has been attributed to the PP2A phosphatase (Chowdhury et al., 2005), the PP4 phosphatase family also deactivates γH2AX and is required for recovery from checkpoint-mediated arrest, suggesting that checkpoint recovery by PP4 phosphatases may be conserved (Nakada et al., 2008).

## 1.9   Responding to replication stress

### 1.9.1   The S-phase checkpoint

S-phase is a critical time for the cell as it must coordinate complex processes such as origin firing as well as unwinding and duplicating large and complex DNA molecules. In addition, the replicating cell may have to deal with various exogenous and endogenous blocks to DNA replication, which can hinder the progression of the replication fork and lead to genomic instability. DNA damage incurred within S-phase has severe consequences on the progression of the replication fork as the fork arrests whenever it encounters a site of DNA damage. Replication fork stalling can also occur at natural pause sites or due to a shortage of dNTP precursors or inhibition of the replicative polymerases (Section 1.4.3). In addition, as fragile sites replicate late in S-phase they are thought to be areas of the chromosome which are prone to fork stalling (Section 1.2.2.1). Similarly, *RSZs* are fork-slowing regions of the chromosome where forks stall in the absence of Mec1 activity (Section 1.2.3.1).

Stalled forks arise when either the polymerase or DNA helicase are prevented form progressing (Tourriere and Pasero, 2007). For example, hydroxyurea (HU) depletes dNTP pools, thereby blocking DNA synthesis without affecting the helicase. Similarly, aphidicolin, which inhibits the replicative polymerases, inhibits progression of the polymerase but not DNA unwinding. In contrast, inter-strand crosslinks (ICLs) and bulky adducts block progression of the replicative helicase. Lesions on the DNA induced by methylmethane sulfonate (MMS) or ultra violet (UV) light inhibit DNA polymerases on only one template strand, thereby uncoupling leading- and lagging-strand synthesis (Tourriere and Pasero, 2007).

Arrested replication forks can activate the S-phase DNA checkpoint pathway (Figure 1.6). Most arrested replication forks expose large regions of ssDNA, either because of uncoupled leading- and lagging-strand synthesis or inhibition of polymerases (Neecke et al., 1999; Sogo et al., 2002). Note that inhibition of the DNA helicase may not result in the exposure of ssDNA and, therefore, may only weakly activate the S-phase checkpoint (Lambert et al., 2005). In addition, forks stalled at natural

pause sites such as the RFB on rDNA do not accumulate ssDNA nor do they elicit a checkpoint response (Gruber et al., 2000; Labib and Hodgson, 2007).

Exposed ssDNA rapidly becomes coated with RPA and is detected by Mec1$^{ATR}$, which in turn activates the S-phase checkpoint (Zou and Elledge, 2003). However, not all ssDNA elicits a checkpoint response. For example, ssDNA generated by replication unwinding during normal replication does not activate the S-phase checkpoint. In *S. cerevisiae*, the widely held view is that a certain threshold of RPA-coated ssDNA must be present in order to create the necessary signal to activate the checkpoint (Shimada et al., 2002; Tercero et al., 2003). This threshold would prevent unnecessary activation of the checkpoint. In vertebrates, RPA may not be critical for activating the checkpoint in response to replication stress. Addition of RPA-coated ssDNA alone to *Xenopus* egg extracts is not sufficient to activate checkpoint (Stokes and Michael, 2003) suggesting that other factors such as TopBP1$^{Dpb11}$, which interacts directly with ATR, may play a role in checkpoint activation (Kumagai et al., 2006).

There is considerable overlap between the proteins involved in activating the S-phase checkpoint response and those required for the DNA damage response. Mec1, Rad53, the PCNA-like checkpoint clamp (Mec3-Rad17-Ddc1), and the Rad24/RFC2-5 checkpoint-specific clamp loader all play crucial roles in the activation of the S-phase checkpoint (Nyberg et al., 2002). In addition, proteins localised to the replication fork also contribute to the overall checkpoint response during S-phase. These include the replicative polymerase itself, Sld2, Dpb11, and the DNA helicases Sgs1 and Srs2 (Branzei and Foiani, 2006; Nyberg et al., 2002). The Mrc1 and Tof1 factors that move with the elongating replication fork also contribute significantly to the S-phase checkpoint (Alcasabas et al., 2001; Foss, 2001). It is thought that Mrc1 plays a major role in activating the S-phase checkpoint, whereas Tof1 plays a minor role (Tourriere et al., 2005). In the S-phase checkpoint cascade, Mrc1 (Claspin in mammals), replaces the role of Rad9 in activating Rad53 and amplifying the checkpoint (Alcasabas et al., 2001; Osborn and Elledge, 2003). Although Rad9 is, to some extent, capable of carrying out the Mrc1-specific role in the checkpoint response to replication stress (Alcasabas et al., 2001), it is likely that Rad9 and Mrc1 mediate the formation of different phophoisoforms of Rad53 that

channel activated Rad53 towards the appropriate response (Pellicioli and Foiani, 2005; Tourriere and Pasero, 2007).

Together, these proteins function to activate the checkpoint kinases, Mec1 and Rad53, in order to carry out the common S-phase responses. These include inhibition of late origin firing, stabilisation of stalled replication forks, cell cycle delay, DNA repair and fork restart.

### 1.9.2   Inhibition of late origin firing

Activation of the S-phase checkpoint slows down the progression of replication and delays entry into G2 (Nyberg et al., 2002). The primary means of increasing the length of S-phase is by delaying of origin firing (Larner et al., 1999; Santocanale and Diffley, 1998; Tercero and Diffley, 2001). As most early firing origins will have already fired by the time the checkpoint is activated, the S-phase checkpoint relays its inhibitory effect on origin firing almost specifically to late-firing origins. By delaying firing of late replication origins, the cell acquires more time to repair the DNA damage obstructing the fork before new replication forks are formed.

The checkpoint-dependent delay in origin firing is thought to operate through the Rad53-dependent phosphorylation of Dbf4. This decreases the activity of the S-phase promoting Dbf4-Cdc7 kinase, which prevents the initiation of replication from late origins (Pasero et al., 1999; Weinreich and Stillman, 1999). In higher eukaryotes, it has been suggested that regulation of origin firing appears to depend on an ATM and ATR feedback mechanism that senses ongoing replication and down-regulates both CDK and DDK activities thereby inhibiting distal origins (Shechter and Gautier, 2005).

Figure 1.6    The replication stress response

### 1.9.3    Stabilisation of stalled forks

When faced with stalled replication forks, the most crucial function of the S-phase checkpoint is to stabilise the stalled forks and maintain them in a replication-competent state so that replication can resume once the impediment to replication has been relieved (Lopes et al., 2001). A clear example is the *mec1-100* mutant that is viable despite an inability to delay late origin firing in response to DNA damage. Although partially deficient in the checkpoint response, *mec1-100* cells retain some ability to stabilise stalled forks, which allows these cells to remain viable in DNA damaging situations (Cobb et al., 2005; Paciotti et al., 2001). Stabilising a stalled fork entails the maintenance of the replisome at the site of the stalled fork so that DNA synthesis can easily be resumed (Cobb et al., 2003; Lucca et al., 2004).

A stalled replication fork is said to have "collapsed" when the replisome has dissociated from the replication fork. Collapsed replication forks exhibit abnormal DNA structures, including single-stranded gaps, hemi-replicated bubbles, and events (Cotta-Ramusino et al., 2005; Lopes et al., 2001; Sogo et al., 2002). These abnormal structures accumulate in Mec1- and Rad53-deficient cells exposed to DNA damaging agents, indicating that the S-phase checkpoint functions to prevent the collapse of the replication fork (Lopes et al., 2001; Sogo et al., 2002). How the S-phase checkpoint prevents the accumulation of such structures at stalled replication forks remains unclear, although recent reports suggest that Rad53 is required to retain MCM proteins at the fork whereas Mec1 stabilises polymerases, presumably by phosphorylating these replisome components (Bjergbaek et al., 2005; Cobb et al., 2005; Gabrielse et al., 2006). Although replication fork collapse is thought to be irreversible in yeast, studies in *Xenopus* suggest that DNA polymerases may be able to assemble *de novo* in vertebrates in an ATR- and ATM-dependent manner (Trenz et al., 2006).

Besides the Mec1/Rad53 pathway, checkpoint-independent mechanisms of replisome stabilisation also exist. Mrc1 and Tof1 form a complex that travels with the replication fork in normal S-phase and are required to couple the replisome to the site of DNA synthesis (Katou et al., 2003). The absence of Mrc1 or, to a lesser extent,

Tof1 results in a drastic retardation in the progression of replication forks that is independent of their checkpoint functions (Osborn and Elledge, 2003; Szyjka et al., 2005; Tourriere et al., 2005). Furthermore, *mrc1Δ* and *tof1Δ* mutants exhibit extensive DNA unwinding when exposed to HU suggesting that both polymerases and DNA helicases move ahead of the site of DNA synthesis (Katou et al., 2003). This is different to the situation in *mec1* or *rad53* mutants treated with HU where the replisome completely dissociates from the DNA.

### 1.9.4   Restarting stalled forks

Homologous recombination (HR) is crucial for restarting an arrested replication fork in bacteria. However, its role in fork recovery in eukaryotes is more contentious as forks initiated from adjacent origins may replicate a region in which the original fork has collapsed (Michel et al., 2004). Nevertheless, it is now clear that the S-phase checkpoint controls HR in both positive and negative ways. Indeed, unscheduled recombination at stalled forks in yeast is thought to be a major source of genomic instability and must, therefore, be tightly regulated in S-phase. Evidence for this stems from observations in *S. pombe* that the recombination proteins, Mus81 and Rad60, are repressed by the S-phase checkpoint (Boddy et al., 2003; Kai et al., 2005). In *S. cerevisiae*, the absence of an intact checkpoint, or the presence of defective polymerases, results in an accumulation in Rad52 foci compared with wild type cells (Lisby et al., 2001). On the other hand, all known recombination enzymes in budding yeast are sensitive to HU, indicating that HR must also play a role in restarting replication forks in yeast (Pan et al., 2006). In addition, Rad55, a paralogue of Rad51 that aids the assembly of the Rad51 filament during HR, is phosphorylated in response to replication stress and promotes fork recovery, further supporting the notion that HR is involved in restarting stalled replication forks (Herzberg et al., 2006).

Abnormal structures at stalled forks such as reversed forks resemble double Holliday junctions (dHJ) and could be processed by recombination proteins, leading to inappropriate or "toxic" recombination (Fabre et al., 2002). Current models suggest that the Sgs1 helicase functions in a complex with the type I topoisomerase, Top3, to promote the resolution of recombination intermediates during the restart of blocked or stalled replisomes (Fabre et al., 2002; Kaliraman et al., 2001). Sgs1 is also required for complete activation of Rad53 and for contributes to pol $\varepsilon$ and pol $\alpha$ stabilisation at the stalled forks (Bjergbaek et al., 2005; Cobb et al., 2003; Cobb et al., 2005; Frei and Gasser, 2000). Mus81 and Mms4 form an endonuclease complex that may also process stalled forks, possibly in a parallel pathway to Sgs1, by cleaving stalled forks to enable the resumption of replication (Fabre et al., 2002; Kaliraman et al., 2001). Although Mus81 is negatively controlled by the S-phase checkpoint in *S. pombe*, it is currently unclear whether such checkpoint-mediated regulation for Mus81 exists in budding yeast. Similarly, the link between the role of Sgs1 in the S-phase checkpoint response and its function at stalled forks is not clearly understood (Barbour and Xiao, 2003; Lambert et al., 2007).

In addition to recombination, fork progression through damaged DNA can occur by post-replicative repair (PRR). In *S. cerevisiae*, PRR comprises one error-free pathway and two translesion synthesis sub-pathways (Barbour and Xiao, 2003; Branzei and Foiani, 2007). Translesion synthesis (TLS) uses specific polymerases to replicate across a lesion often in an error-prone manner (Branzei and Foiani, 2007; Lehmann et al., 2007). Template switching (TS) is an error-free pathway that uses the newly synthesised sister chromatid as a template to bypass DNA damage (Branzei and Foiani, 2007). All PRR pathways in *S. cerevisiae* depend on the ubiquitin conjugating and ligating activities of RAD6 and Rad18, respectively, and are controlled through ubiquitination of PCNA (Branzei and Foiani, 2007; Hoege et al., 2002; Prakash, 1981). Mono-ubiquitination of PCNA promotes translesion synthesis pathways (Stelter and Ulrich, 2003), whereas multi-ubiquitinated PCNA favours the error-free TS pathway (Hoege et al., 2002). It has been suggested that the Srs2 DNA helicase functions as a molecular switch to inhibit some recombination events and promote a template-switching mode of replication (Barbour and Xiao, 2003; Zhang and Lawrence, 2005). Srs2 is phosphorylated in response to replication

stress in a Mec1-dependent manner (Liberi et al., 2000), suggesting that the S-phase checkpoint may influence choice of fork restart pathway by phosphorylating Srs2, although direct evidence for this is still lacking.

### 1.9.5   Restarting stalled forks as a model for fragile site expression

The current models for chromosome instability at common fragile sites are based on the intrinsic and unique properties of these sites in addition to their regulation by checkpoint proteins. The established hypothesis is that common fragile sites are chromosomal regions that are inherently difficult to replicate, so that even low doses of replication inhibitors stall replication forks at these sites. When cells undergo mild replication stress, the polymerases slow or pause, leaving the helicase to continue unwinding DNA ahead of it. The result is long stretches of ssDNA that can activate the ATR-dependent S-phase and/or G2/M checkpoint, leading to stabilization of the fork and/or proper resolution of structures derived from the stalled fork. Due to the highly flexible AT-rich composition of common fragile site sequences, the long stretches of ssDNA may snap together to form secondary structures that can further impede replicative polymerases (Durkin and Glover, 2007; Zhang and Freudenreich, 2007).

The prevailing model is that gaps at common fragile sites represent persisting ssDNA, whereas breaks at these sites result from the aberrant processing of Holliday junctions at damaged forks within these regions (Figure 1.7). The accumulation of DSBs at common fragile sites subsequently leads to deletions or rearrangements in the chromosome, particularly in the event of defective repair pathways or in the absence of an intact replication checkpoint. In the absence of ATR, reversed forks or structures containing large regions of single-stranded DNA accumulate at the stalled fork and are inappropriately resolved by recombination enzymes, BLM/Sgs1 helicase, or the Mus81-Mms4 complex (Durkin and Glover, 2007; Zhang and Freudenreich, 2007).

Models for fragile site expression in yeast, particularly at sites of inverted repeats (e.g. the FS2 site), suggest that secondary structures formed at these sites are processed in such a way as to generate DSBs. For example, a hairpin can be

processed at its single-stranded loop region that separates the Ty repeats. This is followed by dissociation of the hairpin stem resulting in the formation of a recombinogenic DSB (Lemoine et al., 2005). Cruciforms generated at fragile sites could be processed by a DNA resolvase that could cleave this structure producing an intermediate similar to that resulting from processing a hairpin (Lemoine et al., 2005). Candidate enzymes that could generate a DSB from either of these structures include the MRX complex and the Mus81-Mms4 complex that is proposed to act as a resolvase for processing HJ-like molecules (Cote and Lewis, 2008; Lobachev et al., 2002).

Figure 1.7      Prevailing models for the accumulation of breaks and gaps at fragile site

## 1.10 DNA damage and/or replication checkpoint response proteins acting at common fragile sites

It is now clear that ATR is the key regulator of common fragile site stability, even in the absence of replication inhibitors, linking checkpoint function to fragile site stability. However, a recent study shows that ATM also contributes towards maintaining the stability of these sites in the absence of ATR function (Ozeri-Galai et al., 2008). Several targets of ATR-pathways have also been shown to influence fragile site stability. These include BRCA1, CHK1, the Fanconi anemia (FA) pathway proteins, and Smc1. BRCA1, a protein that shares some similarities with Rad9 in yeast, suppresses chromosome breakage at common fragile sites by way of its G2/M checkpoint function (Arlt et al., 2004). Both CHK1 (the orthologue of yeast Chk1) and CHK2 (the orthologue of Rad53 in yeast) are activated upon treatment with aphidicolin, and a lack of CHK1 results in an increase in fragile site expression in the presence of this replication inhibitor (Durkin et al., 2006). Similarly, disruption of FANCD2, a component of the Fanconi anemia pathway that is activated following replication stress, results in an increase in fragile site expression (Howlett et al., 2005). SMC1 deficiency also increases the incidence of chromosome breakage at common fragile sites (Musio et al., 2005). Moreover, Werner syndrome helicase, WRN (the mammalian orthologue of Sgs1 in yeast), forms nuclear foci following treatment with aphidicolin, and disruption of this helicase is accompanied by an increase in fragile site expression even in the absence of aphidicolin (Pirzio et al., 2008). Finally, the Hus1 component of the Rad9-Rad1-Hus1 complex (Section 1.8.1) has also been shown to play a role at common fragile sites, as mouse cells lacking Hus1 display elevated levels of breakage at these loci (Zhu and Weiss, 2007).

# 1.11 The spindle assembly checkpoint

Accurate chromosome segregation requires the bipolar attachment of sister chromatids to the mitotic spindle, mediated by connections between the proteinaceous structure assembled at the centromere known as the kinetochore and the spindle microtubules. Inappropriate attachment of the kinetochores to the spindle results in mis-segregation of chromosomes and genome instability. The spindle assembly checkpoint (SAC) monitors this process and delays the onset of anaphase if proper attachments are not made.

### 1.11.1 What is sensed?

The SAC senses incorrect kinetochore to microtubule attachments by monitoring microtubule occupancy of the kinetochores and/or tension generated across the chromosome/kinetochores (Musacchio and Salmon, 2007). The two modes of sensing incorrect attachments are not necessarily mutually exclusive. For instance, microtubule-kinetochore attachments are destabilised at low tension and stabilised by high tension between the sister kinetochores (Nicklas, 1997; Nicklas et al., 2001). In addition, tension can provide a means of discriminating against incorrect attachments. For example, syntelic attachments, where sister kinetochores are attached to spindles emanating from the same pole, do not generate enough tension and microtubule-kinetochore attachment is destabilised to correct the problem. This correction of syntelic attachments requires the aurora B kinase, or Ipl1 in yeast (Pinsky and Biggins, 2005; Tanaka et al., 2002).

### 1.11.2 Checkpoint proteins

Like the other checkpoint systems, the SAC is a signal transduction cascade mediated by the Mad1-3 (mitotic arrest deficient) proteins, Bub1-3 (budding uninhibited by benzimidazole) proteins, and the Mps1 kinase that is essential for spindle pole body duplication (Hoyt et al., 1991; Li and Murray, 1991; Weiss and Winey, 1996). The function of the SAC is intimately linked to the kinetochore. In *S. cerevisiae*, mutations that impair centromeric DNA or kinetochore activate the SAC

in order to block the metaphase-anaphase transition (Pangilinan and Spencer, 1996; Spencer and Hieter, 1992; Wang and Burke, 1995). In animal cells, all known SAC components localise to the kinetochore. By contrast, in yeast, Bub1 and Bub3 are found on kinetochores early on during unchallenged mitosis, but Mad1 and Mad2 only bind kinetochores in the event of spindle damage or kinetochore defects. This difference is likely due to the fact that kinetochores of *S. cerevisiae* chromosomes are seldom unattached to spindle microtubules (Gillett et al., 2004).

Upon SAC activation, Mps1, Mad1, Mad2, Mad3/BubR1, Mps1, and Bub3 localise to unattached kinetochores (Cleveland et al., 2003). Fluorescence recovery after photobleaching (FRAP) experiments show that Mad2, Mad3/BubR1, Mps1, and Bub3 all cycle on and off the kinetochore with a high rate whereas Bub1 and Mad1 are more stably bound (Howell et al., 2004; Shah et al., 2004). As soon as microtubule attachment and chromosome biorientation are achieved, the SAC proteins then become depleted from kinetochores (Griffis et al., 2007; Wojcik et al., 2001).

The MEN inhibitor, Bub2, was initially isolated as a component of the SAC (Lew and Burke, 2003). Unlike the other Mad and Bub proteins, Bub2 localises to the SPB and is not required to prevent Pds1 degradation and cohesin cleavage. Instead, Bub2 acts during every cell cycle to negatively regulate MEN function and cytokinesis (Lee et al., 2001). Upon activation of the SAC, this function of Bub2 is thought to be protracted thereby stabilising the mitotic cyclin and preventing mitotic exit and cytokinesis (Alexandru et al., 1999; Fesquet et al., 1999; Li, 1999). Therefore, activation of the SAC in response to kinetochore and spindle damage prevents the metaphase-anaphase transition through a Mad2-dependent pathway, whereas Bub2 functions in a parallel, late regulatory branch of the SAC to delay mitotic exit (Alexandru et al., 1999; Krishnan et al., 2000; Figure 1.8). Loss of Bub2 results in partial defects in delaying the transition to anaphase upon treatment with spindle poisons, suggesting that Bub2 may play a role in maintaining the Mad2-mediated inhibition of sister chromatid separation (Pangilinan and Spencer, 1996). In addition to its role in mitotic exit and the SAC, Bub2 plays a role in the spindle orientation checkpoint that regulates the position of the spindle within a dividing yeast cell (Lew and Burke, 2003).

Figure 1.8 The two branches of the spindle assembly checkpoint

### 1.11.3 Effectors of the SAC

In order to delay anaphase onset in response to incorrect kinetochore-microtubule attachments, the SAC prevents cohesin cleavage by inhibiting APC activity until correct attachments are created (Lew and Burke, 2003). The target of the SAC is therefore the APC specificity factor, Cdc20, and mutations in this protein cause dominant checkpoint defects (Hwang et al., 1998). During prometaphase, all components of the SAC and Cdc20 concentrate at the kinetochores, which provides a platform on which the SAC can carry out its response (Cleveland et al., 2003; Maiato et al., 2004). Mad2 binds Cdc20 directly and inhibits its activity (Chan and Yen, 2003). BubR1 binds Cdc20 as well as components of the APC complex (Fang, 2002). The SAC components are thought to function within a complex referred to as the mitotic checkpoint complex (MCC), which binds the APC and strongly inhibits it (Musacchio and Salmon, 2007; Sudakin et al., 2001). Two such checkpoint complexes have been identified in *S. cerevisiae*, the Mad1-Bub1-Bub3 complex and the Mad2-Mad3/BubR1-Bub3-Cdc20 that is similar to the vertebrate MCC (Lew and Burke, 2003). Within the MCC, Mad2 and Mad3/BubR1 bind Cdc20 in a manner that depends on other SAC components. By binding different sites on Cdc20, Mad2 and BubR1 can exert a synergistic effect on APC inhibition (Davenport et al., 2006; Fang, 2002; Musacchio and Salmon, 2007). Exactly how the MCC inhibits APC activity is unclear, but there is at least some evidence to suggest that BubR1 enables the MCC to bind APC and that the MCC must disassemble from the APC at metaphase in order to elicit anaphase (Musacchio and Salmon, 2007).

## 1.12 Additional roles of checkpoint proteins

In addition to controlling the cell cycle, checkpoint proteins also have many additional roles in DNA metabolism. For instance, both *TEL1* and *ATM* are required for telomere maintenance, and mutations in these genes give rise to chromosomes with short, but stable, telomeres (Pandita, 2002; Ritchie et al., 1999). In *S. pombe*, Tel1 and Rad3, the homologue of Mec1, are required for telomere addition

(Matsuura et al., 1999). In *S. cerevisiae*, Tel1 recruits telomerase to telomeres for *de novo* telomere addition (Ritchie et al., 1999). Although no direct role for Mec1 in telomere maintenance has been identified in *S. cerevisiae*, combined defects in Mec1 and Tel1 functions generate short telomeres that are also unstable, indicating a role for Mec1 in maintaining telomere length (Ritchie et al., 1999).

In budding yeast, the essential function of Mec1 and Rad53 is the up-regulation of dNTP synthesis prior to DNA replication to ensure that cells generate sufficient dNTPs to complete S-phase (Zhao et al., 1998). Mec1 and Rad53 also drastically increase dNTP synthesis in response to genotoxic stress, presumably to generate additional dNTPs for DNA repair processes. Mec1 and Rad53 increase dNTP synthesis in three ways: (*i*) by allowing the relocalisation of ribonucleotide reductase (RNR) subunits to the cytoplasm where they can assemble a functional RNR (Yao et al., 2003), (*ii*) by phosphorylating Sml1, the inhibitor of RNR, thereby targeting it for degradation (Zhao et al., 2001; Zhao et al., 1998), and (*iii*) by increasing transcription of RNR subunits (Huang et al., 1998). Conditions that elevate dNTP levels such as deletion of *SML1* and over-expression of the *RNR1* subunit of RNR rescue the lethality of *mec1Δ* cells. However, these cells are unable to respond to genotoxic stress (Craven et al., 2002).

In higher eukaryotes, ATR is also essential (Brown and Baltimore, 2000). Unlike in *S. cerevisiae*, it is the checkpoint function of ATR that is essential (Brown and Baltimore, 2000; Cortez et al., 2001; Garcia-Muse and Boulton, 2005). The reason for the difference between yeast and metazoans in the essential requirement for a functional DNA damage response remains unclear. However, it has been proposed that the more complex and repetitive genome of metazoan cells renders it more difficult to replicate and, hence, more reliant on the genotoxic stress response of ATR (Callahan et al., 2003; Dart et al., 2004).

In metazoans, the S-phase checkpoint plays a role in promoting replication fork progression as depletion of Chk1 or Claspin reduces fork rates during unperturbed DNA replication (Petermann and Caldecott, 2006; Petermann et al., 2008; Petermann et al., 2006). In contrast, the S-phase checkpoint does not appear to be required to regulate fork progression in yeast as fork rates are not altered in *mec1Δ tel1Δ sml1Δ*

(compared to *sml1Δ*) or in *rad53-11* mutants (Katou et al., 2003; Versini et al., 2003). However, Mec1 is required to promote replication fork progression through replication slow zones (Cha and Kleckner, 2002), although whether this is due to its role in dNTP regulation or a novel role is unclear. In support of the former possibility, deletion Sml1, the inhibitor of RNR, which increases dNTP synthesis, prevents fork stalling and chromosome breakage at *RSZs* (Cha and Kleckner, 2002). Similarly, common fragile sites rely on ATR for their stability (Casper et al., 2002), although whether this simply reflects the essential (Cha and Kleckner, 2002) function of ATR in higher eukaryotes is unknown.

## 1.13 Aims of this project

Despite numerous studies aimed at understanding the molecular basis of chromosome instability at common fragile sites, the precise mechanism by which breaks are generated at these sites remains unknown. Using *RSZs* as a model for common fragile sites, this project aims to develop our current understanding of fragile sites, the mechanism by which genomic instability is generated at these sites, and the factors involved in maintaining their stability. The first aim of this study is to characterise *RSZs* in terms of chromosomal features in order to understand the sequence characteristics of *RSZs* further and in order to assess the suitability of utilising *RSZs* as a model system for studying mammalian fragile sites. The second aim is to test the proposed models for endogenous chromosome breakage for their involvement in chromosome breakage at *RSZs*. These include fork restart mechanisms, HR, spindle force, cytokinesis, condensation, and decatenation. The final aim of the project is to understand the interplay of factors governing chromosome stability at *RSZs*.

# Chapter 2

# Materials and Methods

## 2.1   Commonly used buffers and solutions

The details of commonly used buffers and solutions are given in Table 2.1. All chemicals were purchased from Sigma unless otherwise indicated.

**Table 2.1 Commonly used buffers and solutions**

| Buffer/Solution | Composition |
|---|---|
| PBS (1x) | 137 mM NaCl, 2.7 mM KCl, 10 mM $Na_2HPO_4$, 1.8 mM$KH_2PO_4$ |
| PCR[a] buffer (1x) | 2.25 mM $MgCl_2$, 50 mM KCl, 10 mM Tris-HCl pH 8.4 |
| Phosphate buffer pH6.5 (1M stock) | 685 mM $NaH_2PO_4$, 315 mM $Na_2HPO_4$ |
| TAE (1x) | 40 mM Tris base, 40 mM acetic acid, 1 mM EDTA |
| TBE (1x) | 45 mM Tris base, 45 mM boric acid, 1 mM EDTA |
| TE (1x) | 10 mM Tris-HCl pH 8.0, 1 mM EDTA |

[a] polymerase chain reaction (PCR)

[b] ethlenediaminetetra-acetic acid (EDTA)

## 2.2   Bacterial techniques

### 2.2.1   Bacterial strains

*Eschericia coli* (*E. coli*) strain DH5α□ □*F' endA1 hsdR17 [$r_K^- m_K^+$] supE44 thi-1 recA1 gyrA [Nal^r]relA1 Δ[lacZYA-argF]U169 deoR [ϕ80dlacΔ(lacZ)MI5]*) was used for all bacteriological work.

### 2.2.2    *E. coli* **media and growth conditions**

*E. coli* were grown in Luria-Bertani broth (1% [w/v] bacto-tryptone, 0.5% [w/v] yeast extract, 1% [w/v] NaCl pH 7.5) supplemented with 100 μg/ml ampicillin (LB-Amp) or 50 μg/ml kanamycin (LB-Kan) for plasmid selection. Liquid cultures were grown at 37°C in a gyratory shaker at 300 rpm. For solid LB media, 1.5% (w/v) bacto-agar was added to LB-broth. *E. coli* were grown on LB-agar plates in a constant temperature incubator at 37°C. For long-term storage, 1 ml of an overnight *E. coli* culture grown in either LB-Amp or LB-Kan was added to 1 ml of 2x LB/glycerol (2x LB-broth, 50% [v/v] glycerol) and stored at -80°C.

### 2.2.3    *E. coli* **transformation**

To make chemically competent *E. coli* cells for transformation, DH5α cells were grown overnight with shaking in 2 ml of LB broth (no selection) at 37°C. The following morning, 100 ml of LB broth (no selection) was inoculated with 0.5 ml of the overnight culture and grown to an $OD_{600}$ of 0.5. The culture was chilled on ice before the cells were pelleted (10,000 rpm, 1 min, 4°C). The cells were resuspended in 30 ml of filter-sterilised ice-cold buffer 1 (10 mM potassium acetate, 50 mM $MnCl_2$, 100 mM RbCl, 10 mM $CaCl_2$, 15% [v/v] glycerol, adjusted to pH 5.8 with dilute acetic acid) and left on ice for 90-120 min at 4°C. The cells were pelleted (5000 rpm, 1 min, 4°C) and gently resuspended in 4 ml of filter-sterilised ice-cold buffer 2 (10 mM MOPS, 75 mM $CaCl_2$, 10 mM RbCl, 15% [v/v] glycerol, adjusted to pH 7.0 with HCl). After addition of 60 μl of dimethyl sulphoxide (DMSO) to the cells in buffer 2, the mixture was divided into aliquots of 100 μl in pre-chilled microfuge tubes and stored at –80°C.

To transform *E. coli* cells, 1-5 μl of transforming DNA was added to 50 μl of chemically competent cells. The mixture was incubated on ice for 10 minutes then heat-shocked at 42°C for 1 minute. 1 ml of LB-broth was added and the cells were incubated at 37°C in a hot-block for 1 hour to recover. Aliquots of 100 μl and 900 μl were plated onto either LB-Amp or LB-Kan agar and grown overnight at 37°C.

### 2.2.4   Purification of *E. coli* plasmid DNA

Plasmid DNA was extracted from a 2 ml overnight culture using a QuantumPrep Plasmid Miniprep kit [BioRad] according to the manufacturer's instructions.

## 2.3   Yeast techniques

### 2.3.1   Yeast media and growth conditions

Details of the yeast media used in this study are described in Table 2.2.

**Table 2.2 Yeast growth media**

| Medium | Composition |
| --- | --- |
| YEP | 1% (w/v) yeast extract, 2% (w/v) bacto-peptone |
| YPD | 1% (w/v) yeast extract, 2% (w/v) bacto-peptone, 2% (w/v) glucose |
| YPG agar | 1% (w/v) yeast extract, 2% (w/v) bacto-peptone, 3% (v/v) glycerol, 2% (w/v) bacto-agar |
| SD | 0.67% (w/v) yeast nitrogen base, with either appropriate amino acid supplements at 40 μg/ml or 0.8 g/L amino acid dropout mix, 2% (w/v) glucose |
| Amino acid dropout mix | 800 mg adenine, 800 mg arginine, 800 mg histidine, 2400 mg leucine, 1200 mg lysine, 800 mg methionine, 2000 mg phenylalanine, 8000 mg threonine, 800 mg tryptophan, 1200 mg tyrosine, 800 mg uracil (with the appropriate amino acid dropped out) |
| SPM | 1% (w/v) potassium acetate, 2% (w/v) bacto-agar |

Routinely, yeast strains were grown either in YPD rich media or, for auxotrophic selection, in synthetic dextrose media (Table 2.2). SD media supplemented with all the amino acids listed in the dropout mix in Table 2.2 (i.e. with no amino acid dropped out) is referred to as synthetic complete (SC) media. Liquid cultures were grown in a gyratory shaker [New Brunswick] at 175 rpm. For growth on solid media 2% (w/v) bacto-agar was added to the media. Yeast strains were incubated on agar plates in a constant temperature incubator. The standard growth temperature for wild type strains was 30°C. Temperature sensitive strains were grown at the permissive temperature of 23°C and the restrictive temperature as indicated.

Overnight growth on YPG agar (Table 2.2) was used to select against petite mutants.

To select for drug resistance, 200 μg/ml G-418 [GIBCO] or 300 μg/ml Hygromycin B [Sigma] was added to YPD agar.

Growth on 5'-fluoro-orotic acid (5'FOA) [Apollo] containing solid media (SC-media or the appropriate SD-dropout media containing uracil, 3% [w/v] bacto-agar, 1 mg/ml 5'FOA) was used to select against *URA3* gene expression.

To induce DNA replication stress, cells were grown in the presence of hydroxyurea (HU) at the indicated concentrations.

To induce spindle damage and G2/M arrest, cells were grown in the presence of either 15μg/ml nocodazole [Sigma-Aldrich] or 40μg/ml carbendazim (MBC) [Sigma-Aldrich].

For long-term storage, freshly grown yeast cells were removed from agar plates and inoculated into 1.8 ml of 25% (v/v) glycerol. The strain stocks were then stored at -80°C.

### 2.3.2   Mating yeast strains

To generate diploid strains, two haploid strains of opposite mating types were mixed in a patch on a YPD agar plate and incubated overnight at 23°C or 30°C, depending on the strain genotype.

Where possible diploids were isolated by auxotrophic selection. If auxotrophic selection was not possible, cells from the mating patch were streaked for single colonies on a YPD agar plate and diploids were selected by microscopic screening (Section 2.3.10, Figure 2.1) and their ability to sporulate.

Figure 2.1     Haploid and diploid SK1 *S. cerevisiae* cells

### 2.3.3    Tetrad dissection

Diploid strains were incubated on minimal sporulation media (SPM; Table 2.2) at 23°C or 30°C for a minimum of 24 hours. The walls of the asci were digested for 30 minutes with 50 μl of 5 mg/ml Zymolyase-20T [ICN Biomedicals] in SCE buffer (1 M sorbitol, 100 mM sodium citrate, 60 mM EDTA) at 37°C. Tetrads were dissected using a Singer MSM micromanipulator.

The genotype of the haploid strains resulting from tetrad dissection was determined by replica plating onto the appropriate SD-dropout media or drug selection media.

The mating type of the resulting haploid strains after tetrad dissection was determined by their ability to mate with mating type tester strains (RCY313 and RCY314; Table 2.8) to produce a prototrophic diploid.

### 2.3.4    Determination of cell density

The cell density of yeast cultures was determined either by counting cell numbers or by the optical density at 600 nm ($OD_{600}$).

To obtain a cell count, 50 μl of liquid culture was diluted into 10 ml Casyton [Scharfe System] solution and sonicated using a Status US200 sonicator [Philip Harris Scientific] for 3 seconds at 20% power to separate the cells. Cell numbers were counted using a CASY1 (model TT) particle counter [Scharfe System] according to the manufacturer's instructions.

The $OD_{600}$ of a culture was measured in a CO8000 cell density meter [WPA], using a cuvette [Fisherbrand] containing 1 ml of liquid culture (diluted up to 10x if necessary).

### 2.3.5    Growth synchronisation

To obtain a synchronous culture for cell cycle analysis, cells were grown to mid-log phase (approximately $8 \times 10^6$ cells/ml or an $OD_{600}$ of 0.4) and arrested for 2.5 hours with 5 μg/ml α-factor [Polypeptide synthesis lab, NIMR]. To release from the G1

block, the cells were pelleted (3000 rpm, 2 min), washed twice with pre-warmed saline and resuspended in fresh pre-warmed YPD.

### 2.3.6   Fluorescence activated cell sorting (FACS)

Cells from 1 ml of a mid-log phase or synchronous culture were pelleted (13,000 rpm, 1 min) and resuspended in 1 ml of fixative (40% [v/v] ethanol, 0.1 M sorbitol). After a minimum of 3 hours in fixative, cells were pelleted (13,000 rpm, 1 min), resuspended in 250 μl of ribonuclease (RNase) solution (50 mM Tris-HCl pH 7.5, 100 μg/ml RNaseA) and incubated overnight at 37°C. The next day the cells were pelleted (13,000 rpm, 1 min), resuspended in 500 μl of pepsin solution (50 mM HCl, 5 mg/ml pepsin) and incubated for a minimum of 5 minutes at room temperature. The cells were then pelleted (13,000 rpm, 1 min), resuspended in 1 ml SYTOX solution (50 mM Tris-HCl pH 7.5, 1 μM SYTOX Green nucleic acid stain [Invitrogen Molecular Probes]) and incubated overnight at 4°C.

The samples were analysed on a Becton Dickinson FACScan using CellQuest software [Becton Dickinson] according to the manufacturer's instructions.

### 2.3.7   Temperature sensitivity assays

Yeast cultures were grown to mid-log phase. The $OD_{600}$ of the cultures was measured and adjusted to 0.4 before making 10-fold serial dilutions of the cultures. The dilution series was spotted (4-5 μl) onto YPD agar plates. Once dry, the agar plates were incubated at the indicated temperature for 1-5 days as necessary. All drug and temperature sensitivity assays were repeated at least twice, using independent clones of each strain. One representative experiment is shown in each case in the Results chapters.

### 2.3.8   Yeast transformation

Yeast strains were transformed by a standard lithium acetate method as described in (Gietz and Woods, 2002). To prepare competent cells, a 50 ml culture was grown to mid-log phase. The cells were pelleted (3000 rpm, 2 min) and washed once with 25

ml sterile $H_2O$. The cells were resuspended at $10^9$ cells/ml in sterile $H_2O$ and 100 μl of this cell suspension was used per transformation. The cells were pelleted (13,000 rpm, 1 min) and resuspended in 360 μl of transformation mix (30% [w/v] polyethylene glycol $(PEG)_{3350}$, 100 mM lithium acetate, 100 μg single-stranded carrier DNA, 1-10 μg of transforming DNA). The cells were incubated in the transformation mixture at 42°C for 40 minutes. Temperature-sensitive strains were incubated in transformation mixture for 20 minutes at room temperature before heat shocking for 20 minutes at 42°C. For auxotrophic selection, cells were pelleted (6000 rpm, 1 min) after the heat shock treatment and resuspended in 500 μl sterile $H_2O$. Aliquots of 200 μl were plated directly onto SD-dropout agar plates. To select for drug resistance, the cells were pelleted (6000 rpm, 1 min) after the heat shock treatment, resuspended in 1 ml YPD rich media and allowed to recover for 2-3 hours before plating onto selective media as before.

### 2.3.9   Isolation of yeast genomic DNA

Cells from a 2 ml overnight culture were pelleted (13,000 rpm, 1 min), washed with 500 μl $H_2O$, and resuspended in 100 μl breakage buffer (50 mM Tris-HCl pH 7.6, 20 mM EDTA, 1% [w/v] sodium dodecyl sulphate [SDS]). Glass beads (0.5 mm) [BioSpec Products] were added to the level of the liquid and the cells were lysed by two 10 second pulses at speed setting 4 in a RiboLyser [Hybaid] with 1 minute on ice between pulses. The lysate was collected by piercing the bottom of the tube with a red-hot needle, placing this tube inside a clean 1.5 ml tube supported by a 15 ml tube, and centrifuging for 30 seconds at 3000 rpm. The lysate was then incubated for 10 minutes at 70°C in a hot block. After mixing briefly using a vortex, 200 μl of 5 M potassium acetate and 150 μl of 5 M NaCl were added to the lysate and the mixture was incubated on ice for 20 minutes. The cell debris was removed by centrifugation (13,000 rpm, 20 min, 4°C). The supernatant was transferred to a clean 1.5 ml tube and 150 μl 30% (w/v) $PEG_{6000}$ was added. The mixture was incubated on ice for 10 minutes and then the DNA was recovered by centrifugation (13,000 rpm, 10 min, 4°C). The supernatant was removed and the DNA pellet resuspended in 40 μl of nuclease-free $H_2O$.

### 2.3.10  Microscopy

An Eclipse E200 phase-contrast microscope [Nikon] with a 40x objective was used to routinely view yeast cultures. An Olympus DP12 [Olympus Optics] digital camera was used to capture images.

## 2.4  DNA manipulations

### 2.4.1  Agarose gel electrophoresis

Routine agarose gel electrophoresis was carried out in 1% (w/v) agarose gels (electrophoresis grade) [Invitrogen] with TBE electrophoresis buffer (Table 2.1). Use of alternative percentage agarose gels is indicated. Where the DNA fragments were to be subsequently purified, low melting point (LMP) agarose [Invitrogen] and TAE electrophoresis buffer (Table 2.1) were used.

DNA was loaded with 1/6 volume 6x DNA loading buffer (0.2% [w/v] bromophenol blue, 30% [v/v] glycerol) and run with a constant voltage of 75 volts. DNA was stained using 0.05% (w/v) ethidium bromide [GIBCO] (which was added directly to the molten agarose before pouring the gel) and visualised under short wave ultra-violet radiation using a BioDoc-It System transilluminator [UVP]. The size of DNA fragments was estimated by comparison to the DNA markers in a 1 kilo base pair (kb) DNA ladder [Invitrogen].

### 2.4.2  Recovery of DNA fragments from agarose gels

DNA fragments were extracted from TAE agarose gels using a Wizard PCR Preps DNA purification system [Promega] according to the manufacturer's instructions.

### 2.4.3  Pulsed-field gel electrophoresis (PFGE)

To prepare agarose plugs containing chromosome-sized DNA, cell pellets were collected and stored in 1 ml 50 mM EDTA. The number of plugs that could be prepared from each cell pellet was determined by the weight of the dry pellet. For each plug 0.1 g of cells was used. To the cell pellet, 25 μl of solution I (1 M sorbitol,

100 mM sodium citrate, 60 mM EDTA, 5% [v/v] β-mercaptoethanol, 5 mg/ml zymolyase-20T) per plug (i.e. per 0.1 g cells) was added and stirred into the cell pellet. Next, 75 μl of melted 1.5% (w/v) LMP agarose [Invitrogen] was added per plug and mixed into the cell pellet. The mixture was placed into plug moulds and left to set at $4^oC$ for 10 minutes. Plugs were dispensed from the mould into a 2 ml plastic tube. The plugs were treated with 2 ml of solution II (0.45 M EDTA, 10 mM Tris-HCl pH 7, 7.5% [v/v] β-mercaptoethanol, 10 μg/ml RNaseA) for a minimum of 6 hours at 37°C. The tube was then chilled on ice for 10 minutes before replacing solution II with 2 ml solution III (0.25 M EDTA, 10 mM Tris-HCl pH 7, 1% [w/v] sarkosyl, 1 mg/ml Proteinase K [Roche]). The plugs were incubated overnight in solution III at 37°C. The next day the tube was chilled on ice for 10 minutes, before removing solution III and replacing it with 1 ml storage solution (50 mM EDTA, 50% [v/v] glycerol). The prepared agarose plugs were stored at –20°C.

Electrophoresis was performed using 1/3 plug per lane in a Bio-Rad CHEF Mapper according to the parameters listed in Table 2.3. Lambda Ladder PFG marker [New England Biolabs] was used to estimate the sizes of chromosome VI fragments (Section 2.4.4).

**Table 2.3 Parameters for PFGE**

| Parameters | Chromosome III | Chromosome VI |
|---|---|---|
| Voltage gradient | 6 V/cm$^2$ | 6 V/cm$^2$ |
| Switch times | 5- 30sec | 5- 30sec |
| Run time | 24 hours | 20 hours |
| Temperature | $14^oC$ | $14^oC$ |
| % Agarose[a] | 1% (w/v) | 1.2% (w/v) |
| TBE (Table 2.1) | 0.5X | 0.5X |

[a]Pulsed Field Certified Agarose [Bio-RAD]

## 2.4.4   Estimation of chromosome fragment sizes in Pulsed-field gels

The sizes of chromosome fragments separated by PFGE were determined based on the migration distances of the Lambda Ladder PFG marker [New England Biolabs].

The distance that each marker band migrated was measured from the midpoint of the well to the midpoint of the respective marker band. A curve of distance migrated versus band size was then plotted for all the bands within the marker lane. A mathematical formula relating the distance migrated and band size was drived from this curve using the Trendline tool in Excel. This formula was then used to calculate the size of the chromosome fragments in the other lanes of the PFG from the distance they migrated from the well. As the distances that the marker bands migrated varied slightly in each gel, a separate curve and formula were derived for each gel.

### 2.4.5   Southern blot analysis

The agarose gel to be blotted was rinsed in water for 10 minutes, followed by depurination in 0.25 M HCl for 20 minutes. The gel was then rinsed again in water and denatured in 0.4 M NaOH for 30 minutes. The gel was blotted overnight in 0.4 M NaOH onto Hybond-N+ positively charged nylon transfer membrane [GE Healthcare].

The blotted membrane was neutralised with 50 mM sodium phosphate buffer pH 6.5 for 15 minutes. The membrane was then placed in a hybridisation tube [Hybaid] with 15 ml of prehybridisation buffer (7% [w/v] SDS, 0.5 M sodium phosphate buffer pH 6.5, 1 mM EDTA) rotating at 65°C for a minimum of 10 minutes. DNA probes were made either by restriction enzyme digest (Sections 2.4.2 and 2.4.5) or by PCR (Section 2.4.7). The DNA probe was labelled with $^{32}$P-dCTP [GE Healthcare] using a Prime-It RmT Random Primer Labeling kit [Stratagene] according to the manufacturer's instructions. Before addition to a fresh 15 ml of prehybridisation buffer, the $^{32}$P-labelled probe was denatured by incubation in a hot block at 95°C for 5 minutes. The prehybridisation buffer containing the denatured $^{32}$P-labelled probe was then transferred to the hybridisation tube with the membrane. The membrane was incubated with the $^{32}$P-labelled probe overnight, rotating at 65°C.

To remove non-specific signal the membrane was washed twice for 20 minutes in ~500 ml wash buffer (1% [w/v] SDS, 40 mM sodium phosphate buffer, 1 mM EDTA) before being wrapped in Saran wrap and exposed to a storage phosphor screen [Kodak] for 1-3 days.

The screen was scanned using a Storm 860 Phosphorimager and band intensity was quantified with ImageJ software [NIH].

See Table 2.4 for a list of DNA probes used in this study.

**Table 2.4 DNA probes used in this study**

| Probe name | Probe size (bp) | Source |
| --- | --- | --- |
| *CHA1* | ~800 | *Hind*III/*Kpn*I digest of pRSC38 |
| *COS4* | 1139 | PCR product using primers P676 and P677 |
| *IRC7* | 1022 | PCR product using primers P678 and P679 |
| Lambda DNA-*HindIII* Digest | Not applicable | New England Biolabs |

## 2.4.6   Restriction endonuclease digestions

DNA was incubated with the required restriction endonuclease enzyme(s) [New England Biolabs or Roche] in the appropriate restriction endonuclease buffer according to the manufacturer's instructions at 37°C for a minimum of 2 hours.

## 2.4.7   DNA ligations

Following restriction enzyme digestion (Section 2.4.5), plasmid vector DNA to be used for ligation was incubated with 1 U calf intestine alkaline phosphatase [Roche] at 37°C for 1 hour.

Ligation of DNA fragments was carried out in a 20 μl reaction mixture containing 1x T4 DNA ligase buffer [Promega], 1.5 U T4 DNA ligase [Promega] and a 1:3 molar ratio of vector:insert DNA (roughly estimated from an ethidium bromide stained agarose gel). A control reaction without any insert DNA was carried out alongside. Ligation reactions were incubated overnight at 18°C and 5 μl of the reaction mix was transformed into competent *E. coli* cells (Section 2.2.3) the following day.

## 2.4.8   Polymerase chain reaction (PCR)

Polymerase chain reactions were carried out in a Biometra T3 thermocycler [Thistle Scientific].

DNA fragments for genomic modifications were made by PCR (as described in (Longtine et al., 1998) in a 100 μl reaction containing 1x PCR buffer, 2 μM of each primer, 200 μM dNTPs [GE healthcare], 5 U Taq polymerase [Abgene] and 100 ng

template plasmid DNA. The PCR program was an initial denaturation at 94°C for 5 minutes, followed by 20 cycles of 94°C (1 min), 55°C (30 sec), 72°C (1 min), and a final elongation step at 72°C for 10 minutes.

DNA probes for Southern blot analysis were made as above except with 1 μl of a genomic DNA prep from a wild type yeast strain (Section 2.3.10) as the template DNA.

Diagnostic colony PCR was carried out in 50 μl reactions containing 1x PCR buffer, 1 μM of each primer, 100 μM dNTPs, 2.5 U Taq polymerase. The yeast colony was smeared onto the bottom of the PCR tube and microwaved for 1 minute on full power (900 W), before being resuspended in the reaction mixture. The colony PCR program was an initial denaturation at 94°C for 5 minutes, followed by 30 cycles of 94°C (1 min), 50°C (30 sec), 72°C (1 min), and a final elongation step at 72°C for 10 minutes.

Details of the primers [Eurogentec] used in this study are shown in Table 2.3. All primers were supplied desalted.

**Table 2.5 Primers used in this study**

| Name | Sequence 5'-3' | Source |
| --- | --- | --- |
| P219 | TCT GCT GAT TTG CAA CAA GGC ACT ACA AAT GCG GCT GAT TTC TCT CTG ACC AGC TGA AGC TTC GTC CGC | This study |
| P220 | TCA TCA CTA TCA CCT TGG CTC AAA ACA ACT CTA GAC TTT TTG CCA AAA AGG CAT AGG CCA CTA GTG GAT CTG | This study |
| P267 | ATG TTC AGG TCG CAT GCC TCC GGT AAC AAG AAG CAA TGG TCA GCT GAA GCT TCG TAC GC | This study |
| P268 | TCA TTT CAA AGT TTC TAA ACG TTT ATA GAA ATC TTT TAC TGC ATA GGC CAC TAG TGG ATC TG | This study |
| P289 | GGTGGAGTAGATAATCGATG | This study |
| P521 | AGCTGCATCAGGTCGGAGAC | Cha lab |

| Name | Sequence 5'-3' | Source |
|------|----------------|--------|
| P617 | AAG ACA GCT TCT GGA GTT CAA TCA ACT TCT TCG GAA AAG ATA AAA AAC CAC ACA TAC GAT TTA GGT GAC AC | This study |
| P618 | CTA AGG AAG TTC GTT ATT CGC TTT TGA ACT TAT CAC CAA ATA TTT TAG TGA ATA CGA CTC ACT ATA GGG AG | This study |
| P619 | TGCGTTGCTGTGGTCTTCAG | This study |
| P620 | GGCAGGAAGAGAGAGCAAAAG | This study |
| P649 | CTGGAATGCTGTTTTGCC | Cha lab |
| P672 | AGGTCCGTCGAGTAGTAGAAGATTG | Oscar Aparicio |
| P673 | GTTGGTAACGAATTCTCACTCC | Oscar Aparicio |
| P674 | GAA AAC CAA GGA TCA GAT GTT TCG TTC AAT GAA GAG GAT TCC CAC CAC CAT CAT CAT CAC | This study |
| P675 | TAT AAA CAT ATA AAA AGA ATG GCG CTT TCT CTG GAT AAT TAT TAT ACT ATA GGG AGA CCG GCA GAT C | This study |
| P676 | GCA GCT TTA CCT GGT TTT G | This study |
| P677 | CTC ACT GCA GGA TAA TTG CGC | This study |
| P678 | GAT CGT ACC GAG TTA TCG AAG | This study |
| P679 | TCC GGG ACA ATC TTC AAA GG | This study |
| P680 | CAC GAA CAC CGT CAT TGA TC | This study |
| P681 | GAT GAG GAA CTG GTG CCA GTC | This study |

## 2.5  Protein techniques

### 2.5.1  Preparation of yeast TCA extracts

Yeast cells (~$10^7$-$10^8$ cells) were pelleted (3000 rpm, 2 min) and resuspended in 1 ml 20% (w/v) trichloroacetic acid (TCA) [Fisher Scientific]. Cells were transferred to a 2 ml tube, pelleted (13,000 rpm, 1 min) and resuspended in 200 μl 20% (w/v) TCA. Glass beads (0.5 mm) [BioSpec Products] were added up to the level of the liquid and mixed vigorously for 4 minutes using a vortex. Next, 400 μl of 5% (w/v) TCA was added to the tube and the whole aqueous extract removed to a new 2 ml tube. The precipitated proteins were pelleted (3000 rpm, 10 min, 4°C) and the supernatant

removed. To the protein pellet, 100 μl of 3x Laemmli buffer (150 mM Tris-HCl pH 6.8, 6% [w/v] SDS, 30% [v/v] glycerol, 0.3% [w/v] bromophenol blue, 15% [v/v] β-mercaptoethanol) and 50 μl of Tris-HCl pH 9.4 were added and mixed using a vortex for 10 seconds. The protein extract was incubated at 95°C in a hot block for 5 minutes. Insoluble material was pelleted (3000 rpm, 10 min, 4°C) and the soluble supernatant removed to a fresh tube for storage at -20°C.

## 2.5.2   SDS polyacrylamide gel electrophoresis

Proteins were separated by denaturing sodium-dodecyl-sulphate polyacrylamide gel electrophoresis (SDS-PAGE). Polyacrylamide gels (7 x 9 cm) were assembled in a Hoefer Dual Gel Caster vertical apparatus [Amersham Biosciences]. The resolving gel (% acrylamide [Protogel] as indicated, 0.04% [w/v] SDS, 375 mM Tris-HCl pH 8.8, polymerised with 0.1% [w/v] ammonium persulphate [APS] [Bio-Rad] and 0.05% [v/v] N,N,N',N'-tetramethyl-ethylenediamine [TEMED] [Bio-Rad]) was overlaid with stacking gel (5% [w/v] acrylamide, 0.04% [w/v] SDS, 375 mM Tris-HCl pH 6.8, polymerised as before) and left at room temperature to set with a well-forming comb in place. Protein samples were incubated in a hot block at 95°C for 5 minutes prior to loading on the gel and 5-10 μl of a TCA protein extract was loaded per lane. Electrophoresis was performed at a constant current of 35 mA in electrophoresis running buffer (365 mM glycine, 50 mM Tris base, 0.1% [w/v] SDS) until the bromophenol blue dye reached the bottom of the resolving gel. Proteins on the gel were detected by Western blot analysis (Section 2.6.3). The molecular weight of proteins was estimated by comparison with high-range rainbow molecular weight markers (5 μl per gel lane) [Amersham Biosciences].

## 2.5.3   Western blot analysis

The proteins separated by SDS-PAGE (Section 2.6.2) were transferred to a Protran nitrocellulose membrane [Schleicher & Schnell]. The V10-SDB semi-dry electroblotter apparatus [BDH] was assembled using Whatman 3MMChr filter paper, the membrane and the gel according to the manufacturer's instructions. The filter paper, membrane and gel were all pre-incubated in transfer buffer (40 mM glycine,

48.5 mM Tris base, 0.04% [w/v] SDS, 20% [v/v] methanol) for at least 10 minutes. The transfer was performed at 2-5 mA/cm$^2$ of gel area for 2 hours.

After transfer, the membrane was incubated with blocking buffer (phosphate-buffered-saline [PBS; Table 2.1] containing 0.2% [v/v] Tween-20 [PBS-T], 5% [w/v] dried milk [Marvel]) for 1 hour at room temperature. Then the membrane was probed with the indicated primary antibody (Table 2.5) at the appropriate dilution in blocking buffer, gently shaking overnight at 4°C. The next day the membrane was washed in PSB-T (3 x 20 min), and then incubated with the appropriate horseradish peroxidase-conjugated secondary antibody [Sigma] at a 1:10,000 dilution in blocking buffer for 1 hour. The membrane was washed (3 x 10 min) in PBS and the signal visualised by enhanced chemiluminescence (ECL) [GE healthcare]. The two ECL reagents were mixed in a 1:1 ratio and the membrane was incubated with a total volume of 3 ml of the ECL reagents for 1 minute at room temperature. The excess liquid was drained off the membrane, which was then wrapped in Saran wrap and exposed to autoradiography film [Kodak] in the dark in an exposure cassette. The time of exposure varied depending on the intensity of the signal. Multiple exposures were taken when the signal was to be subsequently quantified to obtain a signal in the linear range. Films were developed in an X150 X-ray film processor [X-ograph Imaging Systems]. Developed films were scanned and the images were saved as TIFF files. The band intensity was quantified with ImageJ software [NIH].

**Table 2.6 Antibodies used in this study**

| Antibody | Type | Dilution for Western blotting | Source |
|---|---|---|---|
| α-Clb2 | rabbit polyclonal | 1:1000 | Santa Cruz Biotechnology Inc. |
| α- Flag (M2) | mouse monoclonal | 1:5000 | Jean-Paul Vincent |
| α-HA (12CA5) | mouse monoclonal | 1:1000 | NIMR, London |
| α-MYC (9E10) | mouse monoclonal | 1:1000 | NIMR, London |
| α-phospho-Histone H3 | rabbit polyclonal | 1:1000 | Upstate Biotechnology |
| α-phospho-Rad53 (F9) | mouse monoclonal | 1:1000 | Marco Foiani |

| Antibody | Type | Dilution for Western blotting | Source |
|---|---|---|---|
| α-Rad53 (EL7) | mouse monoclonal | 1:1000 | Marco Foiani |
| α-tubulin (YL1/2) | rat monoclonal | 1:5000 | Abcam |

## 2.6  Fluorescence microscopy

### 2.6.1  Preparation of cells expressing green fluorescent protein (GFP)

A 900 μl sample of a mid-log phase culture was incubated with 100 μl of 37% (w/v) formaldehyde [Fisher Scientific] for 10 minutes at room temperature. The cells were pelleted (5000 rpm, 1 min), washed twice with 1 ml PBS, and then resuspended in 200 μl PBS. A 10 μl sample of the cell suspension was spread onto a glass microscope slide and left to dry. Before application of the glass coverslip, 2 μl of 4,6-diamino-2-phenylindole (DAPI) solution (1.5 μg/ml DAPI [Sigma] in Vectashield mounting medium [Vector Lab]) was dotted onto the dried cells.

### 2.6.2  Fluorescence microscopy

Fluorescence microscopy was performed on a Deltavision Spectris system containing a photometrics CH350L liquid cooled charge-coupled device camera and an Olympus IX70 inverted microscope with a 100x objective equipped with Deltavision data collection system [Applied Precision].

For each image, 20 images (0.2 μm apart) were acquired. Images were processed using SoftWoRx image processing suite [Applied Precision] and PhotoShop version CS [Adobe] software. Out of focus images were discarded prior to projecting the stack of images onto one plane. Exposure times varied and were dependent upon the intensity of the observed fluorescence.

## 2.7   Plasmid construction

The plasmids used in this study are summarised in Table 2.6. Details of the plasmid constructed in this study are given in Section 2.7.1.

**Table 2.7 Plasmids used in this study**

| Plasmid Name | Details | Reference/Source |
|---|---|---|
| pAG32 | PCR template for gene manipulation (pFA6a-hphMX4) | (Goldstein and McCusker, 1999) |
| pCLE5 | Original library clone. YEp24-*MEC1* | Cha lab |
| pKGFP-*MYO1* | *MYO1-GFP* integrative plasmid (*kan$^r$*) | Johnston lab stocks |
| pNH1 | YCpLac111-*RRM3* | Virginia Zakian |
| pNH2 | YCpLac111-*rrm3K260A* | Virginia Zakian |
| pNH20 | PCR template for gene manipulation (pU6His-10FLAG) | Katsuhiko Shirahige |
| pNH21 | pRS406-*MYO1-GFP* integrative plasmid | This study |
| pRSC38 | PUC19-*CHA1* | Cha lab |
| pRSC49 | PCR template for gene manipulation (pFA6kanMX4) | Wach et al., 1994 |
| pRS405-*mrc1-AQ* | *Mrc1-AQ-LEU2* integrative plasmid | Oscar Aparicio |
| pRS406-*CYK1-GFP* | *CYK1-GFP* integrative plasmid (*URA3*) | Johnston lab stocks |
| YCpLac111 | *LEU2,* ARS/CEN cloning vector | Johnston lab stocks |
| YIp5-*top2-1* | *top2-1* integrative plasmid | John Nitiss |

### 2.7.1   pRS406-*MYO1-GFP*

Plasmids pKGFP-*MYO1* and pRS406-*CYK1-GFP* were digested with *Sal*I and *Not*I. The resulting ~1 kb DNA fragment containing the C-terminus of *MYO1* fused to *GFP* was ligated into the purified pRS406 vector backbone to make plasmid pNH21. The resulting clones were checked by restriction enzyme digest.

## 2.8   Yeast strain construction

Details of all the strains used in this study are given in Table 2.8. Most strains are of the SK1 strain background, except for strain NHY421 and its derivatives where the S288C FLY30 strain (Johnston lab stocks, Luca and Winey, 1998) was backcrossed 5 times with SK1 wild type NHY233.

Details of strains constructed in this study by genomic modification are given below in Sections 2.8.1-2.8.6.

Details of strains constructed in this study by standard yeast methods (mating [Section 2.3.2], tetrad dissection [Section 2.3.3] and transformation [Section 2.3.8]) are given in Table 2.8.

### 2.8.1   Integration of a *MYO1-GFP* containing plasmid

To construct strain NHY449, the integrative plasmid pNH21 (pRS406-*MYO1*-GFP) was digested with *AflII* and transformed into NHY400 (SK1 wild type haploid). Stable integrants were selected on SD-URA media. Expression of Myo1-GFP was confirmed by fluorescence microscopy (Section 2.6.2). Transformation of strains NHY447, NHY411, NHY410, NHY448, and NHY425 with *AflII*-digested pNH21 generated the strains NHY450, NHY451, NHY452, NHY453, and 466, respectively.

### 2.8.2   Integration of a *top2-1* containing plasmid

Strains NHY30 and NHY31 were constructed as described previously (Nitiss et al., 1993). The integrative plasmid YIp5-*top2-1* was linearised with *Kpn*I and transformed into RCY1047 (SK1 wild type haploid). Stable integrants were selected on SD-URA media at 23$^{\mathrm{o}}$C. The transformants were then patched onto SC-5'-FOA media to select for elimination of the partial direct repeat of the wild type *TOP2* gene. The resulting strain was viable at 23$^{\mathrm{o}}$C and lethal at 37$^{\mathrm{o}}$C, consistent with published reports that *top2-1* converts strains to temperature sensitivity for growth (Nitiss et al., 1993).

### 2.8.3   C-terminal tagging of *Top2* with a *10FLAG* epitope tag

Strain NHY369 was generated by tagging the genomic copy of *TOP2* with a *10FLAG* epitope tag in the SK1 wild type strain, RCY682, using a PCR-based gene integration technique. A DNA fragment containing ten copies of the *FLAG* epitope flanking a kanamycin resistance gene (*kanMX4*) was generated by PCR from the template plasmid pNH20 (pU6His-*10FLAG*) using the 5' primer, P674, and the 3' primer, P675. The PCR product was then transformed into NHY682 and stable integrants were selected on YPD agar containing 200 µg/ml G-418.

Expression of *TOP2-10FLAG* was tested by Western blot.

### 2.8.4   Deletion of *TOF1*

The entire *TOF1* ORF was deleted using PCR-based gene disruption (Wach et al., 1994). A disruption cassette containing a marker gene encoding the hygromycin B phosphotransferase gene (*hphMX4*), which confers resistance to hygromycin B, was amplified from plasmid pAG32 (pFA6-hphMX4) using the 5' primer P219 and the 3' primer P220. The PCR product was transformed into RCY606 (SK1 diploid strain heterozygous for *mec1-4-URA3*) and stable integrants were selected on YPD-Hygro media.

Integration was confirmed by colony PCR using the 5' primer P619 with homology to the region upstream of the *TOF1* locus and the 3' primer P512 with homology to the hygromycin B resistance gene.

### 2.8.5   Deletion of *MRC1*

The entire *MRC1* ORF was deleted using PCR-based gene disruption (Wach et al., 1994). A disruption cassette containing a marker gene encoding the kanamycin resistance gene (*kanMX4*) was amplified from plasmid pRSC49 (pFA6-KanMX4) using the 5' primer P617 and the 3' primer P618. The PCR product was transformed into RCY606 (SK1 diploid strain heterozygous for *mec1-4-URA3*) and stable integrants were selected on YPD-Kan media.

Correct integration was confirmed by colony PCR using the 5' primer P620 with homology to the region upstream of the *MRC1* locus and the 3' primer P649 with homology to the kanamycin resistance gene.

### 2.8.6   Integration of *mrc1$^{AQ}$* containing plasmid

In order to construct strain NHY413, the integrative plasmid pRS405-*mrc1$^{AQ}$*, which integrates upstream of the *MRC1* locus was digested with *Nde*I and transformed into NHY237 (SK1 *mrc1Δ::KanMX4* haploid strain). Stable integrants were selected on SD-LEU media.

Correct integration was confirmed by colony PCR using the 5' primer P672 with homology to a region upstream of the *MRC1* locus and the 3' primer P673 with homology to the *mrc1*$^{AQ}$ gene.

### 2.8.7   Deletion of *RRM3*

The entire *RRM3* ORF was deleted using PCR-based gene disruption (Wach et al., 1994). A disruption cassette containing a marker gene encoding the hygromycin B resistance gene, *hphMX4*, was amplified from plasmid pAG32 using the 5' primer P267 and the 3' primer P268. The PCR product was transformed into RCY606 (SK1 diploid strain heterozygous for *mec1-4-URA3*) and stable integrants were selected on YPD-Hygro media.

Integration was confirmed by colony PCR using the 5' primer P289 with homology to the region upstream of the *RRM3* locus and the 3' primer P512 with homology to the hygromycin resistance gene.

# Chapter 3

# Characterisation of Replication Slow Zones

## 3.1  Introduction

Chromosome common fragile sites are specific loci that readily exhibit chromosome gaps and breaks on metaphase chromosomes, particularly following partial inhibition of DNA replication. They are evolutionarily conserved among mammalian species (Elder and Robinson, 1989; Ruiz-Herrera et al., 2004; Stone et al., 1991; Yang and Long, 1993) and are also found in lower eukaryotes including yeast (Admire et al., 2006; Lemoine et al., 2005). In humans, fragile sites have been associated with genome instability and tumourigenesis. Fragile sites that have acquired breaks are referred to as 'expressed' fragile sites. Conditions that contribute to fragile site expression include mild replication stress (Glover et al., 1984), premature chromosome condensation (El Achkar et al., 2005), and inactivation of ATR (Casper et al., 2002), an essential, evolutionarily conserved signal transduction protein.

In *S. cerevisiae*, chromosome breakage has been observed in late replicating regions of the chromosome known as replication slow zones (*RSZs*) in the absence of functional Mec1, the yeast homologue of ATR, during an otherwise unperturbed S-phase (Cha and Kleckner, 2002). Due to the essential function of Mec1 in dNTP synthesis, loss of Mec1 likely leads to the failure to up-regulate dNTP levels in late S-phase. Indeed, chromosome breakage in these cells is alleviated by deletion of the ribonucleotide reductase inhibitor, Sml1. Another region that displays fragility is located immediately adjacent to the early-firing origin ARS310 when polymerase levels are limiting (Lemoine et al., 2008; Lemoine et al., 2005). Interestingly, it was independently shown that cells lacking an intact replication checkpoint (*mec1* or *rad53* mutants) exhibit chromosome fragility at this same site (Raveendranathan et al., 2006). Taken together, these studies in yeast, in addition to evidence from

mammalian systems, suggest that chromosome fragility occurs at specific sites in the genome that are more sensitive to replication stress than other regions and, as a result, require S-phase checkpoint proteins for timely fork progression (Casper et al., 2002).

*RSZs* are thought to be genetic determinants that are about 10kb in size and are found in alternation with active replication origins along the entire length of a chromosome excluding the centromere region (Cha and Kleckner, 2002) (Figure 3.1). The name *RSZ* stems from the observation that the rate of replication fork progression slows down as the forks enter these zones when compared to non-*RSZs* in the same chromosome (Cha and Kleckner, 2002). It is unknown why fork progression is delayed in these regions, however, the fact that these are late replicating regions of the chromosome suggests that dNTP pools might be limiting by the time replication forks reach the *RSZs*. Other hypotheses include chromosome architecture or the formation of secondary structures at these sites may physically hinder fork progression. In wild type cells, replication forks continue to progress through these zones, albeit more slowly, eventually completing the duplication of the *RSZs*. Upon thermal inactivation of a temperature-sensitive allele of Mec1, replication forks stall permanently at *RSZs* until they give rise to chromosome breaks (Cha and Kleckner, 2002).

Budding yeast *RSZs* and the mammalian fragile sites share a number of characteristics (discussed in Section 3.3.3), including the involvement of Mec1 and ATR in suppressing their expression. These considerations suggest a common mechanism underlying fragile site expression in the two systems.

As a starting point to this thesis, genomic features and characteristics of *RSZs* were investigated further in order to gain a better understanding of the nature of these sites and to establish whether *RSZs* are a suitable model for studying the factors underlying chromosome stability at common fragile sites.

Figure 3.1 The distribution of *RSZs* on chromosome III relative to chromosomal determinants

## 3.2   Results

### 3.2.1   Mapping *RSZs* on chromosome VI

Currently, *RSZs* have only been mapped on chromosome III. According to their distribution along this chromosome, *RSZs* occur in regular alternation with active origins of replication along the entire length of the chromosome except in the centromere region. Although they do not correspond to known pause sites, *RSZs* tend to coincide with replication termination zones and sites of transposon insertion (Cha and Kleckner, 2002). In order to see if this distribution of *RSZs* holds true on other chromosomes, *RSZs* were mapped on chromosome VI.

The positions of *RSZs* along chromosomes were mapped using pulsed-field gel electrophoresis (PFGE) followed by indirect end-labelling Southern analysis, as described previously (Cha and Kleckner, 2002). Chromosomes were separated by PFGE with the parameters described in Section 2.4.3. Indirect labelling of one chromosome was performed by Southern analysis using probes that hybridise to either the right or the left sub-telomeric region of that chromosome. During PFGE, branched structures such as replication intermediates remain in the well (Hennessy et al., 1991), whereas linear species such as the full-length chromosome and chromosome fragments extending from the labelled end are separated according to size. The positions of break points along the chromosome were deduced from the length of the chromosome fragments (Figure 3.2).

Wild type cells and cells expressing the temperature-sensitive allele of *MEC1*, *mec1-4*, were grown to mid-log phase in YPD at the permissive temperature of $23^{o}$C. The cells were then synchronised in G1 with $\alpha$-factor for two hours at $23^{o}$C and then for a further half hour at $37^{o}$C, the restrictive temperature for the *mec1-4* strain. The cultures were washed and released into pre-warmed YPD at $37^{o}$C. Samples were harvested 5 hours after release from $\alpha$-factor and processed for PFGE and Southern analysis. For analysis of chromosome VI species, the *COS4* and *IRC7* probes that hybridise to regions approximately 6 kb from the left telomere and 11 kb from the right telomere, respectively, were used. In order to determine the sizes of the chromosome fragments, the lambda ladder PFG size marker [New England Bioloabs]

Figure 3.2     Procedure for mapping chromosome break sites using PFGE and indirect end-labelling Southern analysis

was loaded alongside the wild type and *mec1-4* samples. To visualise the lambda ladder, 5 ng of *HindIII*-digested lambda DNA [New England Biolabs] was added to the labelling mix along with the *COS4* and *IRC7* probes. The fragment sizes were estimated as described in Section 2.4.4.

Hybridisation with *COS4* revealed three break regions on the left arm of chromosome VI while hybridisation with the *IRC7* probe revealed two breakage zones on the right arm of chromosome VI (Figure 3.3A and B). The *IRC7* probe was also able to detect two of the three break zones on the left arm of chromosome VI (Figure 3.3B). The chromosome breaks generally formed a broad band in the PFG consistent with the notion that breaks occur throughout a broad region rather than at a specific point. The positions of break zones along chromosome VI is depicted in Figure 3.4. Since *RSZs* are defined as breakage regions following inactivation of Mec1, from here on these breakage zones identified on chromosome VI are referred to as *RSZs*. Similar to the pattern of *RSZs* along chromosome III, *RSZs* occurred in alternation with replication origins on chromosome VI, except between origins surrounding the centromere. All the *RSZs* on this chromosome seem to coincide with termination sites, although the two termination sites close to the centromere do not correspond to *RSZs*. Two of the *RSZs* identified on chromosome VI correspond to sites of transposon insertion with one these *RSZs* also associating with a tRNA gene. The other three *RSZs* do not appear to correlate with these or other known chromosomal determinants. However, it must be noted that although the chromosome fragment sizes (and therefore the positions of the *RSZs*) were determined mathematically, the precise coordinates of the *RSZs* as well as the exact width of each *RSZ* remains an approximation and it is conceivable that the real chromosomal features corresponding to each *RSZ* may be different from those presented in this thesis.

This result confirms the observed distribution of *RSZs* on chromosome III in relation to the location of active replication origins, the centromere, and sites of transposon insertion, suggesting that this pattern of positioning might constitute a general feature of *RSZs*.

Figure 3.3     Mapping *mec1-ts* break zones on chromosome VI

Figure 3.4    Distribution of *RSZs* on chromosome VI in relation to chromosomal determinants

### 3.2.2    Flexibility peaks define a new chromosomal determinant

Among the proposed characteristics for mammalian common fragile sites is their propensity to contain areas of high DNA flexibility (Mishmar et al., 1998; Zlotorynski et al., 2003). To our knowledge, DNA flexibility of yeast chromosomes has not been measured previously, so it was necessary to characterise flexible regions on yeast chromosomes and determine whether they correspond to previously identified chromosomal features. To this end, the DNA flexibility was measured in all sixteen chromosomes of *S. cerevsiae* and compared to positions of centromeres, origins, termination zones, tRNA genes, and transposon insertion.

Evaluation of the potential DNA flexibility of the yeast chromosomes was performed by Peter Rosenthal (Division of Physical Biochemistry, National Institute for Medical Research) using the TwistFlex computer program (a gift from Catherine Freudenreich, Tufts University). The program predicts the flexibility of the DNA helix by using measurements of potential fluctuations of the twist angle between consecutive base pairs in a sequence of DNA (Sarai et al., 1989). This measure provides average twist angle fluctuations for each of the possible dinucleotides and thus enables the evaluation of the flexibility of a DNA sequence by averaging these values in a sliding window. The analysis was performed as described previously for mammalian common fragile sites (Zlotorynski et al., 2003) using sliding windows of 100 bp and where deviations of the twist angle higher than $13.7^{o}$, the default theshold value used in the program, were considered high flexibility peaks. The DNA sequence used for this analysis was that of the fully sequenced S288C strain and was retrieved from the *Saccharomyces* Genome Database (SGD; www.yeastgenome.org).

The regions containing high DNA flexibility peaks were correlated with other chromosomal features including centromeres, tRNA genes, Ty and Δ elements, as well as origins of replication and termination sites. The chromosomal coordinates of centromeres, tRNA genes, and Ty/Δ elements for each chromosome was obtained from the SGD database.

Replication origins were plotted according to the distribution of origin recognition complex (ORC) and minichromosome maintenance (MCM) proteins (Wyrick et al.,

2001). ORC is a six-subunit complex that binds to replication origins and coordinates the assembly of the pre-replicative complex (pre-RC) at each origin that, in turn, is required for initiation of DNA replication (Toone et al., 1997) (Section 1.4). One of the components of the pre-RC is the MCM complex (Toone et al., 1997). Sites where ORC and MCM complexes bind simultaneously were shown to correlate well with experimentally detected origin activity, suggesting that ORC-MCM binding sites represent landmarks of replication origins (Wyrick et al., 2001).

The location of replication termination zones on chromosomes III, VI, and X was deduced from the replication profiles of these chromosomes (Raghuraman et al., 2001). Raghuraman et al. (2001) grew cells in isotopically dense culture medium before allowing the cells to enter synchronous S-phase in isotopically light medium. Replicated DNA [heavy-light (HL)] and DNA that remained un-replicated [heavy-heavy (HH)] was isolated at various time points throughout S-phase and hybridised to a whole genome microarray to reveal the relative level of chromosome sequences that are replicated versus un-replicated at different times in S-phase. The replication profile of a certain chromosome is constructed by plotting the extent of replicated DNA ($\%HL_{(total)}$) as a function of the chromosome coordinate. In these replication profiles, peaks represent regions that replicate earlier than the surrounding sequences and must therefore correspond to origins of replication while the troughs are indicative of the sites at which replication forks terminate (Raghuraman et al., 2001). As the replication profiles of only chromosomes III, VI, and X were determined, termination zones could only be plotted on these chromosomes. This type of replication profile can also be used to identify and map origins of replication, in particular taking into account the activity of each origin; however, as the authors did not assess the replication profiles of all sixteen chromosomes, the distribution of ORC-MCM binding sites was chosen in order to plot origins of replication along each of the sixteen chromosomes. Note that while the position of ORC-MCM complexes almost accurately identifies the location of replication origins, it cannot distinguish between origins that are active from those that are dormant.

The positions of high flexibility peaks (above $13.7^\circ$) in relation to the distribution of chromosomal features for each chromosome is shown in Figures 3.5 and 3.6. In total, 133 high flexibility peaks were found, averaging one peak every 121 kb and ranging

between 52 kb (chromosome V) and 261 kb (chromosome XIV) apart. The average distance between the high flexibility peaks and other chromosomal determinants is shown in Table 3.1 (a complete list of the distances between each Flexibility peak and the nearest chromosomal feature can be found in Appendix I). Statistical analysis revealed that the observed distance between sites of high DNA flexibility and centromeres, Ty elements, and $\Delta$ elements was not significantly different from the distance expected if the flexibility sites were distributed renadomly in the genome (Table 3.1 and Appendix 2). On the other hand, the P-values of the distances between regions of high DNA flexibility and either tRNA genes or replication origins suggests that these features are actually further away from the flexibility sites than would be expected by chance (Table 3.1 and Appendix 2). Taken together, these data suggest that high DNA flexibility peaks do not coincide significantly with centromeres, replication origins, tRNA genes, and Ty/$\Delta$ elements. In contrast, on the three chromosomes where termination sites could be mapped, there was slightly more overlap with sites of replication termination where 36% of the peaks occurred within 5 kb of a termination site and 64% of the flexibility peaks were found within 10 kb of a termination site (Table 3.2). Statistical analysis of these values could not be performed as the number of mapped termination sites is too low.

**Table 3.1 Average distance between peaks of high DNA flexibility and other chromosomal determinants.**

|  | Centromere | Origin | Ty | $\Delta$ | tRNA |
|---|---|---|---|---|---|
| **Distance from Flex[a] (kb)** | 294.5 | 15.8 | 124.3 | 45.5 | 32.3 |
| **P-values[b]** | 0.281 | 0 | 0.164 | 0.07 | 0.002 |

[a] Average distance a flexibility peak is from the nearest chromosomal feature (e.g. origin of replication) in kb.
[b] P-values were calculated by Mario Dos-Reis (Mathematical Biology, NIMR). Calculations were based on a simulation of 1000 sets of flexibility sites, each sampled from a uniform distribution. Details of these calculations are shown in Appendix II.

**Table 3.2 Overlap between peaks of high DNA flexibility and termination zones on chromosomes III, VI, and X.**

| | **Flexibility peaks (Flex)** | **Termination site[a] (5 kb from Flex)** | **Termination site[a] (10 kb from Flex)** |
|---|---|---|---|
| **Number** | 14 | 5 | 9 |
| **Percentage[b]** | 100% | 36% | 64% |

[a]The number of termination sites on each chromsome was deduced from replication profiles of these chromosomes (Raghuraman et al., 2001)
[b]Values correspond to the number of flexibility peaks that coincide with the indicated chromosomal determinants expressed as a percentage of the total number of flexibility peaks in the genome.

Taken together, these results indicate that the occurrence of regions of high DNA flexibility and centromeric regions are mutually exclusive. Regions of high DNA flexibility do not tend to correspond to origins of replication and are, therefore, more likely to correlate with sites of replication termination. Indeed, a higher degree of correlation was observed between termination sites and regions of high DNA flexibility. However, it is important to note that this correlation was based on the distribution of termination sites on only three chromosomes and, therefore, may not be a true representation of the situation on all chromosomes. Regions of high DNA flexibility do not correlate significantly with tRNA genes or with sites of transposon insertion. The lack of a strong correlation with these previously determined chromosomal features suggests that high flexibility regions may define a new chromosomal determinant.

Figure 3.5    Flexibility analysis of chromosomes I to VIII in relation to relevant chromosomal determinants

Figure 3.6      Flexibility analysis of chromosomes IX to XVI in relation to relevant chromosomal determinants

### 3.2.3   *RSZs* correlate with either regions of high DNA flexibility or transposon insertion sites

One feature of mammalian common fragile sites is that they contain a high number of flexibility peaks that are extremely AT-rich and often occur in clusters (Mishmar et al., 1998; Zlotorynski et al., 2003). No correlation between the location of *RSZs* and the nucleotide composition of the chromosome could be determined, however, this could be attributed to the fact that the yeast genome is generally AT-rich and may obscure the identification of distinctly AT-rich regions corresponding to *RSZs* (A. Johnson, personal communication). In Section 3.2.2, regions of high DNA flexibility were identified as chromosomal determinants whose distribution does not correlate strongly with any other chromosomal feature. Considering the similarities between the properties of *RSZs* and mammalian fragile sites, it was necessary to determine whether *RSZs* also correlate with regions of high DNA flexibility.

As performed in Section 3.2.2, flexibility peaks exceeding $13.7^{o}$ were considered areas of high DNA flexibility. The chromosomal coordinates of the other features were retrieved from the SGD database. The distribution of high flexibility regions on chromosomes III and VI, where *RSZs* have been mapped (Section 3.2.1), was analysed in more detail. On chromosome III, four of the six flexibility peaks identified was found within or at the edge of a *RSZ* (Figure 3.7; *RSZ-I* and *-V*). Three of the *RSZs* that did not contain a high flexibility peak, coincided with regions of transposon insertion (Figure 3.7; *RSZ-II*, *-III*, and *-VI*). The sixth *RSZ* identified on chromosome III (*RSZ-IV*) did not appear to correlate with either of these chromosomal determinants.

Similarly, all four of the high flexibility peaks identified on chromosome VI are located within or close to a *RSZ* (Figure 3.8; *RSZ-II*, *-III*, and *-V*). Of the remaining two *RSZs* that do not contain a region of high DNA flexibility, one is associated with a transposon insertion site (*RSZ-IV*), while the other does not correspond with any chromosomal determinant other than a termination zone (*RSZ-I*).

Therefore, eight out of the ten (80%) high flexibility peaks predicted to occur on chromosomes III and VI fall within or at the edge of a *RSZ*. The remaining two

flexibility peaks occur near the telomeres of chromosome III, where *RSZs* can not be mapped (Cha and Kleckner, 2002), and may therefore not be informative to this study. The flexibility peaks associated with *RSZs* on both chromosomes III and VI generally ranged between $13.75^{o}$ and $14.3^{o}$, with *RSZ-V* on chromosome III containing a very high flexibility peak corresponding to a twist angle value of $15.7^{o}$. Of the six *RSZs* on chromosomes III and VI that are not associated with a high DNA flexibility peak, four correspond to Ty/$\Delta$ elements (67%). Taken together, these results suggest that *RSZs* tend to occur either at regions of high DNA flexibility or at sites of transposon insertion. However, some *RSZs* that were identified did not correspond to either of these chromosomal determinants, suggesting that DNA flexibility and transposon insertion may not be strictly defining features of *RSZs*. Monitoring the pattern of breakage at *RSZs* in a *mec1-4* strain where either a Ty/$\Delta$ element or a high DNA flexibility peak is deleted should provide some insight into whether these elements are absolutely responsible for the fragility of these sites.

Figure 3.7    *RSZs* on chromosome III coincide with high DNA flexibility peaks and transposon insertion sites

Figure 3.8     *RSZs* on chromosome VI coincide with high DNA flexibility peaks and transposon insertion sites

### 3.2.4 Low levels of Hydroxyurea (HU) induce chromosome breakage at *RSZs* in *mec1Δ sml1Δ*

*RSZs* are thought to be genetic determinants of the normal yeast chromosome that hinder or slow replication fork progression in wild type cells, and drastically stall the fork in the absence of Mec1 function. However, elimination of the ribonucleotide reductase (RNR) inhibitor, *SML1*, prevents fork stalling and chromosome breakage at these sites, presumably by increasing dNTP levels (Cha and Kleckner, 2002). This suggests that fork slowing and/or stalling at *RSZs* is dependent on dNTP availability. In order to discern whether fork stalling due to dNTP depletion causes DSB formation at *RSZs* or whether these regions are genetic determinants that are prone to fork stalling and chromosome breakage, break formation was monitored in *mec1Δ sml1Δ* cells treated with varying doses of hydroxyurea (HU). HU directly inhibits the activity of RNR by scavenging the tyrosyl-free radical in the active site of the enzyme, thus depleting dNTP pools (Yarbro, 1992). Treatment of wild type cells with this drug results in a delay in replication progression causing S-phase to proceed in slow motion (Alvino et al., 2007).

Log phase cells of *mec1Δ sml1Δ* grown in YPD at $30^oC$ were synchronised in G1 with α-factor for two and a half hours at $30^oC$. The cultures were then split and released into YPD containing either 0 mM, 10 mM, 50 mM, or 100 mM HU at $30^oC$. Samples were collected for PFGE and Southern analysis 5 hours after release from α-factor. Southern hybridisation was performed using the *CHA1* probe previously used to analyse the status of chromosome III (Cha and Kleckner, 2002). As a positive control, DNA extracted from *mec1-4* cells grown for 5 hours the non-permissive temperature of $37^oC$ was loaded in the same gel. To test the viability of *mec1Δ sml1Δ* under these conditions, cells were plated out onto YPD at t=0 and 5 hours after release into HU. The agar plates were incubated at $30^oC$ for three days before the colonies were scored.

Compared to *mec1Δ sml1Δ* cells grown in YPD, *mec1Δ sml1Δ* drastically lost viability in 10 mM, 50 mM, and 100 mM HU (Figure 3.9A). The loss of viability correlated with the concentration of HU used (Figure 3.9A).

As expected, the *mec1-4* strain acquired chromosome breaks at *RSZs* on chromosome III whereas breaks were absent in the *mec1Δ sml1Δ* mutant grown in YPD (Figure 3.9B). Similar to the *mec1-4* control, *mec1Δ sml1Δ* cells accumulated breaks at *RSZs* in the presence of 10 mM HU (Figure 3.9B). Breaks were absent in *mec1Δ sml1Δ* cells treated with either 50 mM or 100 mM of HU. This indicates that, similar to mammalian common fragile sites, the stability of *RSZs* is severely challenged by conditions that slow down DNA replication. In cells treated with high amounts of HU, replication is initiated from early-firing origins but elongating replication forks stall about 8-10 kb away form these origins (Lengronne et al., 2001). Therefore, the observation that breaks are absent in *mec1Δ sml1Δ* cells treated with high doses of HU suggests that replication forks must reach *RSZs* in order to acquire DSBs. As *RSZs* occur in between active origins of replication, a high dose of HU would impede DNA replication shortly after the origins fire whereas a lower dose of HU might allow the replication forks to progress until they reach the *RSZs* where the forks stall due to insufficient dNTP levels, culminating in the eventual formation of DSBs at these sites.

Figure 3.9     Inhibition of DNA replication by low levels of HU induces chromosome breakage at *RSZs*

### 3.2.5   Stalled forks do not immediately collapse in *mec1Δ sml1Δ* cells treated with 10 mM HU

Replication forks progress slowly through *RSZs* in wild type cells. This slowing down of the fork is exacerbated in *mec1-ts* cells such that the fork stalls and chromosome breakage at these sites eventually ensues. This prolonged stalling at *RSZs* in *mec1-ts* is thought to be physiological as cells at this stage resume growth when returned to permissive temperature. It is not until breaks are formed at these sites that the cells are committed to inviability (Cha and Kleckner, 2002). Chromosome breakage at *RSZs* occurs when DNA replication is challenged by low doses of HU, but not by high doses of this drug (Section 3.2.4). Replication forks stalled with DNA damaging agents (including HU) in checkpoint-deficient cells are thought to undergo stochastic fork collapse in S-phase (Sogo et al., 2002; Tercero and Diffley, 2001). In order to ascertain whether forks impeded by low doses of HU collapse stochastically or whether they remain stably stalled until DSBs are formed, the timing of cell death in relation to replication progression in *mec1Δ sml1Δ* strains treated with 10 mM HU was assessed.

Log phase cultures of *mec1Δ sml1Δ* cells grown at $30^{o}$C were synchronised in G1 with α-factor for two and a half hours. The cells were then released into YPD containing either 0 mM, 10 mM, or 100 mM HU at $30^{o}$C. To assess the progression of DNA replication in these cultures, samples were collected every twenty minutes and processed for fluorescence-activated cell scanning (FACS) analysis. At the same time points, cells were removed from the cultures, washed, and plated onto YPD agar plates. The plates were then incubated at $30^{o}$C for three days and colonies were counted in order to determine the kinetics of death in these strains.

As a control, a similar experiment was performed with *mec1-ts* cells. Cells where the *mec1-4* allele replaces the endogenous copy of *MEC1* are viable at $30^{o}$C and undergo several cell cycles before losing viability and accumulating breaks at *RSZs*, even at $37^{o}$C. They are therefore unsuitable for accurate cell cycle analysis of the *mec1-4* allele. Instead, cells where *mec1-4* is placed in the ectopic *ARG4* locus have a lower restrictive temperature than the endogenous *mec1-4* strains as they lose viability and

accumulate breaks at *RSZs* during the first cell cycle at 30°C. As a result, the ectopic *arg4::mec1-4* strain was used for all cell cycle analyses. It is unclear why placing the same allele at two different loci confers a different phenotype, but it is possible that varying levels of gene expression arise from the native promoter when placed at different chromosomal locations.

Log phase cultures of *arg4::mec1-4* cells grown at 23°C were synchronised in G1 with α-factor for two hours and then for a further half hour at 30°C, the non-permissive temperature for ectopic *arg4::mec1-4* cells. The cells were then released into pre-warmed YPD at 30°C and samples collected at the indicated time points for FACS analysis. To assess the kinetics of cell death, cells were also removed at these time points and plated onto YPD agar. The agar plates were then incubated at 23°C for three days.

As expected, *mec1Δ sml1Δ* cells grown in YPD and *arg4::mec1-4* cells grown at permissive temperature (23°C) entered and exited S-phase efficiently at 20 and 40 minutes, respectively (Figure 3.10A). These cells did not lose viability (data not shown). The same strain treated with 100 mM HU lost viability 30 minutes after release into HU, when cells were just entering S-phase (Figure 3.10). However, when *mec1Δ sml1Δ* cells were released into 10 mM HU, the cells maintained viability for a further forty minutes compared to the same strain treated with 100 mM HU (Figure 3.10). FACS analysis of these cells showed that cells entered S-phase 20 minutes after release from α-factor and remained with intermediate DNA content (between 1C and 2C peaks on the FACS profile) for the remainder of the experiment (Figure 3.10). Interestingly, cells in 10 mM HU remained with intermediate DNA content for at least forty minutes before they lost viability, suggesting that forks stalled in this situation may not collapse immediately. However, the timing of break formation at *RSZs* in *mec1Δ sml1Δ* cells in the presence of 10 mM HU in relation to the FACS profiles and the timing of cell death must be assessed in order to confirm this notion.

Figure 3.10 *mec1Δ sml1Δ* cells treated with low doses of HU exhibit loss of viability after a short delay in S-phase

The fact that *mec1Δ sml1Δ* cells lose viability as soon as they enter S-phase in 100 mM HU suggests that replication forks in these cells collapse shortly after replication initiation. On the other hand, there is a clear delay between fork stalling and loss of viability in *mec1Δ sml1Δ* cells treated with a low dose of HU suggesting that, although replication progression is slowed by the treatment with HU, replication forks may not collapse immediately. Similarly, *arg4::mec1-4* showed a comparable delay between fork stalling (as evidenced by the accumulation of cells with intermediate DNA content) and loss of viability. This suggests that, unlike *mec1* cells treated with high doses of HU that induce fork collapse soon after replication initiation, cells treated with low doses of HU may resemble the situation in *arg4::mec1-4* cells where replication forks stall in a replication-competent manner at *RSZs* for some time before being converted into DSBs. However, more detailed analysis of replication intermediates at *RSZs* in presence of varying amounts of HU using two-dimensional (2D) gel electrophoresis is required in order to verify this notion.

## 3.3   Discussion

### 3.3.1   Characteristics of RSZ are maintained in other chromosomes

*RSZs* were previously mapped on chromosome III, the chromosome that has been studied most comprehensively in terms of chromosomal features such as origins of replication and termination sites. On this chromosome, *RSZs* appear to occur between highly active origins of replication, coinciding with sites of replication termination (Cha and Kleckner, 2002). However, not all termination sites correspond to *RSZs*, raising the possibility that these may not be a defining feature of these regions. Interestingly, *RSZs*, or at least breaks at *RSZs*, do not occur between the origins surrounding the centromeric region of chromosome III (Cha and Kleckner, 2002). In addition, evidence of transposon insertion is frequently associated with *RSZs*. There is no obvious correlation between *RSZs* on chromosome III and known natural programmed pause sites that often occur in the genome and include tRNA genes, although these are often also sites for integration of transposable elements (Kim et al., 1998).

In order to determine whether these characteristics of *RSZs* can be applied to *RSZs* on other chromosomes, *RSZs*, defined as preferred breakage zones following Mec1 inactivation, were mapped on chromosome VI, another well-studied chromosome. Positions of *mec1-4* breakpoints corresponding to *RSZs* were mapped on chromosome VI by PFGE followed by indirect end-labelling Southern analysis. This analysis revealed five break sites on chromosome VI. As on chromosome III, *RSZs* occur in alternation with origins of replication on chromosome VI (Figure 3.4). All five sites coincide with replication termination zones but, similar to chromosome III, not all termination sites correspond to *RSZs* (Figure 3.4). Furthermore, no breaks were observed in the centromeric region. Ty elements as well as Δ elements of transposons occur in at least two of the five *RSZs* identified on chromosome VI. Therefore, the distribution of *RSZs* on chromosome VI closely mirrors that on chromosome III suggesting that these characteristics of *RSZs* may be universal.

It is interesting that *mec1-ts* breaks are excluded from centromeric regions on both chromosomes III and VI even though origins of DNA replication are located on either side of the centromere in both chromosomes and termination sites also occur here. Centromeres are packaged by nucleosomes into a specialised and unique form of chromatin (Cleveland et al., 2003). In addition, centromeres are protected from cohesin cleavage until the onset of anaphase (Section 1.5.2). Taking into account the specialised structure of centromeres and the fact that events at these sites are executed differently from other regions on the chromosome arms, it is no surprise that these sites are regulated differently when it comes to break formation at *RSZs*. Perhaps the unusual structure of the centromere renders it resistant to the factors involved in chromosome breakage at *RSZs*. Furthermore, mammalian common fragile sites and *RSZs* tend to be late replicating regions of their respective chromosomes. Centromeres in *S. cerevisiae* replicate early on in S-phase compared to telomeric regions of the chromosome (Raghuraman et al., 2001). This raises the possibility that centromeric regions are, in a way, forced to complete replication early, thereby precluding fork stalling and, consequently, chromosome breakage in these regions. However, centromeres have been identified as natural fork pausing sites (Greenfeder and Newlon, 1992), suggesting that replication forks do stall at these regions despite being replicated early.

*RSZs* on both chromosomes III and VI occur between active origins of replication and, therefore, tend to coincide with sites of replication termination. However, the fact that not all termination sites are *RSZs*, and that structures normally visualised at termination sites by 2D gel electrophoresis are not seen at *RSZs*, argues against these zones being areas where opposing replication forks converge and terminate (Cha and Kleckner, 2002). Furthermore, *RSZs* are thought to be physically determined in that their distribution is not altered upon deletion or inactivation of ARS sequences essential for origin activity (Cha and Kleckner, 2002). However, deletion of these same ARS sequences has been shown to result in the activation of other, more dormant origins (Vujcic et al., 1999). This raises the possibility that in the *mec1-ts* strain lacking active origins of replication on one arm of the chromosome, replication may initiate from origins of replication that are normally dormant, resulting in the termination of replication at or close to the same *RSZ*. Derivatives of chromosome III lacking origins of replication seem to replicate efficiently either by the activation of dormant origins of replication or, when these are also eliminated, by some unknown mechanism (Dershowitz et al., 2007; Theis et al., 2007). Furthermore, replication of *RSZs* occurs towards the end of S-phase when, presumably, dNTP levels are limiting. Similarly, termination sites are the last regions to become replicated as they occur between origins of replication. The observation that fork stalling and chromosome breakage at *RSZs* in *mec1-ts* cells can be averted by increasing dNTP synthesis suggests that forks stall at these sites due to a shortage of dNTPs as the replication forks approach their termini. Although these considerations make it unclear whether *RSZs* are, in fact, physically determined features of the chromosome, the observation that these regions coincide with Ty/Δ elements and/or regions of high DNA flexibility is consistent with the view that these zones are genetically specified rather than being reliant on the position and activation of replication origins. In addition, the finding that chromosome breakage at *RSZs* in *MEC1*-deficient cells occurs after treatment with low levels of HU but is absent in cells treated with high doses of this drug (Section 3.2.4) suggests that replication forks must reach the *RSZs* in order for break formation to ensue (a model depicting this hypothesis is shown in Figure 3.11). This further supports the notion that *RSZs* constitute specialised regions of the chromosome. Alternatively, low doses of HU could delay replication without immediately killing the cells, thereby allowing *mec1Δ sml1Δ* cells to execute G2/M

134

events that generate DSBs at incompletely replicated DNA within *RSZs*. In contrast, *mec1Δ sml1Δ* cells exposed to high amounts of HU could undergo fork collapse and lose viability early on in S-phase, before these G2/M events can take place (Figure 3.11).

Although the distribution of *RSZs* along chromosomes III and VI appears to follow a similar pattern, one factor to consider is that the replication profiles of chromosomes in *mec1-ts* cells may differ significantly from those in wild type cells. Indeed, *mec1Δ sml1Δ* cells treated with HU show a different pattern of origin activation compared to wild type cells whereby dormant origins become activated in these strains (Raveendranathan et al., 2006). This must be taken into consideration when mapping *RSZs*, especially if *RSZs* are not physically determined areas of the chromosome and are, instead, dependent on the activity of replication origins. As mentioned above, it is also important to note that the mapping of *RSZs* on chromosomes III and VI is based on a rough estimation of the length of the chromosome fragments that appear in *mec1-ts* cells and is therefore subject to some level of error. Additionally the precise width of these zones was not acurately determined. One way of mapping these zones more accurately would be to digest DNA extracted from *mec1-4* cells at non-permissive temperature at restriction sites surrounding each *RSZ* and separate the digested DNA by standard agarose gel electrophoresis. Hybridisation with a probe corresponding to a region directly upstream or downstream of the *RSZ* (but still within this restriction fragment) should reveal several bands or a smear that will give a more precise indication of the width of each *RSZ*.

Nevertheless, the observation that the distribution of *RSZs* along chromosomes III and VI follows a similar pattern suggests that, for the most part, the same characteristics could be applied to *RSZs* genome-wide.

Figure 3.11    Chromosome breakage at *RSZs* requires a certain level of replication
progression

### 3.3.2   **Flexibility peaks and *RSZs***

One feature of mammalian common fragile sites is that they are highly flexible compared to other regions of the same chromosome. In order to determine whether *RSZs* also contained regions of high DNA flexibility, the flexibility of yeast chromosomes was predicted using the TwistFlex computer program. As performed in previous studies in mammalian systems, variations in the possible twist angle of values above $13.7^o$ were considered peaks of high DNA flexibility. Interestingly, peaks of high flexibility did not coincide significantly with previously identified chromosomal determinants, including transposon insertion sites, replication origins, tRNA genes, or centromeres, suggesting that DNA flexibility peaks may be considered a novel chromosomal determinant.

A strong correlation between peaks of high DNA flexibility and *RSZs* was detected on chromosomes III and VI where four out of six and four out of four peaks of high DNA flexibility, respectively, appeared to overlap with a *RSZ*. However, the fact that some *RSZs* identified did not contain high flexibility peaks suggests that this may not be a strictly defining feature of *RSZs*. Similarly, chromosome fragility at common fragile sites in humans does not always involve individual flexibility peaks suggesting that other factors may also be required for expression of common fragile sites (Durkin et al., 2008). Another factor to consider is that the threshold value of the twist angle used to determine which peaks are highly flexible may be too high for some chromosomes. Although $13.7^o$ was used as the cut-off threshold level for most flexibility analysis of mammalian common fragile sites, it is likely that chromosomes have different average flexibility values and that the threshold value should be set according to the average flexibility of the chromosome being analysed. Lowering the threshold value may reveal other flexibility peaks that may also correspond to *RSZs*.

The controversy over whether DNA flexibility is a crucial feature of *RSZs* (and possibly mammalian fragile sites) could be settled by testing whether eliminating specific flexibility peaks alters the pattern of breaks at *RSZs* in *mec1-ts*.

It is interesting that high flexibility peaks did not coincide with centromeric regions on any of the 16 chromosomes. Moreover, there was little correlation between these

peaks and origins of DNA replication. In contrast, areas of DNA flexibility have been found near replication origins in Chinese hamster cell lines (Toledo et al., 2000). It is important to note, however, that the values that the authors attributed to high DNA flexibility around replication origins were below the $13.7^o$ threshold used in this study and other fragile site studies; this could account for this discrepancy. Nevertheless, these positioning 'rules' in yeast imply that areas of high flexibility and *RSZs* share similar positional characteristics and support the notion that *RSZs* may coincide with or contain regions of high DNA flexibility. Further analysis of *RSZs* on other chromosomes must be performed before we can truly understand if these sites overlap significantly. However, it is tempting to propose that sites of high DNA flexibility could, in part, predict the location of *RSZs* on other chromosomes. As mentioned above, the predictions in DNA flexibility were derived from the S288C stain background used in the SGD database; this suggests that the location and/or number of peaks identified in this analysis may be slightly different in the SK1 strain background used in this study. Future efforts to generate *mec1-4* strains in the S288C background would facilitate this type of analysis.

Of the *RSZs* on chromosomes III and VI that do not correspond to a flexibility peak, four out of six *RSZs* coincide with sites of transposon insertion. The remaining two *RSZs* do not appear to correlate with any determinant other than termination zones. It is possible that sequence variations between SK1 and S288C backgrounds may mask the presence of a flexibility peak at these two *RSZs* in our SK1 strains. Alternatively, DNA flexibility may not be mechanistically related to chromosome breakage at *RSZs* and, therefore, not all *RSZs* coincide with peaks in DNA flexibility.

Nonetheless, given the high degree of overlap between *RSZs* and flexibility peaks as well as Ty/Δ elements, it is reasonable to infer that *RSZs* tend to either contain areas of high DNA flexibility or correspond with transposon insertion sites. Studies in yeast have indicated that fragile sites are often associated with transposon insertion sites and that low levels of polymerase can induce breakage at these sites (Lemoine et al., 2008; Lemoine et al., 2005; Raveendranathan et al., 2006). Both transposon insertion sites and highly flexible DNA have been implicated with the formation of secondary structures in the DNA (Lemoine et al., 2005; Zhang and Freudenreich, 2007). The current model for mammalian fragile sites proposes that replication fork

pausing at these sites is caused by such secondary structures arising from the highly flexible AT-rich region within these sites. Other studies suggest that inverted repeats found at sites of transposon integration can form DNA hairpins capable of stalling replication forks (Lemoine et al., 2005; Raveendranathan et al., 2006). Perhaps stalling of the replication fork at *RSZs* occurs as a result of secondary structures produced by transposon insertion and/or extremely flexible DNA sequences. This notion is not mutually exclusive with the idea that *RSZs* stall due to limiting amounts of dNTPs. Transient pausing at *RSZs* in wild type cells may arise due to secondary structures formed at these sites. The lack of dNTP up-regulation in *mec1-ts* mutants could exacerbate replication fork stalling at *RSZs* eventually resulting in the accumulation of DSBs at these sites.

### 3.3.3   Are *RSZs* analogous to mammalian common fragile sites?

There are numerous similarities between common fragile sites in mammals and *RSZs* in yeast. Both constitute an integral component of chromosome structure and are, therefore, found on every chromosome in either yeast or mammals. Neither *RSZs* nor common fragile sites are defined by specific sequences, although common fragile sites are relatively AT-rich (Mishmar et al., 1998; Ried et al., 2000; Shiraishi et al., 2001). As mentioned above, the fact that the yeast genome is AT-rich may obscure the ability to identify whether *RSZs* also have some preferred base composition. Although there is no sequence that defines common fragile sites, it is proposed that these sites contain more areas of high DNA flexibility compared to other regions of the chromosome (Arlt et al., 2002; Limongi et al., 2003; Mishmar et al., 1998; Zlotorynski et al., 2003). However, not all chromosomal defects at common fragile sites are associated with individual DNA flexibility peaks suggesting that other chromosomal features may also contribute to chromosome instability at these sites (Durkin et al., 2008; Mimori et al., 1999). Similarly, results from Section 3.2.3 indicate that *RSZs* also tend to be associated with regions of high DNA flexibility, although this does not seem to be true for all *RSZs* identified (Figures 3.7 and 3.8).

Late replication is a feature of both common fragile sites and *RSZs*. Common fragile sites tend to replicate very late in S-phase raising the possibility that these sites experience difficulty in replication fork progression (Hellman et al., 2000; Le Beau

et al., 1998; Palakodeti et al., 2004). Addition of the polymerase inhibitor, aphidicolin, significantly delays replication of these sites further such that these sites remain un-replicated in G2 (Le Beau et al., 1998). Analysis of replication intermediates at *RSZs* in wild type cells shows that these sites are naturally occurring fork slowing zones that delay the completion of replication of these sites until late S-phase (Cha and Kleckner, 2002). These difficulties in replication progression at *RSZs* are exacerbated in *mec1-ts* cells whereby replication forks at these sites stall permanently until they are somehow converted into DSBs.

Support for a mechanistic link between replication fork stalling and expression of common fragile sites stems from monitoring the stability of these sites in cell lines deficient for ATR, the mammalian homologue of Mec1. ATR was found to be crucial to the stability of common fragile sites as these regions are expressed in ATR-deficient cells, even without the addition of aphidicolin (Casper et al., 2002). Furthermore, cells from individuals with Seckel syndrome that have hypomorphic mutations in *ATR* show increased instability at common fragile sites (Casper et al., 2004). As ATR is required for stabilising stalled replication forks, it was deduced that common fragile sites represent regions where forks frequently stall (Casper et al., 2002). Likewise, the fact that increased fork stalling and chromosome breakage at *RSZs* occurs in the absence of Mec1 suggests that this homologue of ATR is also critical in maintaining the stability of fragile sites (Cha and Kleckner, 2002).

In both yeast and mammals, break formation appears to follow an aberrant replication program. Consistent with this, treatment with mild doses of replication inhibitors such as aphidicolin in mammals or HU in yeast results in breakage of the chromosome at common fragile sites and *RSZs*, respectively (Durkin and Glover, 2007). It is important to note that, in yeast, Mec1 function must be absent in order for treatment with HU to induce breaks at *RSZs* as breaks were not observed at these sites in wild type cells treated with HU (data not shown). It is possible that breaks are induced in wild type cells treated with HU but are not frequent enough to be visualised by our system. Alternatively, the requirement for Mec1 may suggest that the Mec1-dependent checkpoint is important in preventing instability at these sites; either by stabilising forks stalled at these sites or by preventing progression into mitosis with incompletely replicated DNA. However, preliminary evidence suggests

that fork stalling at *RSZs* is physiological i.e., in a replication competent manner (Cha and Kleckner, 2002), and thus may not elicit a checkpoint response.

As discussed above, *RSZs* follow a somewhat similar pattern of distribution along different chromosomes in yeast (Section 3.2.1, Figures 3.1 and 3.4). The lack of genome-wide data regarding the position of replication origins and other chromosomal determinants in the mammalian and human genomes hinders our ability to determine the location of fragile sites in relation to these factors. Given the vast differences in chromosome architecture between yeast and mammals, it is unclear whether information regarding the positions of fragile sites along human/mammalian chromosomes can be extrapolated from the distribution of *RSZs* along yeast chromosomes. However, there is some evidence to suggest replication origins may occur within certain common fragile sites (Toledo et al., 2000) suggesting that this may be a possible difference between *RSZs* and common fragile sites. Initial reports suggested that common fragile sites map to R-bands rather than G-bands on chromosomes, even though they display G-band characteristics such as late replication and high A/T content (Mishmar et al., 1999). However, a more recent report mapped common fragile sites to the interface between early-replicating R-bands and late-replicating G-bands, which might act as barriers to replication fork progression (El Achkar et al., 2005). Although *RSZs* do not appear to fall within specific banding isochores, the fact that they overlap with sites of replication termination suggest that they occur within regions that replicate late in S-phase (Cha and Kleckner, 2002). In yeast, *RSZs* also tend to coincide with transposon insertion sites (Cha and Kleckner, 2002). Similarly, viruses such as the human papillomavirus (HPV) often insert their DNA at common fragile sites (Smith et al., 1992; Thorland et al., 2000; Wilke et al., 1996).  This indicates that, in both yeast and mammals, *RSZs* and common fragile sites are preferred sites for integration of foreign DNA.

In conclusion, the multitude of similarities between *RSZs* in yeast and common fragile sites in mammals, in both characteristics and regulation, suggests that *RSZs* provide a good model system for investigating fragile sites, in particular the mechanism by which they become expressed as well as the factors that govern their stability.

# Chapter 4

# Mechanism of budding yeast fragile site expression

## 4.1  Introduction

In both budding yeast and mammalian systems, chromosome breakage at *RSZs* and fragile sites is preceded by perturbations in DNA replication (Casper et al., 2002; Cha and Kleckner, 2002; Richards, 2001; Zhang and Freudenreich, 2007). However, replication fork stalling alone is not sufficient for chromosome breakage. Currently, several hypotheses exist regarding the nature of the additional event that generates a DNA break from a stalled fork. One widely accepted possibility is that chromosome breaks may be generated by the erroneous enzymatic processing of the stalled fork by replication restart pathways (Section 1.9.5). Studies in both prokaryotes and eukaryotes suggest that DSBs may arise spontaneously during DNA replication by the aberrant processing of stalled replication forks by the homologous recombination machinery and recombination-related pathways (Carr, 2002; Cox, 2001; Fabre et al., 2002; Michel et al., 2007; Sogo et al., 2002). This raises the possibility that active processing of replication forks that have stalled at *RSZs* by recombination pathways may generate breaks.

The observation that breaks at *RSZs* are prevented by the spindle depolymerising agent, carbendazim (MBC) (R. Cha unpublished results, Figure 4.1) suggests that the force of the mitotic spindle may be implicated in chromosome breakage at *RSZs*. Alternatively, breaks at *RSZs* may be caused by passage of *mec1-ts* cells through mitosis with incompletely replicated chromosomes. This could involve chromosome condensation, chromosome separation, or cytokinesis. Premature chromosome condensation (PCC) causes expression of common fragile sites in human lymphocytes (El Achkar et al., 2005). Segregation of unreplicated DNA (Krishnan et al., 2004) and the execution of cytokinesis on

142

Figure 4.1    MBC prevents *mec1-4* chromosome breakage

incompletely segregated DNA (Baxter and Diffley, 2008; Holm et al., 1989) have also been shown to generate chromosome breaks, although whether these contribute to breakage at *RSZs* is still unknown.

In this chapter, the potential involvement of stalled fork restart pathways, spindle force, sister chromatid decatenation, chromosome condensation, chromosome segregation, and cytokinesis in *mec1-ts* chromosome breakage was investigated.

## 4.2 Results

### 4.2.1 Break formation in *mec1-4* is not due to aberrant processing of stalled replication forks by recombination pathways

The widely accepted view for the mechanism of endogenous chromosome breakage during S-phase is that certain types of DNA damage or, perhaps, chromosome structure, cause the replication fork to stall. Components of the S-phase checkpoint ensure that this stalled replication fork is maintained in a replication-competent state in order for replication to resume once the damage has been repaired. The S-phase checkpoint is thought to regulate homologous recombination pathways at stalled forks in order to promote fork restart and to suppress toxic recombination events (Fabre et al., 2002; Tourriere and Pasero, 2007). Inappropriate processing of the stalled fork, for example in the absence of an intact checkpoint, may result in the collapse of the stalled replication fork and the formation of a DSB. Although the temporal relationship among the exit from S-phase, chromosome breakage, and loss of viability in *mec1-4* mutants suggests that breaks at *RSZs* arise after S-phase (Cha and Kleckner, 2002), it is still possible that forks stalled at *RSZs* may be processed directly into DSBs by HR or other recombination-dependent pathways.

To assess whether the homologous recombination machinery is involved in generating *mec1-ts* DSBs, *mec1-4* strains carrying deletions of various recombination genes were constructed and analysed for DSBs by PFGE and Southern analysis, the idea being that eliminating the enzyme responsible for generating breaks in *mec1-4* would prevent the formation of DSBs. Wild type and *mec1-4* strains in addition to the recombination mutants, *rad52Δ, rad51Δ, rad54Δ,* and *rad55Δ* in both wild type

and *mec1-4* backgrounds were grown to log phase at 23°C in YPD. The cells were then arrested in G1 with α-factor for two hours at 23°C and then for a further half hour at 37°C, before being released into YPD at 37°C. A sample from each culture was collected five hours after release from α-factor to test for the presence of breaks in each mutant by PFGE and Southern analysis. The *CHA1* probe was used to assess the presence of breaks on chromosome III in the *mec1-4* and recombination mutants. As shown in Figure 4.2A, deletion of the various recombination mutants did not prevent break formation in *mec1-4* cells suggesting that breaks at *RSZs* arise independently of recombination. In conjunction with this experiment, temperature sensitivity assays were also performed on these same mutants. Cells from a mid-log phase culture of each mutant were spotted onto YPD agar plates and incubated for 3 days at the indicated temperatures. As expected, none of the recombination mutants was able to rescue the lethality of *mec1-4* at 37°C (Figure 4.2B). The observation that some of the double mutants were in fact reproducibly more sensitive to higher temperatures than *mec1-4* alone indicates that these gene products may be required in repairing the breaks.

Other enzymes such as the Sgs1 helicase in a complex with topoisomerase III (Top3), the Srs2 helicase, and the Mus81-Mms4 endonuclease have also been shown to process replication forks stalled in the presence of DNA damage (Section 1.9.4). In order to assess whether these proteins were required for break formation in *mec1-ts*, *mec1-4* strains carrying deletions of *SGS1*, *TOP3*, *SRS2*, *MUS81*, or *MMS4* were subjected to the same analysis performed for recombination mutants. Elimination of these enzymes did not affect break formation in the *mec1-4* mutant suggesting that these enzymes are also not required to induce chromosome breakage at *RSZs* (Figure 4.3A). Temperature sensitivity assays performed on these mutants showed that none of these deletions was able to rescue the lethality of *mec1-4* at higher temperatures (Figure 4.3B).

Figure 4.2    Break formation in *mec1-4* arises independently of homologous recombination

Figure 4.3    Break formation in *mec1-4* arises independently of other recombination-related pathways

### 4.2.2   **Mechanism by which spindle poisons prevent *mec1-ts* breaks**

As mentioned above, treatment of *mec1-4* cells with the spindle poison, carbendazim (MBC), prevents break formation in this mutant (Figure 4.1; R Cha, unpublished data). Another, more commonly used, spindle depolymerising agent, nocodazole, also has the same effect on *mec1-4* break formation (see Figures 4.4, 4.9, and 4.10). These spindle poisons prevent anaphase, mitotic exit, and cytokinesis by activating the spindle assembly checkpoint (SAC). In yeast, activation of the SAC by nocodazole or by mutations that arrest cells in metaphase has been reported to enable chromosomes to decondense (Vas et al., 2007). Note that this is different to the situation in mammals where cells treated with spindle poisons display hyper-condensed chromosomes (Vas et al., 2007). Activation of the SAC has also been reported to cause Mec1/Tel1-independent phosphorylation of Rad53 during G2/M (Clemenson and Marsolier-Kergoat, 2006). In yeast, phosphorylation and activation of Rad53 upon DNA damage during S-phase causes an up-regulation of dNTP synthesis (Zhao et al., 2001). Increases in dNTP levels suppress the S-phase defect of *mec1-ts*, prevent breaks from occurring, and rescue the lethality of *mec1-ts* at restrictive temperatures (Cha and Kleckner, 2002). Although the SAC-dependent phosphorylation of Rad53 does not occur via the canonical Mec1/Tel1 pathway and does not result in the hyperactivation of Rad53 that is normally associated with dNTP up-regulation (Clemenson and Marsolier-Kergoat, 2006), the possibility that treatment with MBC prevents *mec1-ts* DSBs by causing an increase in dNTP levels must also be considered.

The observation that spindle depolymerisation prevents breaks at *RSZs* in *mec1-4* can therefore be explained by three possible hypotheses; (*i*) *mec1-4* chromosome breaks are generated by the pulling force of the mitotic spindle on incompletely replicated DNA, (*ii*) the breaks are not generated by the spindle *per se* but are generated by the passage of cells through the different stages of mitosis with incompletely replicated chromosomes, and (*iii*) activation of the SAC results in Rad53-dependent increase in dNTPs.

**4.2.2.1 *mec1-4* breaks arise independently of spindle force**

In order to address the issue of whether breaks at *RSZs* are caused by the mechanical force of the spindle on *mec1-4* chromosomes, a double mutant was generated in which *mec1-4* cells were also deficient for the spindle checkpoint. Deletion of *MAD2* allows cells to condense chromosomes and separate the sister chromatids in the presence of spindle poison (Alexandru et al., 1999; Wasch and Cross, 2002). Note that *mad2*Δ cells treated with spindle poisons do not undergo cytokinesis (Alexandru et al., 1999).

In order to analyse *mec1-4* cells during the first cell cycle, strains in which the endogenous *MEC1* is deleted and the *mec1-4* allele is introduced into the exogenous *arg4* locus were used (see Section 3.2.5). To determine whether the status of the mitotic spindle is important for break formation at *RSZs*, *arg4::mec1-4* and *arg4::mec1-4 mad2*Δ cells were grown to mid-log phase in YPD at 23$^{\circ}$C, arrested with α-factor for two hours at 23$^{\circ}$C and then for a further half hour at 30$^{\circ}$C before being released into fresh YPD containing either nocodazole or dimethylsulfoxide (DMSO), the solvent for nocodazole and MBC, at 30$^{\circ}$C. Samples were collected 150 minutes after release from α-factor and processed for PFGE and Southern analysis. The *CHA1* probe was used to detect breaks at *RSZs* on chromosome III. As expected, the *arg4::mec1-4* strain acquired breaks at non-permissive temperature but breaks were significantly reduced in the culture treated with nocodazole. Breaks were present in the *arg4::mec1-4 mad2*Δ mutants even when treated with nocodazole (Figure 4.4). The observation that *arg4::mec1-4 mad2*Δ mutants acquire DSBs in a situation where spindles are absent (nocodazole) suggests that breaks arise independently of spindle force.

Figure 4.4    *mec1-ts* chromosome breaks arise independently of spindle force

**4.2.2.2 The status of G2/M chromosomal and cellular events in WT and *mec1-4***

Knowing that chromosome breakage in *mec1-4* cells arises during G2/M, and having ruled out the spindle force as a cause for DSB formation, it seemed likely that the breaks are generated by the passage of these cells through mitosis –i.e. condensation, anaphase, or cytokinesis. In order to identify the mitotic event during which breaks are generated, G2/M chromosomal and cellular events were analysed in *arg4::mec1-4* mutants and compared to those in the isogenic wild type strain (*mec1∆, arg4::MEC1*). Phosphorylation of histone H3, cleavage of the cohesin subunit Scc1, and degradation the mitotic cyclin Clb2, were used as markers for chromosome condensation, anaphase onset, and mitotic exit respectively.

Wild type (*arg4::MEC1*) and *arg4::mec1-4* cells expressing C-terminally tagged *SCC1-3HA* were grown to mid-log phase in YPD at 23$^o$C, arrested with α-factor for two hours at 23$^o$C and then for a half hour at 30$^o$C before being released into YPD at 30$^o$C. DMSO was added to these cultures to allow for a more accurate comparison with MBC-treated cultures in the following section (Section 4.2.2.3). Samples were collected at the indicated time points for protein extraction and FACS analysis. Samples were also collected for PFGE and Southern analysis to monitor the timing of break formation in *arg4::mec1-4* cells in relation to G2/M events. Proteins were separated on 10-15% polyacrylamide gels by SDS-PAGE and analysed by Western blot using the following antibodies: (*i*) anti-phospho-H3 to detect the phosphorylated form of histone H3, (*ii*) anti-HA to detect Scc1-HA, and (*iii*) anti-Clb2 to detect Clb2. The gels were subsequently probed with an anti-tubulin antibody that served as a loading control. The antibody signals were quantified from scanned images of the Western blots using ImageJ software; the amount of signal relative to that of tubulin was then calculated for each sample.

As expected, wild type cells executed chromosome condensation, anaphase onset, and mitotic exit in a coordinated and sequential manner (Figure 4.5). Histone H3 became phosphorylated shortly after S-phase (60 min after release from α-factor). The presence of phosphorylated histone H3 at the t=0 time point probably represents the proportion of cells that are in the 2C peak at this time point (see Figure 4.5A).

151

Phosphorylation of histone H3 was followed by cleavage of Scc1 at 75 minutes, and then degradation of Clb2 at 90 minutes after release from α-factor (Figure 4.5C, D, and E). In contrast, these events appeared to be uncoordinated in *arg4::mec1-4* cells. As shown previously, *arg4::mec1-4* cells entered S-phase at the same time as wild type cells (35-40 min) but remained with intermediate DNA content until approximately 150 minutes after release from α-factor (Cha and Kleckner, 2002; Figure 4.6A). PFGE/Southern analysis revealed that DSBs gradually accumulated between 90 and 180 minutes (Figure 4.5B). Histone H3 was phosphorylated with wild type kinetics starting about 60 minutes after release from α-factor, even when the majority of *arg4::mec1-4* cells were in S-phase (Figure 4.5C and G). On the other hand, only a minute amount of Scc1 cleavage product was detected, suggesting that Scc1 is not cleaved efficiently in *arg4::mec1-4* strains (Figure 4.5D and G). Clb2 levels remained fairly stable, with a small amount of degradation observed 120 minutes after release from α-factor (Figure 4.5E and G).  Similar results were observed in YPD cultures lacking DMSO.

Taken together, these results suggest that mitotic events are somewhat uncoordinated in *arg4::mec1-4* mutants. Chromosome condensation, as shown by phosphorylation of histone H3, occurs when the majority of cells are still in S-phase. Anaphase onset defined by the cleavage of Scc1 does not appear to occur, and the cells did not appear to exit mitosis proficiently as only a small amount of Clb2 degradation was detected. The observation that histone H3 phosphorylation occurs in *arg4::mec1-4* while cells are still in S-phase suggests that chromosome condensation may be involved in generating the breaks. Alternatively, the small amount of Clb2 degradation that occurs in *arg4::mec1-4* may indicate that mitotic exit and/or cytokinesis may be required for break formation in these mutants. The finding that Scc1 cleavage does not occur efficiently in these cells, in addition to the observation that the spindle force is not required for break formation (Section 4.2.2.1), indicates that the breaks are unlikely to be generated during anaphase.

Figure 4.5     Chromosome condensation, anaphase onset, and mitotic exit in wild type, *mec1-4*, and *mec1-4* in the presence of MBC

**4.2.2.3 The effect of the spindle poison, MBC, on G2/M events in *mec1-4***

In order to understand how break formation is prevented by treatment of *arg4::mec1-4* with the spindle poisons, MBC and nocodazole, the effect of MBC on the chromosomal and cellular events analyzed above was tested. *arg4::mec1-4* cells were grown to mid-log phase in YPD at $23^o$C , arrested for two hours at $23^o$C with α-factor, and then for a further half hour at $30^o$C. The cells were then released into fresh YPD containing MBC, at $30^o$C. Samples were collected at the indicated time points for protein extraction, FACS analysis, and PFGE/Southern analysis.

The FACS profile of *arg4::mec1-4* cells treated with MBC showed a more prominent 2C DNA content peak and a lesser amount of intermediate DNA content than in untreated *arg4::mec1-4* (Figure 4.5A and Figure 4.6A). This improvement in S-phase progression could be indicative of an increase in dNTP synthesis in the presence of spindle poisons, which prevents fork stalling and chromosome breakage in *mec1-ts* cells. Alternatively, it is possible that the prominent 2C DNA content peak seen in the presence of MBC could be due to the accumulation of cells at this stage of the cell cycle. In support of this, not all cells in an *arg4::mec1-4* culture lacking MBC arrest in S-phase (R. Cha, personal communication). Like other temperature sensitive mutations, it is likely that a minority of cells retain some *MEC1* function and are able to behave as wild type and undergo cell division. The addition of MBC would therefore prevent these cells from progressing beyond the 2C peak.

Phosphorylation of histone H3 in *arg4::mec1-4* cells treated with MBC occurred with similar kinetics to untreated *arg4::mec1-4* cells (Figure 4.5C and H). The overall level of histone H3 phosphorylation detected was slightly, but not significantly, reduced in the presence of MBC compared to the untreated cells (Figure 4.6B). As expected, no Scc1 cleavage or Clb2 degradation was observed in *arg4::mec1-4* cells treated with MBC (Figure 4.5D, E, and H).

Figure 4.6　　Comparison of S-phase and mitotic events in *arg4::mec1-4* cells in the presence and absence of MBC

These results indicate that MBC has a minimal effect on histone H3 phosphorylation. Although this seems to contradict the notion that spindle poisons have an inhibitory effect on condensation (Vas et al., 2007), it is important to note that histone H3 phosphorylation is only correlated with, but not required for, chromosome condensation in *S. cerevisiae* (Section 1.5.1). Furthermore, it has been shown that the reduction in condensation observed in condensin-deficient *Drosophila* cells is not accompanied by a complete absence of histone H3 phosphorylation (Dej et al., 2004; Savvidou et al., 2005; Steffensen et al., 2001). Therefore, it is unclear, from this experiment, whether MBC prevents chromosome breakage in *arg4::mec1-4* by hindering the compaction of the chromosome.

MBC also appears to stabilize Clb2 levels more than what was observed for untreated *arg4::mec1-4* (Figure 4.6C). This raises the possibility that MBC prevents breaks by blocking mitotic exit/cytokinesis. As little or no Scc1 cleavage product was observed in *arg4::mec1-4* cells in the absence or presence of MBC, it seems unlikely that this event is required for *mec1-ts* chromosome breakage.

### 4.2.2.4 Sister chromatid separation is not required for *mec1-ts* DSBs

The occurrence of breaks in a *mad2Δ arg4::mec1-4* mutant in the presence of nocodazole (Section 4.2.2.1) indicates that the breaks arise independently of the tension exerted on the chromosome by the spindle. In addition, the observation that the cohesin subunit, Scc1, does not get cleaved efficiently in *arg4::mec1-4* suggests that sister chromatid separation is not required for break formation. In order to confirm that breaks are not generated by sister chromatid separation, break formation was assessed in *arg4::mec1-4* strains lacking the spindle checkpoint protein Bub2. Bub2 governs a second branch of the spindle assembly checkpoint that inhibits Clb2 degradation in the event of spindle damage but plays no role in the Mad2-dependent branch of the SAC (Alexandru et al., 1999). Therefore, *bub2Δ* mutants treated with spindle poisons do not separate sister chromatids as the Mad2-dependent branch of the SAC is still in tact.

*arg4::mec1-4* and *bub2Δ arg4::mec1-4* cells were grown to mid-log phase in YPD at 23°C, arrested with α-factor for two hours at 23°C and then for half an hour at 30°C before being released into YPD containing either nocodazole or DMSO at 30°C. Samples were collected 150 minutes after release from α-factor and processed for PFGE and Southern analysis. The *CHA1* probe was used to detect breaks at *RSZs* on chromosome III. As expected, DSBs were present in the *arg4::mec1-4* strain at non-permissive temperature but were absent in the culture treated with nocodazole. Breaks were present in both nocodazole-treated and untreated *bub2Δ mec1-4* mutants, confirming the notion that sister chromatid separation is not required for *mec1-ts* break formation (Figure 4.7).

**4.2.2.5 *mec1-ts* breaks are not generated by cytokinesis**

Strains lacking Mad2 or Bub2 do not perform cytokinesis when exposed to spindle antagonists. The results presented in sections 4.2.2.1 and 4.2.2.4 showed that breaks occurred in both *mad2Δ arg4::mec1-4* and *bub2Δ arg4::mec1-4* cells in the presence of nocodazole. This would suggest that cytokinesis might not be required for break formation. However, to confirm that *mad2Δ* and *bub2Δ* cells do not undergo cytokinesis in the context of *arg4::mec1-4*, cytokinesis was examined in *mad2Δ arg4::mec1-4* and *bub2Δ arg4::mec1-4* by monitoring the localisation of Myo1. *MYO1* encodes a component of the actomyosin ring that localises to the bud neck from early S-phase until cytokinesis when the actomyosin ring constricts and Myo1 ring disappears completely from the bud neck (Section 1.6).

Figure 4.7    Breaks arise independently of sister chromatid separation

As a control, the kinetics of Myo1 localisation was monitored in wild type and *arg4::mec1-4* cells expressing *MYO1* tagged at its C-terminus with Green Fluorescent Protein (*MYO1-GFP*) in the absence or presence of nocodazole. Wild type and *arg4::mec1-4* cells were grown to mid-log phase in YPD at 23$^{o}$C, arrested in G1 with α-factor for two hours at 23$^{o}$C and then for half an hour at 30$^{o}$C before being released into YPD containing either nocodazole or DMSO at 30$^{o}$C. In order to restrict the cells that were treated with DMSO to one cell cycle, α-factor was added to the culture 40 minutes after release. Samples were harvested at the indicated time points, fixed, and processed for fluorescence microscopy and FACS. In addition, samples were also collected 120 and 150 minutes post-release for PFGE/Southern analysis.

In the wild type culture, the Myo1 ring appeared simultaneously with the emergence of the bud, 30 minutes after α-factor release (Figure 4.8A and B). The ring was still detectable after nuclear division (Figure 4.8A and B) but disappeared shortly afterward, starting around 90 minutes after release. In the wild type cultures treated with nocodazole, the Myo1 ring remained at the bud neck until the end of the experiment (Figure 4.8B). The Myo1 ring in *arg4::mec1-4* cells was also observable starting t=30 minutes. However, unlike in wild type cells, the Myo1 ring in *arg4::mec1-4* cells remained at the bud neck throughout the duration of the experiment, whether treated with nocodazole or not (Figure 4.8B). Breaks in *arg4::mec1-4* are present at both 120 and 150 minutes after release from α-factor indicating that break formation is independent of cytokinesis (Figure 4.8C). Interestingly, the number of binucleate cells observed in *arg4::mec1-4* was relatively low compared to wild type over the course of the experiment, further supporting the conclusion in Section 4.2.2.4 that anaphase does not occur in these mutants and is, therefore, unlikely to be required for break formation (Figure 4.9).

Figure 4.8    Cytokinesis does not occur in *mec1-ts* at the time of break formation

Figure 4.9     *arg4::mec1-4* cells do not readily reach the binucleate stage compared to wild type cells

The same experiment was performed with *mad2Δ* and *bub2Δ* in wild type and *arg4::mec1-4* backgrounds. The cells were grown to mid-log phase in YPD at 23$^o$C, arrested in G1 with α-factor for two hours at 23$^o$C and then for half an hour at 30$^o$C. The cells were then released into YPD containing nocodazole at 30$^o$C. Samples were collected at the indicated time points and processed for FACS and fluorescence microscopy. As expected, none of the strains performed cytokinesis as judged by the persistence of the Myo1 ring at the bud neck (Figure 4.10A).

The disappearance of Myo1-GFP reflects the completion of cytokinesis, however it is possible that cytokinesis may have initiated in *arg4::mec1-4* cells but failed to complete cell separation. Therefore, as a final confirmation that chromosome breaks in *arg4::mec1-4* cells arise prior to the onset of cytokinesis, the status of *arg4::mec1-4* breaks was assessed in a *mob1-77* background. Mob1 is a component of the mitotic exit network (Section 1.5.3) and is required for cytokinesis (Luca et al., 2001). Cells harbouring a *mob1* mutation arrest in late nuclear division and are defective for cell separation (Luca et al., 2001). Wild type (*arg4::MEC1*), *mob1-77 arg4::MEC1, arg4::mec1-4,* and *arg4::mec1-4 mob1-77* were grown to mid-log phase in YPD at 23$^o$C, arrested in G1 with α-factor for two hours at 23$^o$C and then for half an hour at 37$^o$C, the restrictive temperature for *mob1-77*. The cells were released into fresh YPD at 37$^o$C and samples were collected 5 hours after release for PFGE and Southern analysis. Southern hybridisation was performed using the *CHA1* probe. The *mec1-ts* chromosome breaks were observed in both *MOB1* and *mob1-77* backgrounds (Figure 4.10B) confirming that break formation occurs irrespective of cytokinesis.

Figure 4.10     Cytokinesis is not required for break formation in *mec1-ts*

## 4.2.2.6 MBC does not prevent *mec1-ts* DSBs by phosphorylating Rad53

The third possible mechanism by which treatment of *mec1-ts* cells with spindle depolymerising agents such as MBC and nocodazole prevents chromosome breakage at *RSZs* is that Rad53 may be phosphorylated under these conditions leading to an up-regulation of dNTP synthesis pathways that suppress *mec1-ts* phenotypes. As mentioned above, phosphorylation of Rad53 upon treatment with spindle inhibitors occurs independently of Mec1 and Tel1, the key players in Rad53-dependent up-regulation of dNTP synthesis in response to DNA damage (Clemenson and Marsolier-Kergoat, 2006). Additionally, this SAC-dependent phosphorylation of Rad53 is not accompanied by the hyperactivation and autoactivation of Rad53 that is normally associated with increased dNTP production during DNA damage situations (Clemenson and Marsolier-Kergoat, 2006). Furthermore, phosphorylation of Rad53 by the SAC occurs during G2/M and is therefore unlikely to suppress the S-phase defect of *mec1-ts* cells. However, this does not necessarily rule out the possibility that MBC/nocodazole-induced phosphorylation of Rad53 could circumvent chromosome breakage at *RSZs* by raising dNTP levels in *mec1-ts* cells. Indeed, the improvement of *arg4::mec1-4* progression through S-phase in the presence of MBC (Figure 4.5A) supports the notion that MBC prevents breaks by impacting on dNTP synthesis. Moreover, deletion of *MAD2*, which inhibits nocodazole-dependent phosphorylation of Rad53 (Clemenson and Marsolier-Kergoat, 2006), restores chromosome breakage at *RSZs* in *arg4::mec1-4* cells treated with spindle poisons (Figure 4.4). However, neither Mec1 nor Bub2 is required for nocodazole-induced phosphorylation of Rad53 (Clemenson and Marsolier-Kergoat, 2006). Assuming that Rad53 is, therefore, phosphorylated in *bub2Δ arg4::mec1-4* cells treated with nocodazole, the observation that breaks are present in this condition suggests that nocodazole-induced phosphorylation of Rad53 may not be the mechanism by which spindle depolymerising agents prevent breaks. Further analysis of the status of Rad53 in *mec1-ts* cells treated with spindle inhibitors and under various conditions (e.g. in *bub2Δ arg4::mec1-4* cells) is required in order to completely rule out this possibility.

### 4.2.3    Topoisomerase II mutants suppress *mec1-ts* break formation

The results presented in section 4.2.2 indicate that break formation occurs prior to cytokinesis and anaphase but some time after S-phase. Chromosomal events from late S phase to metaphase include: replication termination, decatenation of the sister chromatids, chromosome individualization, and condensation. Central to these G2-metaphase events is the chromosome scaffold protein, topoisomerase II (Sections 1.4.5 and 1.5.1). Because it can generate DSBs, Top2 is the only eukaryotic topoisomerase capable of decatenating double-stranded DNA; such decatenation is inevitably required at replication termination to separate sister chromatids. Its enzymatic activity is also required for condensation in yeast as well as in higher organisms (Uemura et al., 1987; Vas et al., 2007). It was therefore interesting to assess whether Top2 played a role, either directly or indirectly, in *mec1-ts* chromosome breakage.

As *TOP2* is an essential gene, the *top2-1* allele was used to determine the effect of Top2 inactivation in *mec1-4*. The *top2-1* allele is partially active at $30^{\circ}$C and almost completely inactive at $37^{\circ}$C, the temperature at which the protein is thought to be degraded (J. Nitiss, personal communication). Wild type, *mec1-4*, *top2-1*, and *top2-1 mec1-4* cells were grown to log phase in YPD at the permissive temperature of $23^{\circ}$C. The cells were then arrested with α-factor for two hours at permissive temperature and for a further half hour at $37^{\circ}$C, the non-permissive temperature for both *top2-1* and endogenous *mec1-4*. The cells were released into YPD at $37^{\circ}$C and, after 5 hours, samples were collected for PFGE and Southern hybridisation. Hybridisation was performed using the *CHA1* probe to analyse breaks formation on chromosome III in these mutants. Inactivation of Top2 in *mec1-4* cells significantly reduced the appearance of breaks on chromosome III indicating a possible role for Top2 in *mec1-ts* break formation (Figure 4.11A and B). As expected from the essential nature of *TOP2*, inactivation of Top2 did not rescue the lethality of *mec1-4* at non-permissive temperature (Figure 4.11C).

Figure 4.11     *mec1*-dependent chromosome breaks are suppressed by inactivation of Top2

**4.2.3.1 Top2 does not localise to all *RSZs***

The effect of Top2 on chromosome breakage could be either direct, by generating a DSB at a *RSZ* by way of its decatenating activity, or indirect, by affecting some aspect of chromosome structure such as the chromosome compaction process. However, the fact that raising dNTP levels by deletion of the inhibitor of ribonucleotide reductase, *SML1,* prevents break formation argues against a role for decatenation as a cause for *mec1-ts* break formation since decatenation itself is not reliant on or influenced by dNTP levels. In fact, decatenation of sister chromatids occurs after the chromosome has been fully duplicated. This does not completely rule out the possibility that Top2 generates breaks at *RSZs* independently of its role in decatenating sister chromatids. Therefore, in order to determine if Top2 generates DSBs at *RSZs* in *mec1-ts* directly, the localisation of Top2 tagged with the Flag epitope on chromosomes III and VI was examined by ChIP on chip, based on the assumption that Top2 would be recruited to *RSZs* in order to catalyse the formation of DSBs at these sites. ChIP on chip analysis involves immunoprecipitation of a protein (e.g. Top2) bound to a region of DNA and then hybridising that DNA sequence to a high density oligo microarray to determine the region on the chromosome to which the protein binds.

Wild type (*arg4::MEC1)* and *arg4::mec1-4* cells expressing Flag-tagged Top2 were grown to mid-log phase in YPD at 23$^{\text{o}}$C, synchronised in G1 with α-factor for two hours at 23$^{\text{o}}$C and then for a further half hour at 30$^{\text{o}}$C to inactivate Mec1. The cells were released from α-factor into YPD at 30$^{\text{o}}$C and samples collected three hours after release for ChIP on chip analysis. ChIP on chip analysis was performed by members of Katsuhiko Shirahige's group at the Tokyo Institute of Technology. This analysis was performed for all 16 chromosomes; however, for the purpose of this thesis, Top2-Flag enrichment patterns on only chromosomes III and VI are shown in Figures 4.12 and 4.13 as *RSZs* have only been mapped on these chromosomes (Cha and Kleckner, 2002).

Figure 4.12     Top2 does not localise to all *RSZs* in *mec1-ts* on chromosome III

Figure 4.13    Top2 localises to some *RSZs* in *mec1-ts* on chromosome VI

Although, Top2-Flag was found to localise in the vicinity of *RSZs* on chromosome III in wild type cells, it was not enriched at all *RSZs* in *arg4::mec1-4* cells (Figure 4.12; compare *RSZ-IV* and *–VI* in A and B). Localisation of Top2-Flag on chromosome VI was also examined and found to localise to most, but not all, *RSZs* in *arg4::MEC1* and *arg4::mec1-4* strains (Figure 4.13; see *RSZ-V*). Although this result does not necessarily rule out the possibility that breaks at *RSZs* are generated directly by Top2, the observation that Top2 does not localise to each *RSZ* in *arg4::mec1-4* at the time when breaks are normally observed argues against this notion.

### 4.2.3.2 Suppression of *mec1*-dependent DSBs by Top2 inactivation is not due to phosphorylation of Rad53

The checkpoint kinase, Rad53, is phosphorylated in *top2-1* mutants, presumably during cytokinesis when breaks are generated by segregation of tangled chromosomes or division of the cell before complete segregation of the chromosomes (Bermejo et al., 2007). As mentioned above, Rad53 phosphorylation and activation during S-phase is linked to the up-regulation of dNTPs, a situation known to prevent break formation and rescue the lethality of *mec1-4* mutants. Although activation of Rad53 in *top2-1* is thought to occur well after S-phase (during/after cell division) and is therefore unlikely to improve *mec1*-dependent S-phase defects, it was necessary to rule out the possibility that Rad53 was phosphorylated during S-phase in *top2-1 arg4::mec1-4* mutants. To this end, mid-log phase cultures of wild type (*arg4::MEC1*), *arg4::mec1-4*, *top2-1*, *top2-1 arg4::mec1-4* cells were synchronised in G1 with α-factor for two hours at 23°C and then for a further half hour at 37°C to inactivate both Mec1 and Top2. The cells were then released into YPD at 37°C and samples were collected at the indicated time points for FACS analysis and protein extraction. Protein extracts from samples collected at 30 or 45 minutes, depending on when the cells were in S-phase as determined by FACS, and 150 minutes (post-cytokinesis) after release from α-factor were separated on a 10% polyacrylamide gel by SDS-PAGE and analysed by Western blot using antibodies against phosphorylated Rad53 and the Rad53 backbone. As a positive control, a protein extract from a wild type strain (NHY 343)

172

treated with 0.03% MMS to induce DNA damage was run alongside the samples. Samples were also collected at 150 minutes for PFGE/Southern.

The cell cycle progression of the *top2-1 arg4::mec1-4* strain as measured by FACS showed that inactivation of Top2 may improve the progression of *arg4::mec1-4* cells through S-phase (Figure 4.14A). It is unclear whether this is due to an actual improvement in S-phase progression or if it is simply due to an accumulation of cells in the 2C DNA content peak as often observed in *top2* mutants (Andrews et al., 2006; Downes et al., 1994; Skoufias et al., 2004). At later time points (e.g. 120 and 150 minutes) the double mutant resembled the *top2-1* single mutant in that the 1C and 2C peaks were not clearly identifiable and peaks with less than 1C DNA content were observed, signifying the extensive chromosome breakage expected in *top2* mutants. As expected, no breaks at *RSZs* were detected in the *top2-1 arg4::mec1-4* mutant (Figure 4.14B).

As mentioned above, increases in dNTP levels in *mec1-ts* cells improve S-phase progression, prevent chromosome breakage, and rescue the lethality of *mec1-ts* at high temperatures. As FACS analysis showed that Top2 inactivation seemed to improve the progression of *arg4::mec1-4* cells through S-phase, it was necessary to check whether inactivation of Top2 in the ectopic *arg4::mec1-4* strain improved the viability of *arg4::mec1-4* at restrictive temperatures. Temperature sensitivity assays were, therefore, repeated using the ectopic *arg4::mec1-4* allele. Consistent with the above results (Figure 4.11C), inactivation of Top2 did not improve the viability of *arg4::mec1-4* cells at non-permissive temperatures (Figure 4.14C). However, it remains possible that Top2 inactivation could improve the *mec1*-dependent S-phase defects but render these cells inviable due to *top2*-dependent segregation defects.

Western analysis of protein extracts collected in S-phase and after cytokinesis showed that Rad53 was not phosphorylated in *top2-1 arg4::mec1-4* in either stage of the cell cycle (Figure 4.15). As expected, Rad53 was only phosphorylated in *top2-1* cells after cytokinesis (i.e. not in S-phase). Wild type and *arg4::mec1-4* cells did not phosphorylate Rad53 during S-phase. These results refute the hypothesis that suppression of *mec1-4* breaks by inactivation of Top2 is due to activation of Rad53 and up-regulation of dNTP synthesis during S-phase.

Figure 4.14    The effect of Top2 inactivation on *arg4::mec1-4*

Figure 4.15     Rad53 is not phosphorylated in *top2-1 arg4::mec1-4*

Taken together these results suggest that Top2 may not catalyse the formation of DSBs at *RSZs* directly, although this cannot be ruled out entirely. In addition, suppression of DSBs by Top2 inactivation does not appear to involve Rad53 activation and, presumably, an increase in dNTP availability. Another possibility is that inactivation of Top2 may suppress *mec1-ts* DSBs indirectly by affecting chromosome condensation.

### 4.2.4    Condensin mutants suppress *mec1-ts* break formation

Expression of mammalian common fragile sites is induced when cells undergoing DNA replication are subjected to premature chromosome condensation (El Achkar et al., 2005). Similarly, chromosome condensation in *arg4::mec1-4* mutants as assayed by the phosphorylation of histone H3 occurs when the majority of cells were still in S-phase (Section 4.2.2.2). Results presented in 4.2.2 indicate that break formation occurs prior to cytokinesis and anaphase but some time after S-phase. The fact that spindle poisons have an inhibitory effect on condensation (Vas et al., 2007) and that they also prevent chromosome breakage in *arg4::mec1-4* raises the possibility that these breaks are generated by the chromosome compaction process. Furthermore, inactivation of Top2, an enzyme required for condensation in both yeast and mammals (Gimenez-Abian et al., 1995; Hirano, 2000; Uemura et al., 1987; Vas et al., 2007), prevents break formation in *mec1-4* mutants (Section 4.2.3). It was, therefore, necessary to ascertain whether condensation was required for break formation in *arg4::mec1-4* cells.

To determine whether condensation is required for chromosome breakage in *mec1-ts*, the status of breaks on chromosome III was assessed in *mec1-4* mutants also defective in condensation. The essential genes, *YCG1* and *YCS4*, encode the non-SMC subunits of the condensin complex (Section 1.5.1) and the mutant alleles *ycg1-2* and *ycs4-2* display defects in chromosome condensation (Lavoie et al., 2002). Wild type, *mec1-4*, *mec1-4 ycs4-2*, and *mec1-4 ycg1-2* strains were grown to log phase at 23$^{\circ}$C, arrested in G1 with α-factor for two hours at 23$^{\circ}$C and then for half an hour at 37$^{\circ}$C, the restrictive temperature for condensin and endogenous *mec1-4* mutants. The cells were released into fresh YPD at 37$^{\circ}$C and samples were collected 5 hours after

Figure 4.16    Breaks in *mec1-ts* are suppressed by inactivation of condensin subunits

release from α-factor for PFGE/Southern analysis. Hybridisation with the *CHA1* probe revealed that chromosome breaks occurred in *mec1-4* but not in *mec1-4* mutants carrying the condensin mutations (Figure 4.16). This result supports the hypothesis that condensation is required for break formation in *mec1-ts*.

## 4.3   Discussion

### 4.3.1   DNA breaks at *RSZs* are not the result of aberrant processing of stalled replication forks by recombination pathways

The data presented in this chapter suggest that *mec1-ts* chromosome breaks arise independently of the expected means presumed to generate DSBs from stalled replication forks, namely homologous recombination and the helicases and nucleases implicated in processing stalled forks. Although not all recombination proteins were tested, the fact that breaks arise independently of Rad52, an enzyme required for virtually all types of homologous recombination processes in yeast (Symington, 2002), allows us to conclude that homologous recombination at replication forks stalled at *RSZs* is not required for *mec1-ts* chromosome breakage. Previous studies have proposed that enzymes such as Mus81-Mms4 and Sgs1-Top3 complexes could generate DSBs as an intermediate during the processing of stalled forks via recombination-related pathways (Cote and Lewis, 2008; Kai et al., 2005; Kaliraman et al., 2001; Wu and Hickson, 2003; Zhang et al., 2005). However, this also does not appear to be the case with regard to breakage of DNA at *RSZs* (Section 4.2.1). The observation that *mec1-4* cells that are also defective for recombination were often more sensitive to high temperatures compared to *mec1-4* mutants alone suggests a possible role for homologous recombination in repairing at least some of the DSBs that arise at *RSZs* (Figures 4.2 and 4.3). However, it must be noted that the temperature sensitivity assays were performed using O.D.$_{600}$ measurements to estimate the number of cells spotted for each strain and are therefore not accurate enough to make any significant conclusions. Nevertheless, foci of Rad51 and phospho-DNAPKcs, a component of the non-homologous end-joining (NHEJ) pathway, form at expressed fragile sites on metaphase chromosomes (Schwartz et al., 2005). In addition, down-regulation of Rad51, DNA-PK, and the NHEJ-specific ligase, Ligase IV, leads to a significant increase in fragile site expression under

replication stress (Schwartz et al., 2005), suggesting that expressed fragile sites are often repaired by DSB repair mechanisms. The Mre11-Rad50-Xrs2 (MRX) complex is also required for repair of DNA damage/collapsed replication forks and is implicated in the formation programmed meiosis-induced DSBs (Johzuka and Ogawa, 1995); this raises the possibility that this complex generates breaks at *RSZs*. However, deletion of *MRE11* or *RAD50* does not prevent break formation in *mec1-4* mutants (R. Cha unpublished results) indicating that the MRX complex is not involved in generating *mec1-ts* DSBs.

The fact that chromosome breakage occurs independently of recombination, MRX processing, and other proposed helicases and nucleases lead us to conclude that aberrant processing of replication forks stalled at *RSZs* is not the cause of *mec1-ts* DSBs. However, the involvement of other possible enzymes has not been tested. One example of a candidate enzyme is the flap endonuclease, Exo1, is required for fork collapse in HU-treated *rad53* mutants (Cotta-Ramusino et al., 2005). Deletion of *EXO1* suppresses the sensitivity of *rad53Δ smll1Δ* to MMS, UV, and IR (but not HU) and rescues replication fork breakdown in *rad53Δ smll1Δ* cells subjected to MMS treatment (Segurado and Diffley, 2008). In addition, Yen1 has recently been identified as the yeast HJ resolvase (Ip et al., 2008), raising the possibility that this enzyme may act at forks stalled at *RSZs* to generate a DSB. It is therefore necessary to test the requirement of these enzymes for *mec1-ts* chromosome breakage before completely ruling out replication fork processing as a mechanism for break formation at *RSZs*.

### 4.3.2   *mec1-ts* chromosome breaks are not generated by the mechanical force of the mitotic spindle

The suppression of breaks at *RSZs* by addition of spindle inhibitors lead to the suggestion that the mechanical force of the mitotic spindle could be involved in break formation. However, the presence of breaks in conditions where the spindle is absent (e.g. *mad2Δ arg4::mec1-4* and *bub2Δ arg4::mec1-4* cells treated with nocodazole) argues against this hypothesis (Section 4.2.2.1).

Inappropriate chromosome segregation has been implicated in generating DSBs. For example, the attempted segregation of a dicentric chromosome to opposite poles of the cell is thought to result in breakage of the chromosome (Janson and Tran, 2008). Additionally, segregation of incompletely replicated DNA in the absence of Mec1 results in an increase in Ddc1 foci, signifying the accumulation of DSBs (Krishnan et al., 2004). However, the fact that the mitotic spindle is not involved in *mec1-ts* break formation implies that chromosome segregation is also dispensable for the generating breaks at *RSZs*. This does not necessarily mean that sister chromatid separation is not required; however, it does argue against a role for tension, as well the parties that produce this tension across the chromosome (i.e. sister chromatid cohesion and spindle force), in the formation of *mec1-ts* DSBs.

### 4.3.3   Chromosome breakage at *RSZs* occurs before sister chromatid separation and cytokinesis

Mammalian common fragile sites, the proposed analogues of *RSZs*, are detected on metaphase spreads, presumably before sister chromatid separation, segregation, and cytokinesis. Cleavage of the cohesin subunit, Scc1, was barely detectable in *arg4::mec1-4*, even in the absence of spindle inhibitors suggesting either that cohesin cleavage by Esp1 does not occur efficiently in this mutant, or that *arg4::mec1-4* cells acquire breaks and lose viability prior to sister chromatid separation. In support of the former possibility, *mec1-1* cells treated with HU are reported to undergo reductional nuclear division without the cleavage of Scc1 (Krishnan et al., 2004). However, the observation that *arg4::mec1-4* mutants do not reach a binucleate state (Section 4.2.2.5) suggests that the latter possibility is more probable – i.e., breaks may arise before sister separation. Additionally, deletion of *BUB2*, a condition that allows Scc1 stabilisation in the presence of nocodazole (Alexandru et al., 1999), does not prevent break formation (Section 4.2.2.4). Furthermore, breaks are prevented by inactivation of condensin subunits (Section 4.2.4). Scc1 reportedly associates with and disassociates from chromatin with wild type kinetics in condensin mutants (Bhalla et al., 2002), suggesting that breaks at *RSZs* can be prevented without affecting the status of sister chromatid cohesion. Taken together these results argue against a role for sister chromatid separation in break formation at *RSZs*.

The observation that a minimal amount of the mitotic cyclin, Clb2, is degraded in *arg4::mec1-4* and that this is inhibited, as breaks are, by MBC raises two possibilities. Either, as discussed above, the minimal degradation of Clb2 that occurs is irrelevant, perhaps represents the minority of *mec1-4* cells that act as wild type, and that breaks arise some time before sister chromatid separation and mitotic exit/cytokinesis. Alternatively, the small amount of Clb2 degradation may signify cells that have executed mitotic exit/cytokinesis and have, as a consequence, produced breaks at *RSZs*.

The data presented in Section 4.2.2.5 demonstrates that cytokinesis does not occur in *arg4::mec1-4* mutants, even at the time when breaks are observed, suggesting that cytokinesis is not a contributory factor in break formation at *RSZs* and that these breaks occur prior to this event. The presence of breaks in *mec1-ts* cells defective for the mitotic exit network and cytokinesis confirmed that breaks arise independently of cytokinesis and must therefore occur before this event (Section 4.2.2.5).

### 4.3.4   Breaks may be generated by condensation

A process of elimination of the mitotic stages required for break formation points to a pre-anaphase mitotic event that is affected by spindle depolymerising agents as a cause for chromosome breakage in *mec1-ts*. One obvious chromosomal event that occurs at this stage is condensation or compaction of the chromosome. However, budding yeast chromosomes do not undergo extensive compaction compared to mammals (Guacci et al., 1994; Strunnikov et al., 1995). Is it therefore reasonable to presume that this is the main cause for breaks in *mec1-ts*? Several findings support this hypothesis. First, chromosome breakage at common fragile sites can be induced by forcing S-phase chromosomes to undergo premature chromosome condensation on (El Achkar et al., 2005). Assuming that *RSZs* are the yeast analogue of common fragile sites, then it is possible for chromosome condensation to cause breaks at *RSZs*.

Second, breaks at common fragile sites are observed in metaphase spreads, presumably obtained from cultures treated with spindle poisons such as colchicines. On the other hand, metaphase-arrested *mec1-ts* cells (with MBC or nocodazole) do

not acquire breaks at *RSZs*. These seemingly contrary data can be reconciled if we consider that mammalian chromosomes are hypercondensed when treated with spindle inhibitors, whereas yeast chromosomes decondense in the presence of such agents (Vas et al., 2007). The presence of breaks on hypercondensed chromosomes in mammals and the absence of breaks on decondensed chromosomes in yeast would suggest a link between condensation and chromosome breakage. An alternative explanation for prevention of *mec1-ts* DSBs by spindle inhibitors lies in the apparent phosphorylation of Rad53 following treatment with nocodazole. Phosphorylation of Rad53 is often accompanied by an increase in dNTP synthesis, a condition that prevents break formation in *mec1-ts*. It is arguable whether nocodazole-induced phosphorylation of Rad53 affects dNTP levels as this phosphorylated Rad53 is not regulated in the canonical way (by Mec1 and Tel1) and does not become autophosphorylated. The fact that S-phase progression in *mec1-ts* is improved in the presence of spindle inhibitors (Figure 4.5A) suggests that suppression of breaks by these agents may involve dNTP up-regulation. However, the presence of breaks in *bub2∆ arg4::mec1-4* cells treated with nocodazole (Figure 4.7), where presumably nocodazole-dependent phosphorylation of Rad53 is unaffected, argues against this notion.

Although, histone H3 phosphorylation is not absolutely required for condensation in budding yeast as it is in other organisms, it is still an indicator of chromosome compaction or mitosis in general (Hsu et al., 2000). H3 phosphorylation in *mec1-ts* was the only event that occurred with similar kinetics to wild type cells and prior to the time of break formation, again supporting the notion that condensation might be involved in break formation. One opposing argument is that H3 phosphorylation was not significantly affected in *mec1-ts* treated with MBC. However, studies in *Drosophila* show that reduced defects in condensation are not accompanied by complete loss of H3 phosphorylation (Dej et al., 2004; Steffensen et al., 2001). Another argument against condensation as the cause for chromosome breakage at *RSZs* lies in the fact that metaphase arrests induced by spindle poisons or certain mutations allow chromosomes to initially condense prior to decondensing. If condensation generates DSBs in *mec1-ts* cells, then why doesn't this initial condensation, which occurs even in the presence of spindle inhibitors, generate

182

breaks at *RSZs*? Perhaps, chromosomes must be maintained in a condensed state for chromosome breakage to occur. In agreement with this, DSBs in *arg4::mec1-4* cells do not become visible concomitantly with histone H3 phosphorylation (and presumably initiation of condensation) but shortly afterwards (Figure 4.5).

Finally, the fact that the appearance of DSBs is prevented by inactivation of condensin subunits further supports the notion that chromosome breaks at *RSZs* may be generated by condensation (Figure 4.16). In addition, the genetic requirement for Top2, which is also implicated in condensation, in break formation at *RSZs* may also be consistent with this hypothesis (Figure 4.11). Analysis of Top2 localisation on chromosomes III and VI revealed that Top2 was absent from some *RSZs* while being present at others, reducing the likelihood that Top2 is directly required for break formation in *mec1-ts* (Section 4.2.3.1). Another possibility is that breaks at *RSZs* could be masked by the extensive chromosome breakage that normally occurs in *top2* mutants. The FACS profile of *top2-1 arg4::mec1-4* strains at 120 and 150 minutes after release from α-factor was similar to that of *top2-1* single mutants suggesting that *top2-1 arg4::mec1-4* cells may also undergo extensive breakage of the chromosome (Figure 4.14A). Nevertheless, the fact that breaks are suppressed in both *top2* and condensin mutants, and knowing the common functions of Top2 and condensin regarding chromosome structure and compaction, suggests they may be involved in a common mechanism of chromosome breakage, chromosome condensation.

### 4.3.5   A possible role for sister chromatid decatenation at *RSZs*

Although Top2 and condensin have both been implicated in chromatin compaction at the onset of mitosis, a recent report suggests that condensin is capable of directing the decatenation function of Top2 during rDNA segregation (D'Ambrosio et al., 2008). This raises the possibility that the absence of breaks in *mec1-ts* cells harbouring mutations in condensin is due to a lack of Top2 decatenation activity rather than a defect in condensation. However, rDNA is a specialised locus that recruits condensin in a Fob1-dependent manner during S-phase and in a Cdc14-dependent manner during anaphase (Johzuka et al., 2006; Sullivan et al., 2004; Wang et al., 2004). Therefore, events at the rDNA locus may not reflect events at other loci

within the genome. Nevertheless, topo II-dependent decatenation is reported to be significantly reduced in *Drosophila* cells lacking functional condensin subunits, suggesting that condensation-driven Top2 activity may be a universal phenomenon (Coelho et al., 2003).

The hypothesis that decatenation by Top2 may generate breaks at *RSZs* is supported by the observations that inactivation of Top2 also suppresses *mec1-ts* DSBs (Section 4.2.3) and that these breaks are prevented by treatment with spindle inhibitors, another condition thought to influence Top2 decatenation activity (Holm et al., 1989). However, as mentioned above, Top2 does not localise to all *RSZs*, at least on chromosomes III and VI, arguing against this possibility (Section 4.2.3.1). It is possible that Top2 may have dissociated from the break ends after cleavage of the DNA, and was therefore not enriched at *RSZs*. The localisation of Top2 along chromosomes in conditions where Top2 remains bound to the break ends is currently being assessed in collaboration with the Shirahige group at the Tokyo Institute of Technology. Another possibility is that chromosome breakage at *RSZs* by Top2 does not necessarily require a significant enrichment of Top2 at these sites and may therefore not be detected by ChIP-chip experiments.

One argument against a role for decatenation *per se* in generating DSBs at *RSZs* is that the occurrence of these breaks is dependent on dNTP levels, the idea being that increases in dNTP production prevents fork stalling at *RSZs*, allowing duplication of these regions to be completed prior to mitosis. Top2-dependent sister chromatid decatenation is required for the segregation of fully duplicated (but catenated) sister chromatids and is therefore not influenced by alterations in dNTP levels. Top2 also plays a role in DNA replication to relieve torsional constraints generated during replication elongation (Bermejo et al., 2007). This raises the possibility that Top2 may act at replication forks progressing through the largely unreplicated *RSZs*. However, this role of Top2 can be substituted by Top1 activity, suggesting that, in the absence of Top2, Top1 may act at incompletely replicated *RSZs* to generate breaks instead. Perhaps DNA lesions resulting from Top1 action at *RSZs* in the absence of Top2 cannot be visualised by PFGE and may therefore go undetected in *mec1-4 top2-1* mutants. Furthermore, although condensin promotes Top2-dependent decatenation of rDNA, it is not essential for this process and rDNA is eventually able

to be decatenated in the absence of condensin function (D'Ambrosio et al., 2008). This raises the possibility that Top2-dependent decatenation may eventually occur in *mec1-ts* cells harbouring mutations in condensin subunits without resulting in chromosome breakage at *RSZs*.

### 4.3.6   Model for chromosome break formation in *mec1-ts*

The results presented in this chapter support a model in which chromosome breakage at *RSZs* is produced by a Top2 and condensin-dependent pre-anaphase event. Whether this event is specifically sister chromatid decatenation or chromosome condensation remains unclear. Condensation alone does not normally generate breaks on DNA. As mentioned above, break formation at both common fragile sites in mammals and *RSZs* in yeast occurs after some perturbation in DNA replication. Importantly, these regions replicate late in S-phase and are therefore particularly susceptible to situations where mitosis is not prevented if these regions are not fully replicated – i.e., it is important that these regions have completed replication to avoid breakage of the chromosome.

Perturbations in DNA synthesis resulting in the stalling of the replication fork are a crucial factor in the breakage of the chromosome at fragile sites or *RSZs*. Histone H3 phosphorylation in *arg4::mec1-4* cells occurs when a large proportion of the population is still in S-phase (Section 4.2.2.2) indicating that perhaps condensation is executed with wild type kinetics on incompletely replicated chromosomes in these cells. This would imply that breaks arise when incompletely replicated chromosomes condense. In support of this notion, increasing dNTP synthesis bypasses any replication stalling at *RSZs*, presumably allowing the chromosome to be fully replicated prior to condensation and breaks to be evaded. Alternatively, condensation can promote decatenation of sister chromatids by Top2, resulting in the formation of DSBs at *RSZs*.

Figure 4.18 describes a model to explain chromosome breakage at *RSZs* due to chromosome condensation, either by Top2- and condensin-dependent condensation of the chromosome, or by condensin-dependent decatenation of sister chromatids by Top2. In wild type cells, DNA replication is completed prior to chromosome

condensation. As a result, condensation of the chromosome and possibly also condensin-driven decatenation by Top2 occurs during G2/M, after chromosomes have been fully replicated (Figure 4.17A). Treatment with Calyculin A during late S-phase induces premature condensation on chromosome structures present at this stage, resulting in the generation of breaks at fragile sites/*RSZs* (Figure 4.17B). Likewise, inactivation of Mec1 or treatment with aphidicolin results in stalling of the replication fork at *RSZs* or fragile sites. Condensation is not prevented and occurs at the normal time, possibly due to a lack of checkpoint activity (*mec1-ts* or ATR-deficient cells) or escape from checkpoint arrest (common fragile sites in ATR-proficient cells), leading to chromosome breakage at *RSZs* and fragile sites either by generating a stress on unreplicated DNA at these sites, or by inducing Top2-dependent cleavage of these sites (Figure 4.17C). Increasing dNTPs by deleting *SML1* prevents fork stalling in *mec1-ts* cells and promotes the timely completion of DNA synthesis prior to the onset of chromosome condensation (as in Figure 4.17A). This would eliminate the weak, unreplicated DNA structures that are susceptible to breakage by condensation or condensation-driven Top2 activity by the time condensation initiates. Thus, chromosome breakage at *RSZs* is avoided and the integrity of the genome is maintained.

Figure 4.17    Model for the mechanism for chromosome break formation at *RSZs* and mammalian common fragile sites

# Chapter 5

# Factors that govern chromosome stability at *RSZs*

## 5.1 Introduction

Delayed replication is a defining feature of fragile sites in both mammals and yeast. As mentioned above, two events are required to produce breaks at *RSZs*: *i*) fork stalling or delayed replication at *RSZs*, and *ii*) a process that converts the stalled fork into a DSB. Indeed, chromosome breakage associated with stalled forks has been observed in many organisms including bacteria, yeast, and mammalian cells (Admire et al., 2006; Lundin et al., 2002; Michel et al., 1997; Saintigny et al., 2001; Sorensen et al., 2005). In Chapter 4, the processes involved in producing a DSB from replication forks stalled at *RSZs* were assessed. In this chapter, the factors implicated in fork stalling were examined for their potential effects on break formation at *RSZs*.

Replication forks stall in various circumstances and are regulated or processed according to the context in which they have stalled. Exogenous factors can stall DNA replication by either damaging the DNA template (e.g. MMS) or by depleting dNTP pools (e.g. HU). Under these conditions, the S-phase checkpoint is activated, which in turn stabilises the stalled forks and suppresses genome instability (Section 1.9). Replication forks also stall transiently at natural impediments during unchallenged DNA replication (Section 1.4.3). There are estimated to be over 1000 of these sites scattered throughout the yeast genome. These include tRNA genes, the replication fork barrier (RFB) on rDNA, telomeres, centromeres, silent ARS sequences, and silent mating type loci (Deshpande and Newlon, 1996; Greenfeder and Newlon, 1992; Ivessa et al., 2003; Ivessa et al., 2002; Wang et al., 2001). Unlike forks that stall due to DNA damage, forks that have stalled at natural fork pausing sites are stable, do not elicit or require a checkpoint response for stabilisation, and are unlikely to induce fork collapse (Calzada et al., 2005; Lambert et al., 2005). Rather,

genomic instability at these sites is dependent on other factors in addition to fork pausing such as the surrounding DNA sequence and/or events that occur after pausing (Labib and Hodgson, 2007). Finally, chromosomal determinants such as Ty insertions and other repetitive elements can form secondary structures in the DNA such as hairpins or cruciform structures that can stall a progressing replication fork (Lemoine et al., 2005; Voineagu et al., 2008). In fact, studies in yeast and mammals have proposed that fragile sites are characterised by DNA elements that trigger the formation of secondary structures in the DNA (Lemoine et al., 2005; Raveendranathan et al., 2006; Zhang and Freudenreich, 2007).

When forks stall due to DNA damage, the replication and checkpoint factor, Mrc1, is required to actively and stably stall the replication fork by coupling the helicase and polymerase activities (Katou et al., 2003). The absence of *MRC1* in cells treated with HU results in the uncoupling of the replisome from the site of DNA synthesis, leading to an accumulation of ssDNA at the fork. Unlike in *rad53* mutants treated with HU, uncoupled forks in *mrc1Δ* cells treated with HU do not seem to collapse as the replisome remains bound to DNA (Katou et al., 2003). However, the dependency of *mrc1Δ* cells on Rad9 for viability suggests that damage-like structures are generated by loss of Mrc1 function and activate the DNA damage checkpoint (Alcasabas et al., 2001; Katou et al., 2003). This fork pausing activity of Mrc1 is dispensable for fork stalling at natural programmed pause sites such as the RFB on rDNA as the absence of *MRC1* has no effect on fork stalling at these sites (Calzada et al., 2005; Tourriere and Pasero, 2007). In contrast to its fork stalling function during DNA damage, fork stalling at secondary structures formed on the lagging strand is increased in the absence of *MRC1*, suggesting that Mrc1 is required to counteract fork stalling at these structures, possibly by stabilising the replisome and allowing efficient restart of lagging strand synthesis (Voineagu et al., 2008).

Mrc1 functions in a complex with another checkpoint factor called Tof1 (Katou et al., 2003). Although the function of Tof1 may simply be to recruit Mrc1, deletion of *TOF1* has a similar, albeit more modest, effect on replication fork progression in DNA damaging situations (Tourriere and Pasero, 2007). However, unlike Mrc1, Tof1 is required for fork stalling at natural pause sites, and the absence of *TOF1* reduces fork pausing at these sites (Calzada et al., 2005; Mohanty et al., 2006;

Tourriere and Pasero, 2007). Deletion of *TOF1* increases fork stalling at secondary structures to a similar extent as *mrc1Δ*. Therefore, Tof1 plays an equally important to Mrc1 in counteracting fork stalling at secondary structures (Voineagu et al., 2008).

The helicase, Rrm3, is required at programmed pause sites to enable forks to progress beyond these sites, possibly by displacing bound proteins that may block replication fork progression (Calzada et al., 2005; Mohanty et al., 2006). Deletion of *RRM3* results in an increase in fork stalling accompanied by an increase in chromosome breakage at programmed pause sites (Ivessa et al., 2003; Ivessa et al., 2002). Although Rrm3 is recruited to replication forks just after origin firing, it is not involved in the general progression of the replication fork; instead it seems that Rrm3 is required specifically when the progressing replication fork encounters programmed pause sites (Azvolinsky et al., 2006). Therefore, deletion of *RRM3* does not increase fork stalling and breakage at other sites on the chromosome. It is currently unknown whether Rrm3 plays a role at forks that have stalled at secondary structures; however, Voineagu et al. (2008) postulate that because Tof1 is not specifically involved in fork pausing at these sites, it is unlikely that Rrm3 will be required to process this type of stalled fork.

Similar to the situation at programmed pause sites, fork slowing and/or stalling at *RSZs* in both wild type and *mec1-ts* situations is thought to be physiological, i.e. competent for replication (Cha and Kleckner, 2002). Like the increased fork stalling at pause sites in the absence of *RRM3*, it is the prolonged pausing of the fork at *RSZs*, which occurs when Mec1 is inactivated, that results in chromosome breakage at these sites. However, the factors that contribute to this physiological and stable fork stalling at *RSZs* remain unknown. Therefore, the involvement of Mrc1, Tof1, and Rrm3 at *RSZs* was assessed in order to gain insight into the factors that contribute to stable fork stalling and restart at *RSZs*.

In addition to events that cause replication forks to stall at *RSZs*, factors that may govern the stability of these regions were also investigated in this chapter. The checkpoint protein, Tel1, which can to some extent substitute for Mec1 function, could conceivably play some role at *RSZs*. The Psy2-Pph3 phosphatase complex dephosphorylates Rad53 and, consequently, turns off an activated checkpoint

(O'Neill et al., 2007). Consequently, a deficiency in this phosphatase complex maintains an active checkpoint response even after the source of checkpoint activation (e.g. a replication block) has been repaired. In this chapter, the involvement of checkpoint activity, particularly that of Tel1, at *RSZs* was investigated by examining the effects of Tel1 and the Psy-Pph3 phosphatase complex on break formation at *RSZs* in *mec1-ts* cells.

## 5.2  Results

### 5.2.1  Break formation in *mec1-ts* does not require Tof1 or the checkpoint function of Mrc1.

As mentioned above, chromosome breakage and genomic instability are closely associated with replication fork stalling. This is also true at *RSZs* where prolonged stalling of the replication fork leads to the formation of DSBs (Cha and Kleckner, 2002). In order to discern the factors that contribute to fork stalling at *RSZs*, the effect of the fork stability proteins, Mrc1 and Tof1, on break formation was assessed. In addition to their role in amplifying checkpoint signals, Mrc1 and Tof1 play a structural role at stalled forks independently of the replication checkpoint (Katou et al., 2003). In the event of DNA damage, Mrc1 and Tof1 act together to form a stable fork pausing complex that serves to anchor the replisome to the site of DNA synthesis so that the fork can restart efficiently once the damage has been repaired. At programmed pause sites, Tof1, but not Mrc1, seems to be required to stably stall the replication fork (Calzada et al., 2005; Hodgson et al., 2007; Szyjka et al., 2005). When forks stall at secondary structures such as DNA hairpins, both Mrc1 and Tof1 contribute equally to the stabilisation of the replisome and are required to counteract fork stalling at these stall sites. In light of the various roles of Mrc1 and Tof1 at replication forks that have stalled in different contexts, the role of these factors at *RSZs* was investigated in order to determine the nature of fork stalling at these sites.

As chromosome breakage and replication stalling are closely linked at *RSZs*, we reasoned that the effect of *mrc1Δ* or *tof1Δ* on break formation at these sites would reflect their involvement in fork stalling at *RSZs*. Wild type and *mec1-4* cells, in addition to *mrc1Δ* and *tof1Δ*, in both wild type and *mec1-4* backgrounds were grown to log phase in YPD at 23$^{\text{o}}$C. The cultures were then synchronized in G1 with α-factor for two hours at 23$^{\text{o}}$C and for a further half hour at 37$^{\text{o}}$C, the restrictive temperature for *mec1-4*. The cells were then released into pre-warmed YPD at 37$^{\text{o}}$C and samples were collected 5 hours after release from α-factor and processed for PFGE/Southern. Southern hybridisation was performed using the *CHA1* probe to analyse the status of chromosome III in these strains. In conjunction with this experiment, the same strains were subjected to temperature sensitivity assays. Log phase cultures of these cells were serially diluted and spotted onto YPD agar. The agar plates were then incubated at the indicated temperatures for three days.

As expected *mec1-4* cells acquired breaks at restrictive temperature. Breaks on chromosome III were absent in *mrc1Δ mec1-4* and seemed somewhat reduced in *tof1Δ mec1-4* (Figure 5.1A). Quantification of the level of chromosome breakage in *tof1Δ mec1-4* indicated that the amount of breaks in this double mutant was not significantly lower than that in *mec1-4* mutants alone (Figure 5.1B). Temperature sensitivity assays of these same strains revealed that neither *mrc1Δ* nor *tof1Δ* were able to rescue the lethality of *mec1-4* at high temperatures. In fact, both *tof1Δ* and *mrc1Δ* reduced the viability of *mec1-4* even at 30$^{\text{o}}$C, where endogenous *mec1-4* strains are normally viable (Figure 5.2).

Figure 5.1     The effect of *tof1Δ* and *mrc1Δ* on break formation in *mec1-4*

Figure 5.2     *mrc1Δ* and *tof1Δ* do not rescue the lethality of *mec1-4* at high temperatures

Mrc1 is required for the normal progression of replication forks as the rate of replication fork progression in *mrc1Δ* cells is about half of the rate in wild type cells (Hodgson et al., 2007; Szyjka et al., 2005; Tourriere et al., 2005). Therefore, one plausible explanation for the absence of breaks in the *mrc1Δ mec1-4* mutant is that the combination of S-phase defects conferred by both *mrc1Δ* and *mec1-4* cause the replication forks to collapse before they reach the *RSZs*. This would be similar to the case in *mec1Δ sml1Δ* mutants exposed to high doses of HU (Sections 3.2.4 and 3.2.5). Although chromosome breaks at *RSZs* arise upon treatment with a low dose of HU, breaks do not form at these sites at high concentrations of HU presumably because replication forks stall and collapse before they reach *RSZs* (Figures 3.9, 3.10, and 3.11). The *mrc1-AQ* mutant is defective for the checkpoint function of Mrc1 as all consensus sites for phosphorylation by Mec1 have been mutated (Osborn and Elledge, 2003). In contrast to *mrc1Δ* mutants, cells carrying the *mrc1-AQ* mutation show no defect in replication fork progression (Osborn and Elledge, 2003). In order to assess whether the checkpoint function of Mrc1 was required for break formation at *RSZs*, the effect of this mutation on *mec1-4* chromosome breaks was tested.

Wild type, *mec1-4*, and *mec1-4* strains carrying either *mrc1Δ* or *mrc1-AQ* mutations were grown to log phase in YPD at 23$^\circ$C. The cultures were then synchronized in G1 with α-factor for two hours at 23$^\circ$C and for a further half hour at 37$^\circ$C. The cells were then released into pre-warmed YPD at 37$^\circ$C. Samples were collected 5 hours after release from α-factor and processed for PFGE/Southern. Southern hybridisation was performed using the *CHA1* probe to analyse the status of chromosome III. In conjunction with this experiment, temperature sensitivity assays were performed on the same mutants. Log phase cultures of these cells were serially diluted and spotted onto YPD agar. The agar plates were then incubated at the indicated temperatures for three days.

While break formation was suppressed in *mec1-4* cells where *MRC1* was deleted, breaks were visible in *mec1-4 mrc1-AQ* cells, suggesting that the checkpoint function of Mrc1 is not involved in fork stalling and chromosome breakage at *RSZs* (Figure 5.3A).  Temperature sensitivity assays showed that *mrc1-AQ* did not significantly

affect the growth of *mec1-4* at 30$^{\circ}$C and, as expected, did not rescue the lethality of *mec1-4* at high temperatures (Figure 5.3B).

Taken together, this data suggests that Tof1 and the checkpoint function of Mrc1 are dispensable for stable fork stalling at *RSZs*. It is unclear whether the absence of breaks in *mrc1Δ mec1-4* cells is due to the combined replication defects of *mrc1Δ* and *mec1-4* mutations or whether it indicates a requirement for the fork pausing functions of Mrc1 at *RSZs*. Two-dimensional (2D) gel analysis of replication intermediates in these mutants should determine whether prolonged stalling of the replication fork at *RSZs* still occurs in *mrc1Δ* and *mrc1Δ mec1-4* mutants.

## 5.2.2    The involvement of Rrm3 helicase at *RSZs*

The Rrm3 helicase is required to enable replication forks that have stalled at natural programmed pause sites to restart and progress beyond these sites (Calzada et al., 2005; Ivessa et al., 2003; Mohanty et al., 2006). In the absence of *RRM3*, fork stalling and chromosome breakage is increased at these pause sites. As *RSZs* could be described as natural impediments to DNA replication, it seemed relevant to address whether Rrm3 played a role at *RSZs*.

### 5.2.2.1 Deletion of *RRM3* prevents *mec1-ts* chromosome breakage

In order to determine if Rrm3 plays a role at *RSZs*, *mec1-ts* chromosome breakage was assessed in *mec1-4* cells where *RRM3* was deleted. Wild type, *mec1-4*, *rrm3Δ*, and *rrm3Δ mec1-4* cells were grown to log phase in YPD at 23$^{\circ}$C, arrested in G1 with α-factor for two hours at 23$^{\circ}$C and then for a further half hour at 37$^{\circ}$C. The cells were then released into fresh, pre-warmed YPD at 37$^{\circ}$C and samples for PFGE were collected 5 hours after release from α-factor. Southern hybridisation was performed using the *CHA1* probe.

Figure 5.3 Chromosome breakage at *RSZs* occurs independently of the checkpoint function of Mrc1

Southern analysis of the above mutants revealed that deletion of *RRM3* suppressed chromosome breakage in *mec1-4* mutants suggesting a possible role for the Rrm3 helicase in break formation at *RSZs* (Figure 5.4A). This result was unexpected as deletion of *RRM3* is generally associated with increased fork stalling and chromosome breakage at programmed pause sites (Ivessa et al., 2002; Prado and Aguilera, 2005; Wellinger et al., 2006).

In order to determine whether the suppression of *mec1-4* breaks by *rrm3Δ* is due to the absence of Rrm3 helicase activity, break formation was assessed in *rrm3Δ mec1-4* strains expressing either wild type *RRM3* or helicase-defective *RRM3* from a plasmid. An ARS-CEN plasmid carrying wild type *RRM3* (YCplac111-*RRM3*) or helicase-defective *RRM3* (YCplac111-*RRM3K260A*) was transformed into *rrm3Δ mec1-4* strains. The empty vector, YCplac111, transformed into *rrm3Δ mec1-4* strains was used as a negative control. Wild type, *mec1-4*, *rrm3Δ*, *rrm3Δ mec1-4*, and *rrm3Δ mec1-4* strains transformed with the indicated plasmids were grown to log phase in YPD at 23$^{\circ}$C. The cells were arrested in G1 with α-factor for two hours at 23$^{\circ}$C and then for a further half hour at 37$^{\circ}$C before being released into fresh, pre-warmed YPD at 37$^{\circ}$C. Samples for PFGE were collected 5 hours after release from α-factor. Southern hybridisation was performed using the *CHA1* probe.

Consistent with the above result, breaks were absent in the *rrm3Δ mec1-4* strain. Introduction of the empty vector into *rrm3Δ mec1-4* strains showed no effect in terms of break formation. In contrast, introduction of wild type *RRM3* into *rrm3Δ mec1-4* restored the appearance of *mec1-4* chromosome breaks confirming that the absence of breaks in *rrm3Δ mec1-4* cells was due to loss of Rrm3 function (Figure 5.4B). Restoration of DSBs was not observed when helicase-defective Rrm3 was introduced into in *rrm3Δ mec1-4* cells, suggesting that loss of the helicase function of Rrm3 was critical for the suppression of *mec1-4* DSBs by *rrm3Δ* (Figure 5.4B).

Figure 5.4     Elimination of the Rrm3 helicase prevents break formation in *mec1-4*

The effect of *rrm3Δ* on the viability of *mec1-4* at non-permissive temperatures was also assessed. Log phase cultures of wild type, *mec1-4*, *rrm3Δ*, and *rrm3Δ mec1-4* strains grown at 23$^{\circ}$C were serially diluted, spotted onto YPD agar plates, and incubated at the indicated temperatures for four days. Deletion of *RRM3* in the endogenous *mec1-4* strain showed improved the viability of *mec1-4* at restrictive temperatures (Figure 5.5).

Taken together, these results indicate that elimination of Rrm3, and more specifically, the helicase function of Rrm3, prevents chromosome breakage at *RSZs* in *mec1-4* strains. This suppression of breaks is also accompanied by an improvement in the viability of endogenous *mec1-4* strain.

### 5.2.2.2 S-phase progression and viability of ectopic *mec1-4* are improved upon deletion of *RRM3*

Replication fork stalling and chromosome breakage at programmed pause sites are increased when *RRM3* is deleted (Ivessa et al., 2003; Ivessa et al., 2002; Prado and Aguilera, 2005; Wellinger et al., 2006); so the observation that *mec1-ts* breaks are prevented in *rrm3Δ mec1-4* mutants was somewhat unexpected. It was, therefore, necessary to understand the mechanism by which deletion of *RRM3* prevents DSBs occurring in *mec1-ts* mutants in order to understand the factors governing chromosome stability at *RSZs*. The first step towards elucidating the effect of *rrm3Δ* on *mec1-ts* was to monitor the effect of *rrm3Δ* on the cell cycle progression of *mec1-ts* mutants, in particular their progression through S-phase.

To this end, cell cycle analysis of *mec1-ts* strains where *RRM3* was deleted was performed using the ectopic *mec1-4* strains that acquire DSBs and lose viability within the first cell cycle. Wild type (*mec1Δ, arg4::MEC1)*, *arg4::mec1-4*, *rrm3Δ arg4::MEC1*, and *rrm3Δ arg4::mec1-4* were grown to mid-log phase in YPD at 23$^{\circ}$C. The cells were then arrested in G1 with α-factor for two hours at 23$^{\circ}$C and for a further half hour at 30$^{\circ}$C, the restrictive temperature for ectopic *mec1-4* strains, before being released into YPD at 30$^{\circ}$C. Samples were collected at the indicated time points for FACS analysis.

Figure 5.5    Deletion of *RRM3* improves the viability of *mec1-4* at high temperatures

Wild type cells entered S-phase (intermediate DNA content on FACS profile) between 30 and 45 minutes after release from α-factor and exited S-phase by 60 minutes (Figure 5.5A). As shown above, *arg4::mec1-4* cells entered S-phase at the same time as wild type cells but remained with intermediate DNA content for the remainder of the experiment. The FACS profile of the *rrm3Δ arg4::mec1-4* double mutant revealed that, unlike *arg4::mec1-4* cells, these cells exited S-phase efficiently 60 minutes after release from α-factor (Figure 5.6A).

The viability of ectopic *arg4::mec1-4* cells deleted for *RRM3* was also assessed. Log phase cultures of wild type (*mec1Δ, arg4::MEC1)*, *arg4::mec1-4*, *rrm3Δ arg4::MEC1*, and *rrm3Δ arg4::mec1-4* grown at 23°C were serially diluted and spotted onto YPD agar. The agar plates were then incubated at the indicated temperatures for three days. In contrast to endogenous *mec1-4* cells, *arg4::mec1-4* strains have a lower restrictive temperature and lose viability at 30°C. Deletion of *RRM3* in the ectopic *arg4::mec1-4* background improved the viability of *arg4::mec1-4* cells significantly at 30°C and, to a lesser extent, at temperatures above 30°C (Figure 5.6B).

Taken together, these results indicate that the deletion of *RRM3* somehow alleviates the *mec1-4* defect, resulting in an improvement in S-phase progression and the viability of *arg4::mec1-4* (and presumably also endogenous *mec1-4* cells), thereby precluding breakage of the chromosome at *RSZs*.

Figure 5.6　　Deletion of *RRM3* improves S-phase progression and the viability of ectopic ar*g4::mec1-4* cells

### 5.2.3   Mechanism of suppression of *mec1-ts* DSBs by *rrm3Δ*

Deletion of *RRM3* results in increased fork stalling at natural pause sites as well as an increase in chromosome breaks. As a result, *rrm3Δ* is an unlikely suppressor of *mec1-ts* DSBs. Studies of mitochondrial DNA stability have reported a link between the deletion of *RRM3* and an increase in dNTP pools (O'Rourke et al., 2005; Taylor et al., 2005). In addition, all known suppressors of *mec1Δ* lethality increase dNTP levels or reduce the rate of dNTP consumption (Desany et al., 1998; Morrow et al., 1995; Sanchez et al., 1996; Vallen and Cross, 1999; Zhao et al., 2001); therefore, it was reasonable to hypothesise that the absence of breaks in *rrm3Δ mec1-ts* mutants may be due to an increase in dNTP synthesis. This hypothesis is supported by the observation that *rrm3Δ* partially rescues the lethality of both endogenous *mec1-4* and ectopic *arg4::mec1-4* cells and improves the progression of *arg4::mec1-4* cells through S-phase, a possible indication of dNTP up-regulation.

In budding yeast, dNTP synthesis is dramatically increased during DNA replication and in response to DNA damage, both of which involve increasing the activity of ribonucleotide reductase (RNR). Upon detection of genotoxic stress, a *MEC1-/TEL1-*dependent signalling cascade is activated resulting in the hyperphosphorylation and activation of the checkpoint kinase, Rad53 (Figure 5.7). Hyperphosphorylated Rad53 activates the downstream kinase, Dun1, which increases dNTP synthesis through several pathways. Dun1 directly phosphorylates Sml1, an inhibitor of the enzymatic activity of RNR, leading to its degradation (Uchiki et al., 2004; Zhao et al., 2001; Zhao and Rothstein, 2002). Crt1, the transcriptional inhibitor of *RNR2, RNR3, RNR4* that encode subunits of RNR, is also phosphorylated in a Dun1-dependent manner (Huang et al., 1998). Hyperphosphorylated Crt1 dissociates from the DNA resulting in an increase in the expression of *RNR2*, *RNR3*, and *RNR4* (Huang et al., 1998). In response to genotoxic stress, the small RNR subunits also relocate from the nucleus to the cytoplasm, where the large subunits are located, resulting in the assembly of a complete RNR capable of synthesising dNTPs (Yao et al., 2003).

Figure 5.7        Mechanisms of dNTP up-regulation in response to DNA damage

Strains defective for Rrm3 display constitutively phosphorylated Rad53, suggesting that this Mec1/Tel1-signalling cascade is activated in this mutant and supporting the hypothesis that *rrm3Δ* suppresses the lethality of *arg4::mec1-4* by modulating dNTP pools (Ivessa et al., 2003; Schmidt and Kolodner, 2006). To test this hypothesis, the status of key mechanisms involved in regulating dNTP availability was assessed in *rrm3Δ arg4::mec1-4* cells.

### 5.2.3.1.1 The effect of *rrm3Δ* on cell cycle-dependent fluctuation of Sml1 levels

In wild type cells, Sml1 is degraded at the G1/S transition and is re-synthesised towards the end of S-phase. This fluctuation of Sml1 levels is dependent on *MEC1* as Sml1 levels remain constant in *mec1Δ* cells rescued by *RNR1* over-expression (Zhao et al., 2001). As deletion of *RRM3* improves the viability of *arg4::mec1-4* as well as its progression through S-phase, it seemed possible that *rrm3Δ* may affect the cell cycle-dependent fluctuation of Sml1.

In order to test this hypothesis, wild type (*arg4::MEC1*), *arg4::mec1-4*, *rrm3Δ arg4::MEC1*, and *rrm3Δ arg4::mec1-4* strains expressing N-terminally MYC-tagged Sml1 were constructed. Log phase YPD cultures of these strains grown at 23$^{\mathrm{o}}$C were arrested in G1 with α-factor for two hours at 23$^{\mathrm{o}}$C followed by a further half hour at 30$^{\mathrm{o}}$C. The cells were then released into fresh, pre-warmed YPD at 30$^{\mathrm{o}}$C and samples were collected every ten minutes for protein extraction and FACS analysis. Proteins were separated on 15% polyacrylamide gels by SDS-PAGE and analysed by Western blot. The blots were probed with an anti-MYC antibody to detect MYC-Sml1. The same blots were then probed with anti-tubulin antibody to serve as a loading control. The signals corresponding to 3MYC-Sml1 and tubulin bands were quantified from scanned images of the Western blots using ImageJ software. The graphs show the levels of 3MYC-Sml1 in each strain, normalised to the tubulin band, and expressed relative to the t=0 sample, which was set to 1.00.

As expected, the wild type *arg4::MEC1 3MYC-SML1* control strain showed a decrease in Sml1 levels as cells entered S-phase. Sml1 levels then increased towards the end of S-phase (approximately 40 minutes after release from α-factor; Figure 5.8). On the other hand, Sml1 levels in *arg4::mec1-4 3MYC-SML1* cells remained

roughly constant throughout the experiment, accumulating slightly towards the end of the experiment. The persistence of Sml1 in these cells correlated with an accumulation of cells with intermediate DNA content (Figure 5.8). Sml1 levels decreased significantly in the *rrm3Δ arg4::MEC1 3MYC-SML1* strain. However, the levels of Sml1 did not subsequently increase by the end of the experiment as it had in the wild type strain (Figure 5.8). This lack of fluctuation in Sml1 levels is observed in DNA damage situations and is, therefore, consistent with the notion that *rrm3Δ* cells activate the DNA damage checkpoint (Zhao et al., 2001). A modest decrease in Sml1 levels before the onset of S-phase was detected in *rrm3Δ arg4::mec1-4 3MYC-SML1* cells. As expected, S-phase progression was improved in these cells compared to *arg4::mec1-4* cells (Figure 5.8C). The decrease in Sml1 levels was less than that observed in wild type strains but was slightly more substantial than that in *arg4::mec1-4* cells. Unlike in *rrm3Δ arg4::MEC1* cells, Sml1 levels increased again to t=0 levels by the end of the experiment (Figure 5.8). Similar results were observed in an independent experiment. These observations suggest that deletion of *RRM3* may, to some extent, restore the cycling of Sml1 levels in *arg4::mec1-4* cells.

### 5.2.3.2 The effect of deletion of *RRM3* on Rad53 activation

Rad53 is spontaneously phosphorylated in *rrm3* mutants in a *MEC1-/RAD9-*dependent manner (Schmidt and Kolodner, 2006). It has been proposed that the increased DNA damage that occurs in *rrm3Δ* mutants (presumably at programmed pause sites) results in the activation of the DNA damage checkpoint (Schmidt and Kolodner, 2006). This raises the possibility that *rrm3Δ* inadvertently causes an increase in dNTP synthesis by generating DNA damage elsewhere in the genome.

The results in section 5.2.3.1 suggest that *rrm3Δ* may have a nominal effect on Sml1 cycling. It was therefore necessary to confirm this result by monitoring an upstream event in the signalling cascade that leads to degradation of Sml1. As mentioned above, the different means implicated in dNTP up-regulation all involve the activation of the checkpoint kinase, Rad53. Therefore, in order to substantiate the observation that Sml1 levels are affected by deletion of *RRM3*, the effect of *rrm3Δ* on Rad53 phosphorylation, and consequently its activation, was examined.

Figure 5.8     Deletion of *RRM3* has a modest effect on Sml1 levels in *arg4::mec1-4*

Wild type (*arg4::MEC1*), *arg4::mec1-4*, *rrm3Δ arg4::MEC1*, and *rrm3Δ arg4::mec1-4* cells were grown to mid-log phase in YPD at 23$^{o}$C. The cells were then arrested in G1 with α-factor for two hours at 23$^{o}$C and for another half hour at 30$^{o}$C. The cells were then released into pre-warmed YPD at 30$^{o}$C. Samples for protein extraction were collected 45 minutes after release. Samples were also collected at t=0 and t=45 minutes for FACS analysis. Proteins were separated on a 10% polyacrylamide gel. Western blot analysis was performed by sequentially probing the blot with antibodies against phosphorylated Rad53 and the Rad53 backbone (Bermejo et al., 2007). As a positive control, protein extracts of a log phase culture of a wild type strain (NHY 342) treated with 0.03% MMS to induce DNA damage were also loaded on the gel.

Rad53 was evidently phosphorylated in the MMS-treated control and to a lesser extent in the *rrm3Δ arg4::MEC1* strain, consistent with published reports (Schmidt and Kolodner, 2006). In contrast, phosphorylation of Rad53 was not detected in *arg4::mec1-4* or *rrm3Δ arg4::mec1-4* cells (Figure 5.9A). FACS analysis confirmed that the protein extracts analysed in Figure 5.9A were made from S-phase cells (Figure 5.9B). This result suggests that the mechanism by which *rrm3Δ* improves the S-phase defect and the viability of *arg4::mec1-4* and prevents the formation of breaks at *RSZs* may not be dependent on Rad53 activation. However, it remains possible that deletion of *RRM3* in *arg4::mec1-4* strains may cause a very slight increase in Rad53 phosphorylation that cannot be detected by our system.

Figure 5.9    No detectable phosphorylation of Rad53 occurs in *rrm3Δ arg4::mec1-4*

### 5.2.4   Checkpoint activity regulates *RSZ* stability

Studies of chromosome fragile sites in both yeast and mammalian systems indicate that instability at these sites increases in the absence of an intact replication checkpoint (Admire et al., 2006; Casper et al., 2002; Cha and Kleckner, 2002; Raveendranathan et al., 2006). This suggests that components of the replication checkpoint are involved in regulating the stability of these fragile sites. Chromosome breaks at *RSZs* arise only when Mec1 is inactivated in *mec1-ts* cells, suggesting that Mec1 is the major regulator of chromosome stability at these sites. However, it is possible that other checkpoint factors are also, to some extent, involved in regulating *RSZ* stability.

*PSY2* encodes a component of the Psy2-Pph3 phosphatase complex that is responsible for dephosphorylating Rad53 and γ-H2AX resulting in the deactivation of the checkpoint (O'Neill et al., 2007) (Section 1.8.5). Eliminating Psy2-Pph3 phosphatase activity by deletion of *PSY2* or *PPH3* results in persistent activation of the checkpoint. Therefore, in order to understand the contribution of checkpoint activity to *RSZ* stability, the effect of *psy2Δ* on chromosome stability at *RSZs* in *mec1-ts* was assessed.

### 5.2.4.1 Deletion of *PSY2* improves the viability of *mec1-4*

In order to determine the effect of Psy2 on the stability of *RSZs*, a *mec1-4* strain harbouring a deletion of *PSY2* was generated. Temperature sensitivity assays were performed on these mutants to determine whether deletion of *PSY2* affected the viability of *mec1-4* mutants at non-permissive temperatures.

Log phase cultures of wild type, *mec1-4*, *psy2Δ*, *psy2Δ mec1-4* cells grown at 23$^\mathrm{o}$C were serially diluted and spotted onto YPD agar. The agar plates were then incubated at the indicated temperatures for three days. As expected, *mec1-4* lost viability at both 34$^\mathrm{o}$C and 37$^\mathrm{o}$C, with 37$^\mathrm{o}$C showing the more severe phenotype. However, the viability of *mec1-4* improved at 34$^\mathrm{o}$C and, to a lesser extent, at 37$^\mathrm{o}$C when *PSY2* was deleted in this strain (Figure 5.10).

Figure 5.10    Deletion of *PSY2* improves the viability of *mec1-4* at high temperatures

**5.2.4.2 Deletion of *PSY2* prevents breaks at *RSZs* in *mec1-4***

As deletion of *PSY2* seemed to improve the viability of *mec1-4* strains at restrictive temperatures, it was necessary to verify that this suppression of lethality in the *psy2Δ mec1-4* double mutant was accompanied by a reduction in chromosome breakage at *RSZs*.

Wild type, *mec1-4*, *psy2Δ*, *psy2Δ mec1-4* cells were grown to mid-log phase in YPD at $23^{o}$C. The cells were synchronised in G1 with α-factor for two hours at $23^{o}$C, and then for a further half hour at $34^{o}$C, the temperature at which suppression of *mec1-4* lethality was more robust. The cells were then released from α-factor arrest into fresh, pre-warmed YPD at $34^{o}$C and samples for PFGE were collected after 5 hours. The same experiment was also repeated at $37^{o}$C. Southern analysis was performed using the *CHA1* probe to detect DSB on chromosome III as well the intact chromosome.

Chromosome breaks at *RSZs* were visible in the *mec1-4* strain at $34^{o}$C, as expected, but were absent in the *psy2Δ mec1-4* double mutant (Figure 5.11A). Breaks at *RSZs* were greatly reduced, albeit still visible, in this double mutant at $37^{o}$C, the temperature at which suppression of *mec1-4* lethality was minimal (Figure 5.11B). This indicates that deletion of *PSY2* reduces break formation in *mec1-4* mutants proportionally to the extent to which it improves their viability.

Taken together, the results in Sections 5.2.4.1 and 5.2.4.2 suggest that maintaining an active checkpoint can improve the viability of *mec1-4* cells and reduce the level of chromosome breakage at *RSZs* in this mutant.

Figure 5.11     *psy2Δ* suppresses break formation in *mec1-4*

### 5.2.5   **Involvement of Tel1 activity at *RSZs***

Results in Section 5.2.4 suggest that increasing checkpoint activity can prevent instability at *RSZs*. In addition, *MEC1* and *TEL1* perform partially redundant roles in the response to genotoxic stress such that over-expression of *TEL1* can rescue the lethality of and partially rescue the DNA damage sensitivity of *mec1Δ* mutants (Clerici et al., 2001; Morrow et al., 1995). This raises the possibility that Tel1 activity may play a minor role in regulating *RSZ* stability in the absence of Mec1 function.

**5.2.5.1 Deletion of *TEL1* increases chromosome breakage at *RSZs* in *mec1-ts***

In order to determine whether Tel1 is involved in *RSZ* stability, the effect of *tel1Δ* on the formation of DSBs at *RSZs* was assessed. Log phase cultures of wild type, *mec1-4*, *tel1Δ*, and *tel1Δ mec1-4* cells were synchronised in G1 with α-factor for two hours at $23^{o}$C and for another half hour at $30^{o}$C. The cells were then released into pre-warmed YPD at $30^{o}$C for 5 hours before samples were collected for PFGE. Southern was performed using the *CHA1* probe for analysis of break formation on chromosome III.

Although break formation was observed in *mec1-4* cells at restrictive temperature, the level of chromosome breakage increased when *TEL1* was additionally deleted (Figure 5.12). Break formation did not occur in *tel1Δ* single mutants. This observation suggests that Tel1 may contribute to the regulation of DNA stability at *RSZs*.

Figure 5.12     Tel1 plays a minor role in maintaining chromosome stability at *RSZs*

**5.2.5.2 Suppression of DSBs in *rrm3Δ arg4::mec1-4* is dependent on Tel1**

Results from Sections 5.2.2 and 5.2.3 show that deletion of *RRM3* prevents break formation at *RSZs* and rescues the lethality of *mec1-4* cells, possibly by subtly restoring Sml1 cycling to *mec1-4* cells. However, Rad53 phosphorylation could not be detected in *rrm3Δ arg4::mec1*-4 cells. A possible mechanism by which the deletion of *RRM3* might influence Sml1 levels in a *MEC1*-independent manner is by increasing Tel1 activity. To test this possibility, the dependence of the suppression of *mec1-ts* breaks by *rrm3Δ* on Tel1 was assessed.

In order to test the dependence of the suppression of *mec1*-dependent DSBs by *rrm3Δ*, break formation was monitored in *rrm3Δ arg4::mec1-4* cells where *TEL1* was deleted. Wild type (*arg4::MEC1), arg4::mec1-4*, *rrm3Δ arg4::MEC1*, *rrm3Δ arg4::mec1-4*, and *tel1Δ rrm3Δ arg4::mec1-4* strains were grown to mid-log phase in YPD at 23$^{\circ}$C. The cells were then arrested in G1 with α-factor for two hours at 23$^{\circ}$C and for another half hour at 30$^{\circ}$C. The cells were then released into pre-warmed YPD at 30$^{\circ}$C for 5 hours before samples were collected for PFGE. Southern was performed using the *CHA1* probe for analysis of break formation on chromosome III.

As expected, breaks were present in the *arg4::mec1-4* strain at restrictive temperature but not in the *rrm3Δ arg4::mec1-4* double mutant. However, breaks were restored in *rrm3Δ arg4::mec1-4* cells where *TEL1* was also deleted indicating that the suppression of breaks by deletion of *RRM3* depends on the presence of Tel1 (Figure 5.13).

Figure 5.13     Suppression of *mec1*-dependent chromosome breaks by *rrm3Δ* requires Tel1 function

This result, in addition to the data presented in Section 5.2.3, suggests that deletion of *RRM3* may affect dNTP levels in *arg4::mec1-4* cells by a *TEL1*-dependent pathway. However, Rad53 phosphorylation could not be detected in *rrm3Δ arg4::mec1-4* cells indicating that either the suppression occurs via a Rad53-independent pathway, or that these cells do phosphorylate Rad53 but that our system was not sensitive enough to detect this modification. Although, it is unclear whether the slight decrease in Sml1 levels observed in *rrm3Δ arg4::mec1-4* cells is significant enough to allow the synthesis of ample dNTPs to enable the completion of S-phase, it is tempting to speculate that deletion of *RRM3* in *mec1-ts* cells may slightly affect dNTP levels, tipping the balance towards viability and prevention of chromosome breakage.

### 5.2.5.3 Suppression of *mec1-4* phenotypes by *psy2Δ* requires Tel1

As all known suppressors of *mec1Δ* lethality increase dNTPs one way or another, the observation that *psy2Δ* improves the viability of *mec1-4* mutants suggests it might be doing so by increasing dNTP levels. Psy2, acting in a complex with Pph3, is required to de-phosphorylate and de-activate Rad53 to allow recovery from checkpoint arrest. Cells lacking Psy2 are unable to switch off the checkpoint response. This raises the possibility that maintaining an active checkpoint response in *mec1-4* mutants – whether it is in the form of residual Mec1 activity or increased Tel1 function-improves the viability of *mec1-4* strains, presumably by up-regulating dNTP synthesis. To test the possibility that *psy2Δ* rescues *mec1-4* phenotypes via a Tel1-dependent pathway, the viability and formation of breaks were assessed in *psy2Δ mec1-4* mutants where *TEL1* was also deleted.

Ten-fold serial dilutions of wild type, *mec1-4*, *psy2Δ*, *psy2Δ mec1-4*, and *tel1Δ psy2Δ mec1-4* strains grown to log phase in YPD at 23°C were spotted onto YPD agar. The plates were then incubated at the indicated temperatures for three days.

As shown above, deletion of *PSY2* improved the viability of *mec1-4* at non-permissive temperatures. In contrast, *tel1Δ psy2Δ mec1-4* strains showed the same pattern of viability as in *mec1-4* suggesting that the suppression of *mec1-4* lethality by *psy2Δ* was dependent on Tel1 (Figure 5.14A).

Figure 5.14 Suppression of lethality and chromosome breakage in *mec1-4* by *psy2Δ* is Tel1-dependent

The Tel1-dependency of *mec1-4* DSB suppression by *psy2Δ* was also assessed. Wild type, *mec1-4*, *psy2Δ*, *psy2Δ mec1-4*, and *tel1Δ psy2Δ mec1-4* cells were grown to mid-log phase in YPD at 23°C. The cells were then arrested in G1 with α-factor for two hours at 23°C, and then for a further half hour at 34°C, the temperature at which suppression of *mec1-4* DSBs and lethality was more obvious. The cells were then released from α-factor arrest into fresh, pre-warmed YPD at 34°C and samples for PFGE were collected after 5 hours. Southern analysis was performed using the *CHA1* probe.

Although breaks at *RSZs* were absent in the *psy2Δ mec1-4* double mutant, break formation was restored in this mutant when *TEL1* was deleted (Figure 5.14B). Taken together, these results indicate that deletion of *PSY2* alleviates the defects conferred by *mec1-4* mutants via a Tel1-dependent mechanism.

## 5.3   Discussion

### 5.3.1   Neither the checkpoint function of Mrc1 nor Tof1 are not required for fork stalling and chromosome breakage at *RSZs*

The fork stabilisation factors Mrc1 and Tof1 are differentially required for stabilisation of replication forks stalled in different contexts. Both factors are involved in DNA damage situations, where they are required to maintain the integrity of the stalled fork by coupling the replisome to the site of DNA synthesis and contribute to the amplification of the replication checkpoint. However, only Tof1 seems to be required for fork pausing at natural programmed pause sites such as the rDNA locus. When forks stall due to the secondary structures in the DNA template, it has been proposed that Mrc1 and Tof1 contribute equally to the stability of the stalled fork to allow efficient restart of the fork in these situations.

The stability of the chromosome at *RSZs* is influenced by dNTP levels, suggesting that fork stalling at these sites could resemble the stalling of replication forks in DNA damaging conditions such as treatment with HU. Alternatively, *RSZs* are a natural component of the chromosome that transiently stall replication forks in unperturbed wild type cells and could, therefore, be regulated in a manner similar to

programmed pause sites such as the RFB at the rDNA locus. Recent evidence supports the hypothesis that fragile sites in mammals and yeast readily generate hairpin structures in the DNA that can stall the replication fork (Lemoine et al., 2005; Zhang and Freudenreich, 2007). This raises the possibility that such structures cause the replication fork to stall at *RSZs* and that these stalled forks will be processed accordingly.

In order to understand better the nature of fork stalling at *RSZs*, it was necessary to assess the requirement for Mrc1 and Tof1 for fork stalling at these sites. In *mec1-ts* cells, forks initially stall at *RSZs* in a stable manner, competent to resume DNA synthesis if returned to permissive temperature (Cha and Kleckner, 2002). Chromosome breakage at *RSZs* therefore follows a prolonged period of stable fork stalling (Cha and Kleckner, 2002). As chromosome breakage is closely associated with stalled forks, we used the appearance of chromosome breaks as an indicator of fork stalling in *mrc1Δ mec1-4* and *tof1Δ mec1-4* mutants. Deletion of *TOF1* reduced *mec1*-dependent DSBs, however, this was not significantly less than in *mec1-4* single mutants, suggesting that the fork pausing activity of Tof1 may not be requisite at *RSZs* as it is at programmed pause sites such as the rDNA locus (Figure 5.1). On the other hand, deletion of *MRC1* seemed to prevent DSBs in *mec1-4* (Figure 5.1). The absence of chromosome breaks at *RSZs* in *mrc1Δ mec1-4* may indicate a requirement for Mrc1 in fork stabilisation at *RSZs*. Alternatively, the combined replication defects of both *mrc1Δ* and *mec1-4* leading to fork stalling and collapse before the replication reaches *RSZs* could equally account for this result. Replication progression is also affected in *tof1Δ* mutants, albeit to a lesser extent, suggesting that this may also explain the reduction of breaks at *RSZs* in *tof1Δ mec1-4* cells. The observation that both *mrc1Δ* and *tof1Δ* exacerbate the lethality of *mec1-4* mutants favours this hypothesis (Figure 5.2). In an attempt to resolve this issue, break formation was monitored in the checkpoint-defective but replication-proficient *mrc1-AQ* mutant in a *mec1-4* background. Chromosome breakage occurred in the *mrc1-AQ mec1-4* mutant, indicating that the checkpoint function of Mrc1 is dispensable for stable fork stalling and chromosome breakage at *RSZs* in *mec1-4* cells (Figure 5.3). However, the fact that Mrc1 contributes to fork stability independently of the S-phase checkpoint should be taken into account. It therefore remains unclear whether Mrc1

is involved in stable stalling of the replication fork at *RSZs*. Monitoring the effects of *mrc1Δ* on fork progression at *RSZs* in both wild type and *mec1-4* cells by 2D gel analysis should provide some insight into the role of Mrc1 at *RSZs*.

The observation that breaks arise in *mec1-4* cells carrying the *mrc1-AQ* mutant but not *mrc1Δ* could also imply that the presence of the Mrc1 protein (for example, in the *mrc1-AQ* mutant) is required to recruit a protein that contributes to break formation at *RSZs*.

*mrc1Δ* mutants show delayed phosphorylation of Rad53 by the Rad9-dependent DNA damage checkpoint (Alcasabas et al., 2001), raising the possibility that the absence of breaks in *mrc1Δ mec1-4* cells is due to a checkpoint-dependent increase in dNTP synthesis, perhaps with Tel1 compensating for loss of Mec1 function. However, the fact that *mrc1Δ mec1-4* are lethal at restrictive temperatures, and that the viability of these double mutants is, in fact, worse than in the *mec1-4* strain, at 30$^{o}$C argues against this idea.

### 5.3.2   Mechanism of the suppression of chromosome breakage at *RSZs* by deletion of *RRM3*

Rrm3 is required at natural fork pausing sites such as rDNA locus and tRNA genes to allow the replication fork to bypass the impediment and restart DNA synthesis. If Rrm3 also acts at *RSZs* to enable forks to progress through these sites, then an increase in fork stalling and, consequently, chromosome breakage should be observed when Rrm3 is eliminated. However, deletion of *RRM3* in *mec1-4* cells suppresses break formation at *RSZs* (Figure 5.4). The suppression of DSBs in *rrm3Δ* was accompanied by an improvement in the viability of both the endogenous *mec1-4* and the ectopic *arg4::mec1-4* strain (Figures 5.5 and 5.6). The S-phase defect of *mec1-ts* was also bypassed in *rrm3Δ arg4::mec1-4* strains (Figure 5.6). As all known suppressors of *mec1Δ* lethality up-regulate dNTP synthesis pathways, these observations point to a possible bypass of the essential function of Mec1 in regulating dNTP synthesis. The fact that deletion of *RRM3* has been shown to increase mitochondrial DNA stability by modulating dNTP pools supports the notion that this may also be the mechanism by which *rrm3Δ* suppresses *mec1-ts* DSBs.

A small degree of Sml1 degradation was observed in *rrm3Δ arg::mec1-4* strains, although it remains uncertain whether this decrease in Sml1 levels is sufficient to account for the improvement in viability of *arg4::mec1-4* cells at 30°C (Figure 5.8). Although Rad53 is phosphorylated in *rrm3Δ arg4::MEC1* cells, it could not be detected in the *rrm3Δ arg4::mec1-4* double mutants (Figure 5.9A). Despite this, the absence of breaks at *RSZs* in the *rrm3Δ arg4::mec1-4* mutant is dependent on *TEL1*, suggesting that the suppression is likely to be due to a Tel1-dependent increase in dNTPs (Figure 5.13). However, a dNTP-independent mechanism of suppression of *mec1-ts* phenotypes by *rrm3Δ* cannot be ruled out.

The fact that phosphorylated Rad53 could not be detected in *rrm3Δ arg4::mec1-4* cells is not surprising given that this phosphorylation is Mec1-dependent (Schmidt and Kolodner, 2006). However, this observation is not consistent with the requirement for Tel1 in the suppression of *arg4::mec1-4* by *rrm3Δ* or with the finding that Sml1 cycling is, to some extent, restored in *rrm3Δ arg4::mec1-4*. The small amount of Sml1 degradation observed in *rrm3Δ arg4::mec1-4* cells suggests that *rrm3Δ* may only cause a subtle increase in dNTP pools. It could also imply that Rad53 is only phosphorylated to a limited extent - perhaps on one or two residues instead of the complete hyper-phosphorylation seen in DNA damage situations - and may remain undetected by our methods. Therefore, it is possible that the increase in Tel1 activity by *rrm3Δ* may only be responsible for phosphorylating a few residues on Rad53, rendering this hypo-phosphorylated form of Rad53 undetectable but able to induce enough dNTP synthesis to prevent fork stalling and chromosome breakage at *RSZs*. Alternatively, it is possible that only a minority of Rad53 molecules are phosphorylated in response to an *rrm3Δ*-dependent increase in Tel1 activity, which may also go undetected by our methods. In support of this, deletion of *YKU70* or *YKU80*, components of the nonhomologous end-joining pathway (NHEJ), rescue the lethality of *mec1Δ* by decreasing SMl1 levels in a Tel1-Mre11-dependent pathway (Corda et al., 2005). Although *RAD53* and *DUN1* are required for this suppression, the authors could not detect a high level of Rad53 phosphorylation in the *yku70Δ* or *yku70Δ mec1Δ* mutants.

Alternatively, Tel1 could increase dNTP levels by activating a different substrate, for example Chk1. However, *chk1Δ* mutants do not show a decrease in Dun1 activity or

Sml1 phosphorylation, suggesting that this is an unlikely means of up-regulating dNTP synthesis (Chen et al., 2007).

How does deletion of *RRM3* cause an increase dNTP levels? Deletion of *RRM3* induces DNA damage at programmed pause sites throughout the genome including the rDNA locus and telomeres. It is thought that the accumulation of damage at all these sites activates the Mec1/Tel1 checkpoint cascade. As Mec1 activity is absent or greatly reduced in *mec1-ts* cells, it is likely that the Tel1 kinase substitutes for Mec1 function in activation of the checkpoint cascade leading to dNTP up-regulation. This is similar to the mechanism of *mec1Δ* suppression by *yku70Δ* (Corda et al., 2005). It is interesting that elimination of the helicase activity of Rrm3 is critical for suppression of *mec1-4* DSBs. One explanation is that the helicase activity is required for fork progression at natural pause sites; eliminating the helicase activity of Rrm3 would result in increased fork stalling and chromosome breakage at these sites leading to activation of a Tel1-dependent checkpoint and, consequently, to the suppression of break formation at *RSZs*.

Although we cannot completely exclude the possibility that suppression of *mec1-ts* DSBs by *rrm3Δ* may be through entirely different means, the fact that *rrm3Δ* improves the S-phase progression of *arg4::mec1-4* and its viability as well as suppressing DSBs in a Tel1-dependent manner supports the idea that it does so via a subtle increase in dNTP synthesis.

### 5.3.3    Increasing Tel1 activity suppresses *mec1-ts* lethality and chromosome breakage

As discussed above, deletion of *RRM3* suppresses chromosome breakage at *RSZs* in *mec1-ts* cells in a Tel1-dependent manner. In Section 5.2.4, another suppressor of *mec1-4* chromosome breakage was identified, the Psy2 component of the Psy2-Pph3 phosphatase. Similar to the effect of *rrm3Δ* on *mec1-4* and *arg4::mec1-4* strains, deletion of *PSY2* improves the viability of endogenous *mec1-4* strains at non-permissive temperatures. The suppression of both chromosome breakage at *RSZs* and the lethality of *mec1-4* by *psy2Δ* requires the action of Tel1 (Figure 5.14). The lethality of the *tel1Δ psy2Δ mec1-4* triple mutant at non-permissive temperature is

not due to the inability of *psy2Δ* to deal with the added defects conferred by *tell1Δ* and inactivation of Mec1 because deletion of *TEL1* lowered the viability of *psy2Δ mec1-4* to *mec1-4* levels. Furthermore, breakage at *RSZs* is a phenotype specific to inactivation of Mec1 but not Tel1 (Figure 5.12). The observation that *tell1Δ* restores chromosome breakage at *RSZs*, a Mec1-specific phenotype, in *psy2Δ mec1-4* cells suggests that Tel1 plays a critical role in the suppression of the *mec1-ts* defects by *psy2Δ*.

The following model, depicted in Figure 5.15C, explains the suppression of *mec1-4* defects by *psy2Δ*. Psy2, in a complex with Pph3, contributes to the deactivation of the checkpoint by dephosphorylating Rad53. Assuming that Tel1 is active in *mec1-ts* cells, deletion of *PSY2* maintains the Tel1-dependent phosphorylation of Rad53, raising Rad53 activity to a certain threshold beyond which enough dNTPs can be synthesised to prevent replication fork stalling and chromosome breakage at *RSZs*.

Another situation that influences Tel1 activity is the *rad50S* mutation. This mutation has been shown to constitutively activate Tel1 and Rad53 in yeast and mammalian systems (Usui et al., 2001; Usui et al., 2006). Like *rrm3Δ* and *psy2Δ*, *rad50S* also improves the viability of *mec1-4* and *arg4::mec1-4* at restrictive temperatures in a Tel1-dependent manner, further supporting the notion that increasing Tel1 activity suppresses *mec1-ts* phenotypes (J. Carballo and S. Rowbotham, unpublished work).

Further support for a role for Tel1 in maintaining the integrity of *RSZs* comes from monitoring break formation in *tell1Δ* and *tell1Δ mec1-4* mutants. As mentioned above, deletion of *TEL1* alone does not result in break formation at *RSZs*. However, deletion of *TEL1* in a *mec1-ts* background results in an increase in chromosome breakage at *RSZs,* suggesting that Tel1 may play a minor role alongside Mec1 in preventing fork stalling and chromosome breakage at *RSZs*. This is in agreement with findings in humans that the level of aphidicolin-induced chromosome breakage at common fragile sites is increased in $ATM^-/ATR^-$ cells compared to $ATM^+/ATR^-$ cells, indicating a role for ATM in maintaining genome stability following replication stress in the absence of ATR (Ozeri-Galai et al., 2008). Alternatively, it is possible that Tel1 may reduce the level of *mec1*-dependent chromosome breaks by channelling a fraction of these breaks to a repair pathway. Like-wise, down-

regulation of components of homologous recombination and/or NHEJ repair pathways increase the level of breakage at *RSZs* and common fragile sites (Schwartz et al., 2005; Section 4.2.1).

Taken together, these results indicate that Tel1 plays a minor role at *RSZs* and that increasing Tel1 activity by various means affects chromosome stability at these sites, presumably through dNTP up-regulation pathways. Given that *RSZs* are especially sensitive to variations in dNTP levels and that checkpoint activity is closely linked to dNTP up-regulation in budding yeast, situations that tip the balance below or above a certain threshold for checkpoint activity can influence the stability of *RSZs*. Figure 5.15 depicts a model for the interplay of these mechanisms at *RSZs*. In wild type cells, Mec1 is the major player in the cascade that governs dNTP regulation at *RSZs* while Tel1 plays a minor role. In situations that inactivate Mec1, Tel1 remains active, perhaps slightly reducing the amount of chromosome breakage generated at *RSZs*. However, this activity of Tel1 is not enough to completely prevent fork stalling and chromosome breakage at these sites. Only in conditions that increase the activity of Tel1 beyond a certain threshold for Tel1 activity can a sufficient amount of dNTPs be synthesised to prevent fork stalling at and maintain the integrity of *RSZs*.

Figure 5.15     Increasing Tel1 activity suppresses *mec1-ts* lethality and chromosome breakage at *RSZs*

# Chapter 6

# General Discussion

## 6.1   Mechanism of break formation at *RSZs*

### 6.1.1   Chromosome breakage at *RSZs* does not involve the proposed enzymatic processing of stalled forks

The established view of the mechanism of fragile site expression in both mammals and yeast is that replication forks encounter difficulties when progressing through these regions, resulting in fork stalling at these fragile sites (Durkin and Glover, 2007). It is widely believed that the homologous recombination machinery and other fork restart pathways erroneously process replication forks that have stalled at these fragile sites into DSBs. Candidate enzymes include: members of the *RAD52* epistasis group, the MRX complex, the Sgs1$^{BLM}$-Top3 complex, and the Mus81-Mms4 endonuclease and putative resolvase (Lemoine et al., 2005; Lobachev et al., 2002; Zhang and Freudenreich, 2007). In Chapter 4, these hypotheses for the mechanism of break formation at common fragile sites were examined using *RSZs* as a model. Chromosome breakage at *RSZs* was tested in *mec1-ts* mutants lacking various recombination enzymes, the Sgs1 and Srs2 helicases, Top3, and the Mus81-Mms4 endonuclease. None of these double mutants were able to prevent break formation at *RSZs* indicating that these enzymes are not involved in generating breaks at these sites (Figures 4.2 and 4.3; Section 4.2.1). The observation that the elimination of Rad52, which is required for all forms of recombination in yeast, could not suppress the formation of breaks at *RSZs* suggests that these breaks are not induced by inappropriate recombination at the stalled fork. Deletion of components of the MRX complex also had no effect on chromosome breakage at *RSZs* (R. Cha unpublished results). These results lead to the conclusion that the formation of DSBs at *RSZs*, and by implication possibly also at common fragile sites, does not involve the direct processing of stalled forks or secondary structures by the proposed enzymes.

However, the involvement of other enzymes including the Exo1 exonuclease and Yen1, the recently identified yeast HJ resolvase (Ip et al., 2008), at *RSZs* must be assessed in order to conclude that stalled forks are not enzymatically processed into DSBs at *RSZs*.

### 6.1.2   Timing of break formation in *mec1-ts*

 The prevailing model for the mechanism of break formation at common fragile sites is not applicable to *RSZs*. Previous analysis of chromosome breakage at *RSZs* indicates that these sites acquire DSBs at some point in the G2/M transition (Cha and Kleckner, 2002), raising the possibility that mitotic events such as decatenation, chromosome condensation, anaphase, and cytokinesis are responsible for generating breaks at *RSZs*. Based on the observation that spindle poisons prevent the formation of breaks at *RSZs*, it was proposed that the pulling force of the spindle during mitosis could generate breaks at forks stalled at these sites. However, elimination of the spindle checkpoint proteins, Mad2 and Bub2, in *mec1-ts* cells allowed chromosome breakage at *RSZs* to occur even in the presence of the spindle inhibitor, suggesting that these breaks were not generated by the spindle force but rather by the execution of mitotic events in the presence of incompletely replicated DNA (Figures 4.4 and 4.9).

In order to determine the mitotic event responsible for generating DSBs at *RSZs*, mitotic events were monitored in *mec1-ts* cells using histone H3 phosphorylation, Scc1 cleavage, and Clb2 degradation as markers for chromosome condensation, anaphase onset, and mitotic exit, respectively. This experiment yielded the following observations: chromosome condensation in *mec1-ts* occurred in an untimely manner (when the majority of cells were in S-phase), whereas anaphase onset and mitotic exit did not occur efficiently in this mutant (Figure 4.6). These results imply that *mec1-ts* cells acquire breaks at *RSZs* and lose viability before undergoing anaphase but after/concomitantly with chromosome condensation. Indeed, cytological analysis of *mec1-ts* cells showed that the majority of these cells arrested with a large bud and a single nucleus at non-permissive temperature (Figure 4.11). Furthermore, deletion of *BUB*2, which allows the Mad2-dependent inhibition of sister chromatid separation, in *mec1-ts* cells subjected to spindle poisons did not eliminate break

formation at *RSZs* (Figure 4.9). This supports the hypothesis that chromosome breakage at *RSZs* occurs independently of sister chromatid separation. The conclusion that break formation in *mec1-ts* occurs prior to cytokinesis was confirmed in two ways. First, cytological analysis of *mec1-ts* cells expressing *MYO1-GFP*, which marks the actomyosin ring, revealed that these cells accumulate DSBs before the constriction and disappearance of the actomyosin ring (Figures 4.10 and 4.12A). Secondly, the *mob1-77* mutant that is unable to exit mitosis and perform cytokinesis did not prevent chromosome breakage at *RSZs* in *mec1-ts* cells (Figure 4.12B).

Taken together these results indicate that chromosome breakage at *RSZs* involves a mitotic event that takes place prior to anaphase and cytokinesis and after or concomitantly with chromosome condensation.

### 6.1.3   Chromosome breakage at fragile sites is induced by chromosome condensation or chromosome decatenation

The data presented in Chapter 4 rules out most proposed mechanisms for chromosome break formation, namely; anaphase, cytokinesis, and fork processing activities. As mentioned above, the analyses also suggest that break formation is likely to occur prior to anaphase, in a mechanism governed by chromosome condensation. The remaining possibilities are therefore chromosome condensation and sister chromatid decatenation. Top2 and condensin subunits have been implicated in both processes, rendering the observation that inactivation of either Top2 (Figure 4.13A) or condensin (Figure 4.18) prevents break formation difficult to interpret. Presented below are the arguments for and against each possibility based on data presented in this study in addition to data from relevant literature.

**6.1.3.1 A possible role for condensation in chromosome breakage at *RSZs***

The observation that histone H3 is phosphorylated at a time when the majority of *mec1-ts* cells are in S-phase lead to the hypothesis that incompletely replicated chromosomes undergoing linear compaction might be susceptible to breakage, particularly at *RSZs* where replication is presumed to have stalled. The finding that condensin and Top2 activity, both of which are implicated in chromosome condensation, are required for break formation at *RSZs* supports this hypothesis.

Furthermore, treatment of *mec1-ts* cells with spindle destabilizing drugs, a condition reported to induce SAC-dependent decondensation of chromosomes in yeast, suppresses break formation at *RSZs* in a Mad2-dependent manner (Figure 4.4).

However, although spindle inhibition prevented chromosome breakage at *RSZs*, it did not completely eliminate the phosphorylation of histone H3 (Figure 4.7C and 4.8), indicating that perhaps condensation alone is not sufficient to generate breaks at *RSZs*. Nevertheless, as mentioned above, histone H3 phosphorylation can be observed in condensation-deficient *Drosophila* cells (Dej et al., 2004; Spencer and Hieter, 1992; Steffensen et al., 2001), suggesting that a lack of condensation does not necessarily correlate with the absence of histone H3 phosphorylation. Another argument against a role for condensation in *mec1*-dependent chromosome breakage is that although treatment with spindle poisons eventually results in decondensed chromosomes, an initial condensation activity does occur, suggesting that chromosome condensation must have initially occurred in *mec1-ts* cells treated with spindle inhibitors without producing breaks at *RSZs*. However, it is possible that this preliminary condensation activity is not sufficient to generate breaks at *RSZs*, and that a certain level of condensation must be maintained for some time before incompletely replicated chromosomes to become susceptible to breakage. This is supported by the observation that there is some delay between phosphorylation of histone H3 and the appearance of *mec1-ts* breaks (Figure 4.6). In addition, phosphorylation of histone H3 is required for the instigation, but not maintenance, of condensation on human chromosomes (Van Hooser et al., 1998), supporting the notion that although initial chromosome condensation (visualised as phosphorylated histone H3) is observed in *mec1-ts* cells in the presence of spindle inhibitors, it may not result in the complete compaction required for break formation at *RSZs*. Future experiments in which condensation is visualised cytologically may be more informative of the extent of condensation that occurs in *mec1-ts* cells treated with spindle inhibitors.

One final consideration is that it is currently unknown whether linear chromosome compaction alone can generate enough force to induce chromosome breakage, even at weakened regions such as the junctions between replicated an unreplicated DNA, and especially as budding yeast chromosomes do not undergo extensive compaction.

**6.1.3.2 Could decatenation play a role in break formation at *RSZs*?**

*RSZs* tend to coincide with sites of replication termination (Section 1.2.3.1 and Section 1.4.5). This raises the possibility that these sites are regions of preferred replication termination and decatenation. Indeed, as mentioned above, inactivation Top2, an enzyme critical for this process, suppresses break formation at these sites. In addition, condensation has been implicated in rDNA decatenation during anaphase (D'Ambrosio et al., 2008), and Top2 localisation to chromatin is aberrant in *ycs4* mutants, which also suppress *mec1-4* DSBs (Bhalla et al., 2002). Furthermore, the mitotic spindle is thought to provide directionality to the decatenation activity of Top2 (Holm et al., 1985), which could explain the absence of breaks in MBC-/nocodazole-treated *mec1-ts* cells. However, the extent to which the spindle influences Top2 activity is unclear, particularly as spindle inhibitors induce a metaphase arrest in higher eukaryotic cells leading to the typical metaphase chromosome with separated (and, therefore, decatenated) arms (Gimenez-Abian et al., 2000). This suggests that these chromosomes have undergone Top2-dependent sister chromatid individualisation in the presence of spindle antagonists. Similarly, although condensation can promote decatenation of rDNA, it is not absolutely required for this activity (D'Ambrosio et al., 2008), suggesting that Top2-dependent decatenation may eventually occur in *mec1-ts* cells carrying mutations in condensin subunits. Another argument against the prospect that Top2 directly catalyses the formation of DSBs at *RSZs* stems from the observation that Top2 does not localise to all *RSZs* on chromosomes III and VI in *mec1-ts* cells (Section 4.2.3.1). However, as discussed in Section 4.3.5, this does not necessarily rule out a role for the enzymatic activity of Top2 in break formation at *RSZs* and further analysis is required in order to confirm these results.

Interestingly, progression of *top2-1 arg4::mec1-4* cells through S-phase (as measured by FACS) appeared improved compared to *arg4::mec1-4* cells alone (Figure 4.16), suggesting that inactivation of Top2 may suppress *mec1-ts* breaks by impacting on the dNTP synthesis pathway, perhaps by activating the DNA damage checkpoint. This idea was ruled out on the basis that no Rad53 phosphorylation was detectable in these cells (Figure 4.17) and that S-phase is reportedly unaffected by the *top2-1* mutation (Bermejo et al., 2007; Holm et al., 1989). However, results from

Chapter 5 show that deletion of *RRM3* alleviates *mec1-ts* defects in a Tel1-dependent manner by moderately increasing dNTP levels, despite a lack of detectable Rad53 phosphorylation (Sections 5.2.3 and 5.2.5.2). It is, therefore, possible that inactivation of Top2, may affect DNA replication in a *mec1-4* background, resulting in a Tel1-dependent increase in dNTP levels without the detection of Rad53 phosphorylation. In addition, a catalytically inactive allele of Top2 has been shown to hinder replication and activate the DNA damage checkpoint (Baxter and Diffley, 2008). Further assessment of the status of break formation in *top2-1 mec1-ts* cells treated with low levels of HU or in *top2-1 tel1Δ mec1-ts* triple mutants is required to confirm that the suppression of DSBs in *top2-1 mec1-ts* cells is independent of dNTP up-regulation pathways.

Finally, sister chromatid decatenation is not affected by dNTP levels, and decatenation occurs efficiently on completely duplicated chromosomes. Therefore, increasing dNTP levels, which prevents breaks formation at *RSZs* in *mec1-ts* cells, would not prevent Top2 from decatenating the sister chromatids at the *RSZs*. However, this does not rule out the possibility that the enzymatic activity of Top2 could generate DSBs at *RSZs* independently of its role in sister chromatid decatenation. Nor does it rule out the possibility that a form of decatenation activity executed on abnormal structures arising from incompletely replicated DNA is responsible for break formation, and may be influenced by alterations in dNTP availability.

### 6.1.4   Model for break formation at *RSZs* and common fragile sites

Taken together, the results presented in Chapter 4 indicate that chromosome breakage at *RSZs* occurs prior to anaphase by a Top2- and condensin-dependent event. Due to the common functions of Top2 and condensins in chromosome condensation and decatenation, and assuming that inactivation of Top2 and condensins prevent DSB formation by a common mechanism, it was deduced that the process of chromosome condensation is required for break formation, either directly, by compacting incompletely replicated chromosomes, or indirectly, by promoting Top2-dependent decatenation.

Could chromosome condensation cause expression of common fragile sites in mammals? It has been shown that breaks and gaps on fragile sites can be induced by forcing chromosomes of late S-phase and G2 cells to undergo premature chromosome condensation (El Achkar et al., 2005). In addition, highly flexible regions of DNA, including fragile sites, are thought to preclude nucleosome binding and, as a consequence, do not condense properly (Lukusa and Fryns, 2008). Thus, it is likely that these undercondensed single-stranded sections of the DNA are weaker than adjacent double-stranded regions that are able to condense efficiently and are, therefore, more susceptible to stresses generated by condensation of the chromosome as a whole. However, condensation has not truly been established as a mechanism of fragile site expression in mammalian systems. Moreover, a requirement for Top2-dependent decatenation at common fragile sites has not been addressed.

The results presented here favour a model in which fragile sites that contain incompletely replicated DNA become expressed when cells enter mitosis and chromosomes undergo condensation and/or decatenation events (Figure 6.1). Mec1/ATR presumably reduce the likelihood of this occurring by imposing a block to mitotic entry and/or promoting replication of these sites (Cha and Kleckner, 2002; Hekmat-Nejad et al., 2000; Nyberg et al., 2002; Petermann and Caldecott, 2006; Petermann et al., 2006). One argument against this model stems from the observation that ATR-deficient mouse cells are still able to arrest the cell cycle in the presence of the replication inhibitor, aphidicolin (Brown and Baltimore, 2003). Unlike ATR-deficient cells treated with ionizing radiation (IR), the same cells treated with aphidicolin were able to prevent chromosome condensation and activation of the mitotic CDK, indicating that ATR-deficient cells are capable of blocking mitosis in response to replication inhibitors. These ATR-deficient cells also displayed phosphorylation of $\gamma$-H2AX, indicating that break formation had occurred even though the cells did not appear to enter mitosis. This raises the possibility that break formation at fragile sites can occur independently of the condensation process. However, it is worth noting that the authors used amounts of aphidicolin that greatly exceed the concentrations routinely used to induce fragile site expression (5 $\mu$M versus 0.4 $\mu$M). Low amounts of aphidicolin only perturb replication of common fragile sites, which are presumed to be intrinsically difficult to replicate, delaying the

replication of these regions until G2/M (Durkin and Glover, 2007; Schwartz et al., 2005) when chromosomes begin to condense and when sister chromatid decatenation is likely to take place. On the other hand, high concentrations of the replication inhibitor are likely to result in immediate fork collapse early on in S-phase, particularly in the absence of the fork-stabilising functions of ATR. This is reminiscent of *mec1Δ sml1Δ* cells treated with high doses of HU compared to low doses of the drug. While low concentrations of HU induce chromosome breakage at *RSZs*, large amounts of HU do not, presumably because replication forks collapse shortly after replication initiation, before they reach the *RSZs* and/or before the cells begin to execute mitotic events (Section 3.2.4).

The possibility that Top2-dependent chromosome condensation or decatenation contributes to fragile site expression is an exciting one. We are currently investigating the effect of Top2 inhibition on fragile site expression in ATR-deficient mouse fibroblasts. Results from this and future work regarding the interplay among chromosome condensation, sister chromatid decatenation, and fragile site expression will be instrumental in our understanding of the basis of chromosome fragility during tumourigenesis.

Figure 6.2     Proposed model for the mechanism of chromosome breakage at common fragile sites

## 6.2 The nature of *RSZs*

### 6.2.1 Characteristics of *RSZs*

Previous analysis of *RSZs* on chromosome III demonstrated that these sites are regions of the chromosome that undergo slower fork progression than other areas within the same chromosome, and are thus among the last regions of the chromosome to be replicated (Cha and Kleckner, 2002). Mapping of *RSZs* along chromosome III showed that these sites occur between active origins of replication and coincide with sites of replication termination, further supporting the notion that *RSZs* are late replicating regions of the chromosome. In Chapter 3, *RSZs* were mapped on chromosome VI and found to adhere to the same positioning pattern as on chromosome III suggesting that this distribution of *RSZs* may be universal (Figure 3.4). On both chromosomes III and VI, *RSZs* are often associated with sites of transposon insertion as evidenced by presence of Ty and Δ /LTR elements within several *RSZs*. *RSZs* also frequently coincide with tRNA genes, known to generate impediments to fork progression, although these also tend to be regions where transposons insert (Kim et al., 1998). Indeed, *RSZs* on both chromosomes III and VI only occur at tRNA genes that are associated with transposon insertion, and not with tRNA genes alone (Figures 3.1 and 3.4). Additionally, *RSZs* −or at least *mec1-ts* chromosome breakage − do not occur at centromeres on either chromosome III or VI. Further analysis of replication intermediates at centromeric regions is required to clarify whether replication forks progress through centromeres efficiently, or whether replication is slowed but chromosome breakage is somehow avoided at these specialised regions of the chromosome.

The presence of *RSZs* on a chromosome does not appear to be associated with a particular sequence of DNA (Cha and Kleckner, 2002). Additionally, *RSZs* do not correlate significantly with the nucleotide composition bias of G-/R-banding isochores, sites of cohesin binding, or DNase hypersensitivity sites (Cha and Kleckner, 2002). In Chapter 3, genome-wide predictions of the flexibility of DNA sequences in yeast chromosomes were measured. Peaks of high DNA flexibility on yeast chromosomes did not correlate significantly with other chromosomal

determinants including origins of replication, centromeres, tRNA genes, or Ty/Δ elements (Figures 3.5 and 3.6; Table 3.1). The distribution of high DNA flexibility peaks in relation to other chromosomal determinants on the chromosomes indicates a possible link between *RSZs* and regions of high DNA flexibility. Like *RSZs*, flexibility analysis in yeast indicated that peaks of high DNA flexibility are excluded from centromeric regions on all chromosomes, and also show higher correlation with mapped termination sites than other chromosomal determinants (Table 3.2). Furthermore, there is a strong correlation between high DNA flexibility peaks and *RSZs* on chromosomes III and VI in that 80% of the flexibility peaks on these chromosomes were found within or very close to a *RSZ* (Figures 3.7 and 3.8). The remaining 20% of flexibility peaks on these two chromosomes occur close to telomeres where *RSZs* cannot be mapped. It is tempting to utilise the chromosome map of high DNA flexibility to predict positions of *RSZs* genome-wide; however, the positions of *RSZs* on at least a few other chromosomes must be mapped in order to consolidate the relationship between high DNA flexibility peaks and *RSZs*.

It is important to point out that while a significant fraction of flexibility peaks on chromosomes III and VI coincide with *RSZs*, the reverse is not true; in fact, a number of *RSZs* do not appear to contain a high flexibility peak. This indicates that features other than high DNA flexibility must also be associated with *RSZs*. Among the *RSZs* that are not highly flexible, most – but not all- overlap with sites of transposon insertion and tRNA genes, whereas the remaining *RSZs* do not map to any known chromosomal determinant other than sites of replication termination (Figures 3.7 and 3.8).

### 6.2.2   Possible mechanisms for fork stalling at *RSZs*

By definition, *RSZs* are regions of a chromosome where the rate of replication fork progression is notably slow compared to other regions of the same chromosome. In addition, chromosome breakage at these sites in *mec1-ts* cells requires the prior stalling of replication forks within these *RSZs* (Cha and Kleckner, 2002). However, the underlying molecular basis for fork stalling at these sites remains unclear.

*RSZs* display a strong correlation with peaks of high DNA flexibility and/or of transposon insertion sites (Section 3.2.3; see Table 6.1 p.242). The presence of highly flexible DNA sequences as well as repetitive DNA sequences including Ty/Δ elements at fragile sites is thought to generate secondary DNA structures that may impede fork progression in these regions (Durkin and Glover, 2007; Zhang and Freudenreich, 2007; Zlotorynski et al., 2003). Flexibility peaks in the DNA tend to consist of AT repeats, which have fast relaxation kinetics, allowing the double helix to unwind and cruciform or hairpin structures to be extruded (Bowater et al., 1991; Dayn et al., 1991; Zhang and Freudenreich, 2007). Repetitive sequences such as palindromes or closely spaced inverted repeats can also be extruded to form cruciform or hairpin structures in the DNA (Lemoine et al., 2005; Lobachev et al., 2002). Events that contribute to the formation of secondary structures in the DNA include processes that increase DNA supercoiling such as replication or active transcription (Dayn et al., 1991; McClellan et al., 1990)**.**

Do forks stall at *RSZs* due to secondary structures in the DNA? The observation that *RSZs* tend to coincide with areas of high DNA flexibility or with sites containing Ty/Δ elements (Section 3.2.3, Table 6.1) suggests that these regions may also have a propensity for forming hairpins or cruciforms that slow or impede the progression of replication forks even in wild type cells. However, the fact that *RSZs* occur between highly active origins of replication and coincide with sites of replication termination suggests that these zones are simply regions where dNTP levels are limiting. In support of this, increasing dNTP levels allows progression of replication forks beyond these sites without the ensuing formation of DSBs (Cha and Kleckner, 2002). The role of Mec1 at these sites may simply be to up-regulate dNTP synthesis as forks approach these sites in order to complete DNA replication. However, it seems unlikely that the cell would not have evolved to generate enough dNTPs to complete replication at the onset of S-phase. Nevertheless, it is possible that replication progression slows as cells near the end of S-phase due to limiting dNTP levels and that Mec1 is required at this point to both up-regulate dNTP synthesis and stabilise the replisome at these sites to ensure that replication is completed efficiently. As mentioned above, fork stalling at these sites is thought to be physiological, even in the context of *mec1-ts* where stalled forks are held in a replication-competent state

until DSBs are generated (Cha and Kleckner, 2002), suggesting that the normal means of stabilising replication forks in the event of DNA damage may not be involved at *RSZs*.

Diminishing dNTP levels and the formation of secondary structures are not necessarily mutually exclusive conditions for fork stalling at *RSZs*. It is possible that low fork processivity, a consequence of approaching the end of S-phase, could favour the formation of secondary structures in the DNA, thereby stalling the replication fork. Low levels of dNTPs could delay the synthesis of Okazaki fragments on the lagging strand leading to an increase in single stranded DNA on this strand, which, in turn, increases the probability of generating hairpin structures. Increasing dNTP levels (for example by deleting *SML1*) could disfavour the formation of these structures and allow replication to proceed beyond the *RSZs*.

### 6.2.3   Factors that govern the stability of fragile sites in yeast and mammals

Despite the intrinsic ability of fragile sites to stall a progressing replication fork, whether it is due to limited dNTP pools or structural impediments, chromosome instability is avoided in wild type cells, suggesting that certain factors play a role in maintaining the stability of fragile sites. Both ATR and its budding yeast homologue, Mec1, are necessary to maintain the stability of common fragile sites in mammals and the various fragile sites in yeast, indicating a crucial and universal role for the replication checkpoint at fragile sites (Admire et al., 2006; Casper et al., 2002; Cha and Kleckner, 2002; Raveendranathan et al., 2006).

An investigation into the factors required for *RSZ* stability revealed that deleting *TEL1* in a *mec1-4* background resulted in an increase in chromosome breakage at *RSZs* compared to *mec1-4* strains alone (Figure 5.12). Similarly, a recent report shows that elimination of ATM increases fragile site expression in the absence of functional ATR (Ozeri-Galai et al., 2008). These results indicate a minor role for ATM/Tel1 at fragile sites/*RSZs* that becomes evident in the absence of ATR/Mec1. Deletion of *RRM3* or *PSY2* in a *mec1-4* background results in the suppression of chromosome breakage at *RSZs* in a manner that is dependent on Tel1 (Sections

5.2.5.2 and 5.2.5.3). This further supports a role for Tel1 in maintaining the stability of *RSZs*. Suppression of DSBs at *RSZs* by *rrm3Δ* and *psy2Δ* is also accompanied by an improvement in the viability of *mec1-4* (ectopic and/or endogenous) strains, and deletion of *TEL1* in *psy2Δ mec1-4* strains restores the lethality of *mec1-4*, suggesting that the mechanism by which *rrm3Δ* and *psy2Δ* prevent break formation at *RSZs* is via a Tel1-dependent increase in dNTP synthesis (Section 5.2.5). In support of this notion, suppression of breaks in *rrm3Δ arg4::mec1-4* mutants was accompanied by a modest restoration of Sml1 cycling compared to *arg4::mec1-4* strains that do not degrade Sml1 (Figure 5.8), indicating that the mechanism of suppression of breaks in this mutant involves a subtle increase in dNTP synthesis.

An increase in *mec1-ts* chromosome breakage at *RSZs* was also observed in *mec1-4* cells carrying mutations in recombination factors, helicases, or nucleases (Figures 4.2 and 4.3). This raises the possibility that chromosome breaks at *RSZs* may be repaired via these recombination-dependent pathways. However, breaks at *RSZs* are thought to persist even after 24 hours, suggesting that they are neither repaired nor degraded (Cha and Kleckner, 2002). One possibility is that only a subset of breaks at *RSZs* is processed before the cells lose viability. The fact that breaks at *RSZs* are not degraded after cells have lost viability suggests that they may be protected by the binding of proteins to the ends of the breaks. Down-regulation of DNA repair genes in mammalian cells treated with aphidicolin results in an increase in fragile site expression (Schwartz et al., 2005), suggesting that these sites are repaired by recombinational repair mechanisms. Recombinational repair of breaks at fragile sites is presumed to generate the sister chromatid exchanges (SCE) often associated with fragile site expression (Glover and Stein, 1987).

The checkpoint factors, Mrc1 and Tof1, are required at stalled replication forks to couple the replisome to the site of the replication fork (Katou et al., 2003). Tof1 is required at natural fork pausing sites to stall the fork, and prolonged stalling of forks at these sites, for example in the absence of Rrm3, results in chromosome breakage (Ivessa et al., 2003). In Chapter 5, an attempt was made to assess the involvement of these fork-stalling factors at *RSZs*. Tof1 and the checkpoint function of Mrc1 did not appear to be involved in chromosome breakage at *RSZs* (Figures 5.1 and 5.3). Chromosome breakage at *RSZs* was absent in *mrc1Δ* cells; however, it is likely that

this is due to the collapse of replication forks early in S-phase, before they reach *RSZs* and/or before mitotic events are initiated. It was inferred from these results that Mrc1 and Tof1 may not be involved in stably stalling the fork at *RSZs*. However, a more comprehensive analysis of the effects of *mrc1Δ* and *tof1Δ* on fork slowing and/or stalling at *RSZs* in both wild type and *mec1-ts* situations must be performed in order to properly decipher the roles of these factors in replication fork stability at *RSZs*.

## 6.3    Comparison between *RSZs* and other yeast fragile sites

### 6.3.1    Other yeast fragile sites

Other fragile sites identified in budding yeast include the 17 CEO-proximal regions (which also include the FS2 site) and the E2 403 site on chromosome VII (Admire et al., 2006; Lemoine et al., 2005; Raveendranathan et al., 2006). These regions are particularly sensitive to replication stresses, suggesting that these yeast fragile sites may be mechanistically similar to *RSZs* and common fragile sites in mammals. However, CEO-proximal regions, including the FS2 site, do not coincide with *RSZs* suggesting that they constitute a distinct class of yeast fragile site. The observation that inverted Ty elements at FS2 cause replication forks to stall and accumulate breaks under conditions of replication stress indicates that fork stalling at these sites may be caused by the formation of secondary structures that inhibit the progression of DNA polymerases (Lemoine et al., 2005). Additional replication stress may exacerbate fork stalling at these sites and may, consequently, induce chromosome instability at these sites (Lemoine et al., 2008; Lemoine et al., 2005). Unlike *RSZs*, this site, as well as other CEOs, are located adjacent to active origins of replication (Raveendranathan et al., 2006), suggesting perhaps a closer similarity to common fragile sites that, at least in some cases, are also located in the vicinity of replication origins (Toledo et al., 2000). One difference between these sites and common fragile sites is the lack of flexibility peaks in these regions, presumably because flexibility peaks in yeast do not significantly overlap with origins of replication (Table 6.1; Figures 3.5 and 3.6). In addition, CEO-proximal fragile sites are not observed on 6 of the 16 yeast chromosomes (Raveendranathan et al., 2006), suggesting that, unlike

mammalian common fragile sites and presumably also *RSZs*, these sites are not a structural component of every chromosome.

**Table 6.1 Chromosomal features that coincide with yeast fragile sites.**

|  | Total Number[a] | Flexibility Peak | CEN | tRNA | Ty | Δ/LTR | No Determinant |
|---|---|---|---|---|---|---|---|
| **CEO** | 17 | 7.7% | 11.7% | 64.7% | 5.8% | 41.2% | 17.6% |
| **RSZ** | 11 | 45.4% | 0% | 45.4% | 9% | 45% | 18.18% |
| **403** | 1 | 0% | 0% | 100% | 100% | 100% | 0% |

[a] The total number of CEOs, *RSZs*, or 403 sites present in the yeast genome.
Other values correspond to the number of CEOs, *RSZs*, or 403 sites that coincide with the indicated chromosomal features, represented as a percentage of the total number of CEOs, *RSZs*, or 403 sites in the genome.

The fact that CEO-flanking regions are adjacent to replication origins that are normally activated early on in S-phase suggests that these sites fall within early-replicating domains of the chromosome rather than late-replicating domains. However, these sites may also represent regions where replication forks stall and could, conceivably, end up replicating towards the end of S-phase despite being situated close to an early-replicating origin. For example, the presence of inverted Ty elements could trigger the formation of secondary structures that stall the replication fork. Alternatively, tRNA genes that can temporarily stall replication forks could be situated in the vicinity of these CEOs. Analysis of chromosomal features surrounding CEOs reveals a higher frequency of Ty/Δ elements and/or tRNA genes within 10 kb from CEOs compared to other replication origins (Raveendranathan et al., 2006). However, not all CEOs exhibit Ty/Δ elements and tRNA genes in their immediate vicinity, suggesting that these chromosomal determinants are unlikely to be the only factors contributing to chromosome fragility (Table 6.1). For example, repetitive DNA elements, which can also trigger secondary structure formation, could affect the fragility of these sites.

The '403' chromosome region identified as fragile by Admire et al. (2005) contains four Ty LTR elements as well as clusters of tRNA genes, further supporting the idea that these elements are associated with fragile sites in yeast. Interestingly, this site is a 4 kb region positioned at chromosome coordinates 403 to 407 kb on chromosome VII and does not contain a peak of high DNA flexibility (see chromosome VII in

Figure 3.5). This region is situated between two replication origins and could, conceivably, correspond to a *RSZ*; however, mapping of *RSZs* on chromosome VII has yet to reveal this association. Interestingly, a CEO (ARS718) is located 20 kb away from this site, raising the possibility that this fragile region may fall into the same category as the CEO-dependent fragile sites. However, the distance between the CEO, ARS310, and the FS2 site identified by Lemoine et al. 2005 is significantly smaller than the distance between ARS718 and the 403 fragile site identified by Admire et al. (3 kb versus 20 kb). Therefore, the observation that the 403 fragile site is not immediately adjacent to the proposed CEO suggests it does not fall into this class of yeast fragile sites.

Chromosome breakage in regions adjacent to CEOs occurs during S-phase (Raveendranathan et al., 2006). In contrast, although replication forks in *mec1-ts* cells stall at *RSZs* during S-phase, it is not until cells enter the G2/M transition that breaks are thought to be generated (Cha and Kleckner, 2002). Similarly, common fragile sites are only visualised on metaphase spreads, indicating that chromosome breakage at these sites may occur after S-phase. However, it is possible that chromosome breakage occurs earlier, during S-phase, but is not visible until metaphase after chromosomes have compacted. Therefore, forks stalled within different regions, including different fragile sites, may not have the same fate. Consistent with this notion is the finding that high levels of HU arrest replication forks early in S-phase in *mec1Δ sml1Δ* cells, and presumably result in the irreversible collapse of these forks during S-phase. On the other hand, treatment of the same cells with low doses of HU stalls replication later on in S-phase and results in the accumulation of DSBs at *RSZs*, presumably by a condensin and Top2 dependent mechanism (Sections 3.2.4 and 3.2.5).

Increasing dNTP levels via deletion of *SML1* can avert chromosome breakage at *RSZs* (Cha and Kleckner, 2002). In contrast, chromosome breakage near CEOs can be detected in the absence of HU, albeit at a lower level than in the presence of HU, suggesting that CEO-proximal fragile sites are physically determined sites that are independent of dNTP levels and are prone to breakage under certain conditions (Raveendranathan et al., 2006). *RSZs* coincide with replication termination regions, which are replicated towards the end of S-phase when the dNTPs are likely to be

limiting (Reichard, 1988). In the absence of Mec1 function, dNTPs presumably fail to be up-regulated and replication forks stall permanently at *RSZs*. The fact that CEO-dependent chromosome breakage occurs close to replication origins suggests that dNTP levels at these sites are unlikely to be limiting and, therefore, not the cause of replication fork stalling and chromosome instability at these sites. On the other hand, the 403 fragile site, like *RSZs*, is sensitive to perturbations dNTP pools as treatment with HU increased instability at this site (Admire et al., 2006). Deletion of *RRM3* suppresses chromosome breakage at *RSZs* presumably by increasing dNTP synthesis (Sections 5.2.3 and 5.2.5). In contrast to *RSZs*, Admire et al. (2006) found that disruption of DNA replication by eliminating the Rrm3 helicase increased chromosome instability at the 403 site (Admire et al., 2006) suggesting a different mode of regulation may exist at *RSZs* and the 403 site.

In summary, no single chromosomal feature appears to be absolutely responsible for genomic instability at yeast fragile sites. *RSZs* correspond to sites of replication termination, although the reverse is not true. They also tend to coincide with either regions of high DNA flexibility or transposition hotspots. CEO-flanking fragile sites occur adjacent to active origins of replication, have a higher frequency of Ty/Δ elements and tRNA genes in their vicinity, but do not correlate strongly with areas of high DNA flexibility. Like-wise, the 403 site contains clusters of tRNA genes and multiple insertions of Ty/Δ elements and does not contain a high flexibility peak but occurs in between two origins of replication. Furthermore, the presence of *RSZs* and CEO-flanking regions that do not adhere to their respective characteristics suggests that other factors must also contribute to DNA instability at fragile sites (Table 6.1). Therefore, it is likely that a culmination of these factors (tRNA genes, Ty/Δ elements, DNA flexibility peaks) in addition to chromosomal determinants renders certain regions of the chromosome more fragile than others.

It is interesting that Ty/Δ element insertions are a frequent feature of chromosome fragile sites in yeast. However, it is not known whether the presence of these foreign DNA sequences actually contribute to chromosome breakage or whether they are simply markers for chromosome instability. In support of the latter possibility, it has been shown that both LTR and mitochondrial sequence fragments insert into sites of

DSBs as a mechanism of DNA repair (Moore and Haber, 1996; Ricchetti et al., 1999). These two possibilities are not necessarily mutually exclusive and a situation could arise whereby the formation of a DSB in a breakage-prone region may trigger the insertion of Ty/Δ elements, which, due to their unstable nature, may perpetuate the instability of the chromosome at this site. However, Admire et al. (2006) argue against a role for Ty elements in initiating cycles of chromosome instability in their system. Instead, the authors propose that the presence of LTR fragments near tRNA genes in their system stems from the association of the retrotransposon integrase with RNA polymerase III at stalled forks. In this manner, the integrase could then direct the cleavage of the fork and insertion of the transposon at these sites.

## 6.4    Are *RSZs* analogous to mammalian common fragile sites?

Mammalian metaphase chromosomes present gaps or breaks at common fragile sites under conditions that partially inhibit DNA replication. As discussed in Chapter 3, there are numerous similarities between common fragile sites in mammals and *RSZs* in yeast. In both systems, common fragile sites and *RSZs* are intrinsic components of the chromosome that are inherently difficult to replicate and/or late replicating. This characteristic is thought to render them particularly sensitive to replication stresses such as inadequate dNTP pools (folate-deficiency in mammals, *mec1-ts* or HU in yeast) and replication inhibitors (aphidicolin in mammals, HU in yeast).

Both *RSZs* and common fragile sites represent relatively large regions of their respective genomes (about 10 kb in yeast, up to 2 Mb in mammals) with breaks and/or gaps occurring throughout these zones. However, due to differences in genome organisation and size, *RSZs* often span one or more entire genes, whereas common fragile sites are usually located within large genes. As mentioned above, *RSZs* do not appear to have any sequence bias, in terms of AT/GC content. On the other hand, common fragile sites tend to contain sequences rich in AT tracts. However, the fact that *RSZs* do not have a preference for AT-rich sequences could be confounded by the fact that the budding yeast genome is AT-rich. Although there is no defining sequence for either *RSZs* or common fragile sites, these sites correlate well with regions of high DNA flexibility in both systems. However, it is clear that,

in both yeast and mammals, other factors may also contribute to defining the nature of *RSZs* and common fragile sites.

Like *RSZs*, common fragile sites require ATR, the orthologue of Mec1, for stability. Conditions that inactivate ATR, including cell lines from patients with Seckel syndrome, significantly increase the fragility of such sites, even in the absence of replication inhibitors, suggesting that ATR is critical for maintaining the stability of replication forks stalled at common fragile sites (Casper et al., 2004; Casper et al., 2002). Furthermore, as mentioned above, it is now evident that ATM and Tel1 may also play a role at both common fragile sites and *RSZs* (Section 6.2.3).

Experimental mapping of common fragile sites in relation to other chromosomal determinants and motifs is still lacking. Due to the differences in complexity between mammalian and yeast genomes, it is unlikely that mammalian common fragile sites follow the same pattern of distribution along mammalian chromosomes as *RSZs*. In fact, at least one report has suggested that some common fragile sites containing regions of high DNA flexibility are located close to mammalian origins of replication in Chinese hamster cells (Toledo et al., 2000). Since replication origins are often associated with AT-rich sequences is, it is, perhaps, not unexpected that AT-rich flexibility peaks coincide with origins of replication. However, it is important to note that the threshold according to which origin sequences were considered flexible in this study falls below that used in most analyses of mammalian common fragile sites. In addition, the observation that common fragile sites are AT-rich, highly flexible DNA sequences has led to the proposal that these sites may be associated with matrix association regions (*MARs*). In support of this notion, putative motifs corresponding to *MARs* have been found in the vicinity of common fragile sites (Morelli et al., 2002; Palin et al., 1998; Wang et al., 1997) and at least one recombination hotspot thought to correspond to a common fragile site in Chinese hamster cells is nested within a topoisomerase II hypersensitivity region, a common feature of *MARs* (Svetlova et al., 2001). However, further studies are required to prove that this is a necessary and defining feature of common fragile sites. It would also be interesting to assess the position of *RSZs* in relation to *MARs* sites in yeast.

Chromosome instability at common fragile sites is presented as breaks, gaps, or constrictions on the metaphase chromosome. The accumulation of DSBs under conditions that induce expression of fragile sites has been observed; however, it is unclear whether the constriction or gaps generated at common fragile sites are all converted into DSBs or whether these DSBs merely represent a subset of the chromosomal aberrations detected at common fragile sites (Ozeri-Galai et al., 2008). However, in yeast, chromosome instability that is detectable at *RSZs* is thought to only comprise DSBs. The lack of cytological capability in yeast may hinder the observation of other types of chromosomal aberrations at *RSZs*.

Despite the probable differences in complexity between *RSZs* and common fragile sites, these regions in yeast are likely to be mechanistically analogous to mammalian common fragile sites. Future research aimed at understanding the properties of *RSZs* and the basis of chromosome instability at these sites could have significant implications for unravelling the mystery behind chromosome fragile sites and the field of cancer biology as a whole.

# References

Abraham, R.T. (2004) PI 3-kinase related kinases: 'big' players in stress-induced signalling pathways. *DNA Repair (Amst)*, **3**, 883-887.

Admire, A., Shanks, L., Danzl, N., Wang, M., Weier, U., Stevens, W., Hunt, E. and Weinert, T. (2006) Cycles of chromosome instability are associated with a fragile site and are increased by defects in DNA replication and checkpoint controls in yeast. *Genes Dev*, **20**, 159-173.

Agarwal, R., Tang, Z., Yu, H. and Cohen-Fix, O. (2003) Two distinct pathways for inhibiting pds1 ubiquitination in response to DNA damage. *J Biol Chem*, **278**, 45027-45033.

Akgun, E., Zahn, J., Baumes, S., Brown, G., Liang, F., Romanienko, P.J., Lewis, S. and Jasin, M. (1997) Palindrome resolution and recombination in the mammalian germ line. *Mol Cell Biol*, **17**, 5559-5570.

Alcasabas, A.A., Osborn, A.J., Bachant, J., Hu, F., Werler, P.J., Bousset, K., Furuya, K., Diffley, J.F., Carr, A.M. and Elledge, S.J. (2001) Mrc1 transduces signals of DNA replication stress to activate Rad53. *Nat Cell Biol*, **3**, 958-965.

Alexandru, G., Uhlmann, F., Mechtler, K., Poupart, M.A. and Nasmyth, K. (2001) Phosphorylation of the cohesin subunit Scc1 by Polo/Cdc5 kinase regulates sister chromatid separation in yeast. *Cell*, **105**, 459-472.

Alexandru, G., Zachariae, W., Schleiffer, A. and Nasmyth, K. (1999) Sister chromatid separation and chromosome re-duplication are regulated by different mechanisms in response to spindle damage. *Embo J*, **18**, 2707-2721.

Alvino, G.M., Collingwood, D., Murphy, J.M., Delrow, J., Brewer, B.J. and Raghuraman, M.K. (2007) Replication in hydroxyurea: it's a matter of time. *Mol Cell Biol*, **27**, 6396-6406.

Andrews, C.A., Vas, A.C., Meier, B., Gimenez-Abian, J.F., Diaz-Martinez, L.A., Green, J., Erickson, S.L., Vanderwaal, K.E., Hsu, W.S. and Clarke, D.J. (2006) A mitotic topoisomerase II checkpoint in budding yeast is required for genome stability but acts independently of Pds1/securin. *Genes Dev*, **20**, 1162-1174.

Anglana, M., Apiou, F., Bensimon, A. and Debatisse, M. (2003) Dynamics of DNA replication in mammalian somatic cells: nucleotide pool modulates origin choice and interorigin spacing. *Cell*, **114**, 385-394.

Arlt, M.F., Miller, D.E., Beer, D.G. and Glover, T.W. (2002) Molecular characterization of FRAXB and comparative common fragile site instability in cancer cells. *Genes Chromosomes Cancer*, **33**, 82-92.

Arlt, M.F., Xu, B., Durkin, S.G., Casper, A.M., Kastan, M.B. and Glover, T.W. (2004) BRCA1 is required for common-fragile-site stability via its G2/M checkpoint function. *Mol Cell Biol*, **24**, 6701-6709.

Aylon, Y., Liefshitz, B. and Kupiec, M. (2004) The CDK regulates repair of double-strand breaks by homologous recombination during the cell cycle. *Embo J*, **23**, 4868-4875.

Azvolinsky, A., Dunaway, S., Torres, J.Z., Bessler, J.B. and Zakian, V.A. (2006) The S. cerevisiae Rrm3p DNA helicase moves with the replication fork and affects replication of all yeast chromosomes. *Genes Dev*, **20**, 3104-3116.

Baker, T.A. and Bell, S.P. (1998) Polymerases and the replisome: machines within machines. *Cell*, **92**, 295-305.

Balasubramanian, M.K., Bi, E. and Glotzer, M. (2004) Comparative analysis of cytokinesis in budding yeast, fission yeast and animal cells. *Curr Biol*, **14**, R806-818.

Balasubramanian, M.K., McCollum, D. and Surana, U. (2000) Tying the knot: linking cytokinesis to the nuclear cycle. *J Cell Sci*, **113 ( Pt 9)**, 1503-1513.

Barbour, L. and Xiao, W. (2003) Regulation of alternative replication bypass pathways at stalled replication forks and its effects on genome stability: a yeast model. *Mutat Res*, **532**, 137-155.

Bartek, J. and Lukas, J. (2007) DNA damage checkpoints: from initiation to recovery or adaptation. *Curr Opin Cell Biol*, **19**, 238-245.

Baumer, M., Braus, G.H. and Irniger, S. (2000) Two different modes of cyclin clb2 proteolysis during mitosis in Saccharomyces cerevisiae. *FEBS Lett*, **468**, 142-148.

Baxter, J. and Diffley, J.F. (2008) Topoisomerase II inactivation prevents the completion of DNA replication in budding yeast. *Mol Cell*, **30**, 790-802.

Bell, S.P. and Dutta, A. (2002) DNA replication in eukaryotic cells. *Annu Rev Biochem*, **71**, 333-374.

Bell, S.P. and Stillman, B. (1992) ATP-dependent recognition of eukaryotic origins of DNA replication by a multiprotein complex. *Nature*, **357**, 128-134.

Bermejo, R., Doksani, Y., Capra, T., Katou, Y.M., Tanaka, H., Shirahige, K. and Foiani, M. (2007) Top1- and Top2-mediated topological transitions at replication forks ensure fork progression and stability and prevent DNA damage checkpoint activation. *Genes Dev*, **21**, 1921-1936.

Bhalla, N., Biggins, S. and Murray, A.W. (2002) Mutation of YCS4, a budding yeast condensin subunit, affects mitotic and nonmitotic chromosome behavior. *Mol Biol Cell*, **13**, 632-645.

Bjergbaek, L., Cobb, J.A., Tsai-Pflugfelder, M. and Gasser, S.M. (2005) Mechanistically distinct roles for Sgs1p in checkpoint activation and replication fork maintenance. *Embo J*, **24**, 405-417.

Blow, J.J., Gillespie, P.J., Francis, D. and Jackson, D.A. (2001) Replication origins in Xenopus egg extract Are 5-15 kilobases apart and are activated in clusters that fire at different times. *J Cell Biol*, **152**, 15-25.

Blow, J.J. and Hodgson, B. (2002) Replication licensing--defining the proliferative state? *Trends Cell Biol*, **12**, 72-78.

Boddy, M.N., Shanahan, P., McDonald, W.H., Lopez-Girona, A., Noguchi, E., Yates, I.J. and Russell, P. (2003) Replication checkpoint kinase Cds1 regulates recombinational repair protein Rad60. *Mol Cell Biol*, **23**, 5939-5946.

Boldog, F., Gemmill, R.M., West, J., Robinson, M., Robinson, L., Li, E., Roche, J., Todd, S., Waggoner, B., Lundstrom, R., Jacobson, J., Mullokandov, M.R., Klinger, H. and Drabkin, H.A. (1997) Chromosome 3p14 homozygous deletions and sequence analysis of FRA3B. *Hum Mol Genet*, **6**, 193-203.

Bowater, R., Aboul-ela, F. and Lilley, D.M. (1991) Large-scale stable opening of supercoiled DNA in response to temperature and supercoiling in (A + T)-rich regions that promote low-salt cruciform extrusion. *Biochemistry*, **30**, 11495-11506.

Branzei, D. and Foiani, M. (2006) The Rad53 signal transduction pathway: Replication fork stabilization, DNA repair, and adaptation. *Exp Cell Res*, **312**, 2654-2659.

Branzei, D. and Foiani, M. (2007) Interplay of replication checkpoints and repair proteins at stalled replication forks. *DNA Repair (Amst)*, **6**, 994-1003.

Branzei, D. and Foiani, M. (2008) Regulation of DNA repair throughout the cell cycle. *Nat Rev Mol Cell Biol*, **9**, 297-308.

Brewer, B.J. and Fangman, W.L. (1994) Initiation preference at a yeast origin of replication. *Proc Natl Acad Sci U S A*, **91**, 3418-3422.

Brown, E.J. and Baltimore, D. (2000) ATR disruption leads to chromosomal fragmentation and early embryonic lethality. *Genes Dev*, **14**, 397-402.

Brown, E.J. and Baltimore, D. (2003) Essential and dispensable roles of ATR in cell cycle arrest and genome maintenance. *Genes Dev*, **17**, 615-628.

Callahan, J.L., Andrews, K.J., Zakian, V.A. and Freudenreich, C.H. (2003) Mutations in yeast replication proteins that increase CAG/CTG expansions also increase repeat fragility. *Mol Cell Biol*, **23**, 7849-7860.

Calzada, A., Hodgson, B., Kanemaki, M., Bueno, A. and Labib, K. (2005) Molecular anatomy and regulation of a stable replisome at a paused eukaryotic DNA replication fork. *Genes Dev*, **19**, 1905-1919.

Cangi, M.G., Piccinin, S., Pecciarini, L., Talarico, A., Dal Cin, E., Grassi, S., Grizzo, A., Maestro, R. and Doglioni, C. (2008) Constitutive overexpression of CDC25A in primary human mammary epithelial cells results in both defective DNA damage response and chromosomal breaks at fragile sites. *Int J Cancer*, **123**, 1466-1471.

Carr, A.M. (2002) Checking that replication breakdown is not terminal. *Science*, **297**, 557-558.

Casper, A.M., Durkin, S.G., Arlt, M.F. and Glover, T.W. (2004) Chromosomal instability at common fragile sites in Seckel syndrome. *Am J Hum Genet*, **75**, 654-660.

Casper, A.M., Nghiem, P., Arlt, M.F. and Glover, T.W. (2002) ATR regulates fragile site stability. *Cell*, **111**, 779-789.

Cha, R.S. and Kleckner, N. (2002) ATR homolog Mec1 promotes fork progression, thus averting breaks in replication slow zones. *Science*, **297**, 602-606.

Champoux, J.J. (2001) DNA topoisomerases: structure, function, and mechanism. *Annu Rev Biochem*, **70**, 369-413.

Chan, G.K. and Yen, T.J. (2003) The mitotic checkpoint: a signalling pathway that allows a single unattached kinetochore to inhibit mitotic exit. *Prog Cell Cycle Res*, **5**, 431-439.

Chen, S.H., Smolka, M.B. and Zhou, H. (2007) Mechanism of Dun1 activation by Rad53 phosphorylation in Saccharomyces cerevisiae. *J Biol Chem*, **282**, 986-995.

Chowdhury, D., Keogh, M.C., Ishii, H., Peterson, C.L., Buratowski, S. and Lieberman, J. (2005) gamma-H2AX dephosphorylation by protein phosphatase 2A facilitates DNA double-strand break repair. *Mol Cell*, **20**, 801-809.

Chuang, R.Y. and Kelly, T.J. (1999) The fission yeast homologue of Orc4p binds to replication origin DNA via multiple AT-hooks. *Proc Natl Acad Sci U S A*, **96**, 2656-2661.

Cimprich, K.A. (2003) Fragile sites: breaking up over a slowdown. *Curr Biol*, **13**, R231-233.

Ciosk, R., Shirayama, M., Shevchenko, A., Tanaka, T., Toth, A., Shevchenko, A. and Nasmyth, K. (2000) Cohesin's binding to chromosomes depends on a separate complex consisting of Scc2 and Scc4 proteins. *Mol Cell*, **5**, 243-254.

Ciosk, R., Zachariae, W., Michaelis, C., Shevchenko, A., Mann, M. and Nasmyth, K. (1998) An ESP1/PDS1 complex regulates loss of sister chromatid cohesion at the metaphase to anaphase transition in yeast. *Cell*, **93**, 1067-1076.

Clemenson, C. and Marsolier-Kergoat, M.C. (2006) The spindle assembly checkpoint regulates the phosphorylation state of a subset of DNA checkpoint proteins in Saccharomyces cerevisiae. *Mol Cell Biol*, **26**, 9149-9161.

Clerici, M., Paciotti, V., Baldo, V., Romano, M., Lucchini, G. and Longhese, M.P. (2001) Hyperactivation of the yeast DNA damage checkpoint by TEL1 and DDC2 overexpression. *Embo J*, **20**, 6485-6498.

Cleveland, D.W., Mao, Y. and Sullivan, K.F. (2003) Centromeres and kinetochores: from epigenetics to mitotic checkpoint signalling. *Cell*, **112**, 407-421.

Cobb, J.A., Bjergbaek, L., Shimada, K., Frei, C. and Gasser, S.M. (2003) DNA polymerase stabilization at stalled replication forks requires Mec1 and the RecQ helicase Sgs1. *Embo J*, **22**, 4325-4336.

Cobb, J.A., Schleker, T., Rojas, V., Bjergbaek, L., Tercero, J.A. and Gasser, S.M. (2005) Replisome instability, fork collapse, and gross chromosomal rearrangements arise synergistically from Mec1 kinase and RecQ helicase mutations. *Genes Dev*, **19**, 3055-3069.

Coelho, P.A., Queiroz-Machado, J. and Sunkel, C.E. (2003) Condensin-dependent localisation of topoisomerase II to an axial chromosomal structure is required for sister chromatid resolution during mitosis. *J Cell Sci*, **116**, 4763-4776.

Cohen-Fix, O. and Koshland, D. (1997) The anaphase inhibitor of Saccharomyces cerevisiae Pds1p is a target of the DNA damage checkpoint pathway. *Proc Natl Acad Sci U S A*, **94**, 14361-14366.

Coquelle, A., Pipiras, E., Toledo, F., Buttin, G. and Debatisse, M. (1997) Expression of fragile sites triggers intrachromosomal mammalian gene amplification and sets boundaries to early amplicons. *Cell*, **89**, 215-225.

Corda, Y., Lee, S.E., Guillot, S., Walther, A., Sollier, J., Arbel-Eden, A., Haber, J.E. and Geli, V. (2005) Inactivation of Ku-mediated end joining suppresses mec1Delta lethality by depleting the ribonucleotide reductase inhibitor Sml1 through a pathway controlled by Tel1 kinase and the Mre11 complex. *Mol Cell Biol*, **25**, 10652-10664.

Cortez, D., Guntuku, S., Qin, J. and Elledge, S.J. (2001) ATR and ATRIP: partners in checkpoint signalling. *Science*, **294**, 1713-1716.

Cote, A.G. and Lewis, S.M. (2008) Mus81-dependent double-strand DNA breaks at in vivo-generated cruciform structures in S. cerevisiae. *Mol Cell*, **31**, 800-812.

Cotta-Ramusino, C., Fachinetti, D., Lucca, C., Doksani, Y., Lopes, M., Sogo, J. and Foiani, M. (2005) Exo1 processes stalled replication forks and counteracts fork reversal in checkpoint-defective cells. *Mol Cell*, **17**, 153-159.

Cox, M.M. (2001) Recombinational DNA repair of damaged replication forks in Escherichia coli: questions. *Annu Rev Genet*, **35**, 53-82.

Craig, J.M. and Choo, K.H. (2005) Kiss and break up--a safe passage to anaphase in mitosis and meiosis. *Chromosoma*, **114**, 252-262.

Craven, R.J., Greenwell, P.W., Dominska, M. and Petes, T.D. (2002) Regulation of genome stability by TEL1 and MEC1, yeast homologs of the mammalian ATM and ATR genes. *Genetics*, **161**, 493-507.

Cuadrado, M., Martinez-Pastor, B., Murga, M., Toledo, L.I., Gutierrez-Martinez, P., Lopez, E. and Fernandez-Capetillo, O. (2006) ATM regulates ATR chromatin loading in response to DNA double-strand breaks. *J Exp Med*, **203**, 297-303.

Cuvier, O. and Hirano, T. (2003) A role of topoisomerase II in linking DNA replication to chromosome condensation. *J Cell Biol*, **160**, 645-655.

D'Ambrosio, C., Kelly, G., Shirahige, K. and Uhlmann, F. (2008) Condensin-dependent rDNA decatenation introduces a temporal pattern to chromosome segregation. *Curr Biol*, **18**, 1084-1089.

D'Amours, D. and Amon, A. (2004) At the interface between signalling and executing anaphase--Cdc14 and the FEAR network. *Genes Dev*, **18**, 2581-2595.

Dart, D.A., Adams, K.E., Akerman, I. and Lakin, N.D. (2004) Recruitment of the cell cycle checkpoint kinase ATR to chromatin during S-phase. *J Biol Chem*, **279**, 16433-16440.

Darwiche, N., Freeman, L.A. and Strunnikov, A. (1999) Characterization of the components of the putative mammalian sister chromatid cohesion complex. *Gene*, **233**, 39-47.

Davenport, J., Harris, L.D. and Goorha, R. (2006) Spindle checkpoint function requires Mad2-dependent Cdc20 binding to the Mad3 homology domain of BubR1. *Exp Cell Res*, **312**, 1831-1842.

Dayn, A., Malkhosyan, S., Duzhy, D., Lyamichev, V., Panchenko, Y. and Mirkin, S. (1991) Formation of (dA-dT)n cruciforms in Escherichia coli cells under different environmental conditions. *J Bacteriol*, **173**, 2658-2664.

de la Barre, A.E., Gerson, V., Gout, S., Creaven, M., Allis, C.D. and Dimitrov, S. (2000) Core histone N-termini play an essential role in mitotic chromosome condensation. *Embo J*, **19**, 379-391.

Debatisse, M., El Achkar, E. and Dutrillaux, B. (2006) Common fragile sites nested at the interfaces of early and late-replicating chromosome bands: cis acting components of the G2/M checkpoint? *Cell Cycle*, **5**, 578-581.

Dej, K.J., Ahn, C. and Orr-Weaver, T.L. (2004) Mutations in the Drosophila condensin subunit dCAP-G: defining the role of condensin for chromosome condensation in mitosis and gene expression in interphase. *Genetics*, **168**, 895-906.

Dershowitz, A., Snyder, M., Sbia, M., Skurnick, J.H., Ong, L.Y. and Newlon, C.S. (2007) Linear derivatives of Saccharomyces cerevisiae chromosome III can be maintained in the absence of autonomously replicating sequence elements. *Mol Cell Biol*, **27**, 4652-4663.

Desany, B.A., Alcasabas, A.A., Bachant, J.B. and Elledge, S.J. (1998) Recovery from DNA replicational stress is the essential function of the S-phase checkpoint pathway. *Genes Dev*, **12**, 2956-2970.

Deshpande, A.M. and Newlon, C.S. (1996) DNA replication fork pause sites dependent on transcription. *Science*, **272**, 1030-1033.

DiNardo, S., Voelkel, K. and Sternglanz, R. (1984) DNA topoisomerase II mutant of Saccharomyces cerevisiae: topoisomerase II is required for segregation of daughter molecules at the termination of DNA replication. *Proc Natl Acad Sci U S A*, **81**, 2616-2620.

Donovan, S., Harwood, J., Drury, L.S. and Diffley, J.F. (1997) Cdc6p-dependent loading of Mcm proteins onto pre-replicative chromatin in budding yeast. *Proc Natl Acad Sci U S A*, **94**, 5611-5616.

Douglas, L.M., Alvarez, F.J., McCreary, C. and Konopka, J.B. (2005) Septin function in yeast model systems and pathogenic fungi. *Eukaryot Cell*, **4**, 1503-1512.

Downes, C.S., Clarke, D.J., Mullinger, A.M., Gimenez-Abian, J.F., Creighton, A.M. and Johnson, R.T. (1994) A topoisomerase II-dependent G2 cycle checkpoint in mammalian cells. *Nature*, **372**, 467-470.

Downs, J.A., Allard, S., Jobin-Robitaille, O., Javaheri, A., Auger, A., Bouchard, N., Kron, S.J., Jackson, S.P. and Cote, J. (2004) Binding of chromatin-modifying activities to phosphorylated histone H2A at DNA damage sites. *Mol Cell*, **16**, 979-990.

Durkin, S.G., Arlt, M.F., Howlett, N.G. and Glover, T.W. (2006) Depletion of CHK1, but not CHK2, induces chromosomal instability and breaks at common fragile sites. *Oncogene*, **25**, 4381-4388.

Durkin, S.G. and Glover, T.W. (2007) Chromosome fragile sites. *Annu Rev Genet*, **41**, 169-192.

Durkin, S.G., Ragland, R.L., Arlt, M.F., Mulle, J.G., Warren, S.T. and Glover, T.W. (2008) Replication stress induces tumor-like microdeletions in FHIT/FRA3B. *Proc Natl Acad Sci U S A*, **105**, 246-251.

Ekholm, S.V. and Reed, S.I. (2000) Regulation of G(1) cyclin-dependent kinases in the mammalian cell cycle. *Curr Opin Cell Biol*, **12**, 676-684.

El Achkar, E., Gerbault-Seureau, M., Muleris, M., Dutrillaux, B. and Debatisse, M. (2005) Premature condensation induces breaks at the interface of early and late replicating chromosome bands bearing common fragile sites. *Proc Natl Acad Sci U S A*, **102**, 18069-18074.

Elder, F.F. and Robinson, T.J. (1989) Rodent common fragile sites: are they conserved? Evidence from mouse and rat. *Chromosoma*, **97**, 459-464.

Fabre, F., Chan, A., Heyer, W.D. and Gangloff, S. (2002) Alternate pathways involving Sgs1/Top3, Mus81/ Mms4, and Srs2 prevent formation of toxic recombination intermediates from single-stranded gaps created by DNA replication. *Proc Natl Acad Sci U S A*, **99**, 16887-16892.

Fang, G. (2002) Checkpoint protein BubR1 acts synergistically with Mad2 to inhibit anaphase-promoting complex. *Mol Biol Cell*, **13**, 755-766.

Fesquet, D., Fitzpatrick, P.J., Johnson, A.L., Kramer, K.M., Toyn, J.H. and Johnston, L.H. (1999) A Bub2p-dependent spindle checkpoint pathway regulates the Dbf2p kinase in budding yeast. *Embo J*, **18**, 2424-2434.

Field, C., Li, R. and Oegema, K. (1999) Cytokinesis in eukaryotes: a mechanistic comparison. *Curr Opin Cell Biol*, **11**, 68-80.

Forsburg, S.L. (2004) Eukaryotic MCM proteins: beyond replication initiation. *Microbiol Mol Biol Rev*, **68**, 109-131.

Foss, E.J. (2001) Tof1p regulates DNA damage responses during S phase in Saccharomyces cerevisiae. *Genetics*, **157**, 567-577.

Freeman, L., Aragon-Alcaide, L. and Strunnikov, A. (2000) The condensin complex governs chromosome condensation and mitotic transmission of rDNA. *J Cell Biol*, **149**, 811-824.

Frei, C. and Gasser, S.M. (2000) The yeast Sgs1p helicase acts upstream of Rad53p in the DNA replication checkpoint and colocalizes with Rad53p in S-phase-specific foci. *Genes Dev*, **14**, 81-96.

Frenz, L.M., Lee, S.E., Fesquet, D. and Johnston, L.H. (2000) The budding yeast Dbf2 protein kinase localises to the centrosome and moves to the bud neck in late mitosis. *J Cell Sci*, **113 Pt 19**, 3399-3408.

Friedman, K.L., Brewer, B.J. and Fangman, W.L. (1997) Replication profile of Saccharomyces cerevisiae chromosome VI. *Genes Cells*, **2**, 667-678.

Fukui, T., Yamauchi, K., Muroya, T., Akiyama, M., Maki, H., Sugino, A. and Waga, S. (2004) Distinct roles of DNA polymerases delta and epsilon at the replication fork in Xenopus egg extracts. *Genes Cells*, **9**, 179-191.

Gabriel, A., Dapprich, J., Kunkel, M., Gresham, D., Pratt, S.C. and Dunham, M.J. (2006) Global mapping of transposon location. *PLoS Genet*, **2**, e212.

Gabrielse, C., Miller, C.T., McConnell, K.H., DeWard, A., Fox, C.A. and Weinreich, M. (2006) A Dbf4p BRCA1 C-terminal-like domain required for the response to replication fork arrest in budding yeast. *Genetics*, **173**, 541-555.

Gadea, B.B. and Ruderman, J.V. (2005) Aurora kinase inhibitor ZM447439 blocks chromosome-induced spindle assembly, the completion of chromosome condensation, and the establishment of the spindle integrity checkpoint in Xenopus egg extracts. *Mol Biol Cell*, **16**, 1305-1318.

Garcia-Muse, T. and Boulton, S.J. (2005) Distinct modes of ATR activation after replication stress and DNA double-strand breaks in Caenorhabditis elegans. *Embo J*, **24**, 4345-4355.

Gardner, R., Putnam, C.W. and Weinert, T. (1999) RAD53, DUN1 and PDS1 define two parallel G2/M checkpoint pathways in budding yeast. *Embo J*, **18**, 3173-3185.

Giet, R. and Glover, D.M. (2001) Drosophila aurora B kinase is required for histone H3 phosphorylation and condensin recruitment during chromosome condensation and to organize the central spindle during cytokinesis. *J Cell Biol*, **152**, 669-682.

Gietz, R.D. and Woods, R.A. (2002) Transformation of yeast by lithium acetate/single-stranded carrier DNA/polyethylene glycol method. *Methods Enzymol*, **350**, 87-96.

Gilbert, C.S., Green, C.M. and Lowndes, N.F. (2001) Budding yeast Rad9 is an ATP-dependent Rad53 activating machine. *Mol Cell*, **8**, 129-136.

Gilbert, D.M. (2001) Making sense of eukaryotic DNA replication origins. *Science*, **294**, 96-100.

Gillett, E.S., Espelin, C.W. and Sorger, P.K. (2004) Spindle checkpoint proteins and chromosome-microtubule attachment in budding yeast. *J Cell Biol*, **164**, 535-546.

Gimenez-Abian, J.F., Clarke, D.J., Devlin, J., Gimenez-Abian, M.I., De la Torre, C., Johnson, R.T., Mullinger, A.M. and Downes, C.S. (2000) Premitotic chromosome individualization in mammalian cells depends on topoisomerase II activity. *Chromosoma*, **109**, 235-244.

Gimenez-Abian, J.F., Clarke, D.J., Mullinger, A.M., Downes, C.S. and Johnson, R.T. (1995) A postprophase topoisomerase II-dependent chromatid core separation step in the formation of metaphase chromosomes. *J Cell Biol*, **131**, 7-17.

Gimenez-Abian, J.F., Sumara, I., Hirota, T., Hauf, S., Gerlich, D., de la Torre, C., Ellenberg, J. and Peters, J.M. (2004) Regulation of sister chromatid cohesion between chromosome arms. *Curr Biol*, **14**, 1187-1193.

Glover, T.W., Arlt, M.F., Casper, A.M. and Durkin, S.G. (2005) Mechanisms of common fragile site instability. *Hum Mol Genet*, **14 Spec No. 2**, R197-205.

Glover, T.W., Berger, C., Coyle, J. and Echo, B. (1984) DNA polymerase alpha inhibition by aphidicolin induces gaps and breaks at common fragile sites in human chromosomes. *Hum Genet*, **67**, 136-142.

Glover, T.W. and Stein, C.K. (1987) Induction of sister chromatid exchanges at common fragile sites. *Am J Hum Genet*, **41**, 882-890.

Glover, T.W. and Stein, C.K. (1988) Chromosome breakage and recombination at fragile sites. *Am J Hum Genet*, **43**, 265-273.

Goldstein, A.L. and McCusker, J.H. (1999) Three new dominant drug resistance cassettes for gene disruption in Saccharomyces cerevisiae. *Yeast*, **15**, 1541-1553.

Goto, H., Tomono, Y., Ajiro, K., Kosako, H., Fujita, M., Sakurai, M., Okawa, K., Iwamatsu, A., Okigaki, T., Takahashi, T. and Inagaki, M. (1999) Identification of a novel phosphorylation site on histone H3 coupled with mitotic chromosome condensation. *J Biol Chem*, **274**, 25543-25549.

Greenfeder, S.A. and Newlon, C.S. (1992) Replication forks pause at yeast centromeres. *Mol Cell Biol*, **12**, 4056-4066.

Griffis, E.R., Stuurman, N. and Vale, R.D. (2007) Spindly, a novel protein essential for silencing the spindle assembly checkpoint, recruits dynein to the kinetochore. *J Cell Biol*, **177**, 1005-1015.

Gruber, M., Wellinger, R.E. and Sogo, J.M. (2000) Architecture of the replication fork stalled at the 3' end of yeast ribosomal genes. *Mol Cell Biol*, **20**, 5777-5787.

Gu, Y., Shen, Y., Gibbs, R.A. and Nelson, D.L. (1996) Identification of FMR2, a novel gene associated with the FRAXE CCG repeat and CpG island. *Nat Genet*, **13**, 109-113.

Guacci, V., Hogan, E. and Koshland, D. (1994) Chromosome condensation and sister chromatid pairing in budding yeast. *J Cell Biol*, **125**, 517-530.

Guacci, V., Koshland, D. and Strunnikov, A. (1997) A direct link between sister chromatid cohesion and chromosome condensation revealed through the analysis of MCD1 in S. cerevisiae. *Cell*, **91**, 47-57.

Haase, S.B., Winey, M. and Reed, S.I. (2001) Multi-step control of spindle pole body duplication by cyclin-dependent kinase. *Nat Cell Biol*, **3**, 38-42.

Hagstrom, K.A., Holmes, V.F., Cozzarelli, N.R. and Meyer, B.J. (2002) C. elegans condensin promotes mitotic chromosome architecture, centromere organization, and sister chromatid segregation during mitosis and meiosis. *Genes Dev*, **16**, 729-742.

Hall, D.D., Markwardt, D.D., Parviz, F. and Heideman, W. (1998) Regulation of the Cln3-Cdc28 kinase by cAMP in Saccharomyces cerevisiae. *Embo J*, **17**, 4370-4378.

Hansen, R.S., Canfield, T.K., Fjeld, A.D., Mumm, S., Laird, C.D. and Gartler, S.M. (1997) A variable domain of delayed replication in FRAXA fragile X chromosomes: X inactivation-like spread of late replication. *Proc Natl Acad Sci U S A*, **94**, 4587-4592.

Harper, J.W. and Elledge, S.J. (2007) The DNA damage response: ten years after. *Mol Cell*, **28**, 739-745.

Harrison, J.C. and Haber, J.E. (2006) Surviving the breakup: the DNA damage checkpoint. *Annu Rev Genet*, **40**, 209-235.

Hartwell, L.H. (1974) Saccharomyces cerevisiae cell cycle. *Bacteriol Rev*, **38**, 164-198.

Hartwell, L.H., Culotti, J. and Reid, B. (1970) Genetic control of the cell-division cycle in yeast. I. Detection of mutants. *Proc Natl Acad Sci U S A*, **66**, 352-359.

Hartwell, L.H. and Weinert, T.A. (1989) Checkpoints: controls that ensure the order of cell cycle events. *Science*, **246**, 629-634.

Harvey, K.J. and Newport, J. (2003) Metazoan origin selection: origin recognition complex chromatin binding is regulated by CDC6 recruitment and ATP hydrolysis. *J Biol Chem*, **278**, 48524-48528.

Hauf, S., Roitinger, E., Koch, B., Dittrich, C.M., Mechtler, K. and Peters, J.M. (2005) Dissociation of cohesin from chromosome arms and loss of arm cohesion during early mitosis depends on phosphorylation of SA2. *PLoS Biol*, **3**, e69.

Hauf, S., Waizenegger, I.C. and Peters, J.M. (2001) Cohesin cleavage by separase required for anaphase and cytokinesis in human cells. *Science*, **293**, 1320-1323.

Hekmat-Nejad, M., You, Z., Yee, M.C., Newport, J.W. and Cimprich, K.A. (2000) Xenopus ATR is a replication-dependent chromatin-binding protein required for the DNA replication checkpoint. *Curr Biol*, **10**, 1565-1573.

Hellman, A., Rahat, A., Scherer, S.W., Darvasi, A., Tsui, L.C. and Kerem, B. (2000) Replication delay along FRA7H, a common fragile site on human chromosome 7, leads to chromosomal instability. *Mol Cell Biol*, **20**, 4420-4427.

Hendzel, M.J., Wei, Y., Mancini, M.A., Van Hooser, A., Ranalli, T., Brinkley, B.R., Bazett-Jones, D.P. and Allis, C.D. (1997) Mitosis-specific phosphorylation of histone H3 initiates primarily within pericentromeric heterochromatin during G2 and spreads in an ordered fashion coincident with mitotic chromosome condensation. *Chromosoma*, **106**, 348-360.

Hennessy, K.M., Lee, A., Chen, E. and Botstein, D. (1991) A group of interacting yeast DNA replication genes. *Genes Dev*, **5**, 958-969.

Herzberg, K., Bashkirov, V.I., Rolfsmeier, M., Haghnazari, E., McDonald, W.H., Anderson, S., Bashkirova, E.V., Yates, J.R., 3rd and Heyer, W.D. (2006) Phosphorylation of Rad55 on serines 2, 8, and 14 is required for efficient homologous recombination in the recovery of stalled replication forks. *Mol Cell Biol*, **26**, 8396-8409.

Hewett, D.R., Handt, O., Hobson, L., Mangelsdorf, M., Eyre, H.J., Baker, E., Sutherland, G.R., Schuffenhauer, S., Mao, J.I. and Richards, R.I. (1998)

FRA10B structure reveals common elements in repeat expansion and chromosomal fragile site genesis. *Mol Cell*, **1**, 773-781.

Hirano, T. (2000) Chromosome cohesion, condensation, and separation. *Annu Rev Biochem*, **69**, 115-144.

Hirano, T., Kobayashi, R. and Hirano, M. (1997) Condensins, chromosome condensation protein complexes containing XCAP-C, XCAP-E and a Xenopus homolog of the Drosophila Barren protein. *Cell*, **89**, 511-521.

Hodgson, B., Calzada, A. and Labib, K. (2007) Mrc1 and Tof1 regulate DNA replication forks in different ways during normal S phase. *Mol Biol Cell*, **18**, 3894-3902.

Hoege, C., Pfander, B., Moldovan, G.L., Pyrowolakis, G. and Jentsch, S. (2002) RAD6-dependent DNA repair is linked to modification of PCNA by ubiquitin and SUMO. *Nature*, **419**, 135-141.

Holm, C., Goto, T., Wang, J.C. and Botstein, D. (1985) DNA topoisomerase II is required at the time of mitosis in yeast. *Cell*, **41**, 553-563.

Holm, C., Stearns, T. and Botstein, D. (1989) DNA topoisomerase II must act at mitosis to prevent nondisjunction and chromosome breakage. *Mol Cell Biol*, **9**, 159-168.

Howell, B.J., Moree, B., Farrar, E.M., Stewart, S., Fang, G. and Salmon, E.D. (2004) Spindle checkpoint protein dynamics at kinetochores in living cells. *Curr Biol*, **14**, 953-964.

Howlett, N.G., Taniguchi, T., Durkin, S.G., D'Andrea, A.D. and Glover, T.W. (2005) The Fanconi anemia pathway is required for the DNA replication stress response and for the regulation of common fragile site stability. *Hum Mol Genet*, **14**, 693-701.

Hoyt, M.A., Totis, L. and Roberts, B.T. (1991) S. cerevisiae genes required for cell cycle arrest in response to loss of microtubule function. *Cell*, **66**, 507-517.

Hsu, J.Y., Sun, Z.W., Li, X., Reuben, M., Tatchell, K., Bishop, D.K., Grushcow, J.M., Brame, C.J., Caldwell, J.A., Hunt, D.F., Lin, R., Smith, M.M. and Allis, C.D. (2000) Mitotic phosphorylation of histone H3 is governed by Ipl1/aurora kinase and Glc7/PP1 phosphatase in budding yeast and nematodes. *Cell*, **102**, 279-291.

Huang, C.E., Milutinovich, M. and Koshland, D. (2005) Rings, bracelet or snaps: fashionable alternatives for Smc complexes. *Philos Trans R Soc Lond B Biol Sci*, **360**, 537-542.

Huang, M., Zhou, Z. and Elledge, S.J. (1998) The DNA replication and damage checkpoint pathways induce transcription by inhibition of the Crt1 repressor. *Cell*, **94**, 595-605.

Hwa Lim, H., Yeong, F.M. and Surana, U. (2003) Inactivation of mitotic kinase triggers translocation of MEN components to mother-daughter neck in yeast. *Mol Biol Cell*, **14**, 4734-4743.

Hwang, L.H., Lau, L.F., Smith, D.L., Mistrot, C.A., Hardwick, K.G., Hwang, E.S., Amon, A. and Murray, A.W. (1998) Budding yeast Cdc20: a target of the spindle checkpoint. *Science*, **279**, 1041-1044.

Hyrien, O. (2000) Mechanisms and consequences of replication fork arrest. *Biochimie*, **82**, 5-17.

Ip, S.C., Rass, U., Blanco, M.G., Flynn, H.R., Skehel, J.M. and West, S.C. (2008) Identification of Holliday junction resolvases from humans and yeast. *Nature*, **456**, 357-361.

Ira, G., Pellicioli, A., Balijja, A., Wang, X., Fiorani, S., Carotenuto, W., Liberi, G., Bressan, D., Wan, L., Hollingsworth, N.M., Haber, J.E. and Foiani, M. (2004) DNA end resection, homologous recombination and DNA damage checkpoint activation require CDK1. *Nature*, **431**, 1011-1017.

Ivessa, A.S., Lenzmeier, B.A., Bessler, J.B., Goudsouzian, L.K., Schnakenberg, S.L. and Zakian, V.A. (2003) The Saccharomyces cerevisiae helicase Rrm3p facilitates replication past nonhistone protein-DNA complexes. *Mol Cell*, **12**, 1525-1536.

Ivessa, A.S., Zhou, J.Q., Schulz, V.P., Monson, E.K. and Zakian, V.A. (2002) Saccharomyces Rrm3p, a 5' to 3' DNA helicase that promotes replication fork progression through telomeric and subtelomeric DNA. *Genes Dev*, **16**, 1383-1396.

Janson, M.E. and Tran, P.T. (2008) Chromosome segregation: organizing overlap at the midzone. *Curr Biol*, **18**, R308-311.

Jaquenoud, M., van Drogen, F. and Peter, M. (2002) Cell cycle-dependent nuclear export of Cdh1p may contribute to the inactivation of APC/C(Cdh1). *Embo J*, **21**, 6515-6526.

Jazayeri, A., Falck, J., Lukas, C., Bartek, J., Smith, G.C., Lukas, J. and Jackson, S.P. (2006) ATM- and cell cycle-dependent regulation of ATR in response to DNA double-strand breaks. *Nat Cell Biol*, **8**, 37-45.

Johnson, R.D. and Jasin, M. (2000) Sister chromatid gene conversion is a prominent double-strand break repair pathway in mammalian cells. *Embo J*, **19**, 3398-3407.

Johzuka, K. and Ogawa, H. (1995) Interaction of Mre11 and Rad50: two proteins required for DNA repair and meiosis-specific double-strand break formation in Saccharomyces cerevisiae. *Genetics*, **139**, 1521-1532.

Johzuka, K., Terasawa, M., Ogawa, H., Ogawa, T. and Horiuchi, T. (2006) Condensin loaded onto the replication fork barrier site in the rRNA gene repeats during S phase in a FOB1-dependent fashion to prevent contraction of a long repetitive array in Saccharomyces cerevisiae. *Mol Cell Biol*, **26**, 2226-2236.

Jonsson, Z.O. and Hubscher, U. (1997) Proliferating cell nuclear antigen: more than a clamp for DNA polymerases. *Bioessays*, **19**, 967-975.

Kai, M., Boddy, M.N., Russell, P. and Wang, T.S. (2005) Replication checkpoint kinase Cds1 regulates Mus81 to preserve genome integrity during replication stress. *Genes Dev*, **19**, 919-932.

Kaliraman, V., Mullen, J.R., Fricke, W.M., Bastin-Shanower, S.A. and Brill, S.J. (2001) Functional overlap between Sgs1-Top3 and the Mms4-Mus81 endonuclease. *Genes Dev*, **15**, 2730-2740.

Katou, Y., Kanoh, Y., Bando, M., Noguchi, H., Tanaka, H., Ashikari, T., Sugimoto, K. and Shirahige, K. (2003) S-phase checkpoint proteins Tof1 and Mrc1 form a stable replication-pausing complex. *Nature*, **424**, 1078-1083.

Keogh, M.C., Kim, J.A., Downey, M., Fillingham, J., Chowdhury, D., Harrison, J.C., Onishi, M., Datta, N., Galicia, S., Emili, A., Lieberman, J., Shen, X., Buratowski, S., Haber, J.E., Durocher, D., Greenblatt, J.F. and Krogan, N.J. (2006) A phosphatase complex that dephosphorylates gammaH2AX regulates DNA damage checkpoint recovery. *Nature*, **439**, 497-501.

Kim, J.M., Vanguri, S., Boeke, J.D., Gabriel, A. and Voytas, D.F. (1998) Transposable elements and genome organization: a comprehensive survey of retrotransposons revealed by the complete Saccharomyces cerevisiae genome sequence. *Genome Res*, **8**, 464-478.

Kimura, K., Hirano, M., Kobayashi, R. and Hirano, T. (1998) Phosphorylation and activation of 13S condensin by Cdc2 in vitro. *Science*, **282**, 487-490.

Kimura, K. and Hirano, T. (1997) ATP-dependent positive supercoiling of DNA by 13S condensin: a biochemical implication for chromosome condensation. *Cell*, **90**, 625-634.

Kimura, K. and Hirano, T. (2000) Dual roles of the 11S regulatory subcomplex in condensin functions. *Proc Natl Acad Sci U S A*, **97**, 11972-11977.

Kimura, K., Rybenkov, V.V., Crisona, N.J., Hirano, T. and Cozzarelli, N.R. (1999) 13S condensin actively reconfigures DNA by introducing global positive writhe: implications for chromosome condensation. *Cell*, **98**, 239-248.

Kitajima, T.S., Kawashima, S.A. and Watanabe, Y. (2004) The conserved kinetochore protein shugoshin protects centromeric cohesion during meiosis. *Nature*, **427**, 510-517.

Kitamura, E., Blow, J.J. and Tanaka, T.U. (2006) Live-cell imaging reveals replication of individual replicons in eukaryotic replication factories. *Cell*, **125**, 1297-1308.

Knapp, D., Bhoite, L., Stillman, D.J. and Nasmyth, K. (1996) The transcription factor Swi5 regulates expression of the cyclin kinase inhibitor p40SIC1. *Mol Cell Biol*, **16**, 5701-5707.

Kobayashi, J., Tauchi, H., Sakamoto, S., Nakamura, A., Morishima, K., Matsuura, S., Kobayashi, T., Tamai, K., Tanimoto, K. and Komatsu, K. (2002) NBS1 localizes to gamma-H2AX foci through interaction with the FHA/BRCT domain. *Curr Biol*, **12**, 1846-1851.

Kobayashi, T. and Horiuchi, T. (1996) A yeast gene product, Fob1 protein, required for both replication fork blocking and recombinational hotspot activities. *Genes Cells*, **1**, 465-474.

Krishnan, R., Pangilinan, F., Lee, C. and Spencer, F. (2000) Saccharomyces cerevisiae BUB2 prevents mitotic exit in response to both spindle and kinetochore damage. *Genetics*, **156**, 489-500.

Krishnan, V., Nirantar, S., Crasta, K., Cheng, A.Y. and Surana, U. (2004) DNA replication checkpoint prevents precocious chromosome segregation by regulating spindle behavior. *Mol Cell*, **16**, 687-700.

Kumagai, A., Lee, J., Yoo, H.Y. and Dunphy, W.G. (2006) TopBP1 activates the ATR-ATRIP complex. *Cell*, **124**, 943-955.

Labib, K. and Hodgson, B. (2007) Replication fork barriers: pausing for a break or stalling for time? *EMBO Rep*, **8**, 346-353.

Lambert, S. and Carr, A.M. (2005) Checkpoint responses to replication fork barriers. *Biochimie*, **87**, 591-602.

Lambert, S., Froget, B. and Carr, A.M. (2007) Arrested replication fork processing: interplay between checkpoints and recombination. *DNA Repair (Amst)*, **6**, 1042-1061.

Larner, J.M., Lee, H., Little, R.D., Dijkwel, P.A., Schildkraut, C.L. and Hamlin, J.L. (1999) Radiation down-regulates replication origin activity throughout the S phase in mammalian cells. *Nucleic Acids Res*, **27**, 803-809.

Lavoie, B.D., Hogan, E. and Koshland, D. (2002) In vivo dissection of the chromosome condensation machinery: reversibility of condensation distinguishes contributions of condensin and cohesin. *J Cell Biol*, **156**, 805-815.

Lavoie, B.D., Hogan, E. and Koshland, D. (2004) In vivo requirements for rDNA chromosome condensation reveal two cell-cycle-regulated pathways for mitotic chromosome folding. *Genes Dev*, **18**, 76-87.

Lavoie, B.D., Tuffo, K.M., Oh, S., Koshland, D. and Holm, C. (2000) Mitotic chromosome condensation requires Brn1p, the yeast homologue of Barren. *Mol Biol Cell*, **11**, 1293-1304.

Le Beau, M.M., Rassool, F.V., Neilly, M.E., Espinosa, R., 3rd, Glover, T.W., Smith, D.I. and McKeithan, T.W. (1998) Replication of a common fragile site, FRA3B, occurs late in S phase and is delayed further upon induction: implications for the mechanism of fragile site induction. *Hum Mol Genet*, **7**, 755-761.

Lee, S.E., Jensen, S., Frenz, L.M., Johnson, A.L., Fesquet, D. and Johnston, L.H. (2001) The Bub2-dependent mitotic pathway in yeast acts every cell cycle and regulates cytokinesis. *J Cell Sci*, **114**, 2345-2354.

Lehmann, A.R., Niimi, A., Ogi, T., Brown, S., Sabbioneda, S., Wing, J.F., Kannouche, P.L. and Green, C.M. (2007) Translesion synthesis: Y-family polymerases and the polymerase switch. *DNA Repair (Amst)*, **6**, 891-899.

Lemoine, F.J., Degtyareva, N.P., Kokoska, R.J. and Petes, T.D. (2008) Reduced Levels of DNA Polymerase {delta} Induce Chromosome Fragile Site Instability in Yeast. *Mol Cell Biol*.

Lemoine, F.J., Degtyareva, N.P., Lobachev, K. and Petes, T.D. (2005) Chromosomal translocations in yeast induced by low levels of DNA polymerase a model for chromosome fragile sites. *Cell*, **120**, 587-598.

Lengauer, C., Kinzler, K.W. and Vogelstein, B. (1998) Genetic instabilities in human cancers. *Nature*, **396**, 643-649.

Lengronne, A., Pasero, P., Bensimon, A. and Schwob, E. (2001) Monitoring S phase progression globally and locally using BrdU incorporation in TK(+) yeast strains. *Nucleic Acids Res*, **29**, 1433-1442.

Leroy, C., Lee, S.E., Vaze, M.B., Ochsenbien, F., Guerois, R., Haber, J.E. and Marsolier-Kergoat, M.C. (2003) PP2C phosphatases Ptc2 and Ptc3 are required for DNA checkpoint inactivation after a double-strand break. *Mol Cell*, **11**, 827-835.

Lew, D.J. and Burke, D.J. (2003) The spindle assembly and spindle position checkpoints. *Annu Rev Genet*, **37**, 251-282.

Lew, D.J. and Reed, S.I. (1993) Morphogenesis in the yeast cell cycle: regulation by Cdc28 and cyclins. *J Cell Biol*, **120**, 1305-1320.

Li, A. and Blow, J.J. (2004) Non-proteolytic inactivation of geminin requires CDK-dependent ubiquitination. *Nat Cell Biol*, **6**, 260-267.

Li, G., Sudlow, G. and Belmont, A.S. (1998) Interphase cell cycle dynamics of a late-replicating, heterochromatic homogeneously staining region: precise choreography of condensation/decondensation and nuclear positioning. *J Cell Biol*, **140**, 975-989.

Liang, B., Qiu, J., Ratnakumar, K. and Laurent, B.C. (2007) RSC functions as an early double-strand-break sensor in the cell's response to DNA damage. *Curr Biol*, **17**, 1432-1437.

Liang, C. and Stillman, B. (1997) Persistent initiation of DNA replication and chromatin-bound MCM proteins during the cell cycle in cdc6 mutants. *Genes Dev*, **11**, 3375-3386.

Liang, F., Han, M., Romanienko, P.J. and Jasin, M. (1998) Homology-directed repair is a major double-strand break repair pathway in mammalian cells. *Proc Natl Acad Sci U S A*, **95**, 5172-5177.

Liang, F. and Wang, Y. (2007) DNA damage checkpoints inhibit mitotic exit by two different mechanisms. *Mol Cell Biol*, **27**, 5067-5078.

Liberi, G., Chiolo, I., Pellicioli, A., Lopes, M., Plevani, P., Muzi-Falconi, M. and Foiani, M. (2000) Srs2 DNA helicase is involved in checkpoint response and its regulation requires a functional Mec1-dependent pathway and Cdk1 activity. *Embo J*, **19**, 5027-5038.

Limongi, M.Z., Pelliccia, F. and Rocchi, A. (2003) Characterization of the human common fragile site FRA2G. *Genomics*, **81**, 93-97.

Lipp, J.J., Hirota, T., Poser, I. and Peters, J.M. (2007) Aurora B controls the association of condensin I but not condensin II with mitotic chromosomes. *J Cell Sci*, **120**, 1245-1255.

Lippincott, J. and Li, R. (1998) Sequential assembly of myosin II, an IQGAP-like protein, and filamentous actin to a ring structure involved in budding yeast cytokinesis. *J Cell Biol*, **140**, 355-366.

Lippincott, J., Shannon, K.B., Shou, W., Deshaies, R.J. and Li, R. (2001) The Tem1 small GTPase controls actomyosin and septin dynamics during cytokinesis. *J Cell Sci*, **114**, 1379-1386.

Lisby, M., Rothstein, R. and Mortensen, U.H. (2001) Rad52 forms DNA repair and recombination centers during S phase. *Proc Natl Acad Sci U S A*, **98**, 8276-8282.

Lobachev, K.S., Gordenin, D.A. and Resnick, M.A. (2002) The Mre11 complex is required for repair of hairpin-capped double-strand breaks and prevention of chromosome rearrangements. *Cell*, **108**, 183-193.

Longtine, M.S., McKenzie, A., 3rd, Demarini, D.J., Shah, N.G., Wach, A., Brachat, A., Philippsen, P. and Pringle, J.R. (1998) Additional modules for versatile and economical PCR-based gene deletion and modification in Saccharomyces cerevisiae. *Yeast*, **14**, 953-961.

Lopes, M., Cotta-Ramusino, C., Pellicioli, A., Liberi, G., Plevani, P., Muzi-Falconi, M., Newlon, C.S. and Foiani, M. (2001) The DNA replication checkpoint response stabilizes stalled replication forks. *Nature*, **412**, 557-561.

Losada, A., Hirano, M. and Hirano, T. (2002) Cohesin release is required for sister chromatid resolution, but not for condensin-mediated compaction, at the onset of mitosis. *Genes Dev*, **16**, 3004-3016.

Losada, A. and Hirano, T. (2001) Shaping the metaphase chromosome: coordination of cohesion and condensation. *Bioessays*, **23**, 924-935.

Lowndes, N.F., Johnson, A.L. and Johnston, L.H. (1991) Coordination of expression of DNA synthesis genes in budding yeast by a cell-cycle regulated trans factor. *Nature*, **350**, 247-250.

Lu, X., Nguyen, T.A. and Donehower, L.A. (2005) Reversal of the ATM/ATR-mediated DNA damage response by the oncogenic phosphatase PPM1D. *Cell Cycle*, **4**, 1060-1064.

Lucas, I., Germe, T., Chevrier-Miller, M. and Hyrien, O. (2001) Topoisomerase II can unlink replicating DNA by precatenane removal. *Embo J*, **20**, 6509-6519.

Lucca, C., Vanoli, F., Cotta-Ramusino, C., Pellicioli, A., Liberi, G., Haber, J. and Foiani, M. (2004) Checkpoint-mediated control of replisome-fork association and signalling in response to replication pausing. *Oncogene*, **23**, 1206-1213.

Lukusa, T. and Fryns, J.P. (2008) Human chromosome fragility. *Biochim Biophys Acta*, **1779**, 3-16.

Lundin, C., Erixon, K., Arnaudeau, C., Schultz, N., Jenssen, D., Meuth, M. and Helleday, T. (2002) Different roles for nonhomologous end joining and

homologous recombination following replication arrest in mammalian cells. *Mol Cell Biol*, **22**, 5869-5878.

Ma, J.L., Lee, S.J., Duong, J.K. and Stern, D.F. (2006) Activation of the checkpoint kinase Rad53 by the phosphatidyl inositol kinase-like kinase Mec1. *J Biol Chem*, **281**, 3954-3963.

Maiato, H., DeLuca, J., Salmon, E.D. and Earnshaw, W.C. (2004) The dynamic kinetochore-microtubule interface. *J Cell Sci*, **117**, 5461-5477.

Mailand, N., Falck, J., Lukas, C., Syljuasen, R.G., Welcker, M., Bartek, J. and Lukas, J. (2000) Rapid destruction of human Cdc25A in response to DNA damage. *Science*, **288**, 1425-1429.

Maiorano, D., Rul, W. and Mechali, M. (2004) Cell cycle regulation of the licensing activity of Cdt1 in Xenopus laevis. *Exp Cell Res*, **295**, 138-149.

Marahrens, Y. and Stillman, B. (1992) A yeast chromosomal origin of DNA replication defined by multiple functional elements. *Science*, **255**, 817-823.

Matsuura, A., Naito, T. and Ishikawa, F. (1999) Genetic control of telomere integrity in Schizosaccharomyces pombe: rad3(+) and tel1(+) are parts of two regulatory networks independent of the downstream protein kinases chk1(+) and cds1(+). *Genetics*, **152**, 1501-1512.

McClellan, J.A., Boublikova, P., Palecek, E. and Lilley, D.M. (1990) Superhelical torsion in cellular DNA responds directly to environmental and genetic factors. *Proc Natl Acad Sci U S A*, **87**, 8373-8377.

McGuinness, B.E., Hirota, T., Kudo, N.R., Peters, J.M. and Nasmyth, K. (2005) Shugoshin prevents dissociation of cohesin from centromeres during mitosis in vertebrate cells. *PLoS Biol*, **3**, e86.

Melo, J.A., Cohen, J. and Toczyski, D.P. (2001) Two checkpoint complexes are independently recruited to sites of DNA damage in vivo. *Genes Dev*, **15**, 2809-2821.

Mendenhall, M.D. and Hodge, A.E. (1998) Regulation of Cdc28 cyclin-dependent protein kinase activity during the cell cycle of the yeast Saccharomyces cerevisiae. *Microbiol Mol Biol Rev*, **62**, 1191-1243.

Michaelis, C., Ciosk, R. and Nasmyth, K. (1997) Cohesins: chromosomal proteins that prevent premature separation of sister chromatids. *Cell*, **91**, 35-45.

Michel, B., Boubakri, H., Baharoglu, Z., LeMasson, M. and Lestini, R. (2007) Recombination proteins and rescue of arrested replication forks. *DNA Repair (Amst)*, **6**, 967-980.

Michel, B., Ehrlich, S.D. and Uzest, M. (1997) DNA double-strand breaks caused by replication arrest. *Embo J*, **16**, 430-438.

Michel, B., Grompone, G., Flores, M.J. and Bidnenko, V. (2004) Multiple pathways process stalled replication forks. *Proc Natl Acad Sci U S A*, **101**, 12783-12788.

Mimori, K., Druck, T., Inoue, H., Alder, H., Berk, L., Mori, M., Huebner, K. and Croce, C.M. (1999) Cancer-specific chromosome alterations in the constitutive fragile region FRA3B. *Proc Natl Acad Sci U S A*, **96**, 7456-7461.

Mirkin, S.M. (2006) DNA structures, repeat expansions and human hereditary disorders. *Curr Opin Struct Biol*, **16**, 351-358.

Mishmar, D., Mandel-Gutfreund, Y., Margalit, H., Rahat, A. and Kerem, B. (1999) Common fragile sites: G-band characteristics within an R-band. *Am J Hum Genet*, **64**, 908-910.

Mishmar, D., Rahat, A., Scherer, S.W., Nyakatura, G., Hinzmann, B., Kohwi, Y., Mandel-Gutfroind, Y., Lee, J.R., Drescher, B., Sas, D.E., Margalit, H., Platzer, M., Weiss, A., Tsui, L.C., Rosenthal, A. and Kerem, B. (1998) Molecular characterization of a common fragile site (FRA7H) on human chromosome 7 by the cloning of a simian virus 40 integration site. *Proc Natl Acad Sci U S A*, **95**, 8141-8146.

Mohanty, B.K., Bairwa, N.K. and Bastia, D. (2006) The Tof1p-Csm3p protein complex counteracts the Rrm3p helicase to control replication termination of Saccharomyces cerevisiae. *Proc Natl Acad Sci U S A*, **103**, 897-902.

Moll, T., Tebb, G., Surana, U., Robitsch, H. and Nasmyth, K. (1991) The role of phosphorylation and the CDC28 protein kinase in cell cycle-regulated nuclear import of the S. cerevisiae transcription factor SWI5. *Cell*, **66**, 743-758.

Moore, J.K. and Haber, J.E. (1996) Capture of retrotransposon DNA at the sites of chromosomal double-strand breaks. *Nature*, **383**, 644-646.

Mora-Bermudez, F., Gerlich, D. and Ellenberg, J. (2007) Maximal chromosome compaction occurs by axial shortening in anaphase and depends on Aurora kinase. *Nat Cell Biol*, **9**, 822-831.

Morelli, C., Karayianni, E., Magnanini, C., Mungall, A.J., Thorland, E., Negrini, M., Smith, D.I. and Barbanti-Brodano, G. (2002) Cloning and characterization of the common fragile site FRA6F harboring a replicative senescence gene and frequently deleted in human tumors. *Oncogene*, **21**, 7266-7276.

Morrow, D.M., Tagle, D.A., Shiloh, Y., Collins, F.S. and Hieter, P. (1995) TEL1, an S. cerevisiae homolog of the human gene mutated in ataxia telangiectasia, is functionally related to the yeast checkpoint gene MEC1. *Cell*, **82**, 831-840.

Mossi, R. and Hubscher, U. (1998) Clamping down on clamps and clamp loaders-- the eukaryotic replication factor C. *Eur J Biochem*, **254**, 209-216.

Murnion, M.E., Adams, R.R., Callister, D.M., Allis, C.D., Earnshaw, W.C. and Swedlow, J.R. (2001) Chromatin-associated protein phosphatase 1 regulates aurora-B and histone H3 phosphorylation. *J Biol Chem*, **276**, 26656-26665.

Musacchio, A. and Salmon, E.D. (2007) The spindle-assembly checkpoint in space and time. *Nat Rev Mol Cell Biol*, **8**, 379-393.

Musio, A., Montagna, C., Mariani, T., Tilenni, M., Focarelli, M.L., Brait, L., Indino, E., Benedetti, P.A., Chessa, L., Albertini, A., Ried, T. and Vezzoni, P. (2005) SMC1 involvement in fragile site expression. *Hum Mol Genet*, **14**, 525-533.

Nakada, D., Hirano, Y. and Sugimoto, K. (2004) Requirement of the Mre11 complex and exonuclease 1 for activation of the Mec1 signalling pathway. *Mol Cell Biol*, **24**, 10016-10025.

Nakada, S., Chen, G.I., Gingras, A.C. and Durocher, D. (2008) PP4 is a gammaH2AX phosphatase required for recovery from the DNA damage checkpoint. *EMBO Rep*.

Nakajima, M., Kumada, K., Hatakeyama, K., Noda, T., Peters, J.M. and Hirota, T. (2007) The complete removal of cohesin from chromosome arms depends on separase. *J Cell Sci*, **120**, 4188-4196.

Nasmyth, K. (1996) At the heart of the budding yeast cell cycle. *Trends Genet*, **12**, 405-412.

Nasmyth, K., Peters, J.M. and Uhlmann, F. (2000) Splitting the chromosome: cutting the ties that bind sister chromatids. *Science*, **288**, 1379-1385.

Neecke, H., Lucchini, G. and Longhese, M.P. (1999) Cell cycle progression in the presence of irreparable DNA damage is controlled by a Mec1- and Rad53-dependent checkpoint in budding yeast. *Embo J*, **18**, 4485-4497.

Newlon, C.S. and Theis, J.F. (1993) The structure and function of yeast ARS elements. *Curr Opin Genet Dev*, **3**, 752-758.

Nicklas, R.B. (1997) How cells get the right chromosomes. *Science*, **275**, 632-637.

Nicklas, R.B., Waters, J.C., Salmon, E.D. and Ward, S.C. (2001) Checkpoint signals in grasshopper meiosis are sensitive to microtubule attachment, but tension is still essential. *J Cell Sci*, **114**, 4173-4183.

Nishitani, H. and Lygerou, Z. (2002) Control of DNA replication licensing in a cell cycle. *Genes Cells*, **7**, 523-534.

Nitiss, J.L., Liu, Y.X. and Hsiung, Y. (1993) A temperature sensitive topoisomerase II allele confers temperature dependent drug resistance on amsacrine and etoposide: a genetic system for determining the targets of topoisomerase II inhibitors. *Cancer Res*, **53**, 89-93.

Nojima, H. (1997) Cell cycle checkpoints, chromosome stability and the progression of cancer. *Hum Cell*, **10**, 221-230.

Noton, E. and Diffley, J.F. (2000) CDK inactivation is the only essential function of the APC/C and the mitotic exit network proteins for origin resetting during mitosis. *Mol Cell*, **5**, 85-95.

Nurse, P. and Thuriaux, P. (1980) Regulatory genes controlling mitosis in the fission yeast Schizosaccharomyces pombe. *Genetics*, **96**, 627-637.

Nyberg, K.A., Michelson, R.J., Putnam, C.W. and Weinert, T.A. (2002) Toward maintaining the genome: DNA damage and replication checkpoints. *Annu Rev Genet*, **36**, 617-656.

O'Neill, B.M., Szyjka, S.J., Lis, E.T., Bailey, A.O., Yates, J.R., 3rd, Aparicio, O.M. and Romesberg, F.E. (2007) Pph3-Psy2 is a phosphatase complex required for Rad53 dephosphorylation and replication fork restart during recovery from DNA damage. *Proc Natl Acad Sci U S A*, **104**, 9290-9295.

O'Rourke, T.W., Doudican, N.A., Zhang, H., Eaton, J.S., Doetsch, P.W. and Shadel, G.S. (2005) Differential involvement of the related DNA helicases Pif1p and Rrm3p in mtDNA point mutagenesis and stability. *Gene*, **354**, 86-92.

Osborn, A.J. and Elledge, S.J. (2003) Mrc1 is a replication fork component whose phosphorylation in response to DNA replication stress activates Rad53. *Genes Dev*, **17**, 1755-1767.

Ozeri-Galai, E., Schwartz, M., Rahat, A. and Kerem, B. (2008) Interplay between ATM and ATR in the regulation of common fragile site stability. *Oncogene*, **27**, 2109-2117.

Pacek, M., Tutter, A.V., Kubota, Y., Takisawa, H. and Walter, J.C. (2006) Localization of MCM2-7, Cdc45, and GINS to the site of DNA unwinding during eukaryotic DNA replication. *Mol Cell*, **21**, 581-587.

Paciotti, V., Clerici, M., Scotti, M., Lucchini, G. and Longhese, M.P. (2001) Characterization of mec1 kinase-deficient mutants and of new hypomorphic mec1 alleles impairing subsets of the DNA damage response pathway. *Mol Cell Biol*, **21**, 3913-3925.

Palakodeti, A., Han, Y., Jiang, Y. and Le Beau, M.M. (2004) The role of late/slow replication of the FRA16D in common fragile site induction. *Genes Chromosomes Cancer*, **39**, 71-76.

Palin, A.H., Critcher, R., Fitzgerald, D.J., Anderson, J.N. and Farr, C.J. (1998) Direct cloning and analysis of DNA sequences from a region of the Chinese hamster genome associated with aphidicolin-sensitive fragility. *J Cell Sci*, **111 ( Pt 12)**, 1623-1634.

Pan, X., Ye, P., Yuan, D.S., Wang, X., Bader, J.S. and Boeke, J.D. (2006) A DNA integrity network in the yeast Saccharomyces cerevisiae. *Cell*, **124**, 1069-1081.

Pandita, T.K. (2002) ATM function and telomere stability. *Oncogene*, **21**, 611-618.

Pangilinan, F. and Spencer, F. (1996) Abnormal kinetochore structure activates the spindle assembly checkpoint in budding yeast. *Mol Biol Cell*, **7**, 1195-1208.

Paques, F. and Haber, J.E. (1999) Multiple pathways of recombination induced by double-strand breaks in Saccharomyces cerevisiae. *Microbiol Mol Biol Rev*, **63**, 349-404.

Paradee, W., Wilke, C.M., Wang, L., Shridhar, R., Mullins, C.M., Hoge, A., Glover, T.W. and Smith, D.I. (1996) A 350-kb cosmid contig in 3p14.2 that crosses the t(3;8) hereditary renal cell carcinoma translocation breakpoint and 17 aphidicolin-induced FRA3B breakpoints. *Genomics*, **35**, 87-93.

Pasero, P., Duncker, B.P., Schwob, E. and Gasser, S.M. (1999) A role for the Cdc7 kinase regulatory subunit Dbf4p in the formation of initiation-competent origins of replication. *Genes Dev*, **13**, 2159-2176.

Paull, T.T., Rogakou, E.P., Yamazaki, V., Kirchgessner, C.U., Gellert, M. and Bonner, W.M. (2000) A critical role for histone H2AX in recruitment of repair factors to nuclear foci after DNA damage. *Curr Biol*, **10**, 886-895.

Pellicioli, A. and Foiani, M. (2005) Signal transduction: how rad53 kinase is activated. *Curr Biol*, **15**, R769-771.

Petermann, E. and Caldecott, K.W. (2006) Evidence that the ATR/Chk1 pathway maintains normal replication fork progression during unperturbed S phase. *Cell Cycle*, **5**, 2203-2209.

Petermann, E., Helleday, T. and Caldecott, K.W. (2008) Claspin promotes normal replication fork rates in human cells. *Mol Biol Cell*, **19**, 2373-2378.

Petermann, E., Maya-Mendoza, A., Zachos, G., Gillespie, D.A., Jackson, D.A. and Caldecott, K.W. (2006) Chk1 requirement for high global rates of replication fork progression during normal vertebrate S phase. *Mol Cell Biol*, **26**, 3319-3326.

Peterson, C.L. and Cote, J. (2004) Cellular machineries for chromosomal DNA repair. *Genes Dev*, **18**, 602-616.

Piatti, S., Bohm, T., Cocker, J.H., Diffley, J.F. and Nasmyth, K. (1996) Activation of S-phase-promoting CDKs in late G1 defines a "point of no return" after which Cdc6 synthesis cannot promote DNA replication in yeast. *Genes Dev*, **10**, 1516-1531.

Pierce, A.J., Stark, J.M., Araujo, F.D., Moynahan, M.E., Berwick, M. and Jasin, M. (2001) Double-strand breaks and tumorigenesis. *Trends Cell Biol*, **11**, S52-59.

Pinsky, B.A. and Biggins, S. (2005) The spindle checkpoint: tension versus attachment. *Trends Cell Biol*, **15**, 486-493.

Pirzio, L.M., Pichierri, P., Bignami, M. and Franchitto, A. (2008) Werner syndrome helicase activity is essential in maintaining fragile site stability. *J Cell Biol*, **180**, 305-314.

Prado, F. and Aguilera, A. (2005) Impairment of replication fork progression mediates RNA polII transcription-associated recombination. *Embo J*, **24**, 1267-1276.

Prakash, L. (1981) Characterization of postreplication repair in Saccharomyces cerevisiae and effects of rad6, rad18, rev3 and rad52 mutations. *Mol Gen Genet*, **184**, 471-478.

Preuss, U., Landsberg, G. and Scheidtmann, K.H. (2003) Novel mitosis-specific phosphorylation of histone H3 at Thr11 mediated by Dlk/ZIP kinase. *Nucleic Acids Res*, **31**, 878-885.

Prigent, C. and Dimitrov, S. (2003) Phosphorylation of serine 10 in histone H3, what for? *J Cell Sci*, **116**, 3677-3685.

Raghuraman, M.K., Brewer, B.J. and Fangman, W.L. (1997) Cell cycle-dependent establishment of a late replication program. *Science*, **276**, 806-809.

Raghuraman, M.K., Winzeler, E.A., Collingwood, D., Hunt, S., Wodicka, L., Conway, A., Lockhart, D.J., Davis, R.W., Brewer, B.J. and Fangman, W.L. (2001) Replication dynamics of the yeast genome. *Science*, **294**, 115-121.

Ragland, R.L., Glynn, M.W., Arlt, M.F. and Glover, T.W. (2008) Stably transfected common fragile site sequences exhibit instability at ectopic sites. *Genes Chromosomes Cancer*, **47**, 860-872.

Raveendranathan, M., Chattopadhyay, S., Bolon, Y.T., Haworth, J., Clarke, D.J. and Bielinsky, A.K. (2006) Genome-wide replication profiles of S-phase checkpoint mutants reveal fragile sites in yeast. *Embo J*, **25**, 3627-3639.

Raynard, S., Niu, H., and Sung, P. (2008) DNA double-strande break processing: the beginning of the end. *Genes Dev*, **22**, 2903-2907.

Reichard, P. (1988) Interactions between deoxyribonucleotide and DNA synthesis. *Annu Rev Biochem*, **57**, 349-374.

Reynolds, A.E., McCarroll, R.M., Newlon, C.S. and Fangman, W.L. (1989) Time of replication of ARS elements along yeast chromosome III. *Mol Cell Biol*, **9**, 4488-4494.

Rhind, N. and Russell, P. (1998a) Mitotic DNA damage and replication checkpoints in yeast. *Curr Opin Cell Biol*, **10**, 749-758.

Rhind, N. and Russell, P. (1998b) Tyrosine phosphorylation of cdc2 is required for the replication checkpoint in Schizosaccharomyces pombe. *Mol Cell Biol*, **18**, 3782-3787.

Ricchetti, M., Fairhead, C. and Dujon, B. (1999) Mitochondrial DNA repairs double-strand breaks in yeast chromosomes. *Nature*, **402**, 96-100.

Richards, R.I. (2001) Fragile and unstable chromosomes in cancer: causes and consequences. *Trends Genet*, **17**, 339-345.

Richards, R.I. and Sutherland, G.R. (1994) Simple repeat DNA is not replicated simply. *Nat Genet*, **6**, 114-116.

Ried, K., Finnis, M., Hobson, L., Mangelsdorf, M., Dayan, S., Nancarrow, J.K., Woollatt, E., Kremmidiotis, G., Gardner, A., Venter, D., Baker, E. and Richards, R.I. (2000) Common chromosomal fragile site FRA16D sequence: identification of the FOR gene spanning FRA16D and homozygous deletions and translocation breakpoints in cancer cells. *Hum Mol Genet*, **9**, 1651-1663.

Ritchie, K.B., Mallory, J.C. and Petes, T.D. (1999) Interactions of TLC1 (which encodes the RNA subunit of telomerase), TEL1, and MEC1 in regulating telomere length in the yeast Saccharomyces cerevisiae. *Mol Cell Biol*, **19**, 6065-6075.

Rogakou, E.P., Pilch, D.R., Orr, A.H., Ivanova, V.S. and Bonner, W.M. (1998) DNA double-stranded breaks induce histone H2AX phosphorylation on serine 139. *J Biol Chem*, **273**, 5858-5868.

Rothkamm, K., Kruger, I., Thompson, L.H. and Lobrich, M. (2003) Pathways of DNA double-strand break repair during the mammalian cell cycle. *Mol Cell Biol*, **23**, 5706-5715.

Rozier, L., El-Achkar, E., Apiou, F. and Debatisse, M. (2004) Characterization of a conserved aphidicolin-sensitive common fragile site at human 4q22 and mouse 6C1: possible association with an inherited disease and cancer. *Oncogene*, **23**, 6872-6880.

Ruiz-Herrera, A., Garcia, F., Fronicke, L., Ponsa, M., Egozcue, J., Caldes, M.G. and Stanyon, R. (2004) Conservation of aphidicolin-induced fragile sites in Papionini (Primates) species and humans. *Chromosome Res*, **12**, 683-690.

Saintigny, Y., Delacote, F., Vares, G., Petitot, F., Lambert, S., Averbeck, D. and Lopez, B.S. (2001) Characterization of homologous recombination induced by replication inhibition in mammalian cells. *Embo J*, **20**, 3861-3870.

Saka, Y., Sutani, T., Yamashita, Y., Saitoh, S., Takeuchi, M., Nakaseko, Y. and Yanagida, M. (1994) Fission yeast cut3 and cut14, members of a ubiquitous protein family, are required for chromosome condensation and segregation in mitosis. *Embo J*, **13**, 4938-4952.

Samadashwily, G.M., Raca, G. and Mirkin, S.M. (1997) Trinucleotide repeats affect DNA replication in vivo. *Nat Genet*, **17**, 298-304.

Sancar, A., Lindsey-Boltz, L.A., Unsal-Kacmaz, K. and Linn, S. (2004) Molecular mechanisms of mammalian DNA repair and the DNA damage checkpoints. *Annu Rev Biochem*, **73**, 39-85.

Sanchez, Y., Bachant, J., Wang, H., Hu, F., Liu, D., Tetzlaff, M. and Elledge, S.J. (1999) Control of the DNA damage checkpoint by chk1 and rad53 protein kinases through distinct mechanisms. *Science*, **286**, 1166-1171.

Sanchez, Y., Desany, B.A., Jones, W.J., Liu, Q., Wang, B. and Elledge, S.J. (1996) Regulation of RAD53 by the ATM-like kinases MEC1 and TEL1 in yeast cell cycle checkpoint pathways. *Science*, **271**, 357-360.

Santocanale, C. and Diffley, J.F. (1996) ORC- and Cdc6-dependent complexes at active and inactive chromosomal replication origins in Saccharomyces cerevisiae. *Embo J*, **15**, 6671-6679.

Santocanale, C. and Diffley, J.F. (1998) A Mec1- and Rad53-dependent checkpoint controls late-firing origins of DNA replication. *Nature*, **395**, 615-618.

Sarai, A., Mazur, J., Nussinov, R. and Jernigan, R.L. (1989) Sequence dependence of DNA conformational flexibility. *Biochemistry*, **28**, 7842-7849.

Savvidou, E., Cobbe, N., Steffensen, S., Cotterill, S. and Heck, M.M. (2005) Drosophila CAP-D2 is required for condensin complex stability and resolution of sister chromatids. *J Cell Sci*, **118**, 2529-2543.

Saxena, S., Yuan, P., Dhar, S.K., Senga, T., Takeda, D., Robinson, H., Kornbluth, S., Swaminathan, K. and Dutta, A. (2004) A dimerized coiled-coil domain and an adjoining part of geminin interact with two sites on Cdt1 for replication inhibition. *Mol Cell*, **15**, 245-258.

Schaarschmidt, D., Baltin, J., Stehle, I.M., Lipps, H.J. and Knippers, R. (2004) An episomal mammalian replicon: sequence-independent binding of the origin recognition complex. *Embo J*, **23**, 191-201.

Schmidt, K.H., Derry, K.L. and Kolodner, R.D. (2002) Saccharomyces cerevisiae RRM3, a 5' to 3' DNA helicase, physically interacts with proliferating cell nuclear antigen. *J Biol Chem*, **277**, 45331-45337.

Schmidt, K.H. and Kolodner, R.D. (2006) Suppression of spontaneous genome rearrangements in yeast DNA helicase mutants. *Proc Natl Acad Sci U S A*, **103**, 18196-18201.

Schmiesing, J.A., Ball, A.R., Jr., Gregson, H.C., Alderton, J.M., Zhou, S. and Yokomori, K. (1998) Identification of two distinct human SMC protein complexes involved in mitotic chromosome dynamics. *Proc Natl Acad Sci U S A*, **95**, 12906-12911.

Schvartzman, J.B. and Stasiak, A. (2004) A topological view of the replicon. *EMBO Rep*, **5**, 256-261.

Schwab, M., Lutum, A.S. and Seufert, W. (1997) Yeast Hct1 is a regulator of Clb2 cyclin proteolysis. *Cell*, **90**, 683-693.

Schwartz, M., Zlotorynski, E., Goldberg, M., Ozeri, E., Rahat, A., le Sage, C., Chen, B.P., Chen, D.J., Agami, R. and Kerem, B. (2005) Homologous recombination and nonhomologous end-joining repair pathways regulate fragile site stability. *Genes Dev*, **19**, 2715-2726.

Schwartz, M., Zlotorynski, E. and Kerem, B. (2006) The molecular basis of common and rare fragile sites. *Cancer Lett*, **232**, 13-26.

Schwartz, M.F., Duong, J.K., Sun, Z., Morrow, J.S., Pradhan, D. and Stern, D.F. (2002) Rad9 phosphorylation sites couple Rad53 to the Saccharomyces cerevisiae DNA damage checkpoint. *Mol Cell*, **9**, 1055-1065.

Schwob, E., Bohm, T., Mendenhall, M.D. and Nasmyth, K. (1994) The B-type cyclin kinase inhibitor p40SIC1 controls the G1 to S transition in S. cerevisiae. *Cell*, **79**, 233-244.

Segurado, M. and Diffley, J.F. (2008) Separate roles for the DNA damage checkpoint protein kinases in stabilizing DNA replication forks. *Genes Dev*, **22**, 1816-1827.

Shah, J.V., Botvinick, E., Bonday, Z., Furnari, F., Berns, M. and Cleveland, D.W. (2004) Dynamics of centromere and kinetochore proteins; implications for checkpoint signalling and silencing. *Curr Biol*, **14**, 942-952.

Shechter, D. and Gautier, J. (2005) ATM and ATR check in on origins: a dynamic model for origin selection and activation. *Cell Cycle*, **4**, 235-238.

Shimada, K., Pasero, P. and Gasser, S.M. (2002) ORC and the intra-S-phase checkpoint: a threshold regulates Rad53p activation in S phase. *Genes Dev*, **16**, 3236-3252.

Shiraishi, T., Druck, T., Mimori, K., Flomenberg, J., Berk, L., Alder, H., Miller, W., Huebner, K. and Croce, C.M. (2001) Sequence conservation at human and mouse orthologous common fragile regions, FRA3B/FHIT and Fra14A2/Fhit. *Proc Natl Acad Sci U S A*, **98**, 5722-5727.

Shroff, R., Arbel-Eden, A., Pilch, D., Ira, G., Bonner, W.M., Petrini, J.H., Haber, J.E. and Lichten, M. (2004) Distribution and dynamics of chromatin modification induced by a defined DNA double-strand break. *Curr Biol*, **14**, 1703-1711.

Sidorova, J.M. and Breeden, L.L. (1997) Rad53-dependent phosphorylation of Swi6 and down-regulation of CLN1 and CLN2 transcription occur in response to DNA damage in Saccharomyces cerevisiae. *Genes Dev*, **11**, 3032-3045.

Simanis, V. (2003) Events at the end of mitosis in the budding and fission yeasts. *J Cell Sci*, **116**, 4263-4275.

Skoufias, D.A., Lacroix, F.B., Andreassen, P.R., Wilson, L. and Margolis, R.L. (2004) Inhibition of DNA decatenation, but not DNA damage, arrests cells at metaphase. *Mol Cell*, **15**, 977-990.

Smeets, D.F. and van de Klundert, F.A. (1990) Common fragile sites in man and three closely related primate species. *Cytogenet Cell Genet*, **53**, 8-14.

Smith, P.P., Friedman, C.L., Bryant, E.M. and McDougall, J.K. (1992) Viral integration and fragile sites in human papillomavirus-immortalized human keratinocyte cell lines. *Genes Chromosomes Cancer*, **5**, 150-157.

Smolka, M.B., Albuquerque, C.P., Chen, S.H., Schmidt, K.H., Wei, X.X., Kolodner, R.D. and Zhou, H. (2005) Dynamic changes in protein-protein interaction and protein phosphorylation probed with amine-reactive isotope tag. *Mol Cell Proteomics*, **4**, 1358-1369.

Sogo, J.M., Lopes, M. and Foiani, M. (2002) Fork reversal and ssDNA accumulation at stalled replication forks owing to checkpoint defects. *Science*, **297**, 599-602.

Sorensen, C.S., Hansen, L.T., Dziegielewski, J., Syljuasen, R.G., Lundin, C., Bartek, J. and Helleday, T. (2005) The cell-cycle checkpoint kinase Chk1 is required for mammalian homologous recombination repair. *Nat Cell Biol*, **7**, 195-201.

Spell, R.M. and Holm, C. (1994) Nature and distribution of chromosomal intertwinings in Saccharomyces cerevisiae. *Mol Cell Biol*, **14**, 1465-1476.

Spencer, F. and Hieter, P. (1992) Centromere DNA mutations induce a mitotic delay in Saccharomyces cerevisiae. *Proc Natl Acad Sci U S A*, **89**, 8908-8912.

Steffensen, S., Coelho, P.A., Cobbe, N., Vass, S., Costa, M., Hassan, B., Prokopenko, S.N., Bellen, H., Heck, M.M. and Sunkel, C.E. (2001) A role for Drosophila SMC4 in the resolution of sister chromatids in mitosis. *Curr Biol*, **11**, 295-307.

Stegmeier, F. and Amon, A. (2004) Closing mitosis: the functions of the Cdc14 phosphatase and its regulation. *Annu Rev Genet*, **38**, 203-232.

Stegmeier, F., Huang, J., Rahal, R., Zmolik, J., Moazed, D. and Amon, A. (2004) The replication fork block protein Fob1 functions as a negative regulator of the FEAR network. *Curr Biol*, **14**, 467-480.

Stegmeier, F., Visintin, R. and Amon, A. (2002) Separase, polo kinase, the kinetochore protein Slk19, and Spo12 function in a network that controls Cdc14 localization during early anaphase. *Cell*, **108**, 207-220.

Stelter, P. and Ulrich, H.D. (2003) Control of spontaneous and damage-induced mutagenesis by SUMO and ubiquitin conjugation. *Nature*, **425**, 188-191.

Stevenson, J.B. and Gottschling, D.E. (1999) Telomeric chromatin modulates replication timing near chromosome ends. *Genes Dev*, **13**, 146-151.

Stokes, M.P. and Michael, W.M. (2003) DNA damage-induced replication arrest in Xenopus egg extracts. *J Cell Biol*, **163**, 245-255.

Stone, D.M., Jacky, P.B., Hancock, D.D. and Prieur, D.J. (1991) Chromosomal fragile site expression in dogs: I. Breed specific differences. *Am J Med Genet*, **40**, 214-222.

Stone, D.M., Stephens, K.E. and Doles, J. (1993) Folate-sensitive and aphidicolin-inducible fragile sites are expressed in the genome of the domestic cat. *Cancer Genet Cytogenet*, **65**, 130-134.

Strom, L., Karlsson, C., Lindroos, H.B., Wedahl, S., Katou, Y., Shirahige, K. and Sjogren, C. (2007) Postreplicative formation of cohesion is required for repair and induced by a single DNA break. *Science*, **317**, 242-245.

Strom, L., Lindroos, H.B., Shirahige, K. and Sjogren, C. (2004) Postreplicative recruitment of cohesin to double-strand breaks is required for DNA repair. *Mol Cell*, **16**, 1003-1015.

Strunnikov, A.V., Hogan, E. and Koshland, D. (1995) SMC2, a Saccharomyces cerevisiae gene essential for chromosome segregation and condensation, defines a subgroup within the SMC family. *Genes Dev*, **9**, 587-599.

Subramanian, P.S., Nelson, D.L. and Chinault, A.C. (1996) Large domains of apparent delayed replication timing associated with triplet repeat expansion at FRAXA and FRAXE. *Am J Hum Genet*, **59**, 407-416.

Sudakin, V., Chan, G.K. and Yen, T.J. (2001) Checkpoint inhibition of the APC/C in HeLa cells is mediated by a complex of BUBR1, BUB3, CDC20, and MAD2. *J Cell Biol*, **154**, 925-936.

Sullivan, M., Higuchi, T., Katis, V.L. and Uhlmann, F. (2004) Cdc14 phosphatase induces rDNA condensation and resolves cohesin-independent cohesion during budding yeast anaphase. *Cell*, **117**, 471-482.

Sullivan, M. and Uhlmann, F. (2003) A non-proteolytic function of separase links the onset of anaphase to mitotic exit. *Nat Cell Biol*, **5**, 249-254.

Sumara, I., Vorlaufer, E., Gieffers, C., Peters, B.H. and Peters, J.M. (2000) Characterization of vertebrate cohesin complexes and their regulation in prophase. *J Cell Biol*, **151**, 749-762.

Sumara, I., Vorlaufer, E., Stukenberg, P.T., Kelm, O., Redemann, N., Nigg, E.A. and Peters, J.M. (2002) The dissociation of cohesin from chromosomes in prophase is regulated by Polo-like kinase. *Mol Cell*, **9**, 515-525.

Sutani, T., Yuasa, T., Tomonaga, T., Dohmae, N., Takio, K. and Yanagida, M. (1999) Fission yeast condensin complex: essential roles of non-SMC subunits for condensation and Cdc2 phosphorylation of Cut3/SMC4. *Genes Dev*, **13**, 2271-2283.

Sutherland, G.R. and Richards, R.I. (1995) The molecular basis of fragile sites in human chromosomes. *Curr Opin Genet Dev*, **5**, 323-327.

Svetlova, E.Y., Razin, S.V. and Debatisse, M. (2001) Mammalian recombination hot spot in a DNA loop anchorage region: a model for the study of common fragile sites. *J Cell Biochem Suppl*, **Suppl 36**, 170-178.

Swedlow, J.R. and Hirano, T. (2003) The making of the mitotic chromosome: modern insights into classical questions. *Mol Cell*, **11**, 557-569.

Symington, L.S. (2002) Role of RAD52 epistasis group genes in homologous recombination and double-strand break repair. *Microbiol Mol Biol Rev*, **66**, 630-670, table of contents.

Szostak, J.W., Orr-Weaver, T.L., Rothstein, R.J. and Stahl, F.W. (1983) The double-strand-break repair model for recombination. *Cell*, **33**, 25-35.

Szyjka, S.J., Viggiani, C.J. and Aparicio, O.M. (2005) Mrc1 is required for normal progression of replication forks throughout chromatin in S. cerevisiae. *Mol Cell*, **19**, 691-697.

Takata, M., Sasaki, M.S., Sonoda, E., Morrison, C., Hashimoto, M., Utsumi, H., Yamaguchi-Iwai, Y., Shinohara, A. and Takeda, S. (1998) Homologous recombination and non-homologous end-joining pathways of DNA double-strand break repair have overlapping roles in the maintenance of chromosomal integrity in vertebrate cells. *Embo J*, **17**, 5497-5508.

Takeda, D.Y. and Dutta, A. (2005) DNA replication and progression through S phase. *Oncogene*, **24**, 2827-2843.

Tanaka, S., Tak, Y.S. and Araki, H. (2007) The role of CDK in the initiation step of DNA replication in eukaryotes. *Cell Div*, **2**, 16.

Tanaka, T., Fuchs, J., Loidl, J. and Nasmyth, K. (2000) Cohesin ensures bipolar attachment of microtubules to sister centromeres and resists their precocious separation. *Nat Cell Biol*, **2**, 492-499.

Tanaka, T.U., Rachidi, N., Janke, C., Pereira, G., Galova, M., Schiebel, E., Stark, M.J. and Nasmyth, K. (2002) Evidence that the Ipl1-Sli15 (Aurora kinase-INCENP) complex promotes chromosome bi-orientation by altering kinetochore-spindle pole connections. *Cell*, **108**, 317-329.

Taylor, S.D., Zhang, H., Eaton, J.S., Rodeheffer, M.S., Lebedeva, M.A., O'Rourke T, W., Siede, W. and Shadel, G.S. (2005) The conserved Mec1/Rad53 nuclear checkpoint pathway regulates mitochondrial DNA copy number in Saccharomyces cerevisiae. *Mol Biol Cell*, **16**, 3010-3018.

Tercero, J.A. and Diffley, J.F. (2001) Regulation of DNA replication fork progression through damaged DNA by the Mec1/Rad53 checkpoint. *Nature*, **412**, 553-557.

Tercero, J.A., Longhese, M.P. and Diffley, J.F. (2003) A central role for DNA replication forks in checkpoint activation and response. *Mol Cell*, **11**, 1323-1336.

Theis, J.F., Dershowitz, A., Irene, C., Maciariello, C., Tobin, M.L., Liberi, G., Tabrizifard, S., Korus, M., Fabiani, L. and Newlon, C.S. (2007) Identification of mutations that decrease the stability of a fragment of Saccharomyces cerevisiae chromosome III lacking efficient replicators. *Genetics*, **177**, 1445-1458.

Thorland, E.C., Myers, S.L., Persing, D.H., Sarkar, G., McGovern, R.M., Gostout, B.S. and Smith, D.I. (2000) Human papillomavirus type 16 integrations in cervical tumors frequently occur in common fragile sites. *Cancer Res*, **60**, 5916-5921.

Tinker-Kulberg, R.L. and Morgan, D.O. (1999) Pds1 and Esp1 control both anaphase and mitotic exit in normal cells and after DNA damage. *Genes Dev*, **13**, 1936-1949.

Toledo, F., Coquelle, A., Svetlova, E. and Debatisse, M. (2000) Enhanced flexibility and aphidicolin-induced DNA breaks near mammalian replication origins:

implications for replicon mapping and chromosome fragility. *Nucleic Acids Res*, **28**, 4805-4813.

Toone, W.M., Aerne, B.L., Morgan, B.A. and Johnston, L.H. (1997) Getting started: regulating the initiation of DNA replication in yeast. *Annu Rev Microbiol*, **51**, 125-149.

Tourriere, H. and Pasero, P. (2007) Maintenance of fork integrity at damaged DNA and natural pause sites. *DNA Repair (Amst)*, **6**, 900-913.

Tourriere, H., Versini, G., Cordon-Preciado, V., Alabert, C. and Pasero, P. (2005) Mrc1 and Tof1 promote replication fork progression and recovery independently of Rad53. *Mol Cell*, **19**, 699-706.

Toyn, J.H., Johnson, A.L., Donovan, J.D., Toone, W.M. and Johnston, L.H. (1997) The Swi5 transcription factor of Saccharomyces cerevisiae has a role in exit from mitosis through induction of the cdk-inhibitor Sic1 in telophase. *Genetics*, **145**, 85-96.

Trenz, K., Smith, E., Smith, S. and Costanzo, V. (2006) ATM and ATR promote Mre11 dependent restart of collapsed replication forks and prevent accumulation of DNA breaks. *Embo J*, **25**, 1764-1774.

Uchiki, T., Dice, L.T., Hettich, R.L. and Dealwis, C. (2004) Identification of phosphorylation sites on the yeast ribonucleotide reductase inhibitor Sml1. *J Biol Chem*, **279**, 11293-11303.

Uemura, T., Ohkura, H., Adachi, Y., Morino, K., Shiozaki, K. and Yanagida, M. (1987) DNA topoisomerase II is required for condensation and separation of mitotic chromosomes in S. pombe. *Cell*, **50**, 917-925.

Uhlmann, F., Lottspeich, F. and Nasmyth, K. (1999) Sister-chromatid separation at anaphase onset is promoted by cleavage of the cohesin subunit Scc1. *Nature*, **400**, 37-42.

Uhlmann, F. and Nasmyth, K. (1998) Cohesion between sister chromatids must be established during DNA replication. *Curr Biol*, **8**, 1095-1101.

Uhlmann, F., Wernic, D., Poupart, M.A., Koonin, E.V. and Nasmyth, K. (2000) Cleavage of cohesin by the CD clan protease separin triggers anaphase in yeast. *Cell*, **103**, 375-386.

Unal, E., Heidinger-Pauli, J.M. and Koshland, D. (2007) DNA double-strand breaks trigger genome-wide sister-chromatid cohesion through Eco1 (Ctf7). *Science*, **317**, 245-248.

Usui, T., Ogawa, H. and Petrini, J.H. (2001) A DNA damage response pathway controlled by Tel1 and the Mre11 complex. *Mol Cell*, **7**, 1255-1266.

Usui, T., Petrini, J.H. and Morales, M. (2006) Rad50S alleles of the Mre11 complex: questions answered and questions raised. *Exp Cell Res*, **312**, 2694-2699.

Vallen, E.A. and Cross, F.R. (1999) Interaction between the MEC1-dependent DNA synthesis checkpoint and G1 cyclin function in Saccharomyces cerevisiae. *Genetics*, **151**, 459-471.

van Gent, D.C., Hoeijmakers, J.H. and Kanaar, R. (2001) Chromosomal stability and the DNA double-stranded break connection. *Nat Rev Genet*, **2**, 196-206.

Van Hooser, A., Goodrich, D.W., Allis, C.D., Brinkley, B.R. and Mancini, M.A. (1998) Histone H3 phosphorylation is required for the initiation, but not maintenance, of mammalian chromosome condensation. *J Cell Sci*, **111 ( Pt 23)**, 3497-3506.

Vas, A.C., Andrews, C.A., Kirkland Matesky, K. and Clarke, D.J. (2007) In vivo analysis of chromosome condensation in Saccharomyces cerevisiae. *Mol Biol Cell*, **18**, 557-568.

Verkerk, A.J., Pieretti, M., Sutcliffe, J.S., Fu, Y.H., Kuhl, D.P., Pizzuti, A., Reiner, O., Richards, S., Victoria, M.F., Zhang, F.P. and et al. (1991) Identification of a gene (FMR-1) containing a CGG repeat coincident with a breakpoint cluster region exhibiting length variation in fragile X syndrome. *Cell*, **65**, 905-914.

Verma, R., Annan, R.S., Huddleston, M.J., Carr, S.A., Reynard, G. and Deshaies, R.J. (1997) Phosphorylation of Sic1p by G1 Cdk required for its degradation and entry into S phase. *Science*, **278**, 455-460.

Versini, G., Comet, I., Wu, M., Hoopes, L., Schwob, E. and Pasero, P. (2003) The yeast Sgs1 helicase is differentially required for genomic and ribosomal DNA replication. *Embo J*, **22**, 1939-1949.

Visintin, R., Craig, K., Hwang, E.S., Prinz, S., Tyers, M. and Amon, A. (1998) The phosphatase Cdc14 triggers mitotic exit by reversal of Cdk-dependent phosphorylation. *Mol Cell*, **2**, 709-718.

Visintin, R., Hwang, E.S. and Amon, A. (1999) Cfi1 prevents premature exit from mitosis by anchoring Cdc14 phosphatase in the nucleolus. *Nature*, **398**, 818-823.

Visintin, R., Stegmeier, F. and Amon, A. (2003) The role of the polo kinase Cdc5 in controlling Cdc14 localization. *Mol Biol Cell*, **14**, 4486-4498.

Vogelauer, M., Rubbi, L., Lucas, I., Brewer, B.J. and Grunstein, M. (2002) Histone acetylation regulates the time of replication origin firing. *Mol Cell*, **10**, 1223-1233.

Voineagu, I., Narayanan, V., Lobachev, K.S. and Mirkin, S.M. (2008) Replication stalling at unstable inverted repeats: interplay between DNA hairpins and fork stabilizing proteins. *Proc Natl Acad Sci U S A*, **105**, 9936-9941.

Vujcic, M., Miller, C.A. and Kowalski, D. (1999) Activation of silent replication origins at autonomously replicating sequence elements near the HML locus in budding yeast. *Mol Cell Biol*, **19**, 6098-6109.

Wach, A., Brachat, A., Pohlmann, R. and Philippsen, P. (1994) New heterologous modules for classical or PCR-based gene disruptions in Saccharomyces cerevisiae. *Yeast*, **10**, 1793-1808.

Waga, S. and Stillman, B. (1998) The DNA replication fork in eukaryotic cells. *Annu Rev Biochem*, **67**, 721-751.

Waizenegger, I.C., Hauf, S., Meinke, A. and Peters, J.M. (2000) Two distinct pathways remove mammalian cohesin from chromosome arms in prophase and from centromeres in anaphase. *Cell*, **103**, 399-410.

Walter, J. and Newport, J. (2000) Initiation of eukaryotic DNA replication: origin unwinding and sequential chromatin association of Cdc45, RPA, and DNA polymerase alpha. *Mol Cell*, **5**, 617-627.

Wang, B.D., Yong-Gonzalez, V. and Strunnikov, A.V. (2004) Cdc14p/FEAR pathway controls segregation of nucleolus in S. cerevisiae by facilitating condensin targeting to rDNA chromatin in anaphase. *Cell Cycle*, **3**, 960-967.

Wang, J.C. (2002) Cellular roles of DNA topoisomerases: a molecular perspective. *Nat Rev Mol Cell Biol*, **3**, 430-440.

Wang, L., Paradee, W., Mullins, C., Shridhar, R., Rosati, R., Wilke, C.M., Glover, T.W. and Smith, D.I. (1997) Aphidicolin-induced FRA3B breakpoints cluster in two distinct regions. *Genomics*, **41**, 485-488.

Wang, N.D., Testa, J.R. and Smith, D.I. (1993) Determination of the specificity of aphidicolin-induced breakage of the human 3p14.2 fragile site. *Genomics*, **17**, 341-347.

Wang, Y. and Burke, D.J. (1995) Checkpoint genes required to delay cell division in response to nocodazole respond to impaired kinetochore function in the yeast Saccharomyces cerevisiae. *Mol Cell Biol*, **15**, 6838-6844.

Wang, Y., Vujcic, M. and Kowalski, D. (2001) DNA replication forks pause at silent origins near the HML locus in budding yeast. *Mol Cell Biol*, **21**, 4938-4948.

Wei, Y., Mizzen, C.A., Cook, R.G., Gorovsky, M.A. and Allis, C.D. (1998) Phosphorylation of histone H3 at serine 10 is correlated with chromosome condensation during mitosis and meiosis in Tetrahymena. *Proc Natl Acad Sci U S A*, **95**, 7480-7484.

Weinreich, M. and Stillman, B. (1999) Cdc7p-Dbf4p kinase binds to chromatin during S phase and is regulated by both the APC and the RAD53 checkpoint pathway. *Embo J*, **18**, 5334-5346.

Weiss, E. and Winey, M. (1996) The Saccharomyces cerevisiae spindle pole body duplication gene MPS1 is part of a mitotic checkpoint. *J Cell Biol*, **132**, 111-123.

Wellinger, R.E., Prado, F. and Aguilera, A. (2006) Replication fork progression is impaired by transcription in hyperrecombinant yeast cells lacking a functional THO complex. *Mol Cell Biol*, **26**, 3327-3334.

West, S.C. (2003) Molecular views of recombination proteins and their control. *Nat Rev Mol Cell Biol*, **4**, 435-445.

Wilke, C.M., Hall, B.K., Hoge, A., Paradee, W., Smith, D.I. and Glover, T.W. (1996) FRA3B extends over a broad region and contains a spontaneous HPV16 integration site: direct evidence for the coincidence of viral integration sites and fragile sites. *Hum Mol Genet*, **5**, 187-195.

Wojcik, E., Basto, R., Serr, M., Scaerou, F., Karess, R. and Hays, T. (2001) Kinetochore dynein: its dynamics and role in the transport of the Rough deal checkpoint protein. *Nat Cell Biol*, **3**, 1001-1007.

Wu, L. and Hickson, I.D. (2003) The Bloom's syndrome helicase suppresses crossing over during homologous recombination. *Nature*, **426**, 870-874.

Wyrick, J.J., Aparicio, J.G., Chen, T., Barnett, J.D., Jennings, E.G., Young, R.A., Bell, S.P. and Aparicio, O.M. (2001) Genome-wide distribution of ORC and MCM proteins in S. cerevisiae: high-resolution mapping of replication origins. *Science*, **294**, 2357-2360.

Xie, A., Puget, N., Shim, I., Odate, S., Jarzyna, I., Bassing, C.H., Alt, F.W. and Scully, R. (2004) Control of sister chromatid recombination by histone H2AX. *Mol Cell*, **16**, 1017-1025.

Yabuuchi, H., Yamada, Y., Uchida, T., Sunathvanichkul, T., Nakagawa, T. and Masukata, H. (2006) Ordered assembly of Sld3, GINS and Cdc45 is distinctly regulated by DDK and CDK for activation of replication origins. *Embo J*, **25**, 4663-4674.

Yang, M.Y. and Long, S.E. (1993) Folate sensitive common fragile sites in chromosomes of the domestic pig (Sus scrofa). *Res Vet Sci*, **55**, 231-235.

Yao, R., Zhang, Z., An, X., Bucci, B., Perlstein, D.L., Stubbe, J. and Huang, M. (2003) Subcellular localization of yeast ribonucleotide reductase regulated by the DNA replication and damage checkpoint pathways. *Proc Natl Acad Sci U S A*, **100**, 6628-6633.

Yarbro, J.W. (1992) Mechanism of action of hydroxyurea. *Semin Oncol*, **19**, 1-10.

Yeong, F.M., Lim, H.H., Padmashree, C.G. and Surana, U. (2000) Exit from mitosis in budding yeast: biphasic inactivation of the Cdc28-Clb2 mitotic kinase and the role of Cdc20. *Mol Cell*, **5**, 501-511.

You, Z., Bailis, J.M., Johnson, S.A., Dilworth, S.M. and Hunter, T. (2007) Rapid activation of ATM on DNA flanking double-strand breaks. *Nat Cell Biol*, **9**, 1311-1318.

Yu, S., Mangelsdorf, M., Hewett, D., Hobson, L., Baker, E., Eyre, H.J., Lapsys, N., Le Paslier, D., Doggett, N.A., Sutherland, G.R. and Richards, R.I. (1997) Human chromosomal fragile site FRA16B is an amplified AT-rich minisatellite repeat. *Cell*, **88**, 367-374.

Zachariae, W. and Nasmyth, K. (1999) Whose end is destruction: cell division and the anaphase-promoting complex. *Genes Dev*, **13**, 2039-2058.

Zhang, H. and Freudenreich, C.H. (2007) An AT-rich sequence in human common fragile site FRA16D causes fork stalling and chromosome breakage in S. cerevisiae. *Mol Cell*, **27**, 367-379.

Zhang, H. and Lawrence, C.W. (2005) The error-free component of the RAD6/RAD18 DNA damage tolerance pathway of budding yeast employs sister-strand recombination. *Proc Natl Acad Sci U S A*, **102**, 15954-15959.

Zhang, R., Sengupta, S., Yang, Q., Linke, S.P., Yanaihara, N., Bradsher, J., Blais, V., McGowan, C.H. and Harris, C.C. (2005) BLM helicase facilitates Mus81 endonuclease activity in human cells. *Cancer Res*, **65**, 2526-2531.

Zhao, X., Chabes, A., Domkin, V., Thelander, L. and Rothstein, R. (2001) The ribonucleotide reductase inhibitor Sml1 is a new target of the Mec1/Rad53 kinase cascade during growth and in response to DNA damage. *Embo J*, **20**, 3544-3553.

Zhao, X., Muller, E.G. and Rothstein, R. (1998) A suppressor of two essential checkpoint genes identifies a novel protein that negatively affects dNTP pools. *Mol Cell*, **2**, 329-340.

Zhao, X. and Rothstein, R. (2002) The Dun1 checkpoint kinase phosphorylates and regulates the ribonucleotide reductase inhibitor Sml1. *Proc Natl Acad Sci U S A*, **99**, 3746-3751.

Zhu, M. and Weiss, R.S. (2007) Increased common fragile site expression, cell proliferation defects, and apoptosis following conditional inactivation of mouse Hus1 in primary cultured cells. *Mol Biol Cell*, **18**, 1044-1055.

Zhu, Z., Chung W.H., Shim E.Y., Lee S.E., Ira G. (2008) Sgs1 helicase and two nucleases Dna2 and Exo1 resect DNA double-strand break ends. *Cell*, **134**, 981-984.

Zlotorynski, E., Rahat, A., Skaug, J., Ben-Porat, N., Ozeri, E., Hershberg, R., Levi, A., Scherer, S.W., Margalit, H. and Kerem, B. (2003) Molecular basis for expression of common and rare fragile sites. *Mol Cell Biol*, **23**, 7143-7151.

Zou, L. and Elledge, S.J. (2003) Sensing DNA damage through ATRIP recognition of RPA-ssDNA complexes. *Science*, **300**, 1542-1548.

Zou, L., Liu, D. and Elledge, S.J. (2003) Replication protein A-mediated recruitment and activation of Rad17 complexes. *Proc Natl Acad Sci U S A*, **100**, 13827-13832.

# Appendices

## Appendix 1

**Table showing the distances (in kb) between the mid-point of each of the 133 high DNA flexibility sites and the mid-point of the nearest chromosomal features.**

|        |        | origin | Ty     | t-RNA  | Δ element | Centromere |
|--------|--------|--------|--------|--------|-----------|------------|
| **chr 1** | **Flex1**  | 11.25  | 75.00  | 46.88  | 46.88     | 63.75      |
| **chr2**  | **Flex2**  | 25.81  | 6.79   | 2.04   | 2.04      | 199.00     |
|        | **Flex3**  | 12.23  | 27.17  | 3.40   | 3.40      | 47.54      |
|        | **Flex4**  | 14.94  | 47.54  | 1.36   | 3.40      | 101.88     |
|        | **Flex5**  | 20.38  | 28.53  | 61.13  | 115.46    | 220.73     |
|        | **Flex6**  | 13.58  | 27.17  | 101.88 | 101.88    | 285.25     |
|        | **Flex7**  | 6.79   | 27.17  | 88.29  | 88.29     | 305.63     |
|        | **Flex8**  | 3.40   | 135.83 | 4.75   | 2.04      | 393.92     |
|        | **Flex9**  | 14.94  | 1.30   | 47.54  | 41.43     | 444.18     |
| **chr3**  | **Flex10** | 1.62   | 2.43   | 89.29  | 93.34     | 133.93     |
|        | **Flex11** | 1.62   | 32.47  | 45.46  | 47.08     | 93.34      |
|        | **Flex12** | 8.93   | 40.58  | 32.47  | 32.47     | 89.29      |
|        | **Flex13** | 16.23  | 178.57 | 20.29  | 56.82     | 137.99     |
|        | **Flex14** | 23.54  | 194.81 | 28.41  | 43.02     | 158.28     |
|        | **Flex15** | 12.99  | 260.55 | 17.05  | 15.42     | 227.27     |
| **chr4**  | **Flex16** | 4.01   | 521.27 | 68.57  | 437.07    | 453.11     |
|        | **Flex17** | 8.02   | 477.97 | 25.66  | 400.18    | 417.02     |
|        | **Flex18** | 8.02   | 356.87 | 200.49 | 282.29    | 296.72     |
|        | **Flex19** | 12.03  | 298.33 | 141.14 | 221.34    | 236.58     |
|        | **Flex20** | 16.04  | 283.09 | 125.91 | 175.23    | 224.55     |
|        | **Flex21** | 4.01   | 192.47 | 40.10  | 118.69    | 136.33     |
|        | **Flex22** | 6.42   | 188.46 | 32.08  | 112.27    | 128.31     |
|        | **Flex23** | 7.22   | 172.42 | 17.64  | 100.24    | 116.28     |
|        | **Flex24** | 34.48  | 144.35 | 8.82   | 72.18     | 88.22      |
|        | **Flex25** | 24.06  | 124.30 | 23.26  | 130.72    | 68.17      |
|        | **Flex26** | 21.65  | 16.84  | 16.84  | 12.03     | 88.22      |
|        | **Flex27** | 2.41   | 38.49  | 12.83  | 32.08     | 112.27     |
|        | **Flex28** | 8.02   | 84.21  | 117.89 | 92.22     | 343.24     |
|        | **Flex29** | 24.06  | 0.00   | 26.46  | 1.60      | 477.16     |
|        | **Flex30** | 4.01   | 48.12  | 17.64  | 18.44     | 505.23     |
|        | **Flex31** | 23.26  | 46.51  | 4.01   | 4.81      | 520.47     |
|        | **Flex32** | 40.10  | 7.22   | 23.26  | 16.04     | 538.11     |
|        | **Flex33** | 20.05  | 8.02   | 33.68  | 9.62      | 824.41     |
|        | **Flex34** | 8.82   | 16.84  | 21.65  | 24.06     | 835.64     |
|        | **Flex35** | 5.61   | 71.37  | 25.66  | 74.58     | 889.37     |
|        | **Flex36** | 8.02   | 105.86 | 9.62   | 40.90     | 922.25     |
|        | **Flex37** | 4.01   | 168.41 | 24.06  | 22.45     | 988.01     |
|        | **Flex38** | 4.81   | 208.51 | 55.33  | 136.33    | 1024.90    |

|      |        | origin | Ty     | t-RNA  | Δ element | Centromere |
|------|--------|--------|--------|--------|-----------|------------|
| **chr5** | **Flex39** | 1.44  | 335.86 | 14.35  | 1.44   | 43.06   |
|      | **Flex40** | 15.07 | 321.51 | 1.44   | 2.15   | 28.71   |
|      | **Flex41** | 7.18  | 305.00 | 3.59   | 5.74   | 16.51   |
|      | **Flex42** | 17.94 | 251.18 | 7.89   | 22.96  | 42.27   |
|      | **Flex43** | 10.05 | 238.26 | 3.59   | 35.88  | 53.11   |
|      | **Flex44** | 9.33  | 222.47 | 21.53  | 5.74   | 53.82   |
|      | **Flex45** | 7.18  | 187.31 | 7.89   | 6.46   | 104.06  |
|      | **Flex46** | 7.18  | 160.04 | 5.74   | 5.74   | 130.61  |
|      | **Flex47** | 14.35 | 45.93  | 48.80  | 42.34  | 349.49  |
|      | **Flex48** | 12.92 | 94.73  | 95.45  | 16.51  | 399.73  |
|      | **Flex49** | 7.89  | 102.62 | 101.19 | 3.59   | 408.34  |
| **chr6** | **Flex50** | 14.05 | 91.86  | 46.65  | 43.06  | 105.49  |
|      | **Flex51** | 18.96 | 47.36  | 7.89   | 7.18   | 61.72   |
|      | **Flex52** | 6.32  | 79.66  | 3.59   | 7.89   | 76.79   |
| **chr7** | **Flex53** | 1.39  | 460.52 | 1.39   | 34.78  | 438.26  |
|      | **Flex54** | 3.48  | 452.87 | 8.35   | 24.35  | 429.91  |
|      | **Flex55** | 13.91 | 372.17 | 29.91  | 47.30  | 351.30  |
|      | **Flex56** | 8.35  | 258.09 | 15.30  | 45.22  | 236.52  |
|      | **Flex57** | 2.78  | 251.83 | 9.04   | 38.96  | 229.57  |
|      | **Flex58** | 13.22 | 217.74 | 10.43  | 6.26   | 196.87  |
|      | **Flex59** | 13.91 | 176.00 | 20.87  | 22.26  | 154.43  |
|      | **Flex60** | 3.48  | 98.78  | 5.57   | 11.83  | 79.30   |
|      | **Flex61** | 3.48  | 97.39  | 11.83  | 25.04  | 73.04   |
|      | **Flex62** | 12.52 | 0.00   | 2.09   | 2.09   | 27.83   |
|      | **Flex63** | 24.35 | 33.39  | 53.57  | 33.39  | 108.52  |
|      | **Flex64** | 6.96  | 62.61  | 53.57  | 64.70  | 146.09  |
|      | **Flex65** | 8.35  | 65.39  | 21.57  | 67.48  | 173.91  |
|      | **Flex66** | 1.39  | 13.91  | 6.61   | 6.96   | 305.39  |
|      | **Flex67** | 27.83 | 198.26 | 28.52  | 99.48  | 542.61  |
| **chr8** | **Flex68** | 3.35  | 16.76  | 6.03   | 14.08  | 42.90   |
|      | **Flex69** | 16.76 | 192.37 | 14.75  | 14.75  | 262.75  |
|      | **Flex70** | 2.01  | 142.10 | 8.04   | 6.70   | 284.87  |
|      | **Flex71** | 20.78 | 118.64 | 28.15  | 26.81  | 305.65  |
|      | **Flex72** | 6.70  | 67.03  | 2.01   | 3.35   | 358.61  |
|      | **Flex73** | 6.03  | 28.15  | 34.18  | 21.45  | 395.47  |
| **chr9** | **Flex74** | 4.21  | 91.12  | 67.99  | 90.42  | 251.64  |
|      | **Flex75** | 7.01  | 14.72  | 2.10   | 14.02  | 173.83  |
| **chr10** | **Flex76** | 6.04  | 111.98 | 35.54  | 21.46  | 355.40  |
|      | **Flex77** | 29.50 | 12.07  | 14.75  | 14.75  | 254.14  |
|      | **Flex78** | 7.38  | 5.70   | 36.21  | 8.18   | 24.81   |
|      | **Flex79** | 21.46 | 3.35   | 42.92  | 3.35   | 38.89   |
| **chr11** | **Flex80** | 1.31  | N/A    | 34.07  | 58.30  | 427.78  |
|      | **Flex81** | 17.69 | N/A    | 22.93  | 21.62  | 302.66  |
|      | **Flex82** | 9.17  | N/A    | 58.96  | 6.55   | 273.83  |
|      | **Flex83** | 24.89 | N/A    | 19.00  | 19.00  | 155.92  |
|      | **Flex84** | 6.55  | N/A    | 10.48  | 9.83   | 32.10   |
|      | **Flex85** | 1.31  | N/A    | 13.76  | 13.10  | 91.39   |
|      | **Flex86** | 2.62  | N/A    | 7.86   | 71.08  | 148.71  |

|  |  | origin | Ty | t-RNA | Δ element | Centromere |
|---|---|---|---|---|---|---|
| **chr12** | **Flex87** | 10.28 | 305.05 | 94.83 | 100.54 | 204.51 |
|  | **Flex88** | 11.43 | 190.80 | 13.71 | 14.85 | 94.83 |
|  | **Flex89** | 36.56 | 157.67 | 78.83 | 81.12 | 61.70 |
|  | **Flex90** | 11.43 | 79.98 | 3.43 | 2.29 | 20.57 |
|  | **Flex91** | 16.00 | 76.55 | 6.86 | 5.71 | 22.85 |
|  | **Flex92** | 35.42 | 55.98 | 25.14 | 21.71 | 41.13 |
|  | **Flex93** | 74.26 | 194.23 | 61.70 | 49.13 | 311.91 |
|  | **Flex94** | 83.40 | 203.37 | 53.70 | 39.99 | 318.76 |
|  | **Flex95** | 62.84 | 57.13 | 62.84 | 57.13 | 694.65 |
|  | **Flex96** | 76.55 | 44.56 | 47.99 | 44.56 | 707.22 |
|  | **Flex97** | 45.70 | 77.69 | 16.00 | 12.57 | 946.00 |
|  | **Flex98** | 5.71 | 186.23 | 8.00 | 17.14 | 1175.65 |
|  | **Flex99** | 5.71 | 171.38 | 22.85 | 34.28 | 1189.36 |
|  | **Flex100** | 83.40 | 97.11 | 8.00 | 91.40 | 1267.05 |
|  | **Flex101** | 3.43 | 63.98 | 62.84 | 49.13 | 1501.26 |
| **chr13** | **Flex102** | 7.63 | 156.95 | 108.02 | 108.02 | 247.18 |
|  | **Flex103** | 9.53 | 94.04 | 45.11 | 45.11 | 183.64 |
|  | **Flex104** | 4.45 | 79.43 | 29.86 | 29.86 | 168.39 |
|  | **Flex105** | 25.42 | 32.41 | 19.06 | 37.49 | 33.68 |
|  | **Flex106** | 26.05 | 9.53 | 6.35 | 9.53 | 73.07 |
|  | **Flex107** | 13.98 | 1.91 | 11.44 | 11.44 | 114.38 |
|  | **Flex108** | 13.34 | 173.47 | 7.63 | 7.63 | 287.21 |
|  | **Flex109** | 17.79 | 198.25 | 5.72 | 18.43 | 312.63 |
|  | **Flex110** | 1.91 | 257.34 | 63.54 | 76.25 | 371.72 |
| **chr14** | **Flex111** | 14.16 | 102.95 | 104.88 | 106.17 | 415.02 |
|  | **Flex112** | 1.93 | 39.89 | 49.55 | 25.74 | 25.09 |
|  | **Flex113** | 3.22 | 125.47 | 28.95 | 27.67 | 77.21 |
| **chr15** | **Flex114** | 20.84 | 72.94 | 64.48 | 67.08 | 280.05 |
|  | **Flex115** | 6.51 | 74.90 | 1.30 | 3.26 | 216.22 |
|  | **Flex116** | 26.05 | 65.13 | 30.61 | 24.75 | 131.56 |
|  | **Flex117** | 53.40 | 93.13 | 1.95 | 1.95 | 103.55 |
|  | **Flex118** | 41.68 | 110.72 | 36.47 | 57.96 | 89.88 |
|  | **Flex119** | 11.72 | 222.08 | 2.61 | 1.95 | 25.40 |
|  | **Flex120** | 31.26 | 181.05 | 32.56 | 29.96 | 82.71 |
|  | **Flex121** | 32.56 | 64.15 | 44.61 | 56.66 | 201.89 |
|  | **Flex122** | 0.65 | 42.33 | 6.51 | 1.95 | 333.45 |
|  | **Flex123** | 20.84 | 4.56 | 1.30 | 1.30 | 386.86 |
|  | **Flex124** | 2.61 | 44.94 | 57.96 | 43.64 | 589.40 |
|  | **Flex125** | 11.72 | 1.30 | 1.30 | 0.00 | 654.53 |
|  | **Flex126** | 5.86 | 6.51 | 6.51 | 3.26 | 658.44 |
|  | **Flex127** | 71.64 | 110.72 | 10.42 | 7.82 | 86.62 |
| **chr16** | **Flex128** | 20.84 | 72.49 | 72.49 | 64.08 | 417.48 |
|  | **Flex129** | 1.94 | 96.44 | 46.60 | 47.25 | 391.59 |
|  | **Flex130** | 2.91 | 142.40 | 3.24 | 3.88 | 344.99 |
|  | **Flex131** | 21.36 | 170.88 | 27.83 | 23.30 | 316.51 |
|  | **Flex132** | 12.95 | 130.75 | 26.54 | 78.32 | 90.62 |
|  | **Flex133** | 22.01 | 11.65 | 3.24 | 2.59 | 212.30 |

# Appendix 2
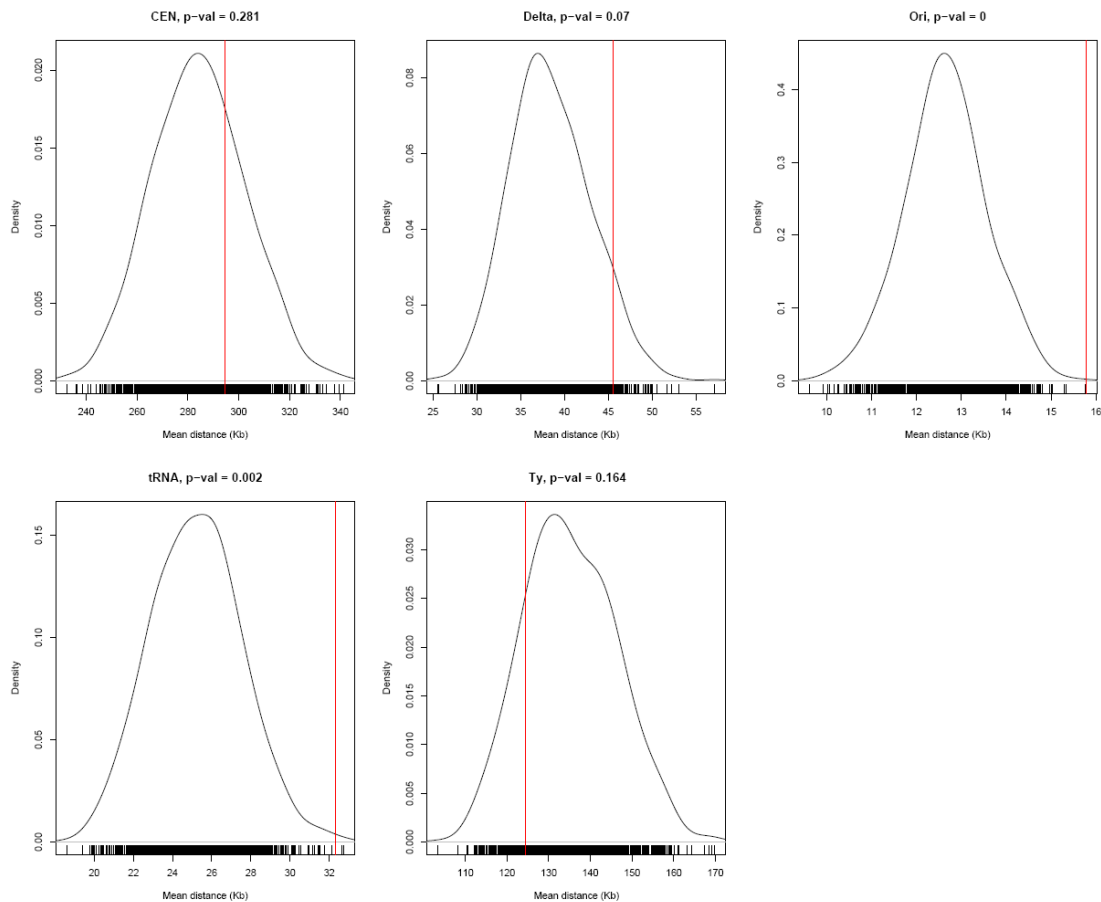


**Statistical analysis of the distance between regions of high DNA flexibility and various chromosomal determinants.** In each plot, the average observed distance between sites of high DNA flexibility and the nearest chromosomal feature (i.e. centromere, origin, Ty, Delements, and tRNA genes; see Table 3.1) is indicated by the vertical red line. 1,000 sets of 133 flexibility sites were simulated, each sampled from a uniform distribution, and were located in their respective chromosomes. For each high flexibility site, the distance between the simulated flexibility sites and the chromosomal feature of interest was calculated. These distances are shown as vertical lines at the bottom of the plot. The histogram represents the density estimate that was fitted to these values and indicates the estimated statistical distribution of the distances. In the case of centromeres, Ty elements, and $\Delta$ elements, the observed distance between high flexibility sites and these chromosomal features (red line) coincides with the histogram, suggesting that these distances are not significantly different than what would be expected if the flexibility sites were distributed randomly. On the other hand, the observed distances between high flexibility sites and either origins or tRNA genes falls outside the histogram, suggesting that flexibility sites seem to be much further away from these features than would be expected by chance. All analyses were performed by Mario Dos-Reis (Mathematical Biology, NIMR).

285